

N° ordre: 41200

# THESE

Presentée à

## Universite Lille1- Sciences et Technologies

Ecole doctorale des Sciences de la Matière, du Rayonnement et de l'Environnement  
U.F.R. de Chimie

## Université Libanaise

Ecole doctorale des Sciences et de Technologie

Par

**Mirna Daye**

Pour obtenir le grade de

**DOCTEUR**

**Specialité: Optique, Lasers, Physico-chimie, Atmosphère**

---

**Etude de la contamination par le mercure dans les milieux  
aquatiques : Devenir et comportement biogeochimique, mise au  
point de methodes d'analyse de trace du mercure**

---

### Membres du Jury

M. Bacquet, Professeur	Université Lille 1, France	Présidente
R.C. Rodriguez Martin-Doimeadios, Professeur	Université Castilla-La Mancha, Espagne	Rapporteur
E. Guillon, Professeur	Université de Reims, France	Rapporteur
B. Ouddane, Professeur	Université Lille 1, France	Directeur
J. Halwani, Professeur	Université Libanaise, Liban	Co-directeur
Z. Saad, Professeur	Université Libanaise, Liban	Examineur
E. Abi-Aad, Professeur	Université littorale côte d'Opale, France	Examineur
L. Quillet, Maître de Conférences	Université Rouen, France	Examineur

---

## ACKNOWLEDGMENTS

---

This thesis has been carried out in collaboration between the University Lille 1 and the Lebanese University. First of all, I would like to express my sincere gratitude to my thesis supervisor prof. Baghdad OUDDANE who welcomed me in his research group. I want to thank him for his phenomenal scientific guidance during my three years Ph.D study, perpetual patience and valuable advice and motivation. Without his constant support and encouragement, I might not been able to accomplish my work.

I am grateful to my co-director in Lebanon prof. Jalal HALWANI, who has guided me during my undergraduate and graduate studies and who helped me to open a new scientific road for continuing my higher studies in France. I greatly appreciate his constant encouragement and his scientific support. I am immensely thankful to Professors Rosa Carmen RODRIGUEZ MARTIN-DOIMEADIOS and Emmanuel GUILLON for accepting to revise and having time to judge this Ph.D work. Their remarks and comments have been substantial to ameliorate this manuscript. I am greatly thankful the president of my Ph.D defence prof. Maryse BACQUET for her good mood and her constructive remarks to improve my manuscript. Also I would like to express my gratitude to prof. Zeinab SAAD, prof. Edmond ABI-AAD and Mr. Laurent QUILLET for accepting being examiners of this work.

I greatly appreciate the friendly welcome and constant smile of prof. Michel WARTEL. I would like to thank him for his motivation and scientific spirit building in the laboratory. Also, I am grateful to him for writing me several letters of recommendation to help me find a postdoctoral position. I am also grateful to Mr. Abdel BOUGHRIET for his scientific advice and his assistance. Besides, I would like to thank prof. Gabriel BILLON for his friendly and practical help. I am also grateful to David DUMOULIN for his immense help and advice in the organic synthesis and analysis. This work would not be possible without the technical assistance in the laboratory including Romain DESCHAMPS for his assistance in sampling and analysis and Christine GRARE for her effective and technical help. I wish to thank all the assistant professors in the Marine Chemistry group including, Sopheak NET, Ludovic LESVEN and Justine CRIQUET. I also appreciate the friendly and the scientific ambience created by the colleagues in the laboratory including Racha Osmani, Mariam hamzeh, Beatriz Lourino-Cabana, Emilie Prygiel, Suzannah Rabodonirina, Pierre-Jean superville, Josselin Gorny, Oscar Aladdin, Eric Foto and also the new colleagues for this year, Inès, Anastasia and Tudor.

I want to thank Sopheak and Racha whom I shared the same office and spent almost three years of family like ambience. Also, I would like to express my sincere gratitude to Catherine Ouddane who welcomed me from my first day in France. I sincerely thank her for her support, concern, advice and encouragement.

Special gratitude to my friends outside the laboratory particularly Farah Kawtharani who works in the same building as I (C8), so I got the chance to let out the work pressure during the end of the day through simple talking, support and encouragement. I also want to thank Rania Badr who is lodged with me in the same student residence, for her motivations and support.

Finally, I would like to express my sincere gratitude to my parents, my two brothers and my sister for their patience, huge support and ultimate loving and caring.

---

# TABLE OF CONTENTS

---

*Résumé*

*Abstract*

ABBREVIATIONS

LIST OF FIGURES

LIST OF TABLES

**Introduction générale..... 1**

**General introduction..... 5**

**Chapter A: Mercury measurement based on solid phase extraction methods,  
Introduction to the biogeochemical behavior of mercury in the  
environment. .... 8**

**Part I: Different analytical methods for measurement of mercury based  
preconcentration principle ..... 9**

**A.I.1. Introduction..... 9**

**A.I.2. Solid phase extraction..... 9**

**A.I.2.1. Conventional adsorbents used in solid phase extraction ..... 11**

*A.I.2.1.1.a. Surface silica modification..... 13*

*A.I.2.1.1.b. Modified silica sorbent..... 14*

*A.I.2.1.2. Various adsorbents used in solid phase extraction of metals ..... 15*

*A.I.2.2. Innovative-new sorbents for solid phase extraction of metals..... 19*

*A.I.2.2.a Surfactant-modified sorbent ..... 19*

*A.I.2.2.b. Immunoassay extraction..... 20*

*A.I.2.2.c. Aptamer based molecular recognition sorbent ..... 20*

*A.I.2.2.d. Carbon nanotubes..... 21*

*A.I.2.2.e. Nano-sized material..... 21*

**A.I.3. Mercury speciation using solid phase extraction..... 24**

**Part II: Biogeochemical behaviour and different transformation of mercury  
in the aquatic environment..... 30**

**A.II.1. Mercury sources ..... 30**

**A.II.2. Mercury exposures..... 31**

**A.II.3. Global Mercury cycle..... 36**

*A.II.3.1. Atmospheric depositions..... 36*

*A.II.3.2. Terrestrial surface-air mercury cycle..... 38*

*A.II.3.3. Freshwater-air mercury cycle ..... 39*

*A.II.3.4. Air-Ocean mercury cycle..... 40*

**A.II.4. Biogeochemical behavior of mercury species in the aquatic  
environments..... 42**

<i>A.II.4.1. Biogeochemical factors affecting mercury methylation</i> .....	44
<b>Refereneecs</b> .....	<b>47</b>
<b>Chapter B: Experimental methods</b> .....	<b>63</b>
<b>Part I: Analytical method development for the determination of mercury in water matrix</b> .....	<b>66</b>
<i>B.I.1. Reagents</i> .....	66
<i>B.I.2. Analytical instruments</i> .....	66
<i>B.I.3. Water sampling for optimization and application studies</i> .....	69
<i>B.I.4.Synthesis of 8-hydroxyquinoline grafted silica gel</i> .....	71
<i>B.I.4.1. Preparation of the hydroxyquinoline functionalized silica gels</i> .....	71
<i>B.I.4.2. Preconcentration procedure using the synthesized chelating resins</i> .....	74
<i>B.I.4.3. Preconcentration procedure using the 5-phenylazo-8-hydroxyquinoline</i> .....	75
<b>B.I.5. Preconcentration strategy using direct addition of reagent to the sample</b> .....	<b>76</b>
<i>B.I.5.1. Preconcentration strategy using the direct addition of 8-hydroxyquinoline to the sample</i> .....	76
<i>B.I.5.2. Preconcentration strategy using the direct addition of iodide and cationic surfactant to the sample</i> .....	77
<b>B.I.6. Batch sorption experiments</b> .....	<b>78</b>
<i>B.I.6.1. Adsorption experiments</i> .....	79
<i>B.I.6.2. Kinetics studies</i> .....	80
<i>B.I.6.3. Adsorption isotherms</i> .....	80
<b>Part II: Biogeochemistry behavior of mercury in aquatic environments</b> ....	<b>82</b>
<i>B.II.1. Study sites</i> .....	82
<i>B.II.1.1.The Deûle river</i> .....	83
<i>B.II.1.2. The Lys river</i> .....	83
<i>B.II.2. Field sampling and sediment processing</i> .....	84
<i>B.II.3. Analysis of mercury species</i> .....	85
<i>B.II.3.1. Mercury species determination in sediments</i> .....	85
<i>B.II.3.2. Total mercury in sediments</i> .....	86
<i>B.II.3.3. Methylmercury in sediments</i> .....	87
<i>B.II.3.4. Dissolved mercury</i> .....	88
<i>B.II.4. Ancillary measurements</i> .....	88
<i>B.II.4.1.Sulfides in sediments</i> .....	88
<i>B.II.4.2. Organic carbon in sediments</i> .....	89
<b>References</b> .....	<b>90</b>
<b>Chapter C: Evaluation of different chelating resins for mercury extraction</b>	<b>92</b>
<b>Résumé</b> .....	<b>93</b>
<b>Summary</b> .....	<b>94</b>

<b>DEVELOPMENT AND EVALUATION OF DIFFERENT CHELATING RESINS BASED ON 8-HYDROXYQUINOLINE FOR THE SOLID PHASE EXTRACTION OF Hg(II) FROM WATER MATRIX .....</b>	<b>95</b>
<b>C.1. Abstract .....</b>	<b>96</b>
<b>C.2. Introduction .....</b>	<b>96</b>
<b>C.3. Experimental procedure .....</b>	<b>100</b>
<i>C.3.1. Instrumentation.....</i>	<i>100</i>
<i>C.3.2. Reagents .....</i>	<i>101</i>
<i>C.3.3. Preconcentration procedure using column method .....</i>	<i>101</i>
<i>C.3.3.1. Preconcentration strategy using direct addition of reagent to the sample ..</i>	<i>101</i>
<i>C.3.3.2. Preparation of the hydroxyquinoline functionalized silica gels.....</i>	<i>101</i>
<b>C.4. Results and discussion.....</b>	<b>104</b>
<i>C.4.1. Optimization direct addition method .....</i>	<i>104</i>
<i>C.4.1.1. Effect of pH.....</i>	<i>104</i>
<i>B.4.1.2. Effect of flowrate of the sample and the eluent.....</i>	<i>106</i>
<i>B.4.1.3. Effect of ligand and eluent concentration.....</i>	<i>106</i>
<i>B.4.1.4. Adsorption capacity.....</i>	<i>107</i>
<i>B.4.1.5. Breakthrough volume and real samples applications .....</i>	<i>107</i>
<i>B.4.1.6. Selectivity and Interferences studies.....</i>	<i>107</i>
<i>B.4.2. Silica functionalized-8-hydroxyquinoline.....</i>	<i>109</i>
<i>B.4.2.1. Immobilization of 8-HQ according to method 1 .....</i>	<i>109</i>
<i>B.4.2.2. Immobilization of 8-HQ according method 2.....</i>	<i>110</i>
<i>B.4.2.3. Immobilization 8-HQ according to method 3.....</i>	<i>111</i>
<i>B.4.2.4. Immobilization of 8-HQ according to method 4 .....</i>	<i>112</i>
<i>B.4.2.5. Immobilization of 8-HQ according to method 5 .....</i>	<i>113</i>
<i>B.4.2.6. Immobilization of 8-HQ according to method 6 .....</i>	<i>114</i>
<b>B.5. Conclusion .....</b>	<b>114</b>
<b>B.6. References.....</b>	<b>115</b>
<b><i>Chapter D: Analytical method development for the measurement of Hg(II) by solid phase extraction onto chelating resin.....</i></b>	<b><i>117</i></b>
<b>Résumé.....</b>	<b>118</b>
<b>Summary .....</b>	<b>120</b>
<b>SOLID PHASE EXTRACTION OF INORGANIC MERCURY USING 5-PHENYLAZO-8-HYDROXYQUINOLINE AND DETERMINATION BY COLD VAPOR FLUORESCENCE SPECTROSCOPY IN NATURAL WATER SAMPLES .....</b>	<b>121</b>
<b>D.1. Abstract .....</b>	<b>122</b>
<b>D.2. Introduction .....</b>	<b>122</b>
<b>D.3. Materials and methods.....</b>	<b>124</b>

D.3.1. Chemicals and materials .....	124
D.3.1.1. Reagents and apparatus .....	124
D.3.2. 5Ph8HQ synthesis .....	125
D.3.3. Adsorption experiments.....	126
D.3.4. Kinetics studies.....	127
D.3.5. Adsorption isotherms .....	128
D.3.6. Preconcentration study .....	128
<b>D.4. Results and discussion.....</b>	<b>129</b>
D.4.1. Effect of pH.....	129
D.4.2. Adsorption dynamics .....	132
D.4.3. Competitive adsorption .....	137
D.4.3.1. Multi-element mixture .....	137
D.4.3.2. Binary and single metal-solution.....	137
D.4.4. Adsorption isotherms .....	139
D.4.5.1. Flow rate optimization .....	142
D.4.5.2. Eluent type and volume optimization .....	143
D.4.5.3. Interferences.....	145
D.4.5.4. Breakthrough volume .....	146
D.4.5.5. Analytical performance and applications .....	146
<b>D.5. Conclusion.....</b>	<b>148</b>
<b>D.6. References .....</b>	<b>150</b>
<b>Chapter E: Analytical method development for the measurement of Hg(II) by direct complexation and subsequent solid phase extraction.....</b>	<b>154</b>
<b>Résumé.....</b>	<b>155</b>
<b>Summary .....</b>	<b>157</b>
<b>PRECONCENTRATION OF TOTAL MERCURY IN RIVER WATER BY ANION EXCHANGE MECHANISM.....</b>	<b>159</b>
<b>Abstract.....</b>	<b>161</b>
<b>Introduction.....</b>	<b>161</b>
<b>Experimental.....</b>	<b>162</b>
<i>Reagents and apparatus</i> .....	162
<i>General extraction procedure</i> .....	162
<b>Results and discussion.....</b>	<b>162</b>
<i>Effect of pH</i> .....	162
<i>Effect of flowrate</i> .....	162
<i>Effect of the eluent type and volume</i> .....	163
<i>Ion pair formation</i> .....	163
<i>Effect of coexisting interferences</i> .....	163
<i>Adsorption capacity</i> .....	165
<i>Breakthrough volume</i> .....	165

<i>Analytical performances and application</i> .....	165
<i>Comparison with other SPE Hg(II) method</i> .....	166
<b>Conclusion</b> .....	<b>166</b>
<b>References</b> .....	<b>166</b>
<b>Chapter F: Mercury distribution, speciation and transport in the aquatic environment</b> .....	<b>167</b>
<b>Résumé</b> .....	<b>168</b>
<b>Summary</b> .....	<b>170</b>
<b>BIOGEOCHEMICAL FACTORS AFFECTING THE DISTRIBUTION, SPECIATION AND TRANSPORT OF Hg SPECIES IN THE DEÛLE AND LYS RIVERS</b> .....	<b>172</b>
<b>F.1. Abstract</b> .....	<b>173</b>
<b>F.2. Introduction</b> .....	<b>173</b>
<b>F.3. Methods and Materials</b> .....	<b>175</b>
<i>F.3.1. Field sampling and sediment processing</i> .....	175
<i>F.3.2. Analysis of mercury species</i> .....	176
<i>F.3.3. Ancillary measurements</i> .....	178
<b>F.4. Results and discussion</b> .....	<b>179</b>
<i>F.4.1. Spatial distribution of HgT and MeHg</i> .....	179
<i>F.4.2. Sulfide and organic carbon distribution</i> .....	183
<i>F.4.3. Effects of geochemical factors on sedimentary Hg species</i> .....	184
<i>F.4.4. Spatial distribution dissolved and particulate HgT in water column</i> .....	193
<i>F.4.5. Porewater distribution</i> .....	196
<i>F.4.6. Controls of mercury porewater</i> .....	198
<i>F.4.7. Mercury partitioning <math>K_D</math></i> .....	202
<i>F.4.8. Estimated sediment-water flux of HgT</i> .....	203
<b>F.5. Conclusion</b> .....	<b>204</b>
<b>Chapter G: Conclusion and perspectives</b> .....	<b>213</b>
<b>Conclusion générale</b> .....	<b>214</b>
<b>General conclusion</b> .....	<b>217</b>
<b>ANNEXES</b> .....	<b>219</b>

## ***Résumé***

Le mercure est un élément omniprésent dans l'environnement et considéré comme un polluant mondial en raison de sa longue portée de transport atmosphérique et de son cycle biogéochimique complexe. Le mercure est parmi les polluants environnementaux les plus dangereux, conféré par sa forme organique, le méthylmercure ( $\text{CH}_3\text{Hg}$  ou MeHg). Le méthylmercure est l'espèce la plus toxiques du mercure, en raison de son caractère bio-accumulatif dans les organismes vivants tout au long de la chaîne alimentaire. Dans les eaux naturelles, le mercure est présent à de très faibles concentrations. Pour cette raison, un grand nombre de techniques analytiques ne permettent pas la mesure directe, ce qui nécessite souvent une étape de préconcentration pour atteindre la limite de détection. Parmi les nombreuses méthodes de préconcentration, l'extraction en phase solide (SPE) est la plus utilisé pour l'extraction de métaux traces. La première partie de cette étude est axée sur le développement des méthodes analytiques pour la mesure du mercure par extraction en phase solide. A la recherche des méthodes d'analyse simples, rapides et peu couteuses pour la détermination du mercure dans les eaux naturelles, deux méthodes analytiques ont été développées. Une technique basée sur le mécanisme d'échange d'anions en utilisant l'ICP-MS (Inductively Coupled Plasma Mass Spectrometry) a été développée. Une autre basée sur l'extraction en phase solide de mercure en utilisant le 5-phenylazo-8-hydroxyquinoline et la détection par CV-AFS (Cold Vapor Atomic Fluorescence Spectroscopy) a été mise au point. La deuxième partie de ce travail est consacrée à l'étude de la distribution et du comportement biogéochimique du mercure dans les rivières Deûle et Lys (Nord de France). Les résultats obtenus montrent des concentrations élevées en mercure total (HgT) dans la Deûle, site contaminé principalement par les activités de l'ancienne fonderie "Metaleurop", les concentrations mesurées dans la Lys sont beaucoup plus faibles. Bien que les sédiments de la Deûle soient très chargés par le mercure total (HgT) par rapport aux sédiments de la Lys, des pourcentages de méthylmercure (% MeHg) beaucoup plus élevés ont été trouvés dans la Lys. Les particules en suspension sont la principale phase porteuse du mercure et considérée comme le véhicule de la pollution de la Deûle vers la Lys. Malgré l'arrêt de l'ancienne fonderie "Metaleurop" depuis près d'une décennie, les niveaux de mercure restent encore trop élevés dans la Deûle.

***Mots Clés :*** mercure, méthylmercure, eau, sédiment, biogéochimie.



## ***Abstract***

Mercury is a very particular element conferred by its high density and vapor pressure. It is an ubiquitous element in the environment and considered as a global pollutant because of its long range atmospheric transport and its complex biogeochemical cycle. Mercury is among the most hazardous environmental pollutants, given by its organic form, methylmercury (MeHg or CH<sub>3</sub>Hg). Methylmercury is the most toxic species of mercury, because of its bio-accumulative character in living organisms throughout the food web. In natural waters, mercury is present at very low concentrations. For this reason, most analytical techniques do not achieve accurate direct measurement of Hg which necessitates preconcentration to meet their limit of detection. Among many preconcentration methods, solid phase extraction (SPE) is the most used for trace metal extraction. The first part of this study focuses on the development of analytical methods for the measurement of mercury by solid phase extraction. In the search of simple, rapid and cheap analytical methods for the measurement of mercury in natural water samples, two analytical methods have been developed. A technique based on the anion exchange mechanism using ICP-MS (Inductively Coupled Plasma Mass Spectrometry) was developed. Another one has been developed and was based on the solid phase extraction of mercury using 5-phenylazo-8-hydroxyquinoline and detection by CV-AFS (Cold Vapor Atomic Fluorescence Spectroscopy). Part of this work also includes the distribution and biogeochemical behavior of mercury in rivers of the Deûle and Lys (Northern France). The results have showed high concentrations of total mercury (HgT) in the Deûle contaminated by a former smelter "Metaleurop". The concentrations of HgT measured in the Lys are much lower. Although the Deûle sediments are highly burdened with HgT as compared to the Lys sediments, much higher percentage of methylmercury is found in Lys river. Suspended particles are the major Hg carrier phase and transporters of Hg pollution from the Deûle to the Lys river. Despite the fact that the former Metaleurop smelter is closed for almost a decade, mercury levels are still high in the Deûle, creating an Hg hotspot for mercury pollution to surrounding environments carrying Hg hundred kilometers downstream the river possibly reaching the sea.

***Keywords:*** mercury, methylmercury, water, sediment, biogeochemistry.

---

## ABBREVIATIONS

---

**AC** Activated carbon

**APDC** Ammonium Pyrrolidine DithioCarbamate

**APSG** Aminopropyl Silica Gel

**AVS** Acid volatile sulfides

**BPDB** 1,4-bis(4-pyridyl)-2,3-diaza-1,3-butadiene

**Bw** Body Weight

**Ce** Concentration at equilibrium

**C<sub>i</sub>/C<sub>0</sub>** Initial concentration

**C<sub>org</sub>** Organic carbon

**CRS** Chromium reducible sulfides

**C<sub>18</sub>** Octadecyl silica phase

**CMC** Micellar Concentration

**CNT** Carbon nanotubes

**CPG-HQ** Hydroxyquiniline Immobilized on Controlled Pore Glass

**CS(NH<sub>2</sub>)<sub>2</sub>** Thiourea

**CV-AAS** Cold vapor-Atomic Absorption Spectrometry

**CV-AFS** Cold vapor-Atomic Fluorescence Spectrometry

**D-R model** Dubinin-Radushkevich model

**DDTP** Dithiophosphoric acid diacyl ester

**DOC** Dissolved organic matter

**DT** Detection technique

**DTAB** DodecylTrimethylAmmonium Chloride

**FeRB** Iron Reducing Bacteria

**FI** Flow injection

**FT-IR** Fourier Transform Infrared Spectroscopy

**GC** Gas Chromatography

**Hg** mercury

**Hg(II)/Hg<sup>2+</sup>/IHg** Inorganic mercury

**Hg<sup>0</sup>** Volatile mercury

**CH<sub>3</sub>Hg<sup>+</sup>/CH<sub>3</sub>Hg(I)/MeHg** Methylmercury

**(CH<sub>3</sub>)<sub>2</sub>Hg/DMHg** Dimethyl mercury

**HgT** Total mercury

**HgT<sub>PW</sub>** Total mercury in porewater

**HgT<sub>S</sub>** Total mercury in solid phase

**HgT<sub>D</sub>** Dissolved mercury in surface water

**HgT<sub>P</sub>** Particulate mercury

**HPLC** High Performance Liquid Chromatography

**8-HQ** 8-Hydroxyquinoline

**5Ph8HQ** 5-PhenylAzo-8-Hydroxyquinoline

**I** Iodide

**IIP** Ionic Imprinted Polymers

**ICP-AES** Inductively Coupled Plasma- Atomic Emission Spectrometry

**ICP-MS** Inductively Coupled Plasma-Mass spectrometry

**ITMS** Ion Trap Mass Spectrometry

**IUPAC** International Union of Pure and Applied Chemistry

**K<sub>D</sub>** Partition coefficient between solid and aqueous phases

**K<sub>d</sub>** Distribution coefficient

**K<sub>f</sub>** Freundlich constant

**K<sub>L</sub>** Langmuir equilibrium constant

**LLE** Liquid-Liquid Extraction

**LOD** Limit of detection

**LogK/LogB** Stability constant

**MIP** Molecular imprinted polymers

**MIP** Microwave induced plasma

**Mg** Mega Gram

**MWCNTs** Multi-wall carbon nanotubes

**NPs** Nanoparticles

**PCR** Polymerase chain reaction

**PF** Preconcentration factor

**PGC** Porous graphitized carbon

**pKa** Acid dissociation constant

**ε Polanyi** potential

**PTFE** Polytetrafluoroethylene

**PUF** Polyurethane Foam

**PVC** PolyVinyl Chloride

**CS-DVB** Copo(styrene-divinyl benzene)  
**Q** Adsorption capacity  
**Q<sub>e</sub>** Amount adsorbed at equilibrium  
**Q<sub>t</sub>** Amount adsorbed at time t  
**Q<sub>m</sub>** Maximum Langmuir uptake  
**R/Ref** Reference  
**R<sup>2</sup>** Correlation coefficient  
**RfD** Reference Dose  
**RGM** Reactive Gaseous Mercury  
**R<sub>L</sub>** Separation factor  
**r.p.m** Round per minute  
**RSD** Relative Standard Deviation  
**S(-II)/S<sup>-2</sup>** Sulfides  
**α** Selectivity Coefficient  
**SDS** Sodium Dodecyl Sulfate  
**S-DVB** Styrene-DivinylBenzene  
**Si-8-HQ** 8-Hydroxyquinoline Immobilized on Silica gel  
**Sil-8-HQ** 8-Hydroxyquinoline Immobilized on Silicone Tubes  
**SMS** Surfactant-modified sorbent  
**SPE** Solid Phase Extraction  
**SRB** Sulfate Reducing Bacteria  
**ST** Separation Technique  
**t<sub>1/2</sub>** Half time sorption  
**TGM** Total gaseous mercury  
**TSS** Total suspended solids

---

## LIST OF FIGURES

---

### CHAPTER A

<b>Figure A.I.1.</b> Different types of solid supports used in the solid phase extraction of metals. <b>12</b>
<b>Figure A.I.2.</b> Silica surface modification by different processes. .... <b>14</b>
<b>Figure A.I.3.</b> Schematic drawing of mercury extraction using mercury-specific aptamer (Wang and Liu, 2008). .... <b>21</b>
<b>Figure A.I.4.</b> Schematic figure of metal extraction using Fe <sub>3</sub> O <sub>4</sub> magnetic nanoparticles. .... <b>22</b>
<b>Figure A.I.5.</b> Schematic drawing IIP-T selective for the extraction of mercury ions (Xu et al 2012)..... <b>23</b>
<b>Figure A.II.1.</b> Bio-magnification of MeHg through a tropical estuarine food chain (Kehrig, 2011)..... <b>33</b>
<b>Figure A.II.2.</b> Hg biogeochemical cycle, an example in the Gulf of Mexico (Harris et al, 2012)..... <b>36</b>

### CHAPTER B

<b>Figure B.1.</b> Different methods used for mercury ions enrichment from water samples. .... <b>64</b>
<b>Figure B.2.</b> (a) Molecular structure of 8-hydroxyquinoline (Arici et al 2005), (b) Hg <sup>2+</sup> -7-formyl-8-hydroxyquinoline complex structure (Asmy et al 1990). .... <b>65</b>
<b>Figure B.I.1.</b> Studied 8-hydroxyquinoline modified silica gels. .... <b>71</b>
<b>Scheme B.I.1.</b> Preparation of phenylazo-8-hydroxyquinoline silica gel 1. .... <b>72</b>
<b>Scheme B.I.2.</b> Preparation of amino-immobilized 8-HQ silica gel 2. .... <b>73</b>
<b>Scheme B.I.3.</b> Preparation of imino-immobilized 8-HQ silica gels 3a and 3b. .... <b>74</b>
<b>Scheme B.I.4.</b> Preparation of amino-immobilized 8-HQ silica gels 4 and 2..... <b>74</b>
<b>Scheme B.I.5.</b> Preparation of imino-immobilized 8-HQ silica gel 5. .... <b>75</b>
<b>Figure B.I.2.</b> Experimental protocols used for the examination of the efficiency 8-HQ based chelating resins for mercury extraction. .... <b>76</b>
<b>Figure B.I.3.</b> Experimental procedure for the solid phase extraction of mercury ions using 5Ph8HQ as chelating resin and CV-AFS as analytical technique..... <b>77</b>
<b>Figure B.I.4.</b> Method optimization of the direct addition of 8-HQ to water samples. .... <b>78</b>
<b>Figure B.I.5.</b> Experimental procedure for the extraction of mercury ions from river water based on I <sup>-</sup> /DTAB/SiO <sub>2</sub> system. .... <b>79</b>
<b>Figure B.I.6.</b> Adsorption dynamics studies of mercury ions on 5-phenylazo-8-hydroxyquinoline using batch experiment mode..... <b>78</b>

<b>Figure B.II.1.</b> Sampling sites in Deûle and Lys Rivers. ....	<b>83</b>
<b>Figure B.II.2.</b> Sampling and processing of sediment cores. ....	<b>85</b>
<b>Figure B.II.3.</b> Schematic diagram of AMA-254 (Costley et al 2000). ....	<b>88</b>

## CHAPTER C

<b>Figure C.1.</b> Studied 8-hydroxyquinoline modified silica gels .....	<b>101</b>
<b>Figure C.2.</b> (a) Effect of solution's acidity on Hg(II) retention . Conditions: concentration of Hg(II): 0.2 µg/mL, sample flowrate: 2 mL/min, elution: 10 mL/HNO <sub>3</sub> (2 M)/ 0.5 mL/min, Concentration 8-HQ: 5×10 <sup>-4</sup> mol/L. (b) Effect of sample flowrate on Hg(II) recovery. Conditions: concentration of Hg(II): 0.2 µg/mL, pH 4, elution: 10 mL/HNO <sub>3</sub> (2 M)/0.5 mL/min, concentration 8-HQ: 5×10 <sup>-4</sup> mol/L (c) Effect of 8-HQ concentration on the retention of Hg(II). Conditions: concentration of Hg(II): 0.2 µg/mL, pH 4, sample flowrate: 2 mL/min, elution: 10 mL/HNO <sub>3</sub> (2 M)/ 0.5 mol/min (d) Effect of nitric acid concentration on the recovery of Hg(II) ions. Conditions: concentration of Hg(II): 0.2 µg/mL, pH 4, sample flowrate: 2 mL/min, concentration 8-HQ: 5×10 <sup>-4</sup> mol/L, elution: 10 mL HNO <sub>3</sub> /0.5 mL/min. (e) Adsorption isotherm. Conditions: pH 4, sample flowrate: 2 mL/min, concentration 8-HQ: 5×10 <sup>-4</sup> mol/L, elution: 10 ml/HNO <sub>3</sub> (4 M)/0.5 mL/min. (f) Breakthrough volume. Conditions: 10 µg Hg(II)/sample volume, pH 4, sample flowrate: 2 mL/min, concentration 8-HQ: 5×10 <sup>-4</sup> mol/L, elution: 10 mL/HNO <sub>3</sub> (4 M)/ 0.5 mL/min. ....	<b>106</b>
<b>Figure C.3.</b> Study of 8-hydroxyquinoline selectivity towards Hg(II) ions. Conditions: concentration of Hg(II): 0.2 µg/mL, pH 4, sample flow rate: 2 mL/min, concentration: 8-HQ: 5 ×10 <sup>-4</sup> mol/L, eluent: 10 mL nitric acid (4 M)/0.5mL/min. ....	<b>109</b>
<b>Figure C.4</b> (a) Effect of pH variation on Hg(II) ions recovery. Conditions: River water, concentration of Hg(II): 0.2 µg/mL, flow rate: 2 mL/min, 300 mg of 8-HQ immobilized on silica gel (1), elution: 10 mL/5 M HCl 5% CS(NH <sub>2</sub> ) <sub>2</sub> / 0.5 mL/min. (b) Effect of pH variation on Hg(II) extraction. Conditions: River water, concentration of Hg(II): 0.2 µg/mL, flow rate: 2 mL/min, 300 mg of 8-HQ immobilized on silica gel (2), elution: 10 mL/2 M HCl 1 M HNO <sub>3</sub> / 0.5 mL/min. (c) Effect of pH variations on Hg(II) retention. Conditions: River water, concentration of Hg(II): 0.2 µg/mL, flow rate: 2 mL/min, 300 mg of 8-HQ immobilized on silica gel (3), elution:10 mL/ 2 M HNO <sub>3</sub> / 0.5 mL/min. (d) Effect of pH variations on Hg(II) ions extraction. Conditions: river water, concentration of Hg(II): 0.2 µg/mL, flow rate: 2 mL/min, 300 mg of 8-HQ immobilized on silica gel (4), elution: 10 mL/2 M HCl 1 M HNO <sub>3</sub> / 0.5 mL/min. (e) Effect of pH variation on the retention of Hg(II) ions. Conditions: river water, concentration of Hg(II): 0.2 µg/mL, flow rate: 2 mL/min, 300 mg of 8-HQ immobilized on silica gel (5), elution:10 mL/ 5 M HNO <sub>3</sub> / 0.5 mL/min. (f) Effect of pH variation on the retention of Hg(II) ions. Conditions: River water, concentration of Hg(II): 0.2 µg/mL, flow rate: 2 mL/min, 300 mg of 8-HQ immobilized on silica gel (physical bonding; resin (6)), elution: 10 mL/2 M HCl 1 M HNO <sub>3</sub> / 0.5 mL/min. ....	<b>111</b>
<b>Figure C.5.</b> Effect of eluent type on the desorption of Hg(II) ions. Conditions: River water, concentration of Hg(II): 0.2 µg/mL, flow rate: 2 mL/min, 300 mg of 8-HQ immobilized on silica gel, elution:10 mL/ 0.5 mL/min. ....	<b>112</b>

**Figure C.6.** Effect of adsorbent amount on the recovery of Hg(II) ions. Conditions: River water, concentration of Hg(II): 0.2 µg/mL, flow rate: 2 mL/min, elution: 10 mL/2 M HCl 1 M HNO<sub>3</sub>/0.5 mL/min. .... 113

**Figure C.7.** Effect of adsorbent amount on the recovery of Hg(II) ions. Conditions: River water, concentration of Hg(II): 0.2 µg/mL, flow rate: 2 mL/min, elution: 10 mL/2 M HCl 1 M HNO<sub>3</sub>/0.5 mL/min. .... 114

## CHAPTER D

**Figure D.1.** Effect of pH variation on the adsorption of metals. Conditions: Volume 200 mL, m(5Ph8HQ): 1g, [M<sup>+</sup>]: 1 µg/mL in single metal solution. Bars represent standard deviation for two replicates. .... 113

**Figure D.2.** Recovery percentage of metals as function of time in a single metal solution. Conditions: V (200 mL), m(5Ph8HQ)=1 g, element optimized pH, [M<sup>+</sup>]= 1µg/mL..... 134

**Figure D.3.** Adsorption kinetics of Hg(II) according to (a) pseudo first order model, (b) pseudo second order model, (c) intra particlar diffusion; [Hg(II)]: 0.005 mmol/L, V(200 mL), pH 4, m(5Ph8HQ): 1g. Adsorption isotherms of Hg(II) by 5Ph8HQ according to (d) Langmuir adsorption model, (e) Freundlich adsorption model, (f) Dubinin-Radushkevich adsorption model; [Hg(II)]: 10-160 µg/mL, V(50 mL), pH 4, m(5Ph8HQ): 1g..... 141

**Figure D.4.** Adsorption profile of Hg(II) as a function of increasing metal concentration. Conditions: [Hg(II)]: 10-160 µg/mL, V(50 mL), pH 4, m(5Ph8HQ): 1g. .... 143

**Figure D.5.** Effect of flowrate mercury by 5Ph8HQ column extraction. Conditions: [Hg(II)]: 2 ng/mL, V(50 mL), pH: 4, eluent: 5 M HCl + 5% CS(NH<sub>2</sub>)<sub>2</sub>/10 mL. Bars represent standard deviation for two replicates. .... 144

**Figure D.6.** Elution recovery of Hg(II) adsorbed on 5Ph8HQ by column method using different types of eluents. Conditions: [Hg(II)]: 2 ng/mL, V(50 mL), pH: 4, eluent volume: 10 mL. Bars represent standard deviation for two replicates. .... 145

**Figure D.7.** Effect of eluent volume on the recovery of Hg(II) adsorbed on 5Ph8HQ by column method. Conditions: [Hg(II)]: 2 ng/mL, V(50 mL), pH: 4, eluent: 5 M HCl + 5% CS(NH<sub>2</sub>)<sub>2</sub>/ 1 M HCl + 2% CS(NH<sub>2</sub>)<sub>2</sub> . Bars represent standard deviation for two replicates. .... 146

## CHAPTER E

**Figure E.1.** Effect of pH on the retention of [HgI<sub>4</sub><sup>2-</sup>][DTA<sup>+</sup>] on silica gel. Conditions: 2 µg Hg(II)/50 mL, flow rate 2 mL min<sup>-1</sup>, [I] 0.01 mol.L<sup>-1</sup>,[DTAB]: 0.0005 mol L<sup>-1</sup>, [HNO<sub>3</sub>]:10 mL/4 mol L<sup>-1</sup>/0.5 mL min<sup>-1</sup> ..... 162

**Figure E.2.** Effect of flowrate on the retention of [HgI<sub>4</sub><sup>2-</sup>][DTA<sup>+</sup>] on silica gel. Conditions: 2 µg Hg(II)/50 mL, pH: 4, [I] 0.01 mol L<sup>-1</sup>, [DTAB]: 0.0005 mol L<sup>-1</sup>, [HNO<sub>3</sub>]: 10 mL/ 4 mol L<sup>-1</sup>/0.5 mL min<sup>-1</sup> ..... 163

<b>Figure E.3.</b> Effect HNO <sub>3</sub> volume on the desorption Hg(II) ions from silica phase. Conditions: 2 µg Hg(II)/50 mL, pH 4, flow rate 2 mL min <sup>-1</sup> , [I <sup>-</sup> ] 0.01 mol L <sup>-1</sup> , [DTAB] 0.0005 mol L <sup>-1</sup> , [HNO <sub>3</sub> ]: 8 mol L <sup>-1</sup> /0.5 mL min <sup>-1</sup> .....	<b>163</b>
<b>Figure E.4.</b> Effect iodide concentration on the adsorption of [HgI <sub>4</sub> <sup>2-</sup> ][DTA <sup>+</sup> ] Hg(II) on silica phase. Conditions: 2 µg Hg(II)/50 mL, pH 4, flow rate 2 mL min <sup>-1</sup> , [DTAB]: 0.0005 mol L <sup>-1</sup> , [HNO <sub>3</sub> ]: 10 mL/8 mol L <sup>-1</sup> /0.5 mL min <sup>-1</sup> .....	<b>164</b>
<b>Figure E.5.</b> Effect DTAB concentration on the adsorption of [HgI <sub>4</sub> <sup>2-</sup> ][DTA <sup>+</sup> ] on silica phase. Conditions: 2 µg Hg(II)/50 mL, pH: 4, flow rate 2 mL min <sup>-1</sup> , [I <sup>-</sup> ] 0.01 mol L <sup>-1</sup> , [HNO <sub>3</sub> ]: 10mL/8 mol L <sup>-1</sup> /0.5 mL min <sup>-1</sup> .....	<b>164</b>
<b>Figure E.6.</b> Maximum adsorption capacity of 1 g silica phase. Conditions: pH: 4, flow rate 2 mL min <sup>-1</sup> , [I <sup>-</sup> ] 0.01 mol L <sup>-1</sup> , [DTAB]: 0.0005 mol L <sup>-1</sup> , [HNO <sub>3</sub> ]: 10 mL/8 mol L <sup>-1</sup> /0.5 mL min <sup>-1</sup> .....	<b>165</b>
<b>Figure E.7.</b> Effect of sample volume on the retention of [HgI <sub>4</sub> <sup>2-</sup> ][DTA <sup>+</sup> ] on silica gel. Conditions: 2 µg Hg(II)/V mL, pH: 4, flow rate 2 mL min <sup>-1</sup> , [I <sup>-</sup> ] 0.01 mol L <sup>-1</sup> , [DTAB]: 0.0005 mol L <sup>-1</sup> , [HNO <sub>3</sub> ]: 10 mL/8 mol L <sup>-1</sup> /0.5mL min <sup>-1</sup> .....	<b>165</b>

**CHAPTER F**

<b>Figure F.1.</b> Sampling sites in Deûle and Lys rivers .....	<b>177</b>
<b>Figure F.2.</b> Sediment depth profiles of Hg species and geochemical determinants in D-A, D-B, L-C and L-D .....	<b>181</b>
<b>Figure F.3.</b> Correlation between percentage organic carbon (% Corg) and percentage methylmercury formation (% MeHg) in Deûle site (D-A and D-B) .....	<b>186</b>
<b>Figure F.4.</b> Associations between acid volatile sulfides (AVS) and percentage of methylmercury formation (% MeHg) in Deûle sites (D-A and D-B) .....	<b>187</b>
<b>Figure F.5.</b> Correlations between chromium reactive sulfides (CRS) and percentage of methylmercury formation (% MeHg) in Deûle sites (D-A and D-B) .....	<b>188</b>
<b>Figure F.6.</b> Correlations between acid volatile sulfides (AVS) and percentage of methylmercury formation (% MeHg) in Lys sites (L-C and L-D).....	<b>189</b>
<b>Figure F.7.</b> Correlations between percentage of organic carbon (% Corg) and percentage of methylmercury (% MeHg) formation in Lys sites (L-C and L-D).....	<b>190</b>
<b>Figure F.8.</b> Correlation between percentage of organic carbon (% Corg) and percentage of methylmercury formation (% MeHg) in all sites (D-A, D-B, L-C & L-D) .....	<b>192</b>
<b>Figure F.9.</b> Correlation between percentage of organic carbon (% Corg) and acid volatile sulfides (AVS) in all sites (D-A, D-B, L-C & L-D).....	<b>193</b>



---

## LIST OF TABLES

---

### CHAPTER A

<b>Table A.I.1.</b> Analytical methods for the measurement of Hg(II) using different types of sorbents.....	<b>19</b>
<b>Table A.I.2.</b> Chromatographic speciation of mercury.....	<b>26</b>
<b>Table A.I.3.</b> Non-chromatographic speciation of mercury .....	<b>28</b>
<b>Table A.II.1.</b> Hg concentrations in water and sediments of the world's largest Hg mines .....	<b>31</b>
<b>Table A.II.2.</b> Worldwide distribution of HgT and MeHg concentrations in muscle tissues of various fish species.....	<b>35</b>
<b>Table A.II.3.</b> Concentration of Hg in open ocean and seawater from around the world.....	<b>40</b>

### CHAPTER B

<b>Table B.I.1.</b> Operating conditions ICP-MS.....	<b>68</b>
<b>Table B.I.2.</b> Deûle water chemical characteristics (Lesven et al 2009; Pygriél, 2013).....	<b>70</b>
<b>Table B.I.3.</b> Drinking water quality limits (CODE DE LA SANTE PUBLIQUE FRANCAISE) .....	<b>70</b>
<b>Table B.II.1.</b> Principal characteristics of Lys and Deûle rivers.....	<b>84</b>

### CHAPTER C

<b>Table C.1.</b> Efficiency of three types of 8-HQ immobilized silica for the retention of metals.	<b>99</b>
<b>Table C.2.</b> Metal recovery results by the direct addition and the adsorption $M^+$ -ligand on silica phase .....	<b>100</b>
<b>Table C.3.</b> Stability constant metal-8HQ .....	<b>110</b>
<b>Table C.4.</b> Effects of different electrolytes on the retention of Hg(II) ions .....	<b>110</b>
<b>Table C.5.</b> Distribution ratios of metals on 8-HQ functionalized silica gel through position 5 on HQ moiety .....	<b>115</b>

### CHAPTER D

<b>Table D.1.</b> Operating conditions ICP-MS .....	<b>126</b>
<b>Table D.2.</b> Adsorption kinetics of metals in single metal solution.....	<b>137</b>
<b>Table D.3.</b> Adsorption kinetics of metals in multi-element mixture at pH=4 .....	<b>137</b>
<b>Table D.4.</b> Metal distribution coefficient ( $K_d$ ) and separation factor ( $\alpha$ ) at pH 4 in Multi-element mixture.....	<b>138</b>
<b>Table D.5.</b> Selectivity of mercury at pH 4 in Binary mixtures.....	<b>139</b>
<b>Table D.6.</b> Metal ion charge to radius ratio.....	<b>139</b>
<b>Table D.7.</b> Distribution coefficients of metals in single-metal solution at element optimized pH.....	<b>140</b>
<b>Table D.8.</b> Langmuir, Freundlich and D-R isotherm constants of Hg .....	<b>141</b>
<b>Table D.9.</b> Effects of different electrolytes on the retention of Hg(II) ions .....	<b>147</b>
<b>Table D.10.</b> Analytical results for the determination of Hg(II) in natural water samples by CV-AFS.....	<b>148</b>

<b>Table D.11.</b> Simultaneous determination of metals in natural water samples by ICP-MS at pH 4.....	<b>149</b>
<b>Table D.12:</b> Comparison of figures of merits for different preconcentration methods for Hg(II) ion.....	<b>150</b>

## CHAPTER E

<b>Table E.1.</b> Operating conditions ICP-MS .....	<b>162</b>
<b>Table E.2.</b> Effect of different concentrations of eluent on the extraction of mercury.....	<b>163</b>
<b>Table E.3.</b> Ligands tested for Hg(II) extraction .....	<b>163</b>
<b>Table E.4.</b> Stability constant for different ligands at 25 C° and 1(NaClO <sub>4</sub> ) as ionic medium .....	<b>163</b>
<b>Table E.5.</b> Effect of electrolytes on the adsorption of Hg(II).....	<b>164</b>
<b>Table E.6.</b> Metal competition in binary element mixture.....	<b>165</b>
<b>Table E.7.</b> Analytical results for the determination of Hg(II) in natural water samples .....	<b>145</b>
<b>Table E.8.</b> Comparison of figures of merits for different preconcentration methods for Hg(II) ion.....	<b>166</b>

## CHAPTER F

<b>Table F.1.</b> Correlation matrix between mercury species and geochemical determinants from Deûle river (D-A (n=8); D-B (n=7)) and Lys river (L-C and L-D (n=12)) .....	<b>194</b>
<b>Table F.2.</b> Concentrations of mercury species and partition coefficient of HgT in surface water and in sediment phase.....	<b>195</b>



## Introduction générale

Le mercure est un élément très particulier connu par sa densité et pression de vapeur élevée. C'est un élément omniprésent dans l'environnement et considéré comme un polluant mondial en raison de son long porté dans l'atmosphère et de son cycle biogéochimique complexe. En effet, le mercure peut atteindre des zones non contaminées éloignées comme les régions Arctiques pouvant agir comme des puits. Par ailleurs, le mercure est parmi les polluants environnementaux les plus dangereux, conféré par sa forme organique, le méthylmercure ( $\text{CH}_3\text{Hg}$  ou MeHg). Le méthylmercure est l'espèce la plus toxique du mercure, en raison de son caractère bio-accumulatif dans les organismes vivants tout au long de la chaîne alimentaire. Il peut s'accumuler dans les organismes et atteindre des concentrations jusqu'au million de fois plus élevé que les eaux environnantes causant des dommages graves au système nerveux et même des décès.

Il y a deux sources principales de mercure dans l'environnement: naturels et anthropiques. Les activités humaines ont contribué au plus grand flux de mercure dans la biosphère où 50-75% des émissions de mercure sont estimées à partir de sources anthropiques. Lorsque le mercure se trouve dans les compartiments de l'environnement (sol, air, eau, biota) il entre dans un cycle biogéochimique complexe des diverses transformations et dégradations des espèces mercuriels. À cette fin, il est essentiel de suivre et de quantifier le mercure dans les écosystèmes afin d'identifier les principaux facteurs qui régissent sa dynamique et de contrôler sa concentration.

Plusieurs facteurs contrôlent la transformation des espèces de mercuriels. Le carbone organique dissous, les sulfates, les sulfures, le pH, la température, les micro-organismes sont tous des facteurs dépendants contrôlant la méthylation du mercure. La dégradation de méthylmercure est possible photochimiquement, ce mécanisme de dégradation est principalement dominant aux eaux de surface. D'un autre côté, la déméthylation biotique peut régir dans les zones dépourvues de soleil. La mobilité et le transport de mercure en phases aqueuse et solide sont principalement contrôlés par les sulfures, la matière organique, oxyhydroxydes de Fe/Mn, le coefficient de partage entre les phases aqueuse et solide et les activités provoquant des remises en suspension de sédiment (Hammerschmidt et al 2004). Les développements récents dans l'utilisation des traceurs isotopiques de mercure ont fourni de nouveaux outils expérimentaux pour mesurer la réactivité et la dynamique du mercure, y

compris les différentes transformations (méthylation, déméthylation, réduction ...). Ainsi, les différents mécanismes de cycle biogéochimique du mercure et des taux de transformation de Hg peuvent être déterminés. Les environnements pollués par le mercure sont connus comme des zones de méthylation actifs dans lequel le suivi et la détermination des différents taux de méthylation et de déméthylation deviennent indispensables. Le canal de la Deûle est situé au nord de la France, est fortement pollué par le mercure à cause d'une ancienne fonderie de minerai qui était opérationnelle depuis plus d'un siècle et finalement fermé en 2003. L'étude de la distribution de mercure et la spéciation peuvent nous permettre de comprendre les facteurs dominants qui contrôlent le comportement, le transport et le devenir de ce métal dans la Deûle.

Dans les eaux naturelles, le mercure est présent à des concentrations très faibles, entre 0,2 à 100 ng/L. Pour cette raison, un grand nombre de techniques analytiques ne permettent pas la mesure directe et précise du mercure ce qui nécessite une étape de préconcentration pour atteindre les limites de détection. Parmi les nombreuses méthodes de préconcentration, l'extraction en phase solide (SPE) est le plus utilisé pour l'extraction de métaux traces. Il existe deux grandes catégories d'adsorbants utilisés dans l'extraction en phase solide, inorganiques et organiques. Le choix de l'agent de sorption approprié dépend de la nature l'élément cible. De nouveaux adsorbants ont été développés pour permettre une détermination plus précise des métaux traces tels que les polymères ion-imprimés, les nanotubes de carbone, l'extraction immunoassay...ect. Afin d'améliorer la sélectivité de l'adsorbant à un métal particulier, le support solide peut être physiquement ou chimiquement modifié par un composé organique. Différents groupes fonctionnels conférés à un ligand particulier, peuvent être immobilisés sur la surface du support solide pour améliorer la stabilité et la fixation des métaux. Cela permet d'avoir un meilleur rendement d'extraction, une amélioration du facteur de préconcentration et une limite de détection basse. Selon la théorie HSAB, le mercure dissous est considéré comme un acide faible, de ce fait les bases contenant des atomes de soufre et d'azote, forment des complexes métalliques stables. Des ligands contenant des groupes fonctionnels mercapto et/ou azoïques/imino sont les plus utilisés pour former des chélates stables avec le mercure pour être extrait ultérieurement sur un support solide. Un autre procédé, se compose de greffer le ligand sur un support solide, les résines obtenues peuvent être utilisés pour l'extraction des métaux. Pour la détermination de mercure, les ligands les plus utilisés pour la fonctionnalisation de l'adsorbant contiennent des dérivés d'

oxine et thiol et/ou des imino. Différents instruments analytiques sont utilisés en conjonction avec l'extraction du mercure en phase solide, tels que CV-AAS, CV-AFS, ICP-AES, ICP-MS. Le choix de l'instrument analytique approprié dépend de sa disponibilité, le coût et les niveaux de mercure dans la matrice de l'échantillon et la limite de détection.

Au regard des différents éléments et problématiques du mercure présentés dans l'introduction, les principaux objectifs de ce travail sont:

- Evaluation des différentes résines pour l'extraction du Hg(II) et de développer des méthodes analytiques pour la mesure de mercure à l'état de trace dans l'eau.
- Étudier la spéciation et la distribution du mercure dans la rivière Deûle, son transport et son devenir potentiel. Ainsi que la détermination des différents facteurs qui régissent la distribution du mercure.

Le manuscrit de thèse est constitué de sept chapitres. Le premier chapitre est consacré à une étude bibliographique basée sur deux aspects: le premier comprend une documentation des techniques de préconcentrations utilisées pour les métaux traces de façon générale et le mercure en particulier avec une description des principaux adsorbants, classiques et nouveaux, utilisées dans l'extraction en phase solide. La deuxième partie comprend, le cycle biogéochimique, la spéciation et les facteurs biogéochimiques contrôlant le comportement du mercure dans l'environnement. Le deuxième chapitre présente les différents matériaux et méthodes expérimentales utilisées au cours de ce travail. Le troisième chapitre présente deux méthodes misent au point pour l'extraction du Hg(II) de l'eau de rivière. La première méthode est basée sur la formation directe de chélates métalliques dans des échantillons d'eau suivie d'une extraction en phase solide. La seconde comprend l'extraction en phase solide de Hg par la 8-hydroxyquinoléine avec une évaluation de différentes résines de chélation pour l'extraction optimale de Hg(II). Le quatrième chapitre présente une étude complémentaire de celle présentée dans le chapitre 3, dans laquelle 5-phenylazo-8-hydroxyquinoline a été utilisé pour le développement d'une méthode de mesure de Hg(II) dans l'eau en utilisant Cold Vapor Atomic Fluorescence Spectrometry (CV-AFS). Le cinquième chapitre décrit une méthode d'analyse simple pour la mesure de Hg(II) dans l'eau. Cette dernière méthode est basée sur la formation des complexes des ions métalliques dans l'échantillon d'eau par la simple addition d'iodure et un agent tensioactif cationique. La formation des complexes d'ions métalliques est suivie d'une extraction en phase solide et analyse par Inductively Coupled Plasma Mass Spectrometry (ICP-MS). Le sixième chapitre, comprend une étude de spéciation et

distribution du mercure dans la Deûle et la Lys, y compris l'identification des principaux facteurs contrôlant le transport, mobilité et la transformation du mercure. Enfin, le septième chapitre, inclut un résumé de toutes les études menées avec une conclusion générale et perspectives.

## General introduction

Mercury (Hg) is a very particular element conferred by its high density and vapor pressure. It is ubiquitous element in the environment and is considered as global pollutant because of its long range atmospheric transport and its complex biogeochemical cycle. Accordingly, mercury can reach remote uncontaminated areas such as Arctic regions, where these potential areas can act as a sink for global mercury. Besides, mercury is among the most hazardous environmental pollutants conferred by its organic form methylmercury ( $\text{CH}_3\text{Hg}^+$  or MeHg). Methylmercury is the most toxic species of mercury, because of its bio-accumulative character in the living organisms throughout the food web. It can accumulate in organisms up to a concentration million times higher than surrounding waters causing damages to the nervous system and possible fatalities.

There are two major inputs of mercury in the environment: natural and anthropogenic. While human activities have contributed to the largest flux of Hg in the biosphere in which 50-75 % of Hg emissions are estimated to be from anthropogenic sources. Once mercury is found in the environmental compartments (air, water, soil and biota) it enters a complex biogeochemical cycle of various transformations and degradations of mercury species. To that end, it is crucial to monitor and quantify mercury in the environmental ecosystems in order to identify the major factors governing mercury dynamics and to control its concentration.

Various factors control the transformation of mercury species. Dissolved organic carbon, sulfate, sulfides, pH, temperature and microorganisms are all dependent factors ruling mercury methylation. Methylmercury degradation is photochemically induced in which this mechanism of degradation is mostly dominant at surface waters. Biotic demethylation can be prevailing in areas lacking of sunlight. Mercury mobility and transport in bulk and aqueous phases are mainly controlled by sulfides, organic matter, fine/coarse fraction, Fe/Mn oxyhydroxides, mercury partition coefficient between aqueous and solid phases and resuspension activities (Hammerschmidt et al 2004). Deûle river located in north of France is highly polluted in Hg because of a former ore smelter that was operational for more than a century and eventually closed in 2003. The study of mercury distribution and speciation can allow us to understand the dominant biogeochemical factors controlling the transport and the fate of mercury in the Deûle river.



In natural waters, Hg is present at a very low concentrations occurring between 0.2-100 ng/L. For this reason, most analytical techniques do not achieve accurate direct measurement of Hg which necessitates preconcentration to meet their limit of detection. Among many preconcentration methods, solid phase extraction (SPE) is the most used for trace metal extraction. There are two major categories of adsorbents used in SPE, inorganic and organic. The choice of the proper sorbent depends on the target analytes. Novel adsorbents have been developed to allow more determinative and precise determination of trace metals such as, ion-imprinted polymers, carbon nanotubes, immunoassay extraction...ect. In order to improve the selectivity of the adsorbent towards a particular metal, the solid support can be physically or chemically modified by an organic modifier. Different functional groups conferred to a particular ligand can be immobilized on the surface of solid support to enhance the stability constant formation with metals. This allows better extraction recoveries, enhanced enrichment factor and lower limits of detection. According to Hard Soft Acid base (HSAB) theory, mercury is considered as soft acid, thereby soft bases containing donor atoms of sulfur and nitrogen form the most stable metal complexes. Ligands containing mercapto or/and azo/ imino functional groups are the most employed to form stable chelates with mercury for the subsequent solid phase extraction. Another method, consists of ligand grafting on a solid support, the following obtained resins can be used for SPE of metals. For Hg determination the most employed ligands used for sorbent functionalization contain oxine and/or thiol and/or imino derivatives. Different analytical techniques are used in conjunction with Hg extraction in an online or offline coupling set-up, such as CV-AAS, CV-AFS, ICP-AES, ICP-MS...ect. The choice of the proper analytical instrument depends on its availability, cost, and levels of mercury in the sample matrix and the instrumental limit of detection.

In the view of different elements and Hg problematic issues presented in the introduction, the main objectives of this work are:

- Evaluation of different chelating resins for the extraction of Hg(II) and analytical methods development for the measurement of trace levels of Hg in river water using solid phase extraction.
- Investigation of Hg speciation and distribution in the Deûle river and its potential fate and transport. As well as, the determination of different factors ruling Hg distribution and mobility.

The following thesis is made up of seven chapters. The first chapter is a bibliographic based study regarding two different aspects: the first part comprises a well-detailed literature of the preconcentration techniques employed for metal extraction. Besides, a description of the major conventional and novel adsorbents used in solid phase extraction. In addition, a description of the major analytical methods based on solid phase extraction for the determination of trace levels of mercury in environmental matrices is provided. The second part includes the biogeochemical cycle, speciation and biogeochemical factors controlling mercury behavior in the environment. The second chapter cites the materials and experimental methods employed during this work. The third chapter includes, a full study comprising two methods of extraction of Hg(II) from river water. The first method is based on the direct formation of metal chelates in water samples followed by solid phase extraction. The second method includes the solid phase extraction of Hg(II) on 8-hydroxyquinoline based resins. As well as, the evaluation of different chelating resins based on 8-hydroxyquinoline for the optimal extraction of Hg(II) from river water. The fourth chapter includes a complementary study of that presented in chapter 3, in which 5-phenylazo-8-hydroxyquinoline was used for the method development for Hg(II) measurement in river water using Cold Vapor Atomic Fluorescence Spectrometry (CV-AFS). The fifth chapter describes an analytical method for the measurement of total mercury in river water. The latter method is based on metal ion chelates formation in water sample by the simple addition of iodide and a cationic surfactant. The formation of metal ion complexes is followed by solid phase extraction on silica phase and detection using Inductively Coupled Plasma Mass Spectrometry (ICP-MS). The sixth chapter presents a study of Hg speciation and distribution in the Deûle and Lys rivers including the identification of major factors controlling the transport and transformation of Hg. Finally, the seventh chapter includes a summary of all studies conducted with a general conclusion and perspectives.

***Chapitre A: Analyse du mercure en utilisant les méthodes d'extraction en phase solide, Introduction sur le comportement biogéochimique du mercure dans l'environnement.***

***Chapter A: Mercury measurement based on solid phase extraction methods, Introduction to the biogeochemical behavior of mercury in the environment.***

## **Part I: Different analytical methods for measurement of mercury based on preconcentration principle**

### **A.I.1. Introduction**

In environmental samples, metal ions exist at trace levels. The low concentration renders their analysis one of the most sophisticated analytical tasks. Most of the modern advanced instrumental methods such as Inductively Coupled Plasma Mass Spectrometry (ICP-MS), often fail in the direct determination of ultra-trace metals because of the inadequate low detection limits and interferences caused by the sample matrix effect. Therefore, a preliminary enrichment step is indispensable to reach quantifiable levels, eliminating interferences and retaining the analyte in a more stable chemical form. The proper choice of efficient preconcentration/separation methods is essential. There are various conventional methods of preconcentration including solvent extraction, precipitation techniques, freezing based concentration methods, distillation, sublimation, evaporation, electrodeposition...ect. Modern techniques of metal enrichment include: solid phase extraction (SPE) by different solid supports (polymeric sorbents, chelating resins, wool, chitosan, activated carbon...ect.), cloud point extraction, liquid-liquid extraction by liquid membrane, stir bar sorptive extraction, single drop microextraction, solid phase microextraction, hollow fibre-liquid phase microextraction, dispersive liquid-liquid microextraction. Solid phase extraction offers many important advantages as compared to liquid-liquid extraction (LLE). It reduces the use of solvents, gives high enrichment factors, recoveries and selectivity. Moreover, it is flexible, simple, economical, and can be automated. Therefore, it is considered as alternative to conventional LLE since the mid-1970 when it was first applied for the preconcentration of trace organic contaminants analysis (Liska et al 2000).

In the following section, a detailed description of solid phase extraction and some examples of the adsorbents used in metal extraction are reported. Moreover, different analytical methods for the measurement of mercury species using solid phase extraction have been also outlined.

### **A.I.2. Solid phase extraction**

Solid phase extraction (SPE) is based on the partitioning of solutes between the sample matrix (liquid) and the solid support (adsorbent). Solid phase extraction technique is based on four successive steps. First, conditioning of the solid support. Its major role is the solvation of the functional group and removal of air and impurities in the packaging of the column.

Conditioning consists of wetting the solid phase with a solvent that depends on the nature of the adsorbent used. Secondly, percolation of the sample through the packing material at a flow rate that should be low enough to allow sufficient retention of analytes. Third, an optional step can be added which is the solid phase washing. Washing with a solvent of low elution strength to remove the matrix effect that can be retained and unbounded analytes. Finally, elution step with solvent capable of stripping off the bonded analytes. The type of elution solvent can vary, depending on the nature of analyte retention. If the retention is due to chelation, the eluent can contain a stronger chelating reagent than that used for the analyte fixation or acid by breaking up the complex formed. The elution flow rate should be lower than the flow rate used for sample percolation.

Retention of analytes on the solid support can be by simple adsorption, chelation or ion exchange depending on the nature of the adsorbent. Adsorption of analytes can be achieved either by physical sorption or chemical sorption due to Van der Waals hydrophobic interactions. Adsorption normally occurs on hydrophobic phases such that of octadecyl-bonded silica and copo(styrene divinylbenzene) polymer. This kind of retention mechanism cannot be applied for metal species as they are considered to be polar. Chelation is a more probable retention for trace metals on adsorbents. Chelation of analytes is achieved by the presence of donor functional group atoms. The most efficient donor atoms for the retention of metals include oxygen, nitrogen, phosphorous and sulfur atoms present in phenol, carbonyl, carboxylic, hydroxyl, ether, phosphoryl, amine, nitro, nitroso, azo, diazo, nitrile, amide, thiol, thioether, thiocarbamate and bisulphite. The selectivity of the functional group towards metal ions can be determined according to the size of the organic modifier, activity of the loaded functional group and the characteristics of hard-soft acid-base (HSAB). Metals can be divided into three groups according to HSAB theory. Hard cations, form weak electrostatic interactions with hard ligands such as oxygen. Hard metals include both alkali and alkaline earth metals ( $\text{Ca}^{2+}$ ,  $\text{Mg}^{2+}$ ,  $\text{Na}^+$ ). Borderline cations have an intermediate interaction that is they form chelates with both hard and soft ligands. Borderline and hard cations enter into competition for O ligand, where they compete with soft metals for the intermediate nitrogen ligand. Such cations belong to transition and post transition metals ( $\text{Fe}^{2+}$ ,  $\text{Co}^{2+}$ ,  $\text{Ni}^{2+}$ ,  $\text{Cu}^{2+}$ ,  $\text{Zn}^{2+}$ ,  $\text{Mn}^{2+}$ ,  $\text{Pb}^{2+}$ ). Finally, soft cations (ex:  $\text{Cd}^{2+}$ ,  $\text{Hg}^{2+}$ ) form covalent bonds with soft sulfur ligands. Retention of metals on solid phase can also be due to ion exchange interactions induced by cationic or anionic functional groups of the sorbent. Sulfonic acid (cation

exchange) and quaternary amines (anion exchange) are strong ion exchange sites that confer ionic interactions at any pH. Carboxylic acid groups (cation exchange) and primary, secondary and tertiary amines (anion exchange) are weak ion exchange sites because they only acquire the ion exchange characteristics at a pH greater or equal to pKa.

When solid phase extraction (SPE) is chosen as a preconcentration method for analytes, a solid support and a ligand should be chosen scrupulously for the efficient extraction of the target analytes. In order to improve the efficiency of the retention of analytes on a particular sorbent, incorporation of donor atoms are required. Chelating sorbents provide better selectivity and enhance the preconcentration factor up to several hundred folds allowing the detection of metals at ultra-trace levels from a large volume of water sample. The resulting selectivity of the chelating resin is owned to the geometrical features of the bonded ligands and their complex forming properties. They are composed of two parts, the chelate comprising the functional group and the polymeric support. Chelating resins can be obtained either by polycondensation or polymerisation of monomers containing a specific chelating group or the inclusion of an active ligand into the polymeric solid support. Functional group incorporation into the polymeric chain is the most used method for the preparation of chelating sorbents. Most polymeric sorbents can be processed using two-step syntheses: First the insertion of an appropriate chelating functional group on the surface of the chelating sorbent. Secondly, immobilization through either physical adsorption or a more stable chemisorption mechanism by forming covalent bonds.

#### **A.I.2.1. Conventional adsorbents used in SPE**

There are two major categories of adsorbents used in solid phase extraction of metals; inorganic corresponding to hydrophobic reversed phase sorbents and organic representing the polar normal phase sorbents (figure A.I.1). Inorganic sorbents include: silica gel  $\text{SiO}_2$ , alumina  $\text{Al}_2\text{O}_3$ , magnesia  $\text{MgO}$ , zirconia  $\text{ZrO}_2$ , titania  $\text{TiO}_2$ , controlled pore glass, mesoporous silica gel, Kieselgur (diatomite, a kind of siliceous sedimentary rock), zeolites...ect. Organic sorbents are comprised of natural polymers (cellulose, dextran, chitosan...ect.) and synthetic polymers. Examples of synthetic polymers such as copo[styrene-divinylbenzene], copo[divinylbenzene-vinylpyrrolidine], polyacrylate, polyurethane, polyacrylonitrile, polystyrene and polytetrafluoroethylene.

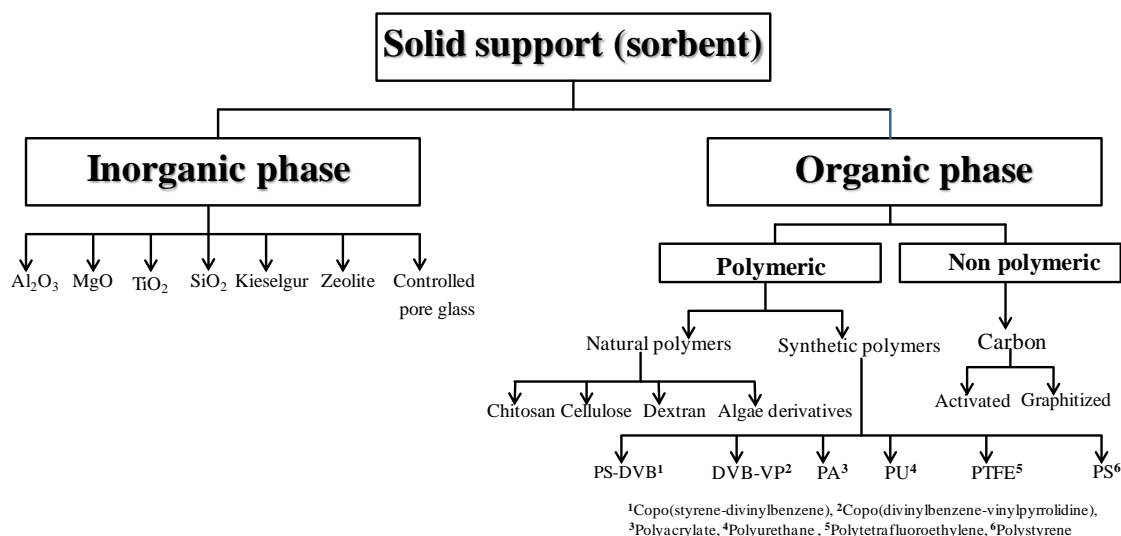


**Figure A.I.1.** Different types of solid supports used in the solid phase extraction of metals.

#### A.I.2.1.1. Silica gel

Silica gel is a polymer of silicic acid in tetrahedral geometry. It is the most used inorganic support since it possesses many advantages. It does not swell nor strain and support heat treatment and is resistant to solvents, thus conferring good mechanical and thermal stability. In addition, it possesses large surface area, which is essential for ion exchange mechanisms. Immobilization of a ligand on this support is easier than any other organic polymeric supports. Moreover, it is characterized by high chemical stability and sorption capacity for various metal ions under different conditions. However, the presence of residual silanol groups attribute to chemical limitations for the usage of silica gel in a narrow pH range. Quantitative retention by silica support occurs in a basic pH range about 7.5-8 even so; it is susceptible to hydrolysis under alkaline conditions. On the other hand, very low pH values protonate silanol groups causing the impairment of the ion exchange properties of silica sites contributing to low extraction of analytes. Modification of silica surface is known as *silylation process* that can allow the attachment of an organic modifier with the desired functional group. In this process, silica forms covalent bond with silane reagent and transforms the surface silanol groups into new organofunctional ones (Unger 1979). Silylation offers a linking group, which permits the attachment of the chelating molecule at the free end away from the silanol sites. This can prevent steric hindrance at the silanol site and maximize the ability of donor atoms of the complexing group to form chelates with metals. Modification of silica support by either loading or immobilizing of a chelating ligand can offer better thermal and chemical

stability, higher selectivity under various conditions, refined porosity and large specific surface area that can attribute to high mass exchange characteristics (Kooshki et al 2007).

#### **A.I.2.1.1.a. Surface silica modification**

First attempts have appeared to introduce an organic modifier on a solid support was in 1952. Selectivity of the sorbent depends principally on the nature of the functional group it holds, and other mechanical, chemical properties of the polymeric matrix such as: fast kinetics, high capacity and regenerability. Therefore, modification of the sorbent is carried out to enhance its selectivity towards particular metal specie. The incorporation of an organic compound with specific Lewis bases properties into the silica support can be accomplished by two methods: physical treatment and chemical treatment (figure A.I.2). The impregnated-loaded sorbent can be obtained by either passing the reagent solution through a column packed with sorbent or by shaking the adsorbent in the reagent solution. In the first approach, the donor atom is directly adsorbed through adhesion process, electrostatic interaction and hydrophobic attractions such as Van der Waals interactions. This leads to changes in the ratio of silanol and siloxane concentrations on the silica surface leading to better performances, since silanol groups are known to be weak ion exchangers.

Chemical modification is achieved by forming chemical bond between the sorbent and the modifier. Chemisorption offers better immobilization of the grafted ligand, mechanical stability and water insolubility ensuing better efficiency and selectivity of the functionalized sorbent. *Functionlization* of the support can be accomplished by two types of modifying agents: organic and inorganic ligands. The most common approach for developing immobilized silica is covalent binding called *covalent grafting* (Tertykh et al 1999). This kind of modification requires silanization procedure, in which the hydrogen atoms of the dispersed surface silanol groups react with organosilyl group conferring an organic nature to the hydrophobic matrix. *Sol-gel process* is another type of covalent grafting, which includes the synthesis of an inorganic-organic hybrid material through the combination of hydroxy and alkoxy groups of silicon atom to organosilicon compound. *Halogenation* is a non-conventional chemical method for the modification of silica surface that leads to the formation of alkyl bonded silica through the direct covalent binding of carbon to silicon atom. This process requires the conversion of surface hydroxyl groups of silica into hydride in the presence of halogenating agent in anhydrous aprotic solvent. Hydride formation is followed by anchoring terminal olefins to the silica surface in the presence of Grignard reagent or metal



catalyst such as organo lithium compound. Silica substrate modification with organic polymers such as vinyl acetate and vinyl pyrrolidine is another potential method for the chemical modification. *Polymer grafting* is performed through covalent binding of organic polymeric chain to silica surface by free radical surface graft polymerisation.

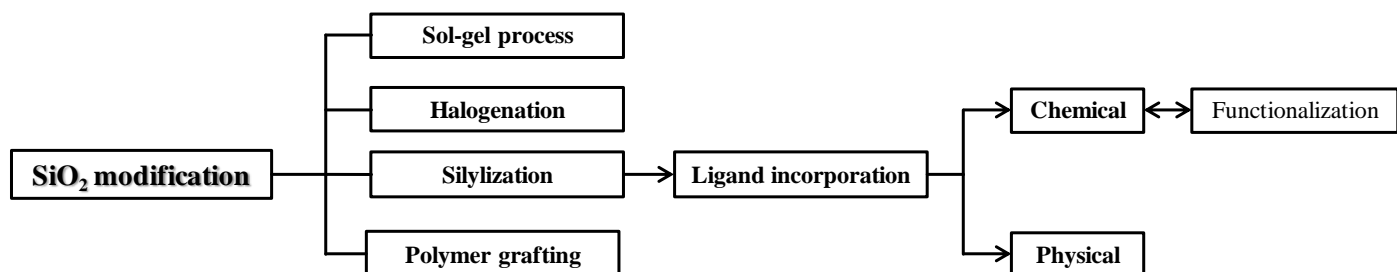


Figure A.I.2. Silica surface modification by different processes.

#### A.I.2.1.1.b. Modified silica sorbent

Numerous ligands were impregnated by physical adsorption on the surface of silica gel. Thionalide for preconcentration of Pb and As from sea water (Terada et al 1983); 2-mercaptobenzothiazole (Terada et al 1983); 3-methyl-1-phenyl-4-stearoyl-5-pyrazolone for the extraction of Cu, Co, Ni from tap water (Tong et al 1990); 8-hydroxyquinoline have been also mechanically impregnated on silica support (Mc Laren et al 1985); hexathia-18-crown tetraone for the extraction of Hg(II) from tap, river and spring waters (Yamini et al 1997); dithizone for the extraction of Hg(II), phenylmercury and methylmercury from synthetic seawaters (Sanchez et al 2000); ammonium pyrrolidine dithiocarbamate (APDC) for the extraction of Cu, Cd from certified sea waters (Liu et al 1992); and Bathophenanthroline for the preconcentration of Fe from tap and well waters (Yamini et al, 2001).

Unmodified silica support can be also used for the preconcentration of metals. The addition of a desired ligand directly into the sample to form stable metal complexes, followed by their subsequent adsorption onto unmodified silica gel. Ammonium pyrrolidine dithiocarbamate was added to sea water samples for the extraction of Se/Sb (Sturgeon et al, 1985). Also, 8-hydroxyquinoline was added to sea water samples for the extraction of Cd, Cu, Zn, Mn, Fe, Ni, Co (Sturgeon et al, 1982).

Immobilization of a complexing agent with a certain functional group (mercapto, oxine, Imino, hydrazide, ethelenamine and ethyleneamine, glyoxime, aniline and acid-base groups

derivatives) through chemical bonding permits more stability and selectivity, thereby allowing metal speciation. Numerous applications were performed for the extraction of mercury and other metals using chelating resins. Selective extraction of Hg(II) using chelating adsorbent from water samples was conducted using: Mercapto functionalized mesoporous crystalline material-41 (MCM-41); mesoporous silica functionalized with 1-furoyl thiourea; and 2,6-pyridine dicarboxylic acid functionalized on nanometer-sized silica (Idris et al 2011, Muresanu et al 2010, Zhang et al 2010). For other metals, 4-amine-2-mercaptopyrimidine immobilized on silica was employed for the removal of Pb ions in river water (Ferreira et al, 2010). Silica gel-polyethylene glycol is used as an efficient adsorbent for the determination of Co, Ni ions in different matrices (Pourreza et al, 2010). Pd(II) was preconcentrated from water samples using highly selective diphenyldiketone-monothiosemicarbazone modified silica (Sharma et al, 2012). Moreover, different metals of Fe, Cr, Cu, Co, Pb, Ni, Zn were solid phase extracted from fuel ethanol using 2, 2' dipyridylamine bonded silica (Vieira et al, 2013).

#### **A.I.2.1.2. Various adsorbents used in solid phase extraction of metals**

In the literature, there is a wide variety of sorbents comprising both organic and inorganic sorbents. Few studies have been reported for the adsorption even the preconcentration of metals using *Alumina*. Metals can be sorbed directly on alumina. However, its modification by organic modifiers can amplify its strength in capturing metals. Most alumina support modification is based on the physical adsorption of donor atoms on its matrix. Chemical bonding of ligands did not exist until Hiraide et al. (1994) developed a method for the immobilization of ligands on alumina. The chemical modification procedure, consists of the introduction of a surfactant, sodium dodecyl sulfate (SDS) on the surface of Al<sub>2</sub>O<sub>3</sub>. Secondly, metal specific chelating ligand can be anchored in the hydrophobic chains of the surfactant.

*Copo[styrene divinyl benzene] (CS-DVB)* are characterized by their high efficiency, robustness and wide pH stability, porosity with uniform pore size distribution, high adsorption capacity of non-ionic adsorbates, high surface area, homogeneous non-ionic structure, durability and purity. The higher the surface area of the sorbent means more number of chelating sites are present allowing higher adsorption capacities and a stronger retention of analytes. It is the amberlite family consisting of XAD-1, XAD-2 and XAD-16 in which the latter resin has the highest surface area among the others. There are different types of CS-DVB. First, the introduction of a hydrophilic functional group by the chemical bonding to the

hydrophobic matrix, results in a more hydrophilic resin. Therefore, the presence of donor atoms (N, O, S) is important for trace metal retention. Addition method, by the formation of ligand-metal complexes and its adsorption on CS-DVB such as the addition of 8-hydroxyquinoline (8-HQ) to natural water samples (Abollino et al 1990). Moreover, the modification of the macroporous resin can be also achieved by physical adsorption or immobilization of a ligand on the macroporous resin, such as the immobilization of ammonium pyrrolidine dithiocarbamate (APDC) on CS-DVB (Ramesh et al, 2002). The most stable resin is the chemically functionalized resin in which the ligand is coupled to the resin backbone through an azo spacer or methylene. No preconcentration studies for mercury have been performed with CS-DVB. Thereby, studies to be realized in this field might be useful to discover the capacity of this resin modified or functionalized for the retention of mercury.

Synthesis of new sorts of resins for the retention of metals seems challenging with the purpose of developing new solid matrices for more stability, selectivity and capacity. Synthesis of new polymers by ring opening metathesis polymerization (ROMP) was first reported by Anderson and Merckling (1995). They patented a procedure to polymerize norbornene. Following these early years, the field of ROMP expanded and was further developed. ROMP is based on the polymerization of prefunctionalized monomers by selective mechanism leading to predetermined, reproducible properties in terms of particle size, porosity, functionality and capacity. A recent SPE was based on a polymer synthesized by ROMP for the selective retention of noble metals. Under competitive conditions, the selectivity order at pH 3.5 was reported to be: Au > Hg > Pd  $\approx$  Ag > Rh > Pt > Ir  $\approx$  Re > Cu > Co  $\approx$  Zn  $\approx$  Cd  $\approx$  Ni > Cr > Mn (Glatz et al, 2003).

***Crosslinked based acrylic polymer*** is a polymer of  $[-CH_2-CH(COONa)-]_n$ . It has the ability to adsorb 300 times its mass in water. It is a large family, playing the role of either an anion exchanger polymer or cation exchanger depending on the active functional group they hold. They are characterized by fast kinetics and mechanical stability and comprise: XAD-7 and XAD-8: (ethylene-dimethacrylate); Amberlite IRC 86 (methacrylic polymer); amberlite XA7HA: (polyacrylic); amberlite IRA 458 (polyacrylic); amberlite CG50 (methacrylic polymer). Rohm and Haas, were first to synthesize polyacrylate anion exchangers (Dardel et al, 2001) comprising amberlite IRA458, amberlite IRA 958, amberlite IRA 670, and amberlite IRA-67 (acrylic). The polarity of acrylic based polymers is considered to be moderate;

therefore, a direct addition of a ligand or its immobilization on the polymer backbone is performed.

**Polyurethane foam (PUF)** is considered as soft and flexible material formed from polyesters and polyethers. Polyurethane foams (PUF) are first used as selective adsorbents by Bowen et al. (1970). Since, then it became widely used for the extraction, sorption, separation and preconcentration. Polyurethane foam is characterized by many advantages: simplicity in preparation, low cost, mechanical stability (stable in wide pH range, strong resistance to organic solvents), high available surface area and cellular structure and easy desorption. The first application of this sorbent was used for the extraction of organic compounds from aqueous solutions. Later on, it was rapidly used for the extraction of metals. Online preconcentration of metals using PUF as solid phase extraction method coupled to modern analytical techniques is recently developed.

In the literature, there are countable studies for the solid phase extraction of mercury by PUF sorbent. In most of the studies, mercury can be retained on unmodified PUF in the form of counter ion complexed with halides. Other form of extraction is ligand physical impregnation of PUF matrix and other possibility is the chemical functionalization of PUF.

**Naphthalene based sorbents** According to our knowledge; it is not widely used for the extraction or for the preconcentration of metals. There are few studies that have discovered its ability for the retention of metals based on naphthalene sorbent. Most of metal recoveries are quantified by spectrophotometric detection. This reveals the weakness of naphthalene for the enrichment of ultra trace levels of metals. Crystalline naphthalene based sorbents are mostly used for metal sorption. Metal retention on this sorbent can be either by the addition of a ligand, naphthalene based sorbent modification or functionalization. Most of the methods developed are based on batch experiments. Most desorption of metals from naphthalene based sorbent is realized by solvents (Dimethylformamide) or by concentrated HCl or HNO<sub>3</sub> (7M). The use of this solid matrix for the preconcentration of mercury is rather uncommon.

**Activated carbon** is produced from carbonaceous materials such as charcoal, coal, lignite, wood, nutshell and peat. There are many types of activated carbon: powdered activated carbon, granular activated carbon, extruded activated carbon, bead activated carbon, impregnated carbon and polymer coated carbon. Activated carbon is characterized by large surface (500-1000 m<sup>2</sup>/g) and different kinds of porosity and micropores. Thus, they are

popular for being good adsorbents of metals and other molecules. Another form of carbon has been developed, porous graphitized carbon (PGC), which has better mechanical stability. Its application is limited to organic compounds where no applications were found for the retention of metals using this sorbent. Retention of metals on activated carbon (AC) can be either through the adsorption of metal chelates on AC or by the adsorption of metals on modified activated carbon by a donor functional group.

**Biosorbents** There are different types of biosorbents employed for metal adsorption including: algae, bacteria and fungus (*Rhizopus Arrhizus*, *Penicillium Spinulum* and *Asperigullus Niger*) (Zouboulis et al 2004, Papageorgiou et al 2006, Yan et al 2003). Moreover, extracellular biopolymer industrial products are also used for the adsorption and removal of metals i.e. waste rubber, coal, industrial waste sludge and agricultural waste. There are a wide repertory of agricultural wastes by-products that are applied for metal adsorption such as tea leaves waste dried plant leaves, roots, wheat shell, tea, coffee grounds, coriander plant (Chinese parsley), barks of tree, pinus bark and different bark samples, modified barks of tree, bicarbonate treated peanut hull, sawdust, coconut husk hyacinth roots (*Eichhornia crassipes*), chitin, Chitosan, wool, seaweeds, biomass, coal-fly ash, bagasse pith, hazelnut shells, peanut hull, red fir, maple sawdusts, palm kernel husk, coconut husk, peanut skins, cellulose, modified cellulosic materials, chemically modified cotton, corncobs, modified corncob, rice hulls, apple wastes, jackfruit peel, coir pith, flax shive, sago waste, wool fibers, olive cake, pine needles, almond shells, cactus leaves, charcoal, lignin, modified lignin, banana, orange peels, modified sugar beet pulp, modified sunflower stalk, palm fruit bunch and maize leaf (Ahalya et al 2003, Cimino et al 2000, Bryant et al 1992, Vazquez et al 1994, Low et al 1999, Macchi et al 1986, Annaduri et al 2002). These biosorbents are mostly used for metal removal. There are few studies reported for the preconcentration of trace levels of metals using biosorbents (Cai et al 1996, Tirtom et al 2008, Rajesh et al 2008).

Different adsorbents used for the preconcentration of mercury from different environmental samples are summarized in table A.I.1.

**Table A.I.1:** Analytical methods for the measurement of Hg(II) using different types of sorbents.

Adsorbent	DT <sup>a</sup>	Matrix	pH	Capacity (mmol L <sup>-1</sup> )	PF <sup>b</sup>	LOD <sup>c</sup> (pg mL <sup>-1</sup> )	R <sup>d</sup>
Alumina modified dimethylsulfoxide	CV-AAS	River water	1-12	1.9	1000	-	1
Polyacrylamide grafted onto crosslinked poly(4-vinylpyridine)	CV-AFS	Seawater	1-8	4	20	2	2
Activated carbon	FI-CV-AFS	Tap water	1.5	-	-	10	3
Multiwall carbonanotubes	AAS	Tap/reservoir water	7	0.01	30	12	4
8-hydroxyquinoline immobilized vinyl copolymer	FI-AAS	Seawater	7	-	100	230	5
Polystyrene-divinylbenzene functionalized 6-mercaptopurine	CV-AAS	Industrial waste water	5.5-6	1.74	-	20	6
Dithizone immobilized ethylene glycol dimethacrylated-hydroxy ethyl methacrylate microbeads	AAS	Distilled water	5-6	0.7	25	0.6	7
Microcrystalline naphthalene immobilized dithizone	CV-AAS	River water	1	0.007	50	14	8
Diphenyldithiocarbazon/Celulose	Spectrophotometer	Tap/seawater	1-4	-	33	2000	9
Sheep wool	FI-CV-AAS	Riverwater	2	0.028	18	10	10
4-(2-pyridylazo)-resorcinol modified nanometer sized particles	CV-AAS	Tap/River water	4	0.001	50	430	11

<sup>a</sup>DT: detection technique, <sup>b</sup>PF: preconcentration factor, <sup>c</sup>LOD: limit of detection, <sup>d</sup>R: reference  
 1 (Soliman et al, 2006) 2 (Yayayuruk et al, 2011), 3 (Ferrua et al, 2007), 4 (Sheikh et al, 2011), 5 (Bravo-Sanchez et al, 2001), 6 (Mondal et al, 2001), 7 (Salih et al, 1998), 8 (Shabani et al, 2004), 9 (Rajesh et al, 2008) 10 (Tirtom et al, 2008), 11 (Zhai et al, 2006)

### A.I.2.2. Innovative-new sorbents for SPE metals

**A.I.2.2.a Surfactant-modified sorbent (SMS):** Micelles are formed above Critical Micellar Concentration (CMC), the hydrophilic end of the molecule becomes in contact with the solvent and the hydrophobic tail in the center of the micelle. For concentration below CMC, the ionic surfactant becomes adsorbed on the surface of the solid support such as silica forming monolayers (Hemimicelles) or Bilayers (admicelles) on the active solid surfaces. In hemimicelle formation, the hydrophobic tail is exposed to the sample corresponding to the affinity towards non-polar compounds. However, in admicelle formation the ionic end of the surfactant is exposed to solution, conferring an affinity towards polar analytes. Solution acidity

plays an important role in surfactant-based sorbent in which it can influence the efficiency and the selectivity. When pH changes, the charge density on the surface of the support changes affecting the type of coacervate present. For metals, surfactant-based sorbents is not widely employed where further research is deemed important. A new mode of modification was recently developed for SMS, which is the introduction of organic ligand in the cores of micelles of the surfactant. An alumina-sodium dodecyl sulfate coated with meso-phenyl bis(indolyl) methane was used for the simultaneous preconcentration of copper, Zinc, lead (Ghaedi et al, 2007). Another SDS-coated alumina was incorporated with bis (2-hydroxyacetophenone)-1,3-propanediimine for the extraction of Zinc, nickel and iron (Ghaedi et al, 2009). Other types of supports were used for metal extraction like poly vinylchloride (Marakel et al, 2009), silica (Shabani et al, 2009) and chromosorb (Ghaedi et al, 2006). Sodium dodecyl sulfate-coated chromosorb P modified with 2-mercaptobenzoxazole was employed for the extraction of trace levels of Hg(II) (Ghaedi et al, 2006).

**A.I.2.2.b. Immunoassay extraction:** it is based on antibody-antigen interactions which are highly selective and specific. This type of extraction requires the development of specific antibodies in the body of a certain animal by eliciting an immune response using hapten. The isolation and purification of plasma of the animal's blood allows to obtain a carrier of the desired adduct. The obtained specific antibodies can be covalently immobilized on a solid support and packed into a cartridge for the subsequent extraction procedure. Immunoassay is widely used for organic compounds and recently, it has been developed for the extraction of metals (Pb, Cd, U, Hg) (Chakrabarti et al 1994; Blake et al 1996; Blake et al 1998; Sasaki et al 2007; Sasaki et al 2009; Date et al 2012; Wang et al 2012).

**A.I.2.2.c. Aptamer based molecular recognition sorbent:** Oligonucleotides (aptamers) are single standard oligonucleotides. Their specificity and recognition to a certain analyte is acquired from the hydrogen bonding or Van der waals forces at dipole and stacking interactions. Specific aptamers are synthesized by doping a random sequence of oligonucleotides. The specific sequence that retain to the target analyte is selected and separated from the aptamer (target analyte). The isolate template can be amplified by PCR. This technique is more employed for the extraction of the organic analytes than metals. Still, very limited number of specific aptamer sorbents for the organic analytes were used in SPE. Recently, a Hg specific oligonucleotide sequence 5'-TTCTTTCTTCCCCTTGTTTGTT-3' was designed based on T-Hg(II)-T (Miyake et al, 2006), since T-T mismatch shows high

selectivity (figure A.I.3) and was used for the selective detection of Hg(II) based on the fluorescence resonance energy transfer (Wang and Liu, 2008). Therefore, additional research in this field is required to apply these mercury specific DNA sorbents for SPE techniques.

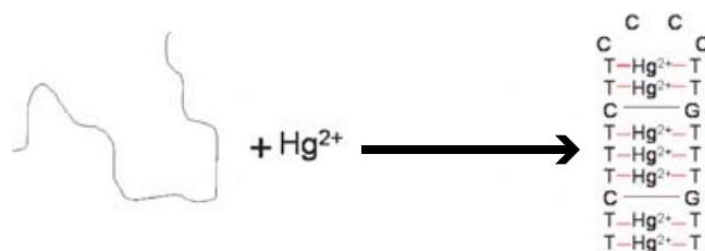


**Figure A.I.3.** Schematic drawing of mercury extraction using mercury-specific aptamer (Wang and Liu, 2008).

**A.I.2.2.d. Carbon nanotubes (CNT):** It is a novel material, which is recently employed for the extraction of both organic and inorganic analytes. CNT are molecular scale tubes of graphitic carbon and are two types single CNT and multi-wall CNT (MWCNT). Single CNT are single rolled graphite lamella in a cylinder and multi-wall CNT consisting of many concentrically arranged CNTs around a common axes. In general, CNTs can have diameters between fraction of nanometers to tens of nanometers and length that can reach several micrometers. CNT have an extraordinary sorptive capacity surpassing activated carbon. This explained by the large surface to volume ratios. In the application of CNTs for metal extraction, it is crucial to regulate pH parameter. pH above "point of zero charge" confer a negative CNT surface for the efficient retention of metal ions. Therefore, the decrease of pH can lead to drop off in the efficiency of extraction. CNTs are used for the preconcentration of metals as unmodified, modified or with addition of a suitable complexing agent. Organometallic compounds of lead and mercury were extracted using MWCNTs and analyzed using GC-MS (Munoz et al, 2005) and non-modified MWCNTs has been demonstrated for its efficiency for Hg(II) extraction (Shang et al 2007; Sheikh et al 2011).

**A.I.2.2.e. Nano-sized material:** The most employed nano-structured materials for sample extraction include nanoparticles (NPs), nanocrystals, nanotubes and nanogels. Nanoparticle material have size range from 1-100 nm, have high surface area-to-volume ratio, short diffusion route, high adsorption capacity, rapid dynamics and high efficiencies of extraction. The most commonly used NPs for the preconcentration of metals are magnetic Fe<sub>3</sub>O<sub>4</sub> and NPs of oxides such as TiO<sub>2</sub> (Mashhadizadeh and Karami 2011; Wang et al 2012). NPs of oxides can be modified or functionalized to attain an upgraded selectivity towards the target analyte.



Magnetic NPs attracted much concern for the extraction of metal ions. The particles used are super-paramagnetic that can be attracted to a magnetic field which is employed during metal extraction (figure A.I.4).

Trace levels of mercury Hg(II) were extracted with dodecyl sulphate coated magnetic nanoparticles and analyzed by ICP-AES with limit of detection as low as 0.011  $\mu\text{g/L}$  (Faraji et al, 2010). Also NPs are functionalized with triazene for the extraction of Hg(II) and quantification using ICP-AES with limit of detection of 0.04  $\mu\text{g/L}$  (Rofouei et al, 2012).

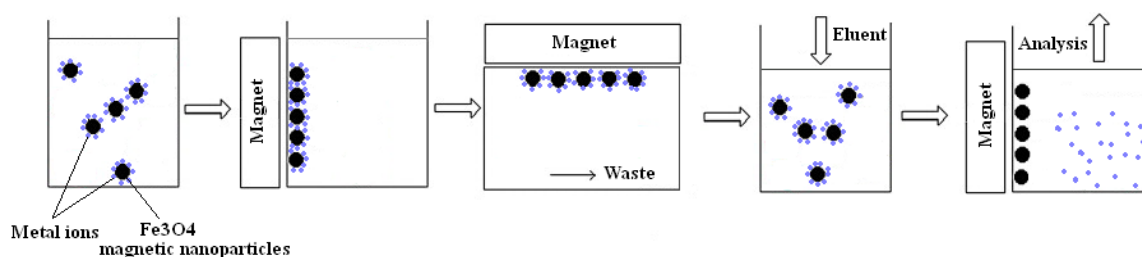


**Figure A.I.4.** Schematic figure of metal extraction using  $\text{Fe}_3\text{O}_4$  magnetic nanoparticles.

**A.II.2.2.f. Ion imprinted polymer:** Molecular imprinted polymers (MIP), is a technique for the creation of molecular recognition system in a three dimensional crosslinked polymer. MIP is synthesized via polymerization in covalent, non-covalent or semi-covalent methods. The copolymerization takes place in the presence of template molecule (inorganic metal ions, organic molecules, or biological macromolecules), cross linking agent and functional monomer. MIPs are used in many domains, including SPE (Xu et al, 2011) and chemosensors (Li et al, 2011). Many advantages are ascribed to MIPs including mechanical and thermal stability, affinity, selectivity and low cost. A small number of functional monomers are used for the synthesis of MIPs such as methacrylic acid, acrylic amide and 4-vinylpyridine. The use of these monomers attribute to MIP that does not have strong selectivity towards the target analytes. Thereby, many attempts have been focused for the synthesis of new functional monomers with specific ligand that has a specific affinity to the searched analyte.

Ionic imprinted polymers (IIP) is a branch of MIPs. Because, the template ion is a metal, therefore, it recognizes metals after imprinting. IIPs form high cross linking functional monomers and align in a predetermined orientation according to their stereo-chemical interaction with template metal ion. The high selectivity of IIPs is attributed to the memory effect towards metal ion interaction with a specific ligand, coordination geometry, number, charge and size. There are some drawbacks encountered with IIPs, i.e. incomplete removal of

the template metal ion, low adsorption capacity and slow mass transfer. To overcome these problems, metal imprinting was developed on surfaces of polymers/silica via sol-gel process (Lin et al, 2010).

A novel Hg(II) imprinted polymer had been reported for the selective preconcentration of Hg(II) from river and tap water. It is based on a new functional monomer; 3-isocyanatopropyltriethoxysilane bearing thymine (T-IPTS). Copolymerisation of the new functional monomer, in the presence of Hg(II) as a template ion, crosslinking agent and an initiator. Consequently, Hg(II) imprinted polymer was synthesized via gel-sol process and based on thymine-Hg(II)-thymine interactions (figure A.I.5). Quantitative recoveries of Hg(II) were recorded (95.2% - 116.3%). Hg(II) analyses was performed using AFS with a limit of detection of 0.03  $\mu\text{g/L}$  and a preconcentration factor of 200 (Xu et al, 2012).

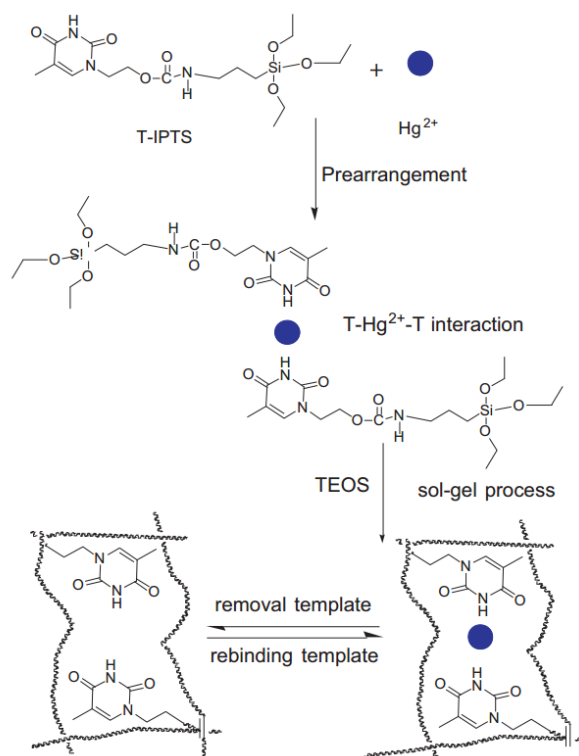


**Figure A.I.5.** Schematic drawing IIP-T selective for the extraction of mercury ions (Xu et al 2012).

### A.I.3. Mercury speciation using solid phase extraction

One of the most sensitive analytical techniques for mercury determination is Cold Vapor Atomic Fluorescence Spectrometry (CV-AFS). Preconcentration of mercury species is employed to enhance the detection limits of the most compatible analytical techniques for mercury measurement. There are many enrichment techniques used for mercury. Solid phase extraction seems to be the most practical preconcentration method for mercury species since it is a green method (no solvents are required). To improve the sensitivity/separation of mercury, derivatization can be employed by the use of  $\text{NaBH}_4$ ,  $\text{NaBEt}_4$  and  $\text{NaBPr}_4$ . In preconcentration techniques, derivatization can be performed, to produce volatile mercury species before the attainment of the final spectroscopic detector.

Non Chromatographic speciation of mercury by Cold Vapor Atomic Absorption Spectrometry (CV-AAS) or CV-AFS, is based on the different behavior of each species, strength of reducing agents ( $\text{SnCl}_2$ ,  $\text{NaHB}_4$ ), different concentrations of sodium tetrahydroborate ( $\text{NaHB}_4$ ), temperature in quartz cell or the use of an oxidant ( $\text{BrCl}$ ,  $\text{KBr/KBrO}_3$ ) for the determination  $\text{HgT}$  and by subtraction with  $\text{Hg(II)}$  (without an oxidant)  $\text{MeHg(I)}$  can be determined. Many procedures are used in several studies for the discrimination of mercury species which are based on the oxidation of the sample using various methods e.g. on-line oxidation decomposition ( $\text{KBr/KBrO}_3$ ) (Hg subtraction method) (Montesinos et al 2001), on-line UV irradiation decomposition (Bagheri et al 2001) or photo-induced chemical vapor generation (subtraction method) (Zheng et al 2005). There are also chromatographic methods for mercury speciation using CV-AAS, CV-AFS and Inductively Coupled Plasma Mass Spectrometry (ICP-MS) coupled with gaseous or liquid chromatography (Stoichev et al 2004; Qvarnstrom et al 2006; Tseng et al 2000).

For the speciation of mercury species using solid phase extraction, there are mainly two methods: (i) Chromatographic separation (ii) non chromatographic speciation of mercury (Table A.I.2 & A.I.3). The first method (i) is based on the online coupling of sorbent extraction preconcentration system to Gaseous Chromatography (GC) or Liquid Chromatography (LC). The second method (ii) is based on the selective separation either by sample pH, elution power or by the concentration of the reducing agent.

- (i) An on line flow-injection preconcentration of mercury species ( $\text{Hg(II)}$ ,  $\text{MeHg(I)}$ ), using dithiocarbamate resin was developed. Mercury species were eluted and

separated with capillary Gas Chromatography with Microwave Induced Plasma emission detection system (GC-MIP). The detection limits (LODs) of the latter analytical method were as low as 0.05 ng/L, 0.15 ng/L for MeHg(I) and Hg(II) respectively (Emteborg et al 1993). Using dithizone immobilized C18 coupled to HPLC-UV-vis detection system, was able to determine low LODs for three mercury species (Hg(II) 0.54 ng, MeHg(I) 0.58 ng, PhHg(I) 0.66 ng) (Sanchez et al 2000). The online preconcentration of mercury species on diethyl dithiocarbamate bonded on polyurethane foam, coupled to HPLC-ICP-MS was also developed (Dos Santos et al 2009). This analytical procedure was able to determine Hg(II) and MeHg(I) with low detection limits (Hg(II) 4.6 ng/L, MeHg(I) 5.2 ng/L).

**TableA.I.2:** Chromatographic speciation of mercury.

Matrix	Species	Adsorbent	Desorption	pH	PF <sup>a</sup>	DT <sup>b</sup> & LOD <sup>c</sup>	R <sup>d</sup>
River water	Hg(II), CH <sub>3</sub> Hg(I)	C18/ammonium pyrrolidine dithiocarbamate	Methanol	3	2500	HPLC-ITMS Hg(II) 90 pg, CH <sub>3</sub> Hg(I) 370 pg,	1
River water	Hg(II), CH <sub>3</sub> Hg(I)	C18 modified diethyldithiocarbamate	Thiourea+ HCl	3-8	150	LC-ICP-MS, Hg(II) 5.2 ng/L CH <sub>3</sub> Hg(I) 5.6 ng/L	2
Marsh water, Riverwater, seawater	CH <sub>3</sub> Hg(I)	Sulphydryl cotton	Acidic KBr/CuSO <sub>4</sub>	2-5	200	GC-AFS MeHg(I) 0.01 ng/L	3
Sea, river water	Hg(II), CH <sub>3</sub> Hg(I)	1, 3 bis( 2- cyanobenzene) triazene) immobilized C18	Acetonitrile	3-5	100	RP-HPLC-UV-Vis Hg(II) 1.3 ng/L CH <sub>3</sub> Hg(I) 1 ng/L	4
Tap, river, seawater	Hg(II), CH <sub>3</sub> Hg(I)	C18 modified dithizone	Na <sub>2</sub> S <sub>2</sub> O <sub>3</sub>	4	Hg(I) 27.8, MeHg(I) 32.2	HPLC-ICP-MS Hg species: 3 ng/L	5
Sediments, zoobenthos, Riverwater	Hg(II), CH <sub>3</sub> Hg(I)	C18 modified 2- mercaptophenol	Methanol	-	1000	HPLC-CV-AFS Hg(II) 0.8µg/L, CH <sub>3</sub> Hg(I) 4.3 µg/L	6
Seawater	Hg(II), CH <sub>3</sub> Hg(I)	Cation exchange resin (sulfonic acid)	Cysteine	7	1250	FI-HPLC-ICPMS Hg(II) 0.042 ng/L CH <sub>3</sub> Hg(I) 0.016 ng/L	7
Tap/brakish water	Hg(II), CH <sub>3</sub> Hg(I)	Dithiocarbamate resin	Acidified thiourea	3-10	555	FI-GC-MIP Hg(II) 0.15 ng/L CH <sub>3</sub> Hg(I) 0.05 ng/L	8
Water & sediment	Hg(II), CH <sub>3</sub> Hg(I)	Diethyldithiocarbamate grafted on polyurethane foam	n-butanol	4-7	100	HPLC-ICP-MS Hg(II) 4.6 ng/L CH <sub>3</sub> Hg(I) 5.2 ng/L	9

PF<sup>a</sup>: preconcentration factor, DT<sup>b</sup>: detection technique, LOD<sup>c</sup>: limit of detection, R<sup>d</sup>: Reference

1 (Houserova et al, 2007), 2 (Blanco et al, 2000), 3 (Cai et al, 1996), 4 (Hashempur et al, 2008), 5 (Yin et al, 2010), 6 (Margetinova et al, 2008), 7 (Jai et al, 2012), 8 (Emteborg et al 1993), 9 (Dos Santos et al 2009)

- (ii) Online preconcentration of mercury species (MeHg(I) and Hg(II)) were preconcentrated on C18 after their complexation with ammoniumpyrrolidine dithiocarbamate (APDC) using Flow Injection-Cold Vapor Atomic Absorption Spectrometry (FI-CV-AAS). The selective separation of mercury species was based on the strength of the reducing agent and solution acidity. The use of (1 mol/L HCl + 0.75% sodium borohydride) and (5 mol/L HCl + 0.0001% sodium borohydride) permitted the selective determination at ng/L levels of MeHg(I) and Hg(II) respectively (Segade et Tyson, 2007). Another online CV-AAS method for the non-chromatographic speciation of mercury using APDC as complexing agent. It is based on the strong adsorption of  $\text{Hg(PDC)}_2$  and the weak adsorption of  $\text{CH}_3\text{HgPDC}$  on polytetrafluoroethylene (PTFE) allowing their separation by using different reducing agents;  $\text{NaBH}_4$  for MeHg(I) and  $\text{SnCl}_2$  for Hg(II) (Zachariadis et al, 2004).

Table A.I.3: Non-chromatographic speciation of mercury.

Matrix	Species	Adsorbent	pH & ST <sup>a</sup>	Eluent	PF <sup>b</sup>	DT <sup>c</sup> & LOD <sup>d</sup>	R <sup>d</sup>
Seawater, estuarine water	Hg(II), CH <sub>3</sub> Hg(I)	poly(acrylamide) grafted onto cross-linked poly(4-vinyl pyridine)	pH: 1-8 Hg(II) pH: 4-5 CH <sub>3</sub> Hg (II)	14.3 M HNO <sub>3</sub>	20	CV-AFS Hg(II): 2 ng/L	1
River water	Hg (II), CH <sub>3</sub> Hg(I)	2-mercaptobenzimidazol loaded on silica gel	pH: 0-10 Hg(II) pH: 2-10 CH <sub>3</sub> Hg(I)	Hg(I): 0.05 M KCN CH <sub>3</sub> Hg(I): 2 M HCl	250	FI-CV-AFS Hg(II): 0.07 ng/L CH <sub>3</sub> Hg(I): 0.05 ng/L	2
NIST 1572, MESS-3, DOLT-2	Hg(II), CH <sub>3</sub> Hg(I)	Diphosphoric acid diacyl ester/C18	pH: 0-5 HgT: (0.3% NaBH <sub>4</sub> + 0.01% FeCl <sub>3</sub> ) Hg(II): 0.1 % NaBH <sub>4</sub>	Ethanol	-	FI-CV-AAS LOD: 10 ng/L	3
River water	Hg(II), CH <sub>3</sub> Hg(I)	Polyaniline	Hg(II) pH: 1-8, CH <sub>3</sub> Hg(I) pH>4	Hg(II): (0.3 % HCl+0.02 % thiourea) CH <sub>3</sub> Hg(I): 0.3 % HCl	Hg(II) 120 CH <sub>3</sub> Hg(I) 60	FI-CV-ICP-MS Hg(II) 2.52 pg, CH <sub>3</sub> Hg (I) 3.24	4
Lake, river, ground, seawater, marine fish	Hg(II), CH <sub>3</sub> Hg(I)	Diethyl dithiophosphate-Hg(II), Dithizone-CH <sub>3</sub> Hg(I)/ Knotted reactor	pH: 2 Hg(II): 0.02 % KHB <sub>4</sub> , MeHg(I): 0.5 % KHB <sub>4</sub>	15 % HCl	Hg(II) 13 CH <sub>3</sub> Hg(I) 24	FI-CV-AFS Hg(II) 3.6 ng/L CH <sub>3</sub> Hg (I) 2 ng/L	5
Tap water, seawater	Hg(II), CH <sub>3</sub> Hg(I)	Staphylococcus aureus loaded Dowex Optipore V-493	pH: 2	Hg(II) : 2 M HCl CH <sub>3</sub> Hg(I): 0.1 M HCl	25	CV-AAS Hg(II) 2.5 ng/L, CH <sub>3</sub> Hg(I) 1.7 ng/L	6
Drinking & pond water	Hg(II), CH <sub>3</sub> Hg(I)	C18/ammonium pyrrolidine dithiocarbamate	pH: 3-9 Hg(II): 5 M HCl+ 0.0001 % NaBH <sub>4</sub> CH <sub>3</sub> Hg(I): 1 M + 0.75% NaBH <sub>4</sub>	Hg(II) : 5 M HCl CH <sub>3</sub> Hg(I): 1 M HCl	9	FI-CV-AAS Hg(II) 0.25 ng/L, CH <sub>3</sub> Hg(I) 0.96 ng/L	7

**Chapter A: Mercury measurement methods, Introduction to the biogeochemical behavior of mercury**

Seawater & urine	Hg(II), CH <sub>3</sub> Hg(I)	Polytetrafluoroethylene/ ammonium pyrrolidine dithiocarbamate	pH: 2-3 Hg(II): SnCl <sub>2</sub> CH <sub>3</sub> Hg(I): NaHB <sub>4</sub> assisted by separation of Hg(PDC) <sub>2</sub> from CH <sub>3</sub> Hg(PDC) <sub>2</sub> by a separation column	Thermal desorption	-	FI-CV-AAS Hg(II) 0.04 µg/L, CH <sub>3</sub> Hg(I) 0.08 µg/L	8
------------------	----------------------------------	---------------------------------------------------------------------	--------------------------------------------------------------------------------------------------------------------------------------------------------------------------------------------------------------	--------------------	---	-------------------------------------------------------------------	---

ST<sup>a</sup>: separation technique, Pf<sup>c</sup>: preconcentration factor, DT<sup>b</sup>: detection technique, LOD<sup>d</sup>: limit of detection, R<sup>e</sup>: Reference

1 (Yayayuruk et al 2011), 2 (Bagheri et al 2001), 3 (Monteiro et al, 2001), 4 (Balarama Krishna et al 2010), 5 ( Wu et al 2006), 6 (Tuzen et al, 2009), 7 (Segade and Tyson 2007), 8 (Zachariadis et al 2004)



## **Part II: Biogeochemical behaviour and different transformation of mercury in the aquatic environment**

### **A.II.1. Mercury sources**

Mercury (Hg) is a global pollutant, because of its long range atmospheric transport conferred to its high volatility. Hg is not only found in uncontaminated sites but also in remote fresh water lakes (Hammersmidt et al, 2006) and Arctic regions (Lamborg et al, 2002). Arctic regions generally act as a sink for the anthropogenic Hg with high an average % MeHg of 2, posing a potential threat to wildlife (Jiang et al, 2011). In arctic Ny-Alesund, values of HgT and MeHg in sediments can reach of 21 - 48 ng/g, 0.4 - 1.1 ng/g respectively (Jiang et al, 2011). Higher concentrations of HgT (102 - 239 ng/g) and MeHg (0.33 - 2.38 ng/g) were found in Alaska (Hammerschmidt et al, 2006). Sonke and Heimbürger (2012) used an advanced transport model for modelling the Arctic Hg cycle. The authors suggest that in Arctic regions riverine and coastal erosion are the same or even greater in magnitude than atmospheric deposition in. Therefore, they assumed that Arctic region is not a sink for anthropogenic Hg emissions.

Mercury is considered as a substantial environmental pollutant. There are two major sources of mercury pollution natural and anthropogenic inputs. Human activities contribute to the largest percentage of mercury flux to the biosphere (Selin 2008). Major anthropogenic mercury emissions are: coal-fired power and heating plants (45 %), gold mining (24 %) and metal smelters (10%) (Lambert et al, 2012). Minor sources are waste incinerators, cement production, chlor-alkali plants and deforestation. Chlor-alkali plants were historically important as a major pollutant. Nowadays, they are not considered as a considerable mercury source. Mercury electrodes were substituted by membrane-based production that contributed to lower levels of pollution. Coal-fired power plants are the largest source of anthropogenic mercury emissions in the US and Canada (Corbitt et al, 2011). The greatest emitting Asiatic countries are China and India contributing to 67% of mercury global emissions (Pacyna et al, 2010). Mercury sources in coastal marine ecosystems originate mainly from atmospheric emissions and of wet and dry depositions (Manson et al, 2012). Inputs to coastal-marine systems are also via watershed either by diffusion or through the direct discharges in the coastal waters (Costa et al, 2012). Legacy sources are other important inputs, through remobilization phenomena or persistence of mercury in the biosphere (Davis et al, 2012).

Mercury mines can contribute to exceedingly high levels of HgT and therefore MeHg in vicinity environments (soil, water, sediment and atmosphere) (table A.II.1). Worldwide famous Hg-mines Almaden (Spain), Wanshan and Xungang (China), Idrija mine (Slovenia), California and Alaska (USA) are the major sources of mercury to the environment and considered as hotspots for Hg pollution. Almaden mine is the largest Hg mine in the world that continued mercury extraction for more than 2000 years and ceased in 2002. Idrijca mine is the second largest Hg mine with more than 500 years of continuous extraction and retorting of Hg ores. Agricultural lands near of these sources have high levels HgT and MeHg in soil enhanced by high levels of gaseous elemental mercury. It has been demonstrated that agricultural soils cultivated with rice near an active Hg mine in Xunyang in China were heavily polluted with mercury. Moreover, significant correlations were found between MeHg in rice, HgT soil, MeHg rice and MeHg soil, MeHg rice and gaseous elemental mercury. These relations indicate a potential bioaccumulation of MeHg in rice, an exposure pathway for humans (Qiu et al, 2012).

**Table A.II.1.** Hg concentrations in water and sediments of the world's largest Hg mines.

Mercury mines	Water		Sediment		R*
	HgT (ng/L)	MeHg (ng/L)	HgT (µg/g)	MeHg (ng/g)	
Almaden mine-Spain	7.6-13000	0.41-30	2.67-2300	0.32-82	1
Idrijca mine- Slovenia	15-283	0.21-0.53	30-4000	0.01-11	2,3
Abbadia San Salvatore mine-Italy	3.8-1400	0.14-3	15-0.26	8.7-0.2	4
Southwest Alaska-USA	1-2500	0.01-1.2	0.9-5500	0.05-31	5
California mine-USA	1400-19000	0.96-4.5	0.4-220	1.1-150	6, 7
Nevada mine-USA	6-2000	0.039-0.92	0.17-170	0.12-0.95	8
Wachuan mine-China	13-2100	0.093-1.1	90-930	3-20	9
Palawan Hg mine- Philippines	170-330	< 0.02-0.33	3.7-15	0.28-3.9	10

1 (Gray et al, 2004), 2 (Hines et al, 2000), 3 (Kocman et al, 2011), 4 (Rimondi et al, 2012), 5 (Gray et al, 2000), 6 (Rytuba et al, 2003), 7 (Davis et al, 2008), 8 (Gray et al, 2002), 9 (Li et al, 2012), 10 (Gray et al, 2003).\* Reference

## A.II.2. Mercury exposures

Mercury pollution is generally localized near estuaries, related to human settlement and industrial activities that are common near coasts. Estuaries include habitats of tidal marshes and sub-tidal marshes, which are potent sites for Hg methylation (Heim et al, 2007). The

highest mercury poisoning incidents was in Minamata 1950. It was due to a production plant for the synthesis of acetaldehyde using mercury as catalyst with effluent discharges to Shiranui Sea. This incident has caused methylmercury biomagnification through the food chain. People who ate the fish have been poisoned and suffered from neurological problems, death of babies in pregnant women and mental retardation. Moreover, born babies have suffered from physical deformation. Adults suffered from problems with vision, sensory disturbances and even difficulties in walking (Harada, 1995). Furthermore, in Iraq Minamata disease have also occurred in 1970, people were exposed to high levels of MeHg by consuming bread treated with fungicide containing mercury (Marsh et al, 1987). Mercury intoxicification is also observed in Canada, which is caused by a caustic soda factory. Hair mercury values of residents have also exceeded 50 mg/Kg (Harada et al, 1977). The U.S EPA reference dose (RfD) for methylmercury is 0.1 µg/kg body weight/day. The World Health organization has set 0.5 mg/Kg dry weight of MeHg in fish as consumption advisory limit for Hg and 5 µg/Kg bw/week as the permitted weekly intake (WHO, 1995).

The bioaccumulative character of mercury enters the food chain first at the base of planktons or benthic fauna and then biomagnifies within the chain to higher trophic levels (figure A.II.1). The greatest bioconcentration of Hg(II) and MeHg occurs between water and macrophytes/epiphytes which is the dominant MeHg source for macroinvertebrate primary consumers (Cremona et al., 2009). The bioaccumulative character of MeHg comes from the cellular distribution coefficient. Its lipophilic properties lead to its prompt passive diffusion into the cytoplasm of organisms whereas inorganic mercury remains adhered to cellular membrane (Mason et al, 1996). Moreover, the rate of MeHg adsorption is much higher than its excretion, explaining the increasing levels of mercury in the biotic chain (Hammerschmidt and Fitzgerald, 2006a). The addition of selenite and/or (Seleno-cystine and selenomethionine) to food is shown to increase MeHg elimination by gold fish (*Carassius Auratus*). MeHg mercury is found to be lost completely from the entire body rather than from a single organ (Bjerregaard et al, 2011). The final product of detoxification process is demonstrated to be mercury selenide complex HgSe(s) with a molar ratio near 1:1.

In fresh water ecosystems, mercury concentration in fish tends to decrease rapidly in response to a decline in mercury atmospheric deposition assisted by a gradual decrease of mercury inputs from watersheds (Knights et al, 2009). High concentrations of mercury were reported for higher trophic level fish species in the Atlantic and Pacific Ocean (Sunderland, 2007). Top

predator species that are commonly consumed by humans are: Tuna (*Scombridae spp.*) and Swordfish (*Xiphias gladius*). These two fish species are reported to have the highest total mercury concentrations in most regions of the world (Lambert et al, 2012). Methylmercury exposure relative to fish-consumption varies between one country and another (Table A.II.2). Tuna and swordfish account for half of mercury intake by the US population (Sunderland et al, 2007). However, in other countries, such as Greenland, whale and seal meat accounts for the dominant population exposure to methylmercury (Johansen et al, 2004).

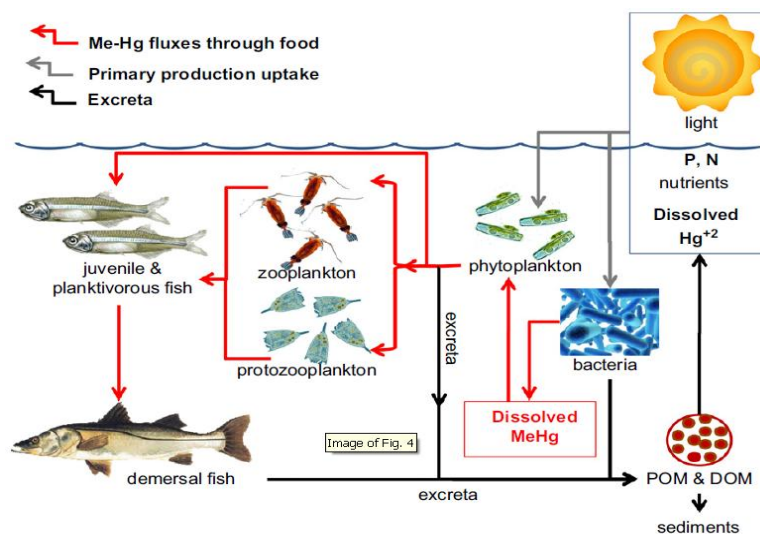


**Figure A.II.1:** Bio-magnification of MeHg through a tropical estuarine food chain (Kehrig, 2011).

Moreover, estuaries are a significant fish source to human and wildlife where estuarine fisheries become the major vector for methylmercury intoxicification (Sunderland 2007). About 90% of total Hg in fish muscle is present as MeHg (Downs et al, 1998). Methyl mercury also poses serious health problems to wild life. Exposure of MeHg to birds and fish leads to reproduction impairments (Scheuhammer et al, 2007). The bird exposure to MeHg in contaminated habitats may lead to defects during early developments (embryos, chicks) or leading to non-hatch eggs and can reduce reproduction. Estuarine mammals are less studied than birds for MeHg bioaccumulation. The most famous bioaccumulators of MeHg are seals and small tidal marsh mammals (endemic shrews). In fish species, MeHg can damage cells and tissues and impair reproduction. Most common species tend to have high MeHg concentrations that is relative to their big-size body are e.g. Leopard Shark, Striped bass, White Sturgeon, King mackerel and Brown Smooth Hound Shark (Davis et al, 2012). Rusty

Black birds breeding in the Acadian forest of northeastern North America are undergoing the fastest decline in population loss due to MeHg bioaccumulation (Edmonds et al, 2012).

Methylmercury is a potent vertebrate neurotoxin and is considered as the most toxic mercury specie. High concentrations of MeHg can cause neurotoxicological and cardiovascular effects in humans. After MeHg exposure through fish consumption, MeHg can be readily adsorbed and distributed throughout the body. Higher levels of MeHg were found in the blood taken from the umbilical cord than the blood in other parts of the body in pregnant women. Therefore, MeHg can easily cross the placenta and accumulates in the fetus. Post-natal mercury exposure can have adverse effects on memory, verbal learning, skills and general intelligence (Axelrad et al, 2007) since the ability of Hg to impair protein synthesis in fetal brains.

**Table A.II.2:** Worldwide distribution of HgT and MeHg concentrations in muscle tissues (dry weight) of various fish species.

Species	HgT (µg/g)	MeHg (µg/g)	Ref
Leporinus sp. (Aracu)- Cahoeira de Piria-Brazil	0.0461-0.271		1
Pseudoplatystoma sp. (Surubim)- Cahoeira de Piria-Brazil	0.375-0.869		1
Hoplias malabaricus (Traira)- Cahoeira de Piria-Brazil	0.231-2.696		1
White fish-Lake, MacKenzie River basin-USA	0.04-0.35		2
Lake Trout- Lake, MacKenzie River basin-USA	0.21-0.77		2
Walleye- Lake, MacKenzie River basin-USA	0.26-1.43		2
Burbot- Lakes Northern Canada	0.21		3
Brook Trout- Lakes Northern Canada	0.106		3
Chinook Salmon- Lakes Northern Canada	0.09		3
Pike- Lakes Northern Canada	0.378		3
Pacific Herring- Lakes Northern Canada	0.031		3
Arctic Charr- French Alps lakes	0.168-0.23		4
Sebastes schlegell (Rockfish)- Lake shihwa, Korea	0.008-0.0364		5
Acanthogobius hasta (Goby)- Lake shihwa, Korea	0.011-0.052		5
Silurus glanis- Ebro River basin, Spain	0.179-1.559	0.285-1.225	6
Gray fish- Ebro River basin, Spain	0.39-0.786	0.283-0.554	6
Cichla spp – Rio Tapajos, Brazilian Amazon		0.038-1.43	7
Acestrorhynchus altus – Itenz River basin, Bolivian Amazon	0.021-0.22		8
Hoplias malabaricus - Itenz River basin, Bolivian Amazon	0.029-0.319		8
Scyliorhinus canicula (Spotted dogfish)- Atlantic Ocean	0.13-0.8	0.05-0.52	9
Salmotrutta- Idrija mercury mine area, Slovenia	0.092-0.33	0.092-0.301	10
Oncorhynchus mykiss- Idrija mercury mine area, Slovenia	0.463-1.44	0.35-0.834	10
Salmo marmoratus- Idrija mercury mine area, Slovenia	0.105-1.15	0.105-1.172	10
Pontoporia blainvillei (Dolphins)- Southwest Brazil *	0.66-9.65	0.12-2.36	11
Ringed seals-Western Arctic	0.11-1.49	0.1-1.58	12
Belgus- Western Arctic	0.35-3.16	0.41-3.44	12
Prionace glauca (Blue sharks)- Atlantic Ocean	0.18-1.95		13
Xiphias gladius (Swordfish) – Atlantic Ocean	0.026-2.4		13
Tiger Shark- Ishigaki Island, Japan	0.38-1.34		14
Silvertip Shark- Ishigaki Island, Japan	1.19-2.35		14
Ziphius Cavirostris –Adriatic sea, Italy	9.68	7	15
Killer Whale-Japan **	17.4-81	10.3-13.3	16
Orcinus orca (Killer Whale) – Northern Japan	1.06-1.46	0.77-1.06	17
Sotalia guianensis (Guinea Dolphins)- Coast Rio de Janeiro, Brazil	0.2-1.66		18
Grampus griseus (Risso dolphin) –Adriatic sea, Italy	30.87	14.96	15
Bottlenose Dolphin –Japan **	6.59-98.9	0.58-15.8	16

1 (Lima et al, 2005), 2 (Evans et al, 2005), 3 (Lockhart et al, 2005), 4 (Maruszczak et al, 2011), 5 (Oh et al, 2010), 6 (Carrasco et al, 2011), 7 (Kehrig et al, 2008), 8 (Pouilly et al, 2012), 9 (Coehlo et al, 2010), 10 (Miklavcic et al, 2013), 11 (Seixas et al, 2008), 12 (Wagemann et al, 1998), 13 (branco et al, 2007), 14 (Endo et al, 2008), 15 (Storelli et al, 1999), 16 (Endo et al, 2004), 17 (Endo et al, 2006), 18 (Moura et al, 2012). \* HgT in liver ; \*\* destined for human consumption

### A.II.3. Global Mercury cycle

Human activities have altered mercury cycle locally, regionally and globally. Mercury emissions and concentrations in the environmental compartments have increased up to 5 times higher than the past 150 years (Sunderland and Mason 2007). Anthropogenic inputs have been decreasing during the past decades; however mercury concentrations in various environmental compartments are still high because of the lag-time in natural systems.

The general biogeochemical cycle of mercury includes atmospheric transport, land and ocean deposition and finally volatilization (figure A.II.2). The lifetime of mercury in atmosphere-ocean-terrestrial system against transfer to sediments is about 3000 years (Selin et al, 2008). It is important to understand the preindustrial mercury emissions to have a global sight on the amount of mercury circulating in the environmental compartments before industrialization. Preindustrial mercury emissions can be evaluated from the ratio of present-day and preindustrial emissions depositions. Mercury deposition is about three to five folds greater than preindustrial mercury depositions. Investigated glacial cores revealed 20 times greater mercury deposition since 1840 (Schuster et al, 2002).

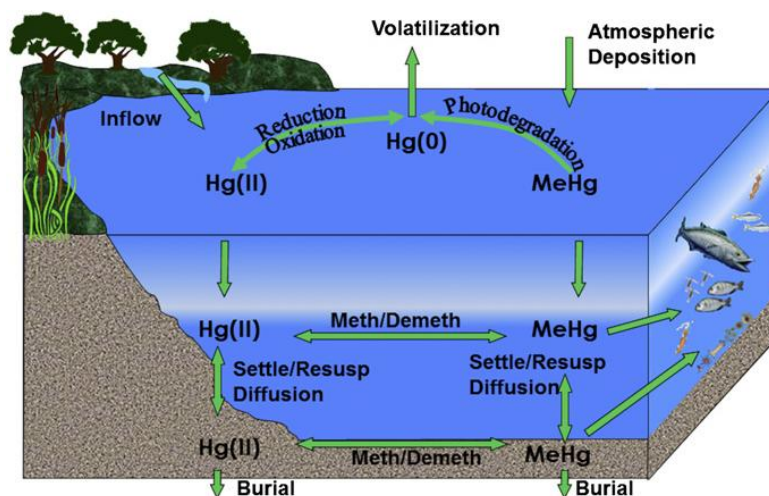


**Figure A.II.2:** Hg biogeochemical cycle, an example in the Gulf of Mexico (Harris et al, 2012).

#### A.II.3.1. Atmospheric depositions

Emissions to the atmosphere can be from natural and anthropogenic sources. Primary emissions include geological activities such as volcanos and land emissions. Primary land emissions are areas around mercurifours belts (North America, Southern china and central Europe). These areas are rich in cinnabar ore (HgS). Estimates of mercury release from Hg-

rich rocks is 10-20 mega gram Mg/year (Gustin et al, 2008) and from land emissions (volcanoes and hot springs) about 60 Mg/year (Varekamp and Buseck 1986). The total mercury budget from geological activities is about 800-3000 Mg/year (Gustin et al, 2008).

The total anthropogenic atmospheric Hg emissions are estimated to be about 2200-4000 Mg/year (Pacyna et al, 2011). The major anthropogenic source is fossil fuel combustion particularly coal. Other industrial activities can also participate in the anthropogenic emissions including gold mining, pig iron, caustic soda production, cement, steel production and waste incineration. About 450 Mg/year, 25 Mg/year, 300 Mg/year mercury emissions from gold mining, fossil fuel combustion and industries respectively (Selin et al, 2008).

Natural emissions of mercury are in the form of  $\text{Hg}^\circ$ , while issued from anthropogenic origin is in the form of  $\text{Hg(II)}$  and particulate mercury  $\text{Hg}_p$ . The major mercury specie in the atmosphere is elemental mercury  $\text{Hg}^\circ$  and other minor species of  $\text{Hg}_p$ , reactive gaseous mercury ( $\text{HgCl}_2$ ) and dimethylmercury (DMHg). The concentration of total gaseous mercury (TGM) in non-polluted zones is 1-2  $\text{ng/m}^3$  (Munthe et al, 2003) and in urbanized areas < 30  $\text{ng/m}^3$  (Fitzgerald and Lamborg, 2005). Mining and industrial zones using Hg in their process, experience TGM 4 times higher than normal levels (Feng and Qui, 2008).  $\text{Hg}^\circ$  is volatile and has a long residence time estimated to be 1.2-1.7 years (6-12 months) (Lamborg et al, 2002). Thus, undergoing long-range transport proven by considerable mercury concentrations in remote Arctic areas. In the atmosphere, mercury reacts with major oxidants, halogen radicals ( $\text{Br}^\circ$ ,  $\text{BrO}^\circ$ ,  $\text{Cl}^\circ$ ,  $\text{ClO}^\circ$ ) catalyzing the photochemical reactions to form reactive gaseous mercury (RGM) and particulate mercury. These two chemical forms have short atmospheric residence time favoring their deposition to the underlying lands and water bodies (Steffen et al, 2008).

The main removal of mercury from atmosphere is by wet deposition of  $\text{Hg(II)}$  (Fitzgerald et al, 1991) and dry deposition of reactive gaseous mercury (RGM) (Mason et al, 2001).  $\text{Hg(II)}$  and  $\text{Hg}_p$  are more soluble in water and tend to deposit more easily by wet and dry processes on terrestrial and water bodies. A MeHg deposit represents about 0.5% of total mercury and thus is not a significant contributor of pollution to the environment (Hammerschmidt et al, 2007). Methylmercury concentrations in the environment are shown to be well correlated with RGM contained in the precipitation (Hammerschmidt et al, 2007).



### *A.II.3.2. Terrestrial surface-air mercury cycle*

Mercuriferous zones are rich in Hg ores, in the form of cinnabar (Red HgS), small quantities of metacinnabar (Black HgS) and rock inclusions of elemental mercury with other minerals. Biomass burning enhances mercury emissions and is estimated to have a global flux of mercury of about 670 Mg/year (Weiss-Penzias et al 2007). For example, 1400-3200 Mg/year is estimated from forest fires of Tennessee (Lindberg et al, 1998). The dominant forms of mercury in soils and sediments are IHg and MeHg. Concentrations of IHg in different types of sediments is between 1 - 10<sup>6</sup> ng/g whereas values of MeHg hovers around between 10<sup>-2</sup> - 10<sup>2</sup> ng/g constituting 0.1 - 2 % of HgT concentrations (Benoit et al, 2003). MeHg concentrations in lacustrine and estuarine sediments are much higher than that of marine sediments (Fitzgerald et al, 2007).

In solid phase, mercury preferentially binds to the fine particles with large specific area. Sediments with high content of organic matter and of clay-silt composition tend to have elevated quantities of mercury. Sediments with gravel, mud and sand have mercury concentrations near background concentration (Loring et al, 1982). In oxic conditions, IHg and MeHg form complexes with iron and manganese oxides and hydroxides (Quemerais et al, 1998). In anoxic sediments, mercury associates with FeS and pyrite FeS<sub>2</sub> where insoluble form of HgS prevails (Morse and Luther III, 1999). However, with increasing sulfur concentrations, soluble complexes are formed HgS<sub>2</sub><sup>2-</sup> (Paquette and Helz, 1997). Therefore, the major solid forms of ambient Hg(II) in anoxic sediments are: complexes with organic matter, complexes at the surface of FeS(s) and complexes with two crystalline forms cinnabar and metacinnabar (Charnock et al, 2003). These solid phases can contribute to bioavailable mercury to methylation through solid-phase dissolution and surface desorption. Methylation rates were highest in the presence of free Hg(II), followed by mercury complexed to organic matter, Hg-FeS complexes, Hg-cinnabar complexes and finally Hg-metacinnabar complexes (Jonsson et al, 2013).

The soil represents a huge mercury reservoir enriched from atmospheric depositions and from the Hg-rich lithosphere. Thereby, soil and forests represent the major sinks of mercury from the atmosphere (Fitzgerald and Lamborg, 2003). The predominant specie of mercury deposition is Hg(II). Deposited Hg(II) is readily available for reduction and evasion as Hg<sup>0</sup>. About 60 % of newly deposited Hg(II) on water and ice is readily re-volatilized and recycled to the atmosphere (Hintelmann et al, 2002). Part of deposited Hg(II) that does not evade is

incorporated by plants. Hg-thiosulphate complexes are mobile (Yin et al, 2012) promoting its bioavailability and its uptake by the plants. Wet and dry Hg deposition can render Hg(II) on vegetation leaves whereas Hg<sup>0</sup> can be incorporated directly into the leaf through gas-exchange at the stomata (Lindberg et al, 1992). Mercury soil enrichment can be by litter-fall of Hg-incorporated plants. Mercury in soil is mostly retained to organic matter particularly sulfides and Fe and Al oxyhydroxides (Skylberg et al, 2003). An important part undergoes physical transformation (erosion) and other part biochemical transformation (methylation biotic and abiotic reduction). The total global soil mercury concentration is in the order 10<sup>6</sup> Mg for the top 15 cm of soil (Selin et al, 2008) and human activities have increased the burden up to 15 %. Exchange reactions with chloride and sulfide mobilizes mercury (Shuster, 1991) where it binds to dissolved organic matter and therefore reaches the aquatic system.

#### ***A.II.3.3. Freshwater-air mercury cycle***

The main dominant mercury species in water ecosystems are IHg and MeHg. In addition, to minor participation of Hg<sup>0</sup> and DMHg (Cossa et al, 1997). In oxic conditions, mercury is complexed by chlorides and hydroxides depending on pH, salinity and concentration (Dyrssen and Wedborg 1980) with dominant binding of IHg and MeHg with chloride (Fitzgerald et al, 2007) and minor participation of hydroxides (Lamborg et al, 2003). For Wallschager et al, (1998), the major Hg forms are: HgCl<sub>2</sub>, Hg(OH)<sub>2</sub>, HgOHCl, Hg-thiol constituting the water-soluble mercury fraction, the mobile and the bioavailable forms. In anoxic conditions, the speciation of IHg, MeHg is controlled by inorganic (Morse and Luther III, 1999) and organic sulfur (Skylberg et al., 2006).

The most significant input of mercury to water bodies is atmospheric mercury deposition. Run-off from continents and river discharges are other sources of inorganic mercury to coastal environments, however it is not considered for the global mercury cycle because of the short residence time of particulate mercury (Lamborg et al, 2002). Wet and dry deposition of mercury enrich freshwater ecosystem with dissolved mercury, in which part of it evades promptly to the atmosphere and only a small part undergoes methylation. Once deposited to the water body, it enters a complex biogeochemical cycle. Biogeochemical cycle controls the speciation of mercury and its availability. It can be reduced, scavenged or methylated depending on the local conditions. In water column it can be methylated and subsequently enters the food chain. Wetland and lake environments are favorable ecosystems for mercury methylation. Methylmercury production occurs at the geochemical interface between oxic

and anoxic conditions (Hintelmann et al, 2000). Many proxies affect MeHg production including Hg(II) availability, sulfide, redox potential and total organic carbon . Inorganic mercury can be scavenged by suspended particles and sulphides to the bottom and can be remobilized by different processes such as bioturbation. Eventually, mercury can be reduced biotically and abiotically and evade into the atmosphere.

#### **A.II.3.4. Air-Ocean mercury cycle**

In marine waters, there are four major mercury species: inorganic mercury Hg(II), volatile mercury Hg<sup>0</sup>, methylmercury (CH<sub>3</sub>Hg<sup>+</sup> or MeHg) and dimethylmercury ((CH<sub>3</sub>)<sub>2</sub>Hg or DMHg) including particulate and colloidal mercury. DMHg is gaseous and considered as toxic species of mercury despite its hydrophilic character (log Kow: 2.59) (Manson et al, 1996). Total mercury concentrations in Oceans ranges from 1.2 pM Pacific Ocean (Laurier et al, 2004), 2.4 pM Northern Atlantic (Sunderland et al, 2007) and 2.5 pM in the Mediterranean (Cossa et al, 1997) (Table A.II.3).

**Table A.II.3:** Concentration of Hg in open ocean and seawater from around the world.

Locations	Unfiltered HgT (ng/L)	Filtered HgT (ng/L)	DGM (fM)	Ref
West Atlantic Ocean	-	0.162	244	1,2
West Atlantic Ocean	2.35	1.19	134	3
East Atlantic Ocean	0.3	-	80	4
North Pacific Ocean	0.34-4.43	-	-	5
Arctic Ocean	-	-	25-67	6
Coastal France	-	0.318	-	7
North Sea & English channel	0.455	0.318	-	8
North Sea	0.181-0.963	-	-	9
Open Baltic Sea	-	0.1-3.9	-	10
Yellow Sea	1.34-5.5	-	30-648	11
Mediterranean Sea	0.082-0.532	-	230	12

1 (Lamborg et al, 2012), 2 (Manson et al, 2001), 3 ( Soerensen et al, 2013), 4 ( Kuss et al, 2011), 5 (Laurier et al, 2004), 6 (Andersson et al, 2008), 7 (laurier et al, 2003), 8 (Leermakers et al, 2001), 9 (Coquery et al, 1995), 10 (Saniewska et al, 2010), 11 (Ci et al, 2011), 12 (Kotnik et al, 2007).

In the marine ecosystem, the major supplier of Hg(II) is by atmospheric deposition. Oceans are considered as a phenomenal sink of atmospheric mercury, which is estimated to be in the order of 2000 Mg/year (Lamborg et al, 2002). Ocean circulation can play the role of a sink or a source of mercury to distant regions such as in North Pacific Ocean where ocean circulation acts as a source of mercury (Lambert et al, 2012). In the euphotic zone, Hg<sup>0</sup> is produced from both photochemical and biological reduction of Hg(II) (Whalin et al, 2007) and MeHg degradation (Chen et al, 2003). Whereas, in the aphotic zone, Hg(II) undergoes biotic reduction and MeHg demethylation in zones where light does not penetrate. Normally, at

surface of water columns, concentrations of methylated mercury are low due to photodemethylation. However, MeHg levels are compensated by the fact that, water column mixing transports MeHg and DMHg from sub surface to surface where primary production is the highest. Vertical mixing attributes to additional MeHg, as DMHg undergoes photodegradation to MeHg (Sommar et al, 1996). Hg(II) can be subjected to lateral transport, vertical settling by suspended particulate matter or evades to the atmosphere as Hg<sup>0</sup>. Hg flux to the atmosphere is estimated to be 0.1-44 ng/m<sup>2</sup>/h for the Mediterranean (Gardfeldt et al, 2003), 14.8 ng/ m<sup>2</sup>/h for the Gironde estuary, 10.7 ng/m<sup>2</sup>/h for the Scheldt estuary, 10.7 ng/m<sup>2</sup>/h for the Arcachon estuary and 4.7 ng/m<sup>2</sup>/h for theThau Lagoon (Sharif et al, 2013). The global mercury flux from oceans is of the order of 800 Mg/year (Lamborg et al, 2002). In most of the scientific observations in oceans, Hg(II) enrichment in subsurface is typically less than surface because of long scales of lateral and vertical transport to deep oceans (Sunderland et Mason , 2007)

Local methylation and demethylation control the quantity of MeHg in water column and how mercury is available to biomagnification throughout the food chain. Hg(II) methylation is the principal source of methylated mercury in water column (Lehnherr et al, 2011). In marine water, DMHg is the principal methylated form of mercury. It is explained to be the primary product of Hg(II) methylation in marine waters and then MeHg is produced by DMHg reduction (Manson et al, 1995). Methylation of mercury is also observed to occur in sub-thermocline depth (Kirk et al, 2008). MeHg production in oceans depends on Hg(II) supply and organic carbon mineralization by microbial decomposition. Hg(II) methylation in sediments can occur, thereby acting as both sink or source of mercury to water column depending on the conditions. Sediments are considered as an important source of MeHg through diffusion, particle settling, resuspension and bioturbation (Hollweg et al, 2009). Moreover, Sediments can sequester Hg through particle settling and sediment burial acting as a sink. Horizontal mixing can be a source for open ocean ecosystems for MeHg formed in coastal ecosystems (River drainage). *In situ* methylation associated with decomposition of organic matter is the major source of MeHg in oceans referred to fluxes from deep sea-sediments. Methylation of mercury is observed in different aquatic environments e.g. water column (Monperrus et al, 2007), continental shelf region (Hammerschmidt et al, 2007), estuaries (Heyes et al, 2006) and hydrothermal vents (Kraepiel et al, 2003). Other minor sources of MeHg to oceans include: atmospheric inputs, hydrothermal fluids, riverine inputs.

Other additional minor sources comprise the decomposition of (CH<sub>3</sub>)<sub>2</sub>Hg and remineralization of sinking particles (Lehnherr et al, 2011).

Demethylation of MeHg can be by both light photodemethylation and dark microbial demethylation (Lehnherr et al, 2011). Microbial demethylation can occur throughout the water column whereas; photodemethylation is restricted to the euphotic zone. It is shown that, the rate of MeHg demethylation is slower in seawater than in fresh water. This is due to the presence of high concentrations of chloride ions, thus controlling the mercury speciation. In marine waters, CH<sub>3</sub>HgCl is the major form of MeHg which is resistant to demethylation explaining therefore the slower rates observed (Zhang and Hsu-Kim, 2010).

#### **A.II.4. Biogeochemical behavior of mercury species in the aquatic environments**

To date, strains of bacteria that were capable of methylating Hg, belong to Delta Proteobacteria classification (Lin et al, 2012). Sulfate-reducing bacteria (SRB) are the major methylators for mercury in nature with favoring conditions: low pH, high DOM and low dissolved oxygen (Acha et al, 2011). Anaerobic biotic conditions are the most favorable conditions for methylation (Rodriguez Martin-Doimeadios et al, 2004). In anoxic sub-surface zone of lakes and sediments rich in sulfate, SRB use sulfate as terminal electron acceptor converting it into sulfides (Harmon et al, 2007).

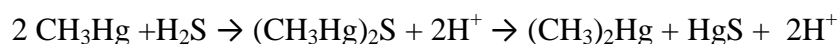


However, studies revealed that there are other types of microorganisms involved in methylation depending on the environmental conditions such as iron reducing bacteria, methanogens and macroalgae (Pongratz and Heumann, 1998). Iron reducing bacteria belonging to Deltaproteo bacteria and are shown to be among the biotic methylators of mercury (Kerin et al, 2006). In summer season, methylation potential is highest because of enhanced sulfate reduction by SRB. However, in winter Iron reducing bacteria (IRB) intervene as important methylators for mercury (Hines et al, 2012). There are microorganisms isolated, showing methanogenic activities and abilities for methylating Hg, such as macrophytic periphyton and methanogens (*Methanococcales*, *Methanobacteriales*, *Methanosarcinales*) (Hamelin et al, 2011). Light conditions are shown to enhance methylation and methylation potentials were found higher in the presence of biogenic particles of phytoplankton and bacterio-plankton. Methylation was found higher in the euphotic zone of

the Mediterranean waters, mainly mediated by heterotrophic microorganisms (phytoplankton) (Monperrus et al, 2007). In deep ocean, MeHg is stable and it can be transported long distances from its origin site of production. In coastal waters, MeHg is rather unstable due to the photochemical reduction and oxidation that are predominantly controlled by photochemical reactions (Whalin et al, 2007). Different pathways for mercury uptake for microbial methylation exist including, enzymatic reduction (Glimour and Henry, 1991) or transmethylation (Quevauviller et al, 1992). Passive diffusion of neutrally charged mercury complexes is thought to be the main transport mechanism of microbial methylation (Najera et al, 2005). However, recent studies have shown that mercury transfer did not occur by passive diffusion but rather by active uptake facilitated by membrane transport proteins (Acha et al, 2011). Scientists have hurdled the knowledge gap of the major biogeochemical pathways for Hg methylation in the microbial cell. One mechanism identified linked to a specific methyltransferase occurring through methylcobalamin compounds and acetyl-coenzyme A (Parks et al, 2013). Recent studies have shown a different type of pathway consisting of corrinoid proteins facilitating methyltransfer and ferredoxin responsible for the corrinoid reduction and the consequent methylation of mercury. Corrinoid proteins and ferredoxin are coded by two gene cluster *hgcA* and *hgcB* evidenced in *Desulfovibrio desulfuricans* ND 132 and *Geobacter sulfurreducens* PCA (Parks et al, 2013).

Mercury can be released from three major bulk phases: the release of Hg trapped in organic matter by oxidation and microbial degradation at the surface-water interface. The release of Hg by reduction of ferrous and manganese bulk phases in suboxic zone or by the active solubilization of oxides by their use by microbes for the degradation of organic matter. Fe hydroxides reduction can release dissolved organic matter providing strong binding phases for mercury, decreasing or enhancing methylation depending on the prevailing geochemical conditions. Reduction of sulfide phases in the anoxic zone can subsequently release trapped Hg. Organic matter is a relevant binding phase to mercury through the thiol functional groups. When retained by sediment organic matter, its mobility is the matter of sediment aging where it gradually becomes associated with stronger binding sites in sediments. Organic matter is also responsible for the removal of Hg from water column through scavenging onto particulate organic matter, which is considered as important transport vectors for Hg pollution (Benoit et al, 2003). Once Hg is released, its mobility and diffusive flux depends on many factors including vertical position of redox transition zone, the activity of methylating and

demethylating bacteria and bioturbation. Elevated sulfide concentrations can enhance Hg solubilization (Benoit et al, 1998; Dyrssen and Wedborg 1991) particularly observed in cinnabar rich sites. Hydrogen sulfide produced from sulfate reduction can decrease Hg levels in pore water, by transforming Hg(II) into metacinnabar (HgS) or convert MeHg to dimethylmercury sulfide which in turn decomposes into volatile dimethyl mercury and metacinnabar (Baldi et al, 1995).



In the absence of sulfides and organic ligands, Hg(OH)<sub>2</sub> and HgCl<sub>2</sub> are two of the most dominant Hg species in natural water (Dyrssen and Wedborg, 1991). While in high salinity environments HgCl<sub>3</sub><sup>-</sup> and HgCl<sub>4</sub><sup>2-</sup> forms become predominant. Negatively charged mercuric chloride produces negative feedback on Hg methylation by reducing Hg bioavailability, while neutral mercuric chlorides (HgCl<sub>2</sub>) induce no effect (Barkay et al, 1997). In sulfidic rich environment, chloride and hydroxides are unlikely to compete with sulfides which are the dominant ligands for mercury complexation with outstanding stability constants, forming HgS<sup>o</sup> with logK: 25 for S<sup>2-</sup> concentration < 10<sup>-5</sup> M (Hammerschmidt et al, 2004) otherwise, HgS<sub>2</sub>H<sup>-</sup> forms with log K: 32 (Benoit et al, 1999a). The presence of super class ligands present in wastewater are capable of competing with sulfides for the speciation of mercury with an estimated logK: 30 (Hsu et Sedlak 2003). In oxic waters, Hg-DOM dominates Hg speciation showing a decline in Hg-S(-II) concentrations (Hsu et Sedlak 2003).

#### **A.II.4.1. Biogeochemical factors affecting mercury methylation**

To favor methylation, two of the most important geochemical factors are the supply of carbon, the electron donor for microbial degradation and electron acceptors such as sulfate. Estuaries and brackish water are characterized by non-limiting supply of sulfate and therefore are considered as hotspots for methylation (Branfireun et al, 2001). High organic matter maintains low redox potential through its degradation by microbes which consume oxygen, and decrease the redox potential close to the surface-water interface, essential for sulfate reduction and the subsequent methylation. Organic matter can simultaneously reduce the bioavailability of Hg(II) in the dissolved phase and stimulate the activity of methylating bacteria. Fine grained sediments rich in organic matter, are efficient scavengers of Hg as they settle out and enrich the bottom sediment with Hg. The Hg partitioning coefficient controls the distribution of Hg between dissolved and solid phases and is a crucial factor determining

the amount of Hg that is bioavailable. Dissolved organic carbon (DOC) is shown to affect the bioavailability of Hg(II) for methylation (Barkay et al, 1997). In sulfidic rich environments, the formation of polysulfides and dissolved organic carbon solubilizes Hg (Paquette et al, 1995). Sedimentary organic matter and AVS are important sinks of Hg in anoxic sediment. However, remobilization or other physical disturbance can cause their oxidation and the release of the scavenged Hg. In oxic sediment layers, Fe-Mn oxyhydroxides are known as important scavengers of Hg that limit their diffusive fluxes to the overlying water. When Fe-Mn oxyhydroxides are buried, they undergo reductive dissolution with the release of sequestered Hg to porewater (Gagnon et al, 1997).

Factors controlling Hg methylation can be also divided into those affecting the bioavailability of Hg for methylation and those affecting the activity of SRB. Factors affecting the activity of SRB are: temperature, sulfates, carbon supply and quality and the competition with other microorganisms. MeHg formation depends on several factors including temperature (Merritt and Amirbahman, 2008), ambient IHg (King et al, 1999), organic substrate (King et al, 2000), bacterial growth (Benoit et al, 2001a), intrinsic characteristics of the site (Canario et al, 2007), seasonal variation concerning the growth phase of vegetation that might influence the composition quality of the organic substances available for SRB (Weber et al, 1998) and AVS (Hammerschmidt and Fitzgerald 2004). The availability of  $\text{SO}_4^{2-}$  for SBR and the bioavailability of  $\text{Hg-S}^\circ$  are the most important factors for the determining of MeHg concentration in an environmental compartment (Skjellberg et al, 2008).

Inorganic mercury is a prerequisite for methylation particularly the dissolved fraction (Hammerschmidt and Fitzgerald 2006). However, Sunderland et al. (2006) have found high MeHg methylation rates in the presence of both high levels of DOM and S(-II). Neutral sulfide mercury complexes Hg-S(-II) ( $\text{HgS}^\circ + \text{Hg}(\text{HS})_2^\circ$ ) particularly those with specific low molecular mass ( $\text{HgS}^\circ$ ) are thought to be the most bioavailable forms for methylation accentuating the role of pore-water S(-II) in controlling Hg speciation (Benoit et al, 1999a). The speciation of Hg species depends on the pH. At pH 7, charged species  $\text{HgS}_2\text{H}^-$  are dominant over neutral species  $\text{Hg}(\text{HS})_2^\circ$  (Benoit et al, 1999a). The solubility of  $\text{HgS}(\text{s})$  is shown to be enhanced in the presence of  $\text{S}^\circ$  generated by polysulfides. S(-II) can even promote the formation of volatile MeHg (Baldi et al, 1993). S(-II) are found to increase in non-methanogenic zone in depth areas populated with SRB (Merritt et al, 2009). It remains confusing whether methylation is favored by low concentrations of S(-II) or it is the matter of



depth of highly populated bacteria and rapid cycling of organic matter. In contrary, Jay et al. (2002) have shown no relation between the increased solubility of IHg and MeHg methylation rates. Recent studies have demonstrated HgS(s) nanoparticles are more available to methylation than crystalline microparticulate HgS(s) attributed to their higher solubility and dissolution (Zhang et al, 2012). In fact, the presence of DOM enhance the bioavailabilty of Hg(II) by stabilizing HgS nanoparticles against growth and aggregation (Gerbig et al, 2011). A recent study has shown that DOM favors methylation by enhancing HgS nanoparticles under low sulfide concentrations of  $< 30 \mu\text{M}$  (Graham et al, 2013).

MeHg production depends on both microbial activity and diffusive uptake of mercury controlled by Hg-S(-II). The optimum S(-II) concentration is  $< 10 \mu\text{M}$  (Munthe et al, 2007). Above which S(-II) has no role in controlling Hg-S(-II) speciation. High levels of S(-II) can totally inhibit methylation. This is due to the formation of anionic Hg-S complexes that are not bioavailable as the neutral Hg-S complexes. Moreover, high concentrations of sulfides can lead to metal complexation with sulfur particularly Co, Ni and Zn that are required for metabolic enzymes (Ekstrom and Morel, 2007) which can induce a change in SBR community. The threshold of reactive sulfide (AVS) that can inhibit methylation is  $>0.03 \mu\text{moleS/g}$  (Hammerschmidt and Fitzgerald 2004).

## Referenecs

- Acha D, Hintelmann H, Yee J. Importance of sulfate reducing bacteria in mercury methylation and demethylation in periphyton from Bolivian Amazon region. *Chemosph.* 82 (2011) 911–916.
- Ahalya N, Ramachandra T.V, Kanamadi R.D. Biosorption of heavy metals, *Res. J. Chem. Environ.* 7 (2003) 71–79.
- Anderson AW, Merckling, NG, 1955, U.S. Patent 2, 721, 198. CA, 50, 3008.
- Andersson M.E, Sommar J, Gardfeldt K, Lindqvist O. Enhanced concentrations of dissolved gaseous mercury in the surface waters of the Arctic Ocean. *Mar. Chem.* 110 (2008) 190–194.
- Annadurai G, Juang R.S, Lee D.L. Adsorption of heavy metals from water using banana and orange peels. *Water Sci. Technol.* 47 (2002) 185–190.
- Axelrad D.A, Bellinger D.C, Ryan L.M, Woodruff T.J. Dose–response relationship of prenatal mercury exposure and IQ: an integrative analysis of epidemiologic data. *Environ. Health Persp.* 115 (2007) 4.
- Abollino O, Mentasti E, Porta V, Sarzanini C. Immobilized 8-oxine units on different solid sorbents for the uptake of metal traces. *Anal. Chem.* 62 (1990) 21–26.
- Balarama Krishna M.V, Chandrasekaran K, Karunasagar D. On-line speciation of inorganic and methyl mercury in waters and fish tissues using polyaniline micro-column and flow injection-chemical vapour generation-inductively coupled plasma mass spectrometry (FI-CVG-ICPMS). *Talanta.* 81 (2010) 462–472
- Baldi F, Parati F, Filippelli M. Dimethylmercury and dimethylmercurysulfide of microbial origin in the biogeochemical cycle of Hg. *Water. Air. Soil. Poll.* 80 (1995) 805–815.
- Baldi F, Pepi M, Filippelli M. Methylmercury resistance in *Desulfovibrio desulfuricans* strains in relation to methylmercury degradation. *Appl. Environ. Microbiol.* 59 (1993) 2479–2485.
- Benoit J.M, Gilmour C.C, Heyes A, Mason R.P, Miller C. 2003. Geochemical and biological controls over methylmercury production and degradation in aquatic ecosystems. In ACS Symp. Ser. 835, ed. Y Chai, O C Braids, pp. 262–97. Washington, DC: Am. Chem. Soc.
- Benoit J.M., Gilmour C.C, Manson R.P. The influence of sulfide on solid mercury bioavailability for methylation by pure cultures of *Desulfobulbus propionicus*(1pr3). *Environ. Sci. Technol.* 35 (2001a) 127–132.
- Benoit J.M, Gilmour C.C, Mason R.P, Heyes A. Sulfide controls on mercury speciation and bioavailability to methylating bacteria in sediment pore waters. *Environ. Sci. Technol.* 33 (1999 a) 951–957.
- Benoit J.M, Gilmour C.C, Mason R.P, Reidel G.S, Reidel G.F, 1998. Behaviour of mercury in Patuxent River estuary. *Biogeochemistry.* 40 (1998) 249–265.
- Blake D.A, Blake R.C, Khosraviani M, Pavlov A.R. Immunoassays for metal ions. *Anal. Chim. Acta.* 376 (1998) 13–19.
- Blanco R.M, Villanueva M.T, Uria J.E.S, Sanz-Medel A. Field sampling, preconcentration and determination of mercury species in river waters. *Anal. Chim. Acta.* 419 (2000) 137–144.

- Bagheri H, Gholami A. Determination of very low levels of dissolved mercury(II) and methylmercury in river waters by continuous flow with on-line UV decomposition and cold-vapor atomic fluorescence spectrometry after pre-concentration on a silica gel-2-mercaptopbenzimidazol sorbent. *Talanta*. 55 (2001) 1141–1150.
- Barkay T, Gillman M, Turner R. Effects of dissolved organic carbon and salinity on bioavailability of mercury. *Appl. Environ. Microb.* 63 (1997) 4267-4271.
- Bjerregaard P, Fjordside S, Hansen M, Petrova M. Dietary Selenium Reduces Retention of Methyl Mercury in Freshwater Fish. *Environ. Sci. Technol.* 45 (2011) 9793–9798.
- Bowen H.J.M, Absorption by Polyurethane Foams; New Method of Separation. *J. Chem. Soc. (A)*. (1970) 1082-1085.
- Branco V, Vale C, Canario J, Santos M. Mercury and selenium in blue shark (*Prionace glauca*, L. 1758) and swordfish (*Xiphias gladius*, L. 1758) from two areas of the Atlantic Ocean. *Environ. Pollut.* 150 (2007) 373-380.
- Branfireun B.A, Bishop K, Roulet N.T, Granberg G, Nilsson M. Mercury cycling in boreal ecosystems : The long term effect of acid rain constituents on peatland porewater methylmercury concentrations. *Geophys. Res. Lett.* 28 (2001) 1227-1230.
- Bravo-Sanchez L.R, Riva B.V, Costa-Fernandez J.M, Pereiro R, Sanz-Medel A. Determination of lead and mercury in sea water by preconcentration in a flow injection system followed by atomic absorption spectrometry detection. *Talanta*. 55 (2001) 1071–1078.
- Bryant P.S, Petersen J.N, Lee J.M, Brouns T.M. Sorption of heavy metals by untreated red fir sawdust, *Appl. Biochem. Biotechnol.* 34–35(1992) 777–778.
- Cai Y, Jaff R, Alli A, Jones R.D. Determination of organomercury compounds in aqueous samples by capillary gas chromatography-atomic fluorescence spectrometry following solid-phase extraction. *Anal. Chim. Acta.* 334 (1996) 251-259.
- Canário J, Prego R, Vale C, Branco V. Distribution of Mercury and Monomethylmercury in Sediments of Vigo Ria, NW Iberian Peninsula. *Water. Air. Soil. Pollut.* 182(2007) 21–29.
- Carrasco L, Benejam L, Benito J, Bayona J, Díez S. Methylmercury levels and bioaccumulation in the aquatic food web of a highly mercury-contaminated reservoir. *Environ. Int.* 37 (2011) 1213–1218.
- Ci Z, Zhang X, Wang Z. Elemental mercury in coastal seawater of Yellow Sea, China: Temporal variation and air-sea exchange. *Atmos. Environ.* 45 (2011) 183-190.
- Cimino G, Passerini A, Toscano G. Removal of toxic cations and Cr(VI) from aqueous solution by hazelnut shell, *Water Res.* 34 (2000) 2955–2962.
- Charnock, J.M, Moyes, L.N, Patrick, R.A.D, Mosselmans J.F.W, Vaughan D.J, Livens F.R. The structural evolution of mercury sulfide precipitate: An XAS and XRD study. *Am. Mineral.* 88 (2003) 1197-1203.
- Chen J, Pehkonen S.O, Lin C.J. Degradation of monomethylmercury chloride by hydroxyl radicals in simulated natural waters. *Water. Res.* 37 (2003) 2496–2504.
- Coelho J.P, Santos H, Reis A.T, Falcão J, Rodrigues E.T, Pereira M.E, Duarte A.C, Pardal M.A. Mercury bioaccumulation in the spotted dogfish (*Scyliorhinus canicula*) from the Atlantic Ocean. *Mar. Pollut. Bull.* 60 (2010) 1372–1375.

- Coquery M, Cossa D. Mercury speciation in surface waters of the North sea. *Neth. J. Sea Res.* 34 (1995) 245-257.
- Corbitt E, Jacob D, Holmes C, Streets D, Sunderland E. Global source– receptor relationships for mercury deposition under present-day and 2050 emissions scenarios. *Environ. Sci. Technol.* 45 (2011) 10477–10484.
- Costa M, Landing W, Kehrig H, Barletta M, Holmes C, Barrocas P, Evers D, Buck D, Vasconcellos A, Hacon S, Moreira J, Malm O. Mercury in tropical and subtropical coastal environments. *Environ. Res.* 119 (2012) 88–100.
- Cossa D, Martin J.M, Takayanagi K, Sanjuan J. The distribution and cycling of mercury in the Western Mediterranean. *Deep Sea Res. II.* 44 (1997) 721-740.
- Cremona F, Hamelin, S, Planas D, Lucotte M. Sources of organic matter and methylmercury in littoral macroinvertebrates: a stable isotope approach. *Biogeochemistry* 94 (2009) 81-94.
- Dardel F, Arden T.V (2001). *Ion Exchangers. Principles and Application*, Ullman's Encyclopedia of Industrial Chemistry, (sixth edition) Wiley–VCH Verlag, GmbH.
- Date Y, Aota A, Terakado S, Sasaki K, Matsumoto N, Watanabe Y, Matsue T, Ohmura N. Trace-Level Mercury Ion ( $Hg^{2+}$ ) Analysis in Aqueous Sample Based on Solid-Phase Extraction Followed by Microfluidic Immunoassay. *Anal. Chem.* 85 (2013) 85 434–440.
- Davis J.A, Greenfield B.K, Ichikawa G.M. S. Mercury in sport fish from the Sacramento– San Joaquin Delta region, California, USA. *Sci. Total. Environ.* 391 (2008) 66–75.
- Davis J.A, Looker R.E, Yee D, Marvin-DiPasquale M, Grenier J.L, Austin C.M, McKee L.J, Greenfield, B.K , Brodberg R, Blum J.D. Reducing methylmercury accumulation in the food webs of San Francisco Bay and its local watersheds. *Environ. Res.* 119 (2012) 3–26.
- Dos Santos J.S, Guardia M, Pastor A, Dos Santos M.L.P. Determination of organic and inorganic mercury species in water and sediment samples by HPLC on-line coupled with ICP-MS. *Talanta.* 80 (2009) 207–211.
- Downs S.G, Macleod C.L, Lester J.N. Mercury in precipitation and its relation to bioaccumulation in fish: a literature review. *Water. Air. Soil. Pollut.* 108 (1998), 149–187. Dyrssen D, Wedborg M. The sulfur-mercury(II) system in natural waters. *Water. Air. Soil. Pollut.* 56 (1991) 507-517.
- Dyrssen D, Wedborg M, 1980. Major and minor elements, chemical speciation in estuarine waters. In: *Chemistry and Biochemistry of estuaries*. Olausson E. and Cato I. (eds.) J.Wiley, Chichester. 329 pp.
- Edmonds S, O’Driscoll N.J, Hillier N, Atwood J. L, Evers D. C. Factors regulating the bioavailability of methylmercury to breeding rusty blackbirds in northeastern wetlands. *Environ. Pollut.* 171 (2012) 148-154.
- Ekstrom E.B, Morel F.M.M. Cobalt limitation of growth and mercury methylation in sulfate-reducing bacteria. *Environ. Sci. Technol.* 42 (2007) 93–99.
- Emteborg H, Baxter D.C, Frech W. Speciation of mercury in natural waters by capillary gas chromatography with microwave-induced plasma emission detector following

- preconcentration using a dithiocarbamate resin microcolumn installed in a closed flow injection system. *Analyst*. 118 (1993) 1007-1013.
- Endo T, Kimura O, Hisamichi Y, Minoshima Y, Haraguchi K, Kakumoto C, Kobayashi M. Distribution of total mercury, methyl mercury and selenium in pod of killer whales (*Orcinus Orca*) stranded in the northern area of Japan: Comparison of mature females with calves. *Environ. Pollut.* 144 (2006) 145-150.
- Endo T, Hisamichi Y, Haraguchi K, Kato Y, Ohta C, Koga N. Hg, Zn and Cu levels in the muscle and liver of tiger sharks (*Galeocerdo cuvier*) from the coast of Ishigaki Island, Japan: Relationship between metal concentrations and body length. *Mar. Pollut. Bull.* 56 (2008) 1774–1780.
- Endo T, Haraguchi K, Cipriano F, Simmonds M.P, Hotta Y, Sakata M. Contamination by mercury and cadmium in the cetacean products from Japanese market. *Chemosphere*. 54 (2004) 1653-1662.
- Evans M.S, Lockhart W.L, Doetzel L, Low G, Muir D, Kidd K, Stephens G, Delaronde J. Elevated mercury concentrations in fish in lakes in the Mackenzie River Basin: The role of physical, chemical, and biological factors. *Sci. Total. Environ.* 351–352 (2005) 479–500.
- Faraji M, Yamini Y, Rezaee M. Extraction of trace amounts of mercury with sodium dodecyl sulphate-coated magnetite nanoparticles and its determination by flow injection inductively coupled plasma-optical emission spectrometry. *Talanta*. 81 (2010) 831–836.
- Feng X, Qiu G, 2008. Mercury pollution in Guizhou, Southwestern China-An overview. *Sci. Total. Environ.* 400 (2008) 227-237.
- Ferreira G, Caetano L, Castro R, Padilha P, Castro G. Synthesis, characterization, and application of modified silica in the removal and preconcentration of lead ions from natural river water. *Clean. Techn. Environ. Policy*. 13 (2011) 397–402.
- Ferrua N, Cerutti S, Salonia J.A, Olsina R.A, Martinez L.D. On-line preconcentration and determination of mercury in biological and environmental samples by cold vapor-atomic absorption spectrometry. *J. Hazard. Mater.* 141 (2007) 693–699.
- Fitzgerald, W.F, Lamborg, C.H. 2005. Geochemistry of mercury in the environment. In *Treatise on Geochemistry*, ed. BS Lollar, pp. 107–48. New York: Elsevier.
- Fitzgerald W.F, Lamborg C.H, Hammerschmidt C.R. Marine biogeochemical cycling of mercury. *Chemical Reviews*. 107 (2007) 641-662.
- Fitzgerald W.F, Mason R.P, Vandal G.M. Atmospheric cycling and air-water exchange of mercury over mid-continental lacustrine regions. *Water. Air. Soil. Poll.* 56 (1991)745–767.
- Gardfeldt K, Sommar j, Ferrara R, Ceccarini C, Lanzillotta E, Munthe J, Wangberg I, Lindqvist O, Pirron, N, Sprovieri F, Pesenti E, Stromberg D. Evasion of mercury from coastal and open waters of the Atlantic ocean and the Mediterranean Sea. *Atmos. Environ.* 37 (2003) 73-84.
- Gagnon C, Pelletier E, Mucci A. Behaviour of anthropogenic mercury in coastal marine sediments. *Mar. Chem.* 59 (1997) 159-176.

- Gerbig C, Kim C, Stegemeier J, Ryan J.N, Aiken G.R. Formation of nanocolloidal metacinnabar in mercury-DOM-sulfide systems. *Environ. Sci. Technol.* 74 (2011) 4693-4708.
- Graham A.M, Aiken G.R, Gilmour C.C. Effect of dissolved organic matter and character on microbial Hg methylation in Hg-S-DOM solutions. *Environ. Sci. Technol.* 47 (2013) 5746-5754.
- Ghaedi M, Fathi M, Shokrollahi A, Shajarat F. Highly Selective and Sensitive Preconcentration of Mercury Ion and Determination by Cold Vapor Atomic Absorption Spectroscopy. *Anal. Lett.* 39 (2006) 1171-1185.
- Ghaedi M, Tavallali H, Shokrollahi A, Zahedi M, Montazerzohori M, Soylak M. Flame atomic absorption spectrometric determination of zinc, nickel, iron and lead in different matrixes after solid phase extraction on sodium dodecyl sulfate(SDS)-coated alumina as their bis (2-hydroxyacetophenone)-1, 3-propanediimine chelates. *J. Hazard. Mater.* 166 (2009) 1441–1448.
- Glatz I, Mayr M, Hoogenboom R, Schubert U, Buchmeiser M. Terpyridine-based silica supports prepared by ring-opening metathesis polymerization for the selective extraction of noble metals. *J. Chromatogr. A* 1015 (2003) 65–71.
- Gilmour C.C, Henry E.A. Mercury methylation in aquatic systems affected by acid deposition. *Environ. Pollut.* 71 (1991) 131-169.
- Gray J.E, Crock J.G, Fey D.L. Environmental geochemistry of abandoned mercury mines in west-central Nevada, USA. *Appl. Geochem.* 17 (2002) 1069–79.
- Gray J.E, Greaves IA, Bustos D.M, Krabbenhoft D.P. Mercury and methylmercury contents in mine-waste calcine, water, and sediment collected from the Palawan Quicksilver Mine, Philippines. *Environ. Geol.* 43 (2003) 298–307.
- Gray J.E, Hines M.E, Higuera P.L, Adatto I, Lasorsa B.K. Mercury speciation and microbial transformations in mine wastes, stream sediments, and surface waters at the Almadén mining district, Spain. *Environ. Sci. Technol.* 38 (2004)4285–92.
- Gray J.E, Theodorakos P.M, Bailey E.A, Turner R.R. Distribution, speciation, and transport of mercury in stream-sediment, stream-water, and fish collected near abandoned mercury mines in southwestern Alaska, USA. *Sci. Total. Environ.* 260 (2000) 21–33.
- Gustin M, Lindberg S.E, Weisberg P.J. An update on the natural sources and sinks of atmospheric mercury. *Appl. Geochem.* 23 (2008) 482–493.
- Hamelin S, Amyot M, Barkay T, Wang Y.P, Planas D. Methanogens: Principal methylators of mercury in lake periphyton. *Environ. Sci. Technol.* 45 (2011) 7693-7700.
- Hashempour T, Rofouei M.K, Khorrami A.R. Speciation analysis of mercury contaminants in water samples by RP-HPLC after solid phase extraction on modified C18 extraction disks with 1, 3-bis(2-cyanobenzene)triazene. *J. Microchem.* 89 (2008) 131–136.
- Harada M. Minamata disease: methylmercury poisoning in Japan caused by environmental pollution. *Crit. Rev. Toxicol.* 25 (1995) 1–24.
- Harada M, Fujino, Akagi T. Mercury contamination in human hair at Indian reserves in Canada. *Kumamoto Med. J.* 30 (1977) 57-64.

- Hammerschmidt C.R, Fitzgerald W.F. Methylmercury cycling in sediments on the continental shelf of southern New England. *Geochim. Cosmochim. Acta.* 70 (2006) 918–930.
- Hammerschmidt, C.R, Fitzgerald, W.F. Geochemical controls on the production and distribution of methylmercury in near-shore marine sediments. *Environ. Sci. Technol.* 38 (2004)1487–1495.
- Hammerschmidt C.R, Fitzgerald W.F, Lamborg C.H, Balcom P.H, Tseng C.M. Biogeochemical cycling of methylmercury in lakes and tundra watersheds of Arctic Alaska. *Environ. Sci. Technol.* 40 (2006) 1204-1211.
- Hammerschmidt C.R, Lamborg C.H, Fitzgerald W.F. Aqueous phase methylation as a potential source of methylmercury in wet deposition. *Atmos. Environ.* 41 (2007) 1663–1668.
- Harmon S.M, King J.K, Gladden J.B, Newman L.A. Using Sulfate-Amended Sediment Slurry Batch Reactors to Evaluate Mercury Methylation. *Arch. Environ. Contam. Toxicol.* 52 (2007) 326–331.
- Harris R, Pollman C, Hutchinson D, Landing W, Axelard D, Morey S.L, Dukhovskoy D, Vijayaraghavan. A screening model analysis of mercury sources, fate and bioaccumulation in the Gulf of Mexico. *Environ. Res.* 119 (2012) 53–63.
- Heim W, Coale K, Stephenson M, Cheo K, Gill G, Foe C. Spatial and Habitat-Based Variations in Total and Methyl Mercury Concentrations in Surficial Sediments in the San Francisco Bay-Delta. *Environ. Sci. Technol.* 41 (2007) 3501-3507.
- Heyes A, Mason R.P, Kim E.H, Sunderland E. Mercury methylation in estuaries: insights from using measuring rates using stable mercury isotopes. *Mar. Chem.* 102 (2006) 134–47.
- Hines M.E, Horvat M, Faganeli J, Bonzongo J.J, Barkay T, Major E.B, Scott J.J, Bailey E.A, Warwick J.J, Berry Lyons W. Mercury biogeochemistry in the Idrija River, Slovenia, from above the mine into the Gulf of Trieste. *Environ. Res. Sect A.* 83 (2000) 129–39.
- Hines M, Poitras E, Covelli S, Faganeli J, Emili A, Zizek S, Horvat M. Mercury methylation and demethylation in Hg-contaminated lagoon sediments (Marano and Grado Lagoon, Italy). *Estuar. Coast. Shelf. Sci.* 113 (2012) 85-95.
- Hintelmann H, Harris R, Heyes A, Hurley J, Kelly C, 2002. Reactivity and mobility of new and old mercury deposition in a boreal forest ecosystem during the first year of the METAALICUS study. *Environ. Sci. Technol.* 36 (2002) 5034–40.
- Hintelmann H, Keppel-Jones K, Evans R. Constants of mercury methylation and demethylation rates in sediments and comparison of tracer and ambient mercury availability. *Environ. Toxicol. Chem.* 19 (2000) 2204–11.
- Hiraide M, Sorouradin M.H, Kawaguchi H. Immobilization of dithizone on surfactant-coated alumina for preconcentration of metal ions. *Anal. Sci.* 10 (1994) 125-127.
- Hollweg T.A, Gilmour C.C, Mason R.P. Methylmercury production in sediments of Chesapeake Bay and the mid-Atlantic continental margin. *Mar. Chem.* 114 (2009) 86–101.
- Houserova P, Matejcek D, Kuban V. High- performance liquid chromatography/ion trap mass spectrometric speciation of aquatic mercury as its pyrrolidinedithiocarbamate complexes (2007). *Anal. Chim. Acta.* 596 (2007) 242-250.

- Hsu H, Sedlack D.L. Strong Hg(II) complexation in municipal wastewater effluent and surface waters. *Environ. Sci. Technol.* 37 (2003) 2743-2702.
- Idris S, Harvey S, Gibson L. Selective extraction of mercury(II) from water samples using mercapto functionalised-MCM-41 and regeneration of the sorbent using microwave digestion. *J. Hazard. Mater.* 193 (2011) 171–176.
- Jay J.A, Murray K.J, Gilmour C.C, Mason R.P, Morel F.M.M, Roberts A.L, Hemond H.F. Mercury methylation by *Desulfovibrio desulfuricans* ND 132 in the presence of polysulfides. *Appl. Environ. Microbiol.* 68 (2002) 5741–5745.
- Jia X, Gong D, Han Y, Wei C, Duan T, Chen H. Fast speciation of mercury in seawater by short-column high-performance liquid chromatography hyphenated to inductively coupled plasma spectrometry after on-line cation exchange column preconcentration. *Talanta.* 88 (2012) 724–729.
- Jiang S, Liu X, Chen Q. Distribution of total mercury and methylmercury in lake sediments in Arctic Ny-Alesund. *Chemosphere.* 83 (2011) 1108–1116.
- Johansen P, Muir D, Asmund G, Riget F. Human exposure to contaminants in the traditional Greenland diet. *Sci. Total. Environ.* 331 (2004) 189–206.
- Jonsson S, Skjellberg U, Nilsson M.B, Westlund P, Shchukarev A, Lundberg E, Bjorn E. Mercury methylation rates for geochemically relevant Hg(II) species in sediments. *Environ. Sci. Technol.* 46 (2012) 11653-11659.
- Kehrig H.A, 2011. Mercury and plankton in tropical marine ecosystems: a review. *Oecol. Aust.* 15 (2011) 868–880.
- Kehrig H.A, Howard B, Malm O. Methylmercury in a predatory fish (*Cichla* spp.) inhabiting the Brazilian Amazon. *Environ. Pollut.* 154 (2008) 68-76.
- Kerin E.J, Gilmour C.C, Roden E, Suzuki M.T, Coates J.D, Mason R.P. 2006. Mercury methylation by dissimilatory iron-reducing bacteria. *Appl. Environ. Microbiol.* 72 (2006) 7919- 7921.
- Kirk J.L, St. Louis V.L, Hintelmann H, Lehnher I, Else B, Poissant L 2008. Methylated mercury species in marine waters of the Canadian High and Sub- Arctic. *Environ. Sci. Technol.* 42 (2008) 8367–8373.
- King J, Saunders S, Lee R.F, Jahnke, R.A. Coupling mercury methylation rates to sulfate reduction rates in marine sediments. *Environ. Toxicol. Chem.* 18 (1999) 1362–1369.
- King J, Kostka J, Frischer M, Saunders F. Sulfate-Reducing Bacteria Methylate Mercury at Variable Rates in Pure Culture and in Marine Sediments. *Appl. Environ. Microbiol.* 66 (2000) 2430-2437
- Knights C, Sunderland E, Barber M, Johnston J, Ambrose R.J. Application of ecosystem scale fate and bioaccumulation models to predict fish mercury response times to changes in atmospheric deposition. *Environ. Toxicol. Chem.* 28 (2009) 881–893.
- Kocman D, Kanduc T, Ogrinc N, Horvat M. Distribution and partitioning of mercury in a river catchment impacted by former mercury mining activity. *Biogeochemistry.* 104 (2011) 183-201.
- Kooshki M, Shams E. Selective response of dopamine in the presence of ascorbic acid on carbon paste electrode modified with titanium phosphated silica gel. *Anal. Chim. Acta* 587 (2007) 110-115.



- Kotnik J, Horvat M, Tessier E, Ogrinc N, Monperrus M, Amouroux D, Fajon V, Gibicar D, Zizek S, Sprovieri F, Pirrone N. Mercury speciation in surface and deep waters of the Mediterranean Sea. *Mar. Chem.* 107 (2007) 13–30.
- Kuss J, Zulicke C, Pohl C, Schneider B. Atlantic Mercury Emission Determined from Continuous Analysis of the Elemental Mercury Sea-Air Concentration Difference within Transects between 50 ° N and 50 ° S. *Glob. Biogeochem. Cycles.* 25 (2011) 1-9.
- Lambert K, Evers D, Warner K, King S, Seline N. Integrating mercury science and policy in the marine context: Challenges and opportunities. *Environ. Res.* 119 (2012) 132–142.
- Lamborg C, Fitzgerald W.F, O'Donnell J, Torgersen T. A non-steady state compartmental model of global-scale mercury geochemistry with interhemispheric gradients. *Geochim. Cosmochim. Acta.* 66 (2002) 1105-1118.
- Lamborg C. H, Hammerschmidt C.R, Gill G.A, Mason R.P, Gichuki S. An Intercomparison of Procedures for the Determination of total Mercury in seawater and recommendations regarding mercury speciation during geotraces cruises. *Limnol. Oceanogr. Methods.* 10 (2012) 90-100.
- Lamborg C, C Tseng, Fitzgerald W, Balcom P, Hammerschmidt C. Determination of the Mercury Complexation Characteristics of Dissolved Organic Matter in Natural Waters with Reducible Hg Titrations. *Environ. Sci. Technol.* 37 (2003) 3316-3322.
- Laurier F, Cossa D, Gonzalez J. L, Breviere E, Sarazin G. Mercury Transformations and Exchanges in a High Turbidity Estuary: The Role of Organic Matter and Amorphous Oxyhydroxides. *Geochim. Cosmochim. Acta.* 67 (2003) 3329-3345.
- Laurier F, Mason R.P, Gill G.A, Whalin L. 2004. Mercury distributions in the North Pacific Ocean 20 years of observations. *Mar. Chem.* 90 (2004) 3–19.
- Leermakers M, Galletti S, De Galan S, Brion N, Baeyens W. Mercury in the Southern North Sea and Scheldt Estuary. *Mar. Chem.* 75 (2001) 229-248.
- Lehnherr I, St. Louis V.L, Hintelmann H, Kirk J.L. Methylation of inorganic mercury in polar marine waters. *Nat. Geosci.* 3 (2011) 298–302.
- Li J.H, Zhang Z, Xu S.F, Chen L.X, Zhou N, Xiong H, Peng H.L. Label-free colorimetric detection of trace cholesterol based on molecularly imprinted photonic hydrogels. *J. Mater. Chem.* 21 (2011) 19267–19274.
- Li P, Feng X, Qui G, Shang L, Wang S. Mercury pollution in Wuchuan mercury mining area, Guizhou, Southwestern China: The impacts from large scale and artisanal mercury mining. *Environ. Int.* 42 (2012) 59–66.
- Lima A, Sarkis J, Shihomatsu H, Muller R. Mercury and selenium concentrations in fish samples from Cachoeira do Piria Municipality, Para State, Brazil. *Environ. Res.* 97 (2005) 236–244.
- Lin C, Wang H, Wang Y, Cheng Z. Selective solid-phase extraction of trace thorium(IV) using surface-grafted Th(IV)-imprinted polymers with pyrazole derivative. *Talanta.* 81 (2010) 30–36.
- Lin C, Yee N, Barkay T. Microbial transformations in the mercury cycle. In *Environmental Chemistry and Toxicology of Mercury*, John Wiley and Sons, Hoboken, NJ, 2012, 155-191.

- Lindberg S.E, Hanson P, Meyers T, Kim K. Air/surface exchange of mercury vapor over forests—the need for a reassessment of continental biogenic emissions. *Atmos. Environ.* 32 (1998) 895–908.
- Lindberg S.E, Meyers T, Taylor G, Turner R, Schroeder. Atmosphere-surface exchange of mercury in a forest: results of modeling and gradient approaches. *J. Geophys. Res.* 97 (1992) 2519–28.
- Liska I, fifty years of solid phase extraction in water analysis historical development and overview, *J. Chromatogr. A.* 885 (2000) 3-16.
- Lockhart W.L, Stern G.A, Low G, Hendzel M, Boila G, Roach P, Evans M.S, Billeck B.N, DeLaronde J, Friesen S, Kidd K, Atkins S, Muir D.C.G, Stoddart M, Stephens G, Stephenson S, Harbicht S, Snowshoe N, Grey B, Thompson S, DeGraff N.A history of total mercury in edible muscle of fish from lakes in northern Canada. *Sci. Total. Environ.* 351–352 (2005) 427–463.
- Loring D.H. Geochemical factors controlling the accumulation and dispersal of heavy metals in the Bay of Fundy region. *Can. J. Earth Sci.* 19 (1982) 930–944.
- Low K.S, Lee C.K, Ng A.Y. Column study on the sorption of Cr(VI) using quaternized rice hulls. *Biores. Technol.* 68 (1999) 205–208.
- Margetinova J, Houserova-Pelcova P, Kuban V. Speciation analysis of mercury in sediments, zoobenthos and river water samples by high-performance liquid chromatography hyphenated to atomic fluorescence spectrometry following preconcentration by solid phase extraction. *Anal. Chim. Acta.* 615 (2008) 115–123.
- Maruszczak N, Larose C, Dommergue A, Paquet S, J Beaulne, R. Maury- Brachet, M Lucotte, R Nedjai, C Ferrari. Mercury and methylmercury concentrations in high altitude lakes and fish (Arctic charr) from the French Alps related to watershed characteristics. *Sci. Total. Environ.* 409 (2011) 1909–1915.
- Marsh D, Clarkson T, Cox C, Myers G, Amin-Zaki L, Tikriti S. Fetal methylmercury poisoning. Relationship between concentration in single strands of maternal hair and child effects. *Arch. Neurol.* 44 (1987) 1017–22.
- Mashhadizadeh M, Karami Z. Solid phase extraction of trace amounts of Ag, Cd, Cu, and Zn in environmental samples using magnetic nanoparticles coated by 3-(trimethoxysilyl)-1-propanol and modified with 2-amino-5-mercapto-1,3,4-thiadiazole and their determination by ICP-OES. *J. Hazard. Mater.* 190 (2011) 1023–1029.
- Macchi G, Marani D, Tirivanti G. Uptake of mercury by exhausted coffee grounds. *Environ. Technol. Lett.* 7 (1986) 431–444.
- Mason R.P, Choi A, Fitzgerald W, Hammerschmidt C, Lamborg C, Soerensen A, Sunderland E. Mercury biogeochemical cycling in the ocean and policy implications. *Environ. Res.* 119 (2012) 101–117.
- Mason R.P, Lawrence A. Concentration, distribution and bioavailability of mercury and methylmercury in sediments of Baltimore Harbor and Chesapeake Bay, Maryland, USA. *Environ. Toxicol. Chem.* 18 (1999) 2438–2447.
- Mason R. P, Lawson N. M, Sheu G.R. Mercury in the Atlantic Ocean: Factors controlling air-sea exchange of mercury and its distribution in the upper waters. *Deep-Sea Res. II.* 48 (2001) 2829–2853.

- Mason R.P, Reinfelder J.R, Morel F.M.M. Uptake, toxicity, and trophic transfer of mercury in coastal diatom. *Environ. Sci. Technol.* 30 (1996) 1835-1845.
- Mason R.P, Rolffhus K.R, Fitzgerald W.F. Methylated and elemental mercury cycling in surface and Deep Ocean waters of the north Atlantic. *Water. Air. Soil. Pollut.* 80 (1995) 665–677.
- Merritt K.A, Amirbahman A. Mercury methylation dynamics in estuarine and coastal marine environments-A critical review. *Earth. Sci. Reviews.* 96 (2009) 54–66.
- Merritt K.A, Amirbahman A. Methylmercury cycling in estuarine sediment porewaters (Penobscot River estuary Maine, USA). *Limnol. Oceanogr.* 53 (2008) 1064–1075.
- Miklavcic A, Mazej D, Jaćimović R, Dizdarevic T, Horvat M. Mercury in food items from the Idrija Mercury Mine area. *Environ Res.* (2013) <http://dx.doi.org/10.1016/j.envres.2013.02.008i>.
- Mondal B, Das D, Das A. Application of a new resin functionalised with 6-mercaptopurine for mercury and silver determination in environmental samples by atomic absorption spectrometry. *Anal. Chim. Acta.* 450 (2001) 223–230.
- Monperrus M, Tessier E, Amouroux D, Leynaert A, Huonnic P, Donard O.F.X. Mercury methylation, demethylation and reduction rates in coastal and marine surface waters of the Mediterranean Sea. *Mar. Chem.* 107 (2007) 49–63.
- Monperrus M, Tessier E, Point D, Vidimova K, Amouroux D, Guyoneaud R, Leynaert A, Grall J, Chauvaud L, Thouzeau G, Donard O.F.X. The biogeochemistry of mercury at the sediment–water interface in the Thau Lagoon. 2. Evaluation of mercury methylation potential in both surface sediment and the water column. *Estuar. Coast. Shelf. Sci.* 72 (2007) 485–496.
- Moura J, Hacon S, Vega C, Davis R, Campos R, Siciliano S. Guiana Dolphins (*Sotalia guianensis*, Van Beneden 1864) as Indicators of the Bioaccumulation of Total Mercury along the Coast of Rio de Janeiro State, Southeastern Brazil. *Bull. Environ. Contam. Toxicol.* 88 (2012) 54–59.
- Monteiro A.C.P, Andrade L.S.N, Campos R.C. Online mercury and methylmercury preconcentration by adsorption of their dithiophosphoric acid diacyl ester chelates on a C18 column and cold vapor atomic absorption detection. *Fresenius J. Anal. Chem.* 371 (2001) 353-357.
- Montesinos P, Dominguez-Vidal A, Luisa Cervera W, Pastor A, Guardia M. On-line speciation of mercury in fish by cold vapour atomic fluorescence through ultrasound-assisted extraction. *J. Anal. At. Spectrom.* 19 (2004) 1386–1390.
- Morse J.W, Luther III G.W. Chemical influences on trace metal-sulfide interactions in anoxic sediments. *Geochim. Cosmochim. Ac.* 63 (1999) 3373-3378.
- Munoz J, Gallego M, Valcárcel M. Speciation of Organometallic Compounds in Environmental Samples by Gas Chromatography after Flow Preconcentration on Fullerenes and Nanotubes. *Anal. Chem.* 77 (2005) 5389-5395.
- Muresanu M, Reiss A, Cioatera N, Trandafir I, Hulea V. Mesoporous silica functionalized with 1-furoyl thiourea urea for Hg(II) adsorption from aqueous media. *J. Hazard. Mater.* 182 (2010) 197-203.

- Munthe J, Wangberg I, Iverfeldt A, Lindqvist O, Stromberg D, Sommar J, Gardfeldt K, Peterson G, Ebinghaus R, Prestbo E, Larjava K, Siemens V. Distribution of atmospheric species in Northern Europe: final results from MOE project. *Atmos. Environ.* 37 (2003) 9-20.
- Munthe J, Bodaly R.A, Branfireun B.A, Driscoll C.T, Gilmour C.C, Harris R, Horvat M, Lucotte M, Malm O. Recovery of mercury-contaminated fisheries. *Ambio* 36 (2007)33-44.
- Najera I, Lin C, Kohbodi G, Jay J. Effect of Chemical Speciation on Toxicity of Mercury to *Escherichia coli* Biofilms and Planktonic Cells. *Environ. Sci. Technol.* 39 (2005)3116-3120.
- Oh S, Kim M, Yi S, Zoh K. Distributions of total mercury and methylmercury in surface sediments and fishes in Lake Shihwa, Korea. *Sci. Total. Environ.* 408 (2010) 1059-1068.
- Pacyna E.G, Pacyna, J.M, Sundseth K, Munthe J, Kindbom K, Wilson S, Steenhuisen F, Maxson P. Global emission of mercury to the atmosphere from anthropogenic sources in 2005 and projections to 2020. *Atmos. Environ.* 44 (2010) 2487-2499.
- Papageorgiou S.K, Fotios K. K. Kouvelos E.P, Nolan J.W, Le Deit H, Kanellopoulos N.K. Heavy metal sorption by calcium alginate beads from *Laminaria digitata*. *J. Hazard. Mater.* 137 (2006) 1765-1772.
- Paquette K.E, Helz G. Inorganic speciation of mercury in sulfidic waters : The importance of Zero-valent sulfur. *Environ. Sci.Technol.* 31 (1997) 2148-2153.
- Paquette K.E, Helz G. Solubility of cinnabar (red HgS) and implications for mercury speciation in sulfidic waters. *Water. Air. Soil. Poll.* 80 (1995) 1053-1056.
- Parks J, Johs A, Podar M, Bridou R, Hurt R, Smith S, Tomanicek S, Qian Y, Brown S, Brandt C, Palumbo A, Smith J, Wall J, Slias D, Liang L. The Genetic Basis for Bacterial Mercury Methylation. *Science.* 339 (2013) 1332-1335.
- Pongratz R, Heumann K.G. Production of methylated mercury and lead by polar macroalgae—a significant natural source for atmospheric heavy metals in clean room compartments. *Chemosphere.* 36 (1998) 1935-1946.
- Pouilly M, Perez T, Rejas D, Guzman F, Crespo G, Duprey J, Guimaraes J. Mercury bioaccumulation patterns in fish from the Itenez river basin, Bolivian Amazon. *Ecotox. Environ. Safe.* 83 (2012) 8-15.
- Qiu G, Feng X, Meng B, Sommara J, Gu C. Environmental geochemistry of an active Hg mine in Xunyang, Shaanxi Province, China. *Appl. Geochem.* 27 (2012) 2280-2288.
- Quemerais B, Cossa D, Rondeau B, Pham T.T, Fortin B, 1998. Mercury distribution in relation to iron and manganese in the waters of St. Lawrence River. *Sci. Total. Environ.* 213 (1998) 193-201.
- Quevauviller P, Donard O.F.X, Wasserman J.C, Martin F.M, Schneider. Occurrence of methylated tin and dimethyl mercury compounds in a mangrove core from Sepetiba Bay, Brazil. *Appl.Organolet.Chem.* 6 (1992) 221-228.
- Qvarnstrom J, Tu Q, Frech W, Ludke C. Flow injection-liquid chromatography-cold vapour atomic absorption spectrometry for rapid determination of methyl and inorganic mercury *Analyst* 125 (2000) 1193-1197.

- Rajesh N, Hari M.S. Spectrophotometric determination of inorganic mercury(II) after preconcentration of its diphenylthiocarbazone complex on a cellulose column. *Spectrochim. Acta. A* 70 (2008) 1104–1108.
- Ramesh A, Mohan K.R, Seshaiiah K. Preconcentration of trace metals on Amberlite XAD-4 resin coated with dithiocarbamates and determination by inductively coupled plasma–atomic emission spectrometry in saline matrices. *Talanta*. 57 (2002) 243–252.
- Rimondi V, Gray J, Costagliola P, Vaselli O, Lattanzi P. Concentration, distribution, and translocation of mercury and methylmercury in mine-waste, sediment, soil, water, and fish collected near the Abbadia San Salvatore mercury mine, Monte Amiata district, Italy. *Sci. Total. Environ.* 414 (2012) 318–327.
- Rodriguez Martin-Doimeadios R.C, Tessier E, Amouroux D, Guyoneaud R, Duran R, Caumette P, Donard O.F.X. Mercury methylation/demethylation and volatilization pathways in estuarine sediment slurries using species-specific enriched stable isotopes. *Mar. Chem.* 90 (2004) 107–123.
- Rofouei M, Rezaei A, Masteri-Farahani M, Khani H. Selective extraction and preconcentration of ultra-trace level of mercury ions in water and fish samples using Fe<sub>3</sub>O<sub>4</sub>-magnetite-nanoparticles functionalized by triazene compound prior to its determination by inductively coupled plasma-optical emission spectrometry. *Anal. Methods*. 4 (2012) 959–966.
- Rytuba J.J. Mercury from mineral deposits and potential environmental impact. *Environ. Geol.* 43 (2003) 326–38.
- Scheuhammer A, Meyer M, Sandheinrich M, Murray M. Effects of environmental methylmercury on the health of wild birds, mammals, and fish. *AMBIO: A J. Hum. Environ.* 36 (2007) 12–19.
- Salih B, Say R, Denizli A, Genc O, Piskin E. Determination of inorganic and organic mercury compounds by capillary gas chromatography coupled with atomic absorption spectrometry after preconcentration on dithizone-anchored poly(ethylene glycol dimethacrylate-hydroxyethylmethacrylate) microbeads. *Anal. Chim. Acta.* 371 (1998) 177–185.
- Sanchez D.M, Martin R, Morante R, Martin J, Munuera M.L. Preconcentration speciation method for mercury compounds in water samples using solid phase extraction followed by reversed phase high performance liquid chromatography. *Talanta*. 52 (2000) 671–679.
- Saniewska D, Beldowska M, Beldowski J, Saniewski M, Kwasniak J, Falkowska L. Distribution of mercury in different environmental compartments in the aquatic ecosystem of the coastal zone of the Southern Baltic Sea. *J. Environ. Sci.* 22 (2010) 1144–1150.
- Sasaki K, Oguma S, Namiki Y, Ohmura N. Monoclonal Antibody to Trivalent Chromium Chelate Complex and Its Application to Measurement of the Total Chromium Concentration. *Anal. Chem.* 81 (2009) 4005–4009.
- Sasaki K, Tawarada K, Okuyama A, Kayama F, Abe K, Okuhata H, Maruyama Y, Arakane T, Miyasaka H, Fujikawa T, Ohmura N. Rapid determination of cadmium in

- rice by immunochromatography using anti-(Cd-EDTA) antibody labeled with gold particle. *Bunseki Kagaku*. 56 (2007) 29–36.
- Schuster E. The behaviour of mercury in the soil with special emphasis on the complexation and adsorption processes: a review of the literature. *Water. Air. Soil. Poll.* 56 (1991) 667–680.
- Schuster P.F, Krabbenhoft D, Naftz D, Cecil L, Olson M. Atmospheric mercury deposition during the last 270 years: a glacial ice core record of natural and anthropogenic sources. *Environ. Sci. Technol.* 36 (2002) 2303–2310.
- Seixas T, Kehrig H, Costa M, Fillmann G, Beneditto A, Secchi E, Souza C, Malm O, Moreira I. Total mercury, organic mercury and selenium in liver and kidney of a South American coastal dolphin. *Environ. Poll.* 154 (2008) 98-106.
- Segade S.R, Tyson J.F. Determination of inorganic mercury and total mercury in biological and environmental samples by flow injection-cold vapor-atomic absorption spectrometry using sodium borohydride as the sole reducing agent, *Spectrochim. Acta. B.* 58 (2003) 797–807.
- Selin E, Jacob D, Yantosca R, Strode S, Jaegle L, Sunderland E. 2008. Global 3-D land-ocean atmosphere model for mercury: present-day versus preindustrial cycles and anthropogenic enrichment factors for deposition. *Glob. Biogeochem. Cycles.* 22 (2008) 1-13.
- Shabani A, Dadfarnia S, Nasirizadeh N. Speciation analysis of mercury in water samples by cold vapor atomic absorption spectrometry after preconcentration with dithizone immobilized on microcrystalline naphthalene. *Anal. Bioanal. Chem.* 378 (2004) 1388–1391.
- Sharif S., Tessier E, Bouchet S, Monperrus M, Pinaly H, Amouroux D, Comparison of different air-water gas exchange models to determine gaseous mercury evasion from different European coastal lagoons and estuaries. *Water. Air. Soil. Pollut.* (2013). DOI: 10.1007/s 11270-013-1606-1.
- Skylberg U. Competition among thiols and inorganic sulfides and polysulfides for Hg and MeHg in wetland soils and sediments under suboxic conditions: Illumination of controversies and implications for MeHg net production. *J. Geophys. Res. Biogeosci.* 113 (2008) G00C03.
- Skylberg U, Bloom P.R, Qian J, Lin C.M, Blears W.F. Complexation of mercury(II) in soil organic matter: EXAFS evidence for linear two-coordination with reduced sulfur groups. *Environ. Sci. Technol.* 40 (2006) 4174-4180.
- Skylberg U, Qian J, Frech W, Xia K, Blears W.F. Distribution of mercury, methyl mercury and organic sulphur species in soil, soil solution and stream of a boreal forest catchment. *Biogeochemistry.* 64 (2003) 53–76.
- Sommar J.M, Hallquist M, Ljungstrom E. Rate of reaction between the nitrate radical and dimethyl mercury in the gas phase. *Chem. Phys. Lett.* 257 (1996) 434–438.
- Soerensen A, Mason R.P, Balcom P, Sunderland E. Drivers of surface ocean mercury concentrations and air-sea exchange in the West Atlantic Ocean. *Environ. Sci. Technol.* (2013) DOI: 10.1021/es401354q.
- Sonke J.E, Blum J.D. Mercury in flux. *Nat. Geosci.* 5 (2012) 447-448.

- Steffen A, Douglas T, Amyot M, Ariya P, Aspmo K, Berg T, Bottenheim J, Brooks S, Cobbett F, Dastoor A, Dommergue A, Ebinghaus R, Ferrari C, Gardfeldt, K., Goodsite M. E, Lean D, Poulain A. J, Scherz C, Skov H, Sommar J, Temme C. A synthesis of atmospheric mercury depletion event chemistry in the atmosphere and snow, *Atmos. Chem. Phys.* 8 (2008) 1445-1482.
- Stoichev T, Rodriguez martin-Doimeadios R.C, Tessier E, Amouroux D, Donard O.F.X. Improvement of analytical performances for mercury speciation by on-line derivatization, cryofocussing and atomic fluorescence spectrometry. *Talanta* 62 (2004) 433-438.
- Storelli M, Zizzo N, Marcotrigiano G. Heavy Metals and Methylmercury in Tissues of Risso's Dolphin (*Grampus griseus*) and Cuvier's Beaked Whale (*Ziphius cavirostris*) Stranded in Italy (South Adriatic Sea). *Bull. Environ. Contam. Toxicol.* 63 (1999) 703-710.
- Sturgeon R.E, Berman S.S, Willie S.N. Concentration of trace metals from seawater by complexation with 8-hydroxyquinoline and adsorption on C18 bonded silica gel. *Talanta*. 29 (1982) 167-171.
- Sturgeon R.E., Willie S.N, Berman S.S. Perconcentration of selenium and antimony from seawater for determination by graphite furnace atomic absorption spectrometry. *Anal. Chem.* 57 (1985) 6-9.
- Sunderland E.M. Mercury exposure from domestic and imported estuarine and marine fish in the U.S. seafood market. *Environ. Health. Perspect.* 115 (2007) 235–242.
- Sunderland E.M, Gobas F.A.P.C, Branfireun B.A, Heyes A, 2006. Environmental controls on the speciation and distribution of mercury in coastal sediments. *Mar. Chem.* 102 (2006) 111–123.
- Sunderland E.M, Mason R.P. Human impacts on open ocean mercury concentrations. *Glob. Biogeochem. Cycles.* 21 (2007)1-15.
- Tertykh V.A and Belyakova L.A. Chemical reactions involving silica surface. *Naukova Dumka, Kiev*, 1991.
- Tirtom V, Goulding S, Henden E. Application of a wool column for flow injection online preconcentration of inorganic mercury(II) and methyl mercury species prior to atomic fluorescence measurement. *Talanta*. 76 (2008) 1212–1217.
- Tuzen M, KaramanI, Citak D, Soylak M. Mercury(II) and methyl mercury determinations in water and fish samples by using solid phase extraction and cold vapour atomic absorption spectrometry combination. *Food. Chem.Toxicol.* 47 (2009) 1648–1652.
- Tseng C.M, Amouroux D, Brindle I.D, Donard O.F.X. J. *Environ. Monit. Field cryofocussing hydride generation applied to the simultaneous multi-elemental determination of alkyl-metal(loid) species in natural waters using ICP-MS detection.* 2 (2000) 603-612.
- Unger K.K (1979). Porous silica, its properties and use as support in column liquid chromatography. *Journal of chromatography*, Volume 16, Elsevier Scientific Publishing Company, Amsterdam-Netherlands.
- Varekamp J, Buseck P. Global mercury flux from volcanic and geothermal sources. *Appl. Geochem.* 1 (1986) 65–73.

- Vazquez G, Antorrena G, Gonzalez J, Doval M.D. Adsorption of heavy metal ions by chemically modified Pinus pinaster bark. *Biores. Technol.* 48 (1994) 251.
- Vieira E, Soares I, Dias Filho N, Silva N, Garcia E, Bastos A, Perujo S, Ferreir T, Rosa A, Fraceto L. Preconcentration and determination of metal ions from fuel ethanol with a new 2,2'-dipyridylamine bonded silica. *J. Colloid. Interf. Sci.* 391 (2013) 116–124.
- Wagemann R, Trebacz E, Boila G, Lockhart W.L. Methylmercury and total mercury in tissues of arctic marine mammals. *Sci. Total. Environ.* 218 (1998) 19-31.
- Wallschläger D, Desai V.M.M, Spengler M, Wilken R. Mercury speciation in floodplain soils and sediments along a contaminated river transect. *J. Environ. Qual.* 27 (1998) 1034–1044.
- Wang Y, Luo X, Tang J, Hu X, Xu Q, Yang C. Extraction and preconcentration of trace levels of cobalt using functionalized magnetic nanoparticles in a sequential injection lab-on-valve system with detection by electrothermal atomic absorption spectrometry. *Anal. Chim. Acta.* 713 (2012) 92–96.
- Wang Y, Yang H, Pschenitza M, Niessner R, Li Y, Knopp D, Deng A. Highly sensitive and specific determination of mercury(II) ion in water, food and cosmetic samples with an ELISA based on a novel monoclonal antibody. *Anal. Bioanal. Chem.* 403 (2012) 2519–2528.
- Wang J, Liu B. Highly sensitive and selective detection of  $Hg^{2+}$  in aqueous solution with mercury-specific DNA and Sybr Green Iw. *Chem. Commun.* (2008) 4759–4761.
- Weber J.H, Evans R, Jones S. H, Hines M.E. Conversion of mercury(II) into mercury(0), monomethylmercury cation, and dimethylmercury in saltmarsh sediment slurries. *Chemosphere.* 36 (1998) 1669–1687.
- Weiss-Penzias P, Jaffe D, Swartzendruber P, Hafner W, Chand D, Prestbo E. Quantifying Asian and biomass burning sources of mercury using the Hg/CO ratio in pollution plumes observed at the Mount Bachelor Observatory. *Atmos. Environ.* 41 (2007) 4366–79.
- Whalin L, Kim E.H, Mason R. Factors influencing the oxidation, reduction, methylation, and demethylation of mercury species in coastal waters. *Mar. Chem.* 107 (2007) 278–294.
- WHO (World Health Organization) Environmental Health Criteria. Methylmercury 1990, vol. 101. Geneva, Switzerland : WHO/IPCS; 1995.
- Wu H, Jin Y, Han W, Miao Q, Bi S. Non-chromatographic speciation analysis of mercury by flow injection on-line preconcentration in combination with chemical vapor generation atomic fluorescence spectrometry. *Spectrochim. Acta. B.* 61 (2006) 831–840.
- Xu S, Chen L, Li J, Guan Y, Lu H. Novel  $Hg^{2+}$ -imprinted polymers based on thymine- $Hg^{2+}$ -thymine interaction for highly selective preconcentration of Hg in water samples. *J. Hazard. Mater.* 237–238 (2012) 347–354.
- Xu S, Chen L, Li J, Qin W, Ma J. Preparation of hollow porous molecularly imprinted polymers and their applications to solid-phase extraction of triazines in soil samples, *J. Mater. Chem.* 21 (2011) 12047–12053.
- Yan G, Viraraghavan T. Heavy-metal removal from aqueous solution by fungus *Mucor rouxii*. *Water. Res.* 37 (2003) 4486–4496.



- Yamini Y, Alizadeh N, Shamsipur M. Solid phase extraction and determination of ultra-trace amounts of mercury(II) using octadecyl-18-crown-6-tetraone and cold vapour atomic absorption spectrometry. *Anal. Chim. Acta.* 355 (1997) 69-74.
- Yayayuruk O, Henden E, Bicak N. Determination of mercury(II) in the presence of methylmercury after preconcentration using poly(acrylamide) grafted onto cross-linked poly(4-vinyl pyridine): Application to mercury speciation (2011). *Anal. Sci.* 27 (2011) 833-838.
- Yin Y, Chen M, Peng J.f, Liu J, Jiang G. Dithizone-functionalized solid phase extraction–displacement elution-high performance liquid chromatography–inductively coupled plasma mass spectrometry for mercury speciation in water samples. *Talanta.* 81 (2010) 1788–1792.
- Yin R, Feng X, Wang J, Bao Z, Yu B, Chen J. Mercury isotope variations between bioavailable mercury fractions and total mercury in mercury contaminated soil in Wanshan Mercury Mine, SW China. *Chem. Geol.* 336 (2013) 80-86.
- Zachariadis G.A, Anthemidis A.N, Daftsis E.I, Stratis J. Online speciation of mercury and methylmercury by cold vapour atomic absorption spectrometry using selective solid phase extraction. *J. Anal. At. Spectrom.* 20 (2004) 63-65.
- Zhai Y, Duan S, He Q, Yang X, Han Q. Solid phase extraction and preconcentration of trace mercury(II) from aqueous solution using magnetic nanoparticles doped with 1,5-diphenylcarbazide. *Microchim. Acta.* 169 (2010) 353–360.
- Zhang L, Chang X, Hu Z, Zhang L, Shi J, Gao R. Selective solid phase extraction and preconcentration of mercury(II) from environmental and biological samples using nanometer silica functionalized by 2,6-pyridine dicarboxylic acid. *Microchim. Acta.* 168 (2010) 79–85.
- Zhang T, Hsu-Kim H. Photolytic degradation of methylmercury enhanced by binding to natural organic ligands. *Nat. Geosci.* 3 (2010) 473–476.
- Zhang T, Kim B, Levard C, Reinsch B.C, Lowry G.V, Deshusses M.A, Hsu-Kim H. Methylation of mercury by bacteria exposed to dissolved, nanoparticulate and microparticulate mercuric sulfides. *Environ. Sci. technol.* 46 (2012) 6950-6958.
- Zheng C.B, Y. Li, He Y.H, Ma Q, Hou X.D. Photo-induced chemical vapor generation with formic acid for ultrasensitive atomic fluorescence spectrometric determination of mercury: potential application to mercury speciation in water. *J. Anal. At. Spectrom.* 20 (2005) 746–750.
- Zouboulis A.I, Loukidou M.X, Matis K.A. Biosorption of toxic metals from aqueous solutions by bacteria strains isolated from metal-polluted soils. *Process. Biochem.* 39 (2004) 909–916.

***Chapitre B: Méthodes expérimentales***

***Chapter B: Experimental methods***

*This chapter* is divided into two parts; the first part comprises the materials and methods used for the development of new analytical methods for the measurement of mercury in natural water samples.

The main objective of the *first part* of the study is to develop analytical methods based on the Solid Phase Extraction (SPE) of analytes, which are at the same time cheap, simple, and rapid and are capable of *in situ* sampling of mercury ions. Two different methods were employed for the solid phase extraction of mercury ions from natural water samples (figure B.1). The first one is based on the simple addition of a ligand to water samples to form ligand-Hg chelates with subsequent extraction on silica phase and detection using a suitable analytical technique. The second method is based on the immobilization of a ligand of a desired functional group (e.g. 8-hydroxyquinoline) on silica phase. Natural water samples are therefore extracted throughout the ligand-functionalized silica and finally the eluted mercury ions can be quantified using an adequate detection technique. Based on the principles of the latter methods, two analytical methods were developed for the measurement of mercury ions in river water. The first one has implicated the solid phase extraction of mercury ions onto a chelating resin (8-hydroxyquinoline-functionalized silica) and detection using CV-AFS. The other one is based on a more simple method of direct addition and complexation of mercury ions in river water using iodide and a cationic surfactant followed by a subsequent extraction on silica phase and detection using ICP-MS.

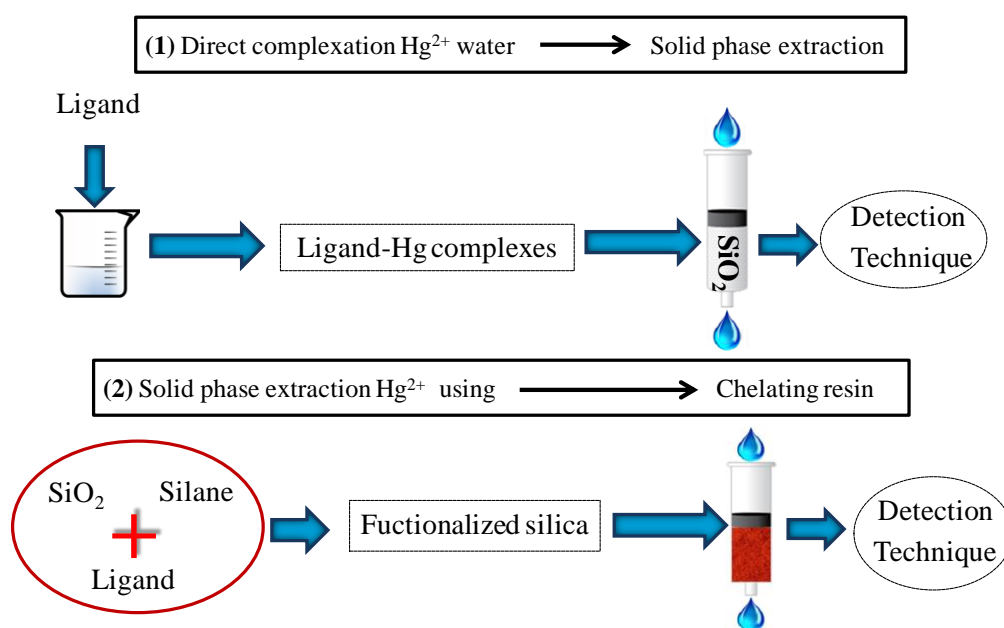


**Figure B.1.** Different methods used for mercury ions enrichment from water samples.

8-Hydroxyquinoline (figure B.2. (a)) has been chosen as a ligand for mercury solid phase extraction studies because of its outstanding characteristics of metal extraction. Even though there are many studies that determined the structure of metal complexes with 8-hydroxyquinoline and their stability constant formation, the latter ligand is poorly studied with mercury ions. In the literature, Asmy et al. (1990) has determined that Hg(II) forms a six-membered ring as a negative bidentate with 7-formyl-8-hydroxyquinoline (figure B.2. (b)). Besides, in the literature there are many studies which have determined the stability constant of different metals with 8-hydroxyquinoline, however; no studies have been performed for its determination with mercury.

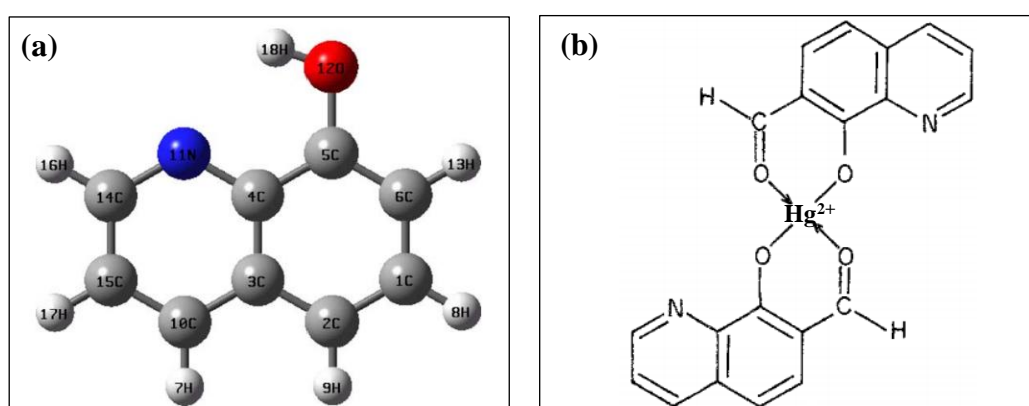


**Figure B.2.** (a) Molecular structure of 8-hydroxyquinoline (Arici et al 2005), (b) Hg<sup>2+</sup>-7-formyl-8-hydroxyquinoline complex structure (Asmy et al 1990).

The *second part* is consecrated to the study of the distribution, speciation and the biogeochemical behavior of mercury in the Deûle and Lys rivers (Northern France). Thereby, this part includes a description of the study sites and the materials and methods utilized for the sampling and analysis of mercury species in the sediment phase and surface water.

## Part I: Analytical method development for the determination of mercury in water matrix

### B.I.1. Reagents

All chemicals and solvents used were analytical grade. Ultrapure water (with a resistivity of 18.2 M $\Omega$ .cm) was obtained using a Milli-Q system (Millipore, USA). Labware was soaked in 20% nitric acid and washed thoroughly with pure water prior to use. Inorganic mercury (Hg(II)) stock solution (1000 mg/L) was prepared from mercuric chloride (Merck) Working solutions of metals (Cr(III), Cu(II), Co(II), Zn(II), Ni(II), Pb(II), Cd(II), As(II), Fe(III), V(II)) were prepared from stock metal nitrate solution (1000 mg/L) (Merck). Silica (100-200 mesh), chemicals and solvents were supplied from Sigma Aldrich (France). Buffer solutions were prepared from 1 M sodium acetate and the pH was adjusted to the desired pH value by addition of 1 M HNO<sub>3</sub>. Ammonium acetate and phosphate buffer were used for obtaining pH 7 and pH 8 respectively.

### B.I.2. Analytical instruments

The pH measurements and adjustments were conducted by pH meter calibrated using two standard buffer solutions of pH 4 and pH 7. The flow rate of the samples was adjusted using a Gilson Miniplus 3 peristaltic pump. PVC tubes (3.18 i.d) were used for the preconcentration process. Self-made PTFE (polytetrafluoroethylene) columns (65 mm  $\times$  4 mm i.d.) were used for packing the examined adsorbent. **Fourier Transform Infrared (FT-IR)** spectra of functionalized silica were recorded using Nicolet 380 Smart iTR spectrometer (ThermoScientific, USA) and were silica-matrix corrected.

During this study, various analytical techniques were employed for the quantification of mercury ions. In *chapter C*, an Inductively Coupled Plasma Atomic Emission Spectroscopy was used for mercury ions quantification. In *chapter D*, Cold Vapor Atomic Fluorescence Spectroscopy was used for the method development of mercury quantification in river waters. In *chapter E*, Inductively Coupled Plasma Mass Spectrometry was utilized as a detection technique for the method developed using I/DTAB/SiO<sub>2</sub> extraction system of mercury ions from river water. The detailed description of the three analytical instruments used was as following:

**Inductively Coupled Plasma Atomic Emission Spectroscopy (ICP-AES)** is a powerful and popular technique for trace element determination within different matrices. In this technique, the sample can be introduced in the plasma core by three different means, by using a nebulizer, hydride generation or by using electrothermal vaporization. However, nebulizers are the most common devices for sample introduction which includes three different types of devices; one referred as concentric nebulizer, the other as cross-flow nebulizer, and the last as Babington nebulizer. The core of the plasma is sustained at a temperature of 10 000 K. Therefore, the aerosols introduced are vaporized and liberated as free atoms and ions at the gaseous state. The collisional excitation within the plasma promotes the excitation of the atoms. When the excited ions and atoms relax to the ground state, they emit photons which are characteristics energies of the target analytes. Thereby, the wavelengths of the photons are used to identify the analytes from which they originated. The photons emitted are then collected and focused with a lens or concave mirror and separated using a monochromator. Finally, the signal is detected using a photodetector after its conversion into electrical signal and its amplification. There are three configurations for observing emissions from ICP: radial, axial and dual. With radial viewing, the plasma is operated in vertical orientation. On the other hand in axial view, the plasma is oriented to a horizontal position. The axial view contributes to better LODs than radial. This is ascribed to the longer viewing path available down the axis of the plasma. The Dual view is employed for complex matrices of wide range of concentrations. This view configuration is a combination of both radial and axial views. In *chapter C*, concentration of Hg(II) ions were determined by using **Inductively Coupled Plasma Atomic Emission Spectroscopy (ICP-AES; Varian Vista Pro, axial view, 253 nm)**. External calibration was performed using standard solution and blank correction was applied if necessary.

**Inductively Coupled Plasma Mass Spectrometer (ICP-MS)** has the same principles as that of ICP-AES, however; in ICP-MS a mass spectrometer is used to separate and quantify ions based on their mass to charge ratio. In *chapter E*, an **Inductively Coupled Plasma Mass Spectrometer**, Thermo-Optek X7 (Thermo Fischer Scientific, USA), equipped with a cross-flow pneumatic nebulizer, a concentric glass-type nebulization chamber and a 1.5 mm i.d. quartz plasma torch, was used for Hg(II) and metal ions determination. All the operating parameters were those recommended by the manufacturer. The optimum operating conditions and measurement parameters for ICP-MS. Measurements were performed with high purity

Argon gas. The optimum operating conditions and measurement parameters for ICP-MS are listed in table.B.I.1.

**Table B.I.1.** Operating conditions ICP-MS.

Forward Power (W)	1050
Nebuliser Gas Flow (L/min)	0.7
Auxiliary Gas Flow (L/min)	0.95
Cool Gas Flow (L/min)	13.5
Quartz Plasma Torch I.D. (mm)	1.5
Cone type	Pt
Glass Impact Bead	3
Spray Chamber temperature (°C)	
Nebulizer type	Concentric glass
Sample Uptake Rate (mL/min)	1
Uptake delay (s)	35
Washout delay (s)	150
Analyte	<sup>202</sup> Hg

**Cold vapor Atomic Fluorescence Spectroscopy (CV-AFS)** uses the characteristics of mercury that allows vapor measurements at room temperature. Mercury ions are excited by a specific wavelength at 253.7 nm by Hg-cathode lamp. Upon the passage of the excited atoms to the background state, they tend to emit photons at the same wavelength of the excitation source. This technique is called atomic fluorescence spectrometry, because the fluorescence signal is measured at 90° angle from the excitation source. CV-AFS as compared to the conventional techniques e.g. Atomic Absorption Spectroscopy (AAS) is considered as more sensitive, more selective and is linear over a wide range of concentrations. In **chapter D**, mercury ions were measured by **Cold Vapor Atomic Fluorescence Spectroscopy** (Tekran, Model 2600 CVAFS Mercury Analysis System, USA). Ionic mercury is reduced with SnCl<sub>2</sub> (2% solution in 1 % HCl), subsequently converting Hg(II) to Hg<sup>0</sup>. The volatile species of mercury are separated from solution by purging with high purity argon gas through a semi permeable dryer tube. Volatile mercury is then carried by argon gas and preconcentrated into

a gold cell of the Cold-Vapor Atomic Fluorescence spectrometer. After thermal desorption, the concentration of Hg is determined by atomic fluorescence spectrometry at 253.7 nm.

### **B.I.3. Water sampling for optimization and application studies**

River water samples were taken by hand into precleaned acid-washed polyethylene bottles. Clean techniques were used for sampling, handling and analyzing the samples. All materials used for sampling and filtration were acid-washed and stored in double polyethylene bags until required. River water was sampled from the Deûle river (northern France); the latter river is shown by many studies to be highly polluted with heavy metals. Water samples collected were filtered directly through cellulose acetate filters of 0.45  $\mu\text{m}$  pore size. Then, the samples were preserved by adding high purity concentrated  $\text{HNO}_3$  (Merck, suprapur) and stored in dark cold place at 4 °C. Tap water was sampled directly from the laboratory's faucet after keeping water running for almost 10 minutes. Tap water was supplied by the North Water Agency "EauxDuNord". Tap water was sampled in precleaned acid washed polyethylene bottles and preconcentrated directly without any preservation techniques. River and tap water characteristics employed throughout the studies of method development are shown in table B.I.2 and B.I.3.



**Table B.I.2.** Deûle water chemical characteristics (Lesven et al 2009; Pygriël, 2013).

Element	C <sup>a</sup> (µS/cm)	T <sup>b</sup> (°C)	D.O <sup>c</sup> (mg/L)	pH	Ca (mg/L)	Cd (ng/L)	Cu (ng/L)	Cr (ng/L)	Fe (ng/L)	Ni (ng/L)	Pb (ng/L)	Zn (ng/L)	SO <sub>4</sub> <sup>2-</sup> (mg/L)	NO <sub>3</sub> <sup>-</sup> (mg/L)	Alc <sup>d</sup> (mmol/L)	DOC <sup>e</sup> (mg/L)
Average Concentration	705	14	9	8	0.069	0.019	0.746	0.076	8.846	0.974	0.327	5.506	550	20	3.4	2.8

a: Conductivity, b:Temperature, c: Dissolved oxygen, d: Alkalinity, e: DOC: dissolved organic carbon

**Table B.I.3.** Drinking water quality limits (CODE DE LA SANTE PUBLIQUE FRANCAISE).

Element	T <sup>a</sup> (°C)	pH	DOC <sup>b</sup>	Conductivity (µS/cm)	Ca (mg/L)	Cd (µg/L)	Cu (mg/L)	Cr (µg/L)	Fe (µg/L)	Ni (µg/L)	Pb (µg/L)	Zn (µg/L)	SO <sub>4</sub> <sup>2-</sup> (mg/L)	NO <sub>3</sub> <sup>-</sup> (mg/L)
Concentration	25	6.5-9	2	200-1100	450	<5	<1	<50	<200	<20	<10	-	<250	<50

a: Temperature b:Dissolved organic matter

## B.I.4. Synthesis of 8-hydroxyquinoline grafted silica gel

### B.I.4.1. Preparation of the hydroxyquinoline functionalized silica gels

Different immobilization procedures were used to produce six immobilized-8-quinolinol silica gels that differ by the nature and the position of the bond connecting the chelating agent to the surface of silica gel (Figure B.I.1). Prior to use, silica gel was activated by hydrochloric acid, neutralized, and then dried at 110°C till total dryness. For the preparation of aminopropyl silica gel (APSG), the dried silica gel (10 g) in toluene (150 mL) was refluxed with aminopropyltriethoxysilane (10 mL) for 18h. The resulting suspension was filtered and washed successively with toluene, diethylether, ethanol (20 mL each) and finally dried at 60°C.

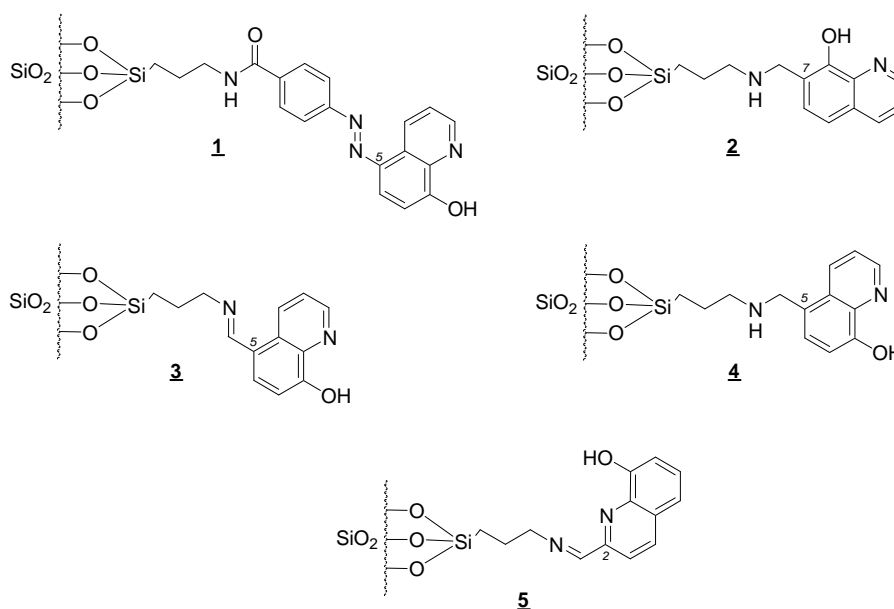


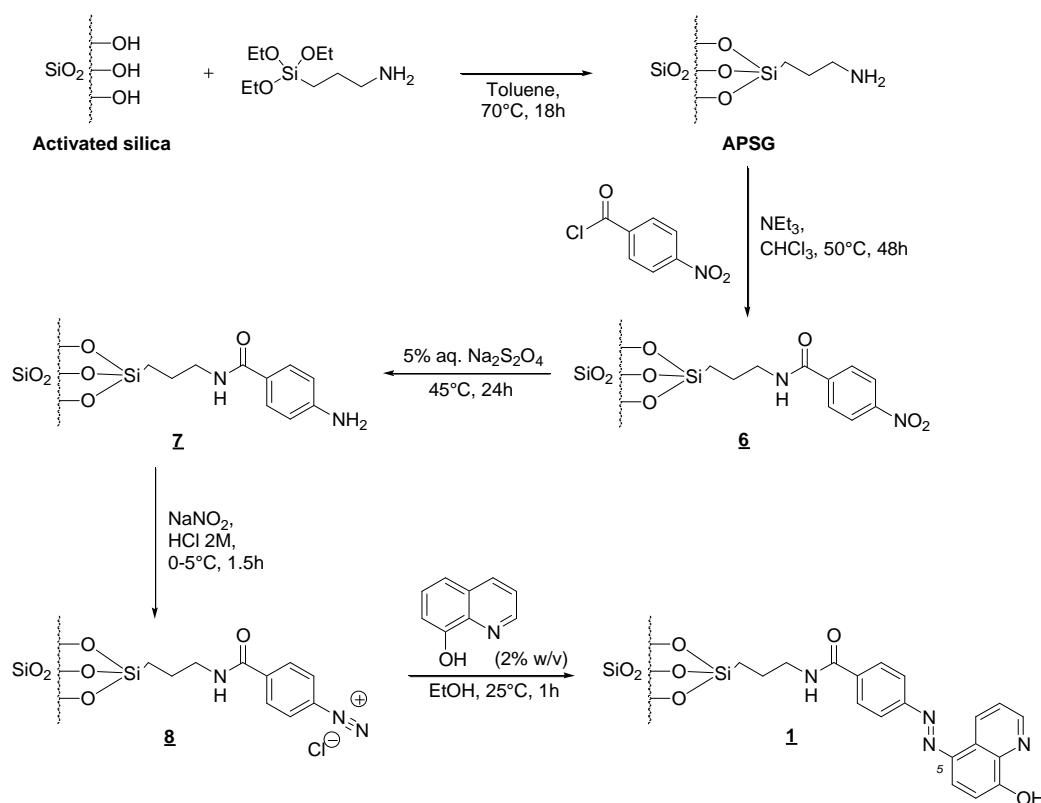
**Figure B.I.1.** Studied 8-hydroxyquinoline modified silica gels.

#### *Method 1*

The first strategy concerned loading of 8-hydroxyquinoline on activated silica gel as described by Kamal et al (2011). The non-covalent procedure for impregnation involved mixing of 8-HQ and silica gel in ethanol and ultra pure water with heating at 60°C for 24 hours to produce resin **6**.

Method 2 (Scheme B.I.1)

Phenylazo-8-hydroxyquinoline silica gel **1** was prepared according to the procedure proposed by Sugawara et al (1974). The procedure firstly consists in a coupling step between an arylamine moiety and aminopropyl silica gel (APSG) to permit further azo-linking of 8-hydroxyquinoline on position 5. APSG (10 g) was also acylated by treatment with *p*-nitrobenzoyl chloride (1 g) in chloroform (60 mL) in the presence of triethylamine (2 mL). The nitro-adduct **6** was then reduced by sodium dithionite (5% w/v solution) to yield aminobenzoyl-APSG **7**. Oxidation of the amino-moiety with sodium nitrite afforded formation of the expected diazonium salt **8**, which was rapidly filtered to be coupled with 8-HQ. Formation of the final adduct **1** was characterized by the rapid development of a deep red color, prominent feature of the formation of the expected diazo-linkage.

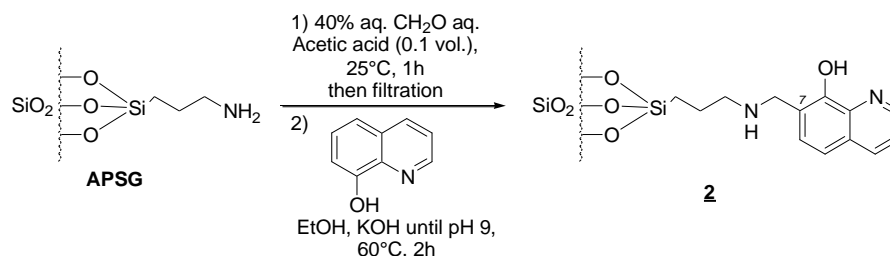


Scheme B.I.1. Preparation of phenylazo-8-hydroxyquinoline silica gel **1**

Method 3 (Scheme B.I.2)

Starting from aminopropyl silica gel (APSG), preparation of the 8-hydroxyquinoline silica gel (**2**) was performed according to the procedure described by Pyell and Stork (1992). Involving a Mannich reaction, this strategy offers immobilization of 8-HQ on position 7 via a secondary

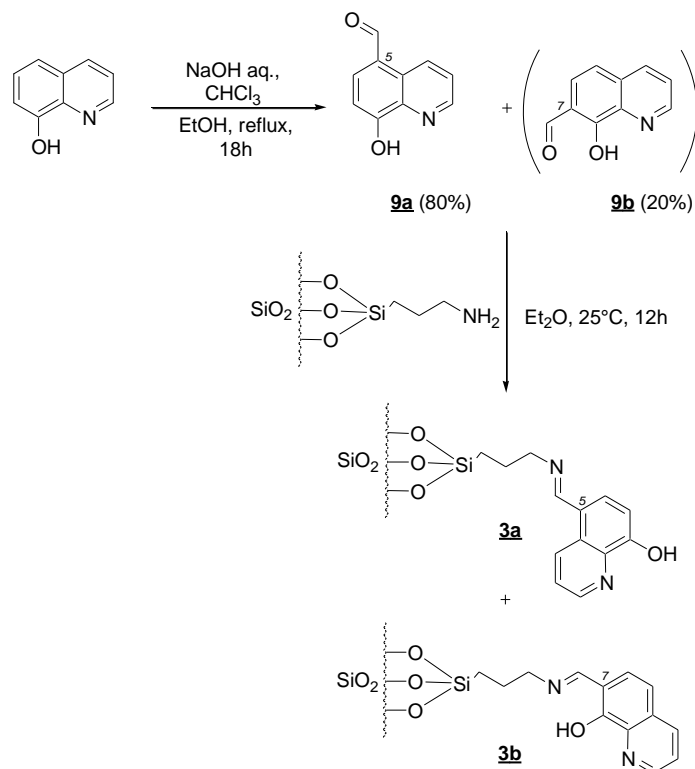
amine bond linkage. Surface functionalization was performed by mixing APSG with formaldehyde (40 % aq.) in the presence of acetic acid, followed by coupling of the intermediate iminium with 8-HQ at pH 9.



**Scheme B.I.2.** Preparation of amino-immobilized 8-HQ silica gel **2**

*Method 4 (Scheme B.I.3)*

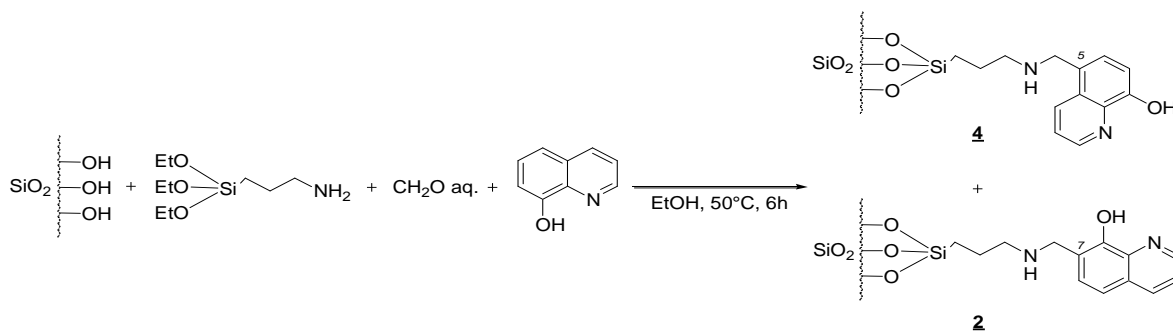
The third strategy involved immobilization of 8-HQ on position 5 via formation of a Schiff base according to Goswami et al (2003). Starting from 8-hydroxyquinoline, installation of the carbaldehyde function was accomplished by a Reimer-Tiemann reaction as described by Clemo et al. (1955). Formation of the corresponding imino-immobilized 8-HQ silica gels **3a** and **3b** was performed by condensing the aldehyde mixture **9a** + **9b** with APSG in anhydrous diethylether.



**Scheme B.I.3.** Preparation of imino-immobilized 8-HQ silica gels **3a** and **3b**

Method 5 (Scheme B.I.4)

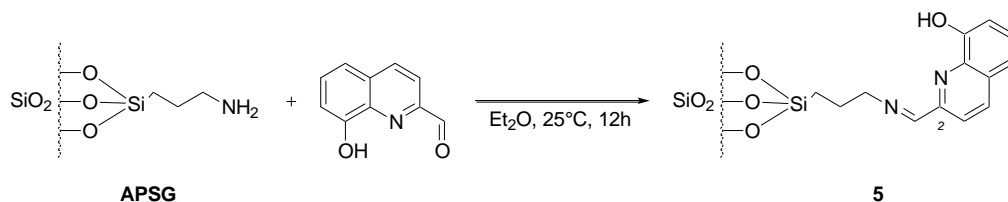
The fourth studied strategy involved the one-step Mannich reaction described by Wang et al. (2006), yielding a mixture of amino-immobilized 8-HQ silica gels **4** and **2**. As stated by the optimized method, 8-HQ was allowed to react with silica gel in presence of formaldehyde and aminopropyltrimethoxysilane (0.8 eq. vs. 8-HQ) for 6 h in ethanol at 50°C.



**Scheme B.I.4.** Preparation of amino-immobilized 8-HQ silica gels **4** and **2**

Method 6 (Scheme B.I.5)

We also embarked on the study of a new anchored silica gel concerned by a Schiff-base functionalization of APSG with 8-hydroxyquinoline on position 2. Here, imino-immobilized 8-HQ silica gel **5** was prepared by condensation of APSG with the commercial 2-formyl-8-hydroxyquinoline as described in scheme 5.



**Scheme B.I.5.** Preparation of imino-immobilized 8-HQ silica gel **5**

**B.I.4.2. Preconcentration procedure using the synthesized chelating resins**

The efficiency of the six above-mentioned immobilized-8-quinolinol silica gels was investigated for Hg(II) extraction from river samples. Three hundred milligrams of Si-8-HQ were packed in the column and plugged with frit caps at both ends. Prior to sample percolation, solid phase was conditioned to the pH of the sample. The packed 8-HQ resins were tested by using river water samples spiked with 0.2 µg/mL of Hg(II). River water samples were then adjusted to the desired pH value with buffer prior to percolation. After

percolation of the water samples, the retained mercury ions were eluted with a suitable eluent and analyzed using ICP-AES (figure B.I.2).

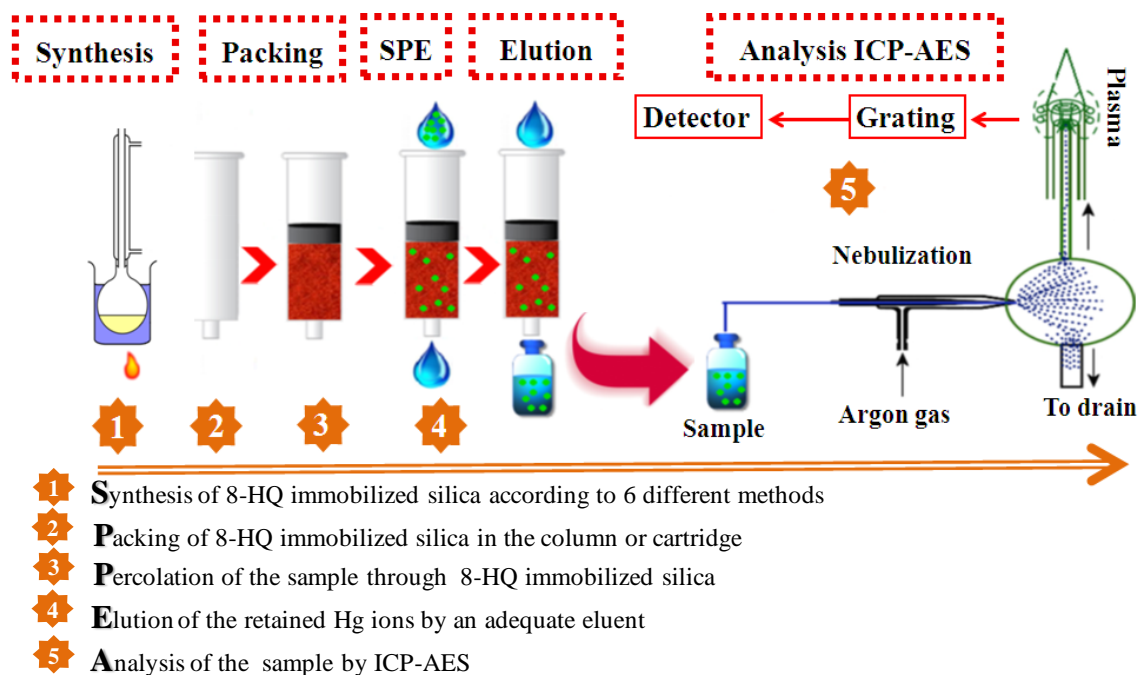


**Figure B.I.2.** Experimental protocol used for the examination of the efficiency 8-HQ based chelating resins for mercury extraction.

#### B.I.4.3. Preconcentration procedure using the 5-phenylazo-8-hydroxyquinoline

5-phenylazo-8-hydroxyquinoline (5Ph8HQ) is chosen among the six different 8-HQ based chelating resins because of its high extraction recoveries of mercury ions from river water, high synthetic yields, low cost of chemical reagent and low toxicity. For optimization procedure (figure B.I.3), the synthesized 5Ph8HQ was cleaned by 20 mL of 2 M HNO<sub>3</sub> at a flow rate 2 mL/min, washed by Milli-Q pure water until free from acid and finally conditioned by acetate-acetic acid buffer system at a flow rate of 1 mL/min. Aliquots of 50 mL of river water containing of 2 ng/mL were adjusted to optimal extraction pH using Ammonia or HNO<sub>3</sub> suprapur solution. Samples were percolated through 300 mg pre-cleaned resin at optimized flow rate, eluted with a suitable eluent and finally analyzed by CV-AFS.

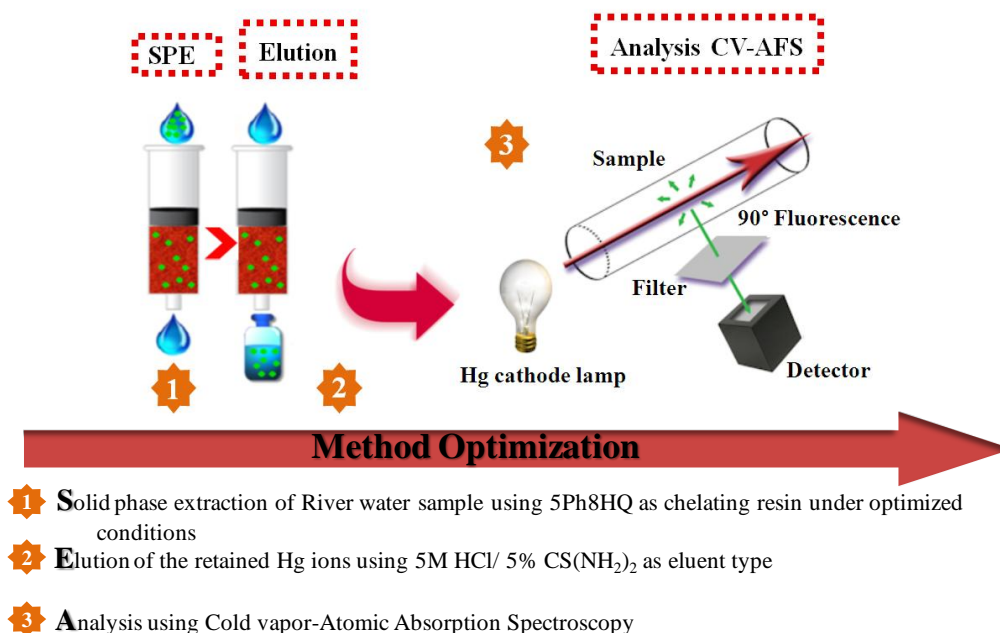


**Figure B.I.3.** Experimental procedure for the solid phase extraction of mercury ions using 5Ph8HQ as chelating resin and CV-AFS as analytical technique.

## B.I.5. Preconcentration strategy using direct addition of reagent to the sample

### B.I.5.1. Preconcentration strategy using the direct addition of 8-hydroxyquinoline to the sample

We were also interested in studying mercury direct complexation with 8-hydroxyquinoline followed by the adsorption of the complex onto octadecyl silica gel.

C<sub>18</sub> cartridges were prepared by activation of a batch of silica gel. Prior to use, C<sub>18</sub>-silica gel was washed with methanol, ultra pure water and 2 M aq. nitric acid HNO<sub>3</sub> in order to remove contaminants. Octadecyl silica gel was then prepared using ultrapure water (20 mL/g silica), methanol (5 mL/g silica) and ultrapure water (20 mL/g silica). PTFE columns (6 ml volume, 4.0 mm i.d., 60 mm length) were packed with one gram of activated silica gel. A suitable 50 mL model solution of 0.2 µg/mL of Hg(II) and 5×10<sup>-4</sup> M of 8-hydroxyquinoline was prepared in ultrapure water. Under optimized conditions, water samples were adjusted to pH 4 and passed through a column containing the tested adsorbent at a constant flowrate of 2 mL/min. Retained Hg(II) ions were stripped off using 10 ml (2 M) HNO<sub>3</sub> at a flowrate of 0.5 mL/min. Quantitative analyses of eluents were performed by ICP-AES in order to determine the percentage of retention (figure B.I.4).

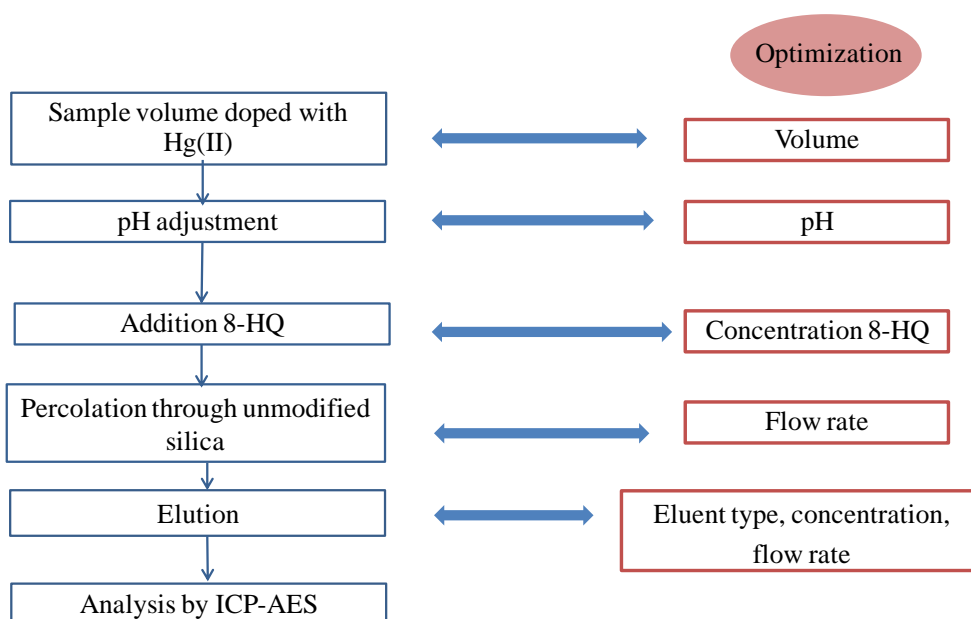


**Figure B.I.4.** Method optimization of the direct addition of 8-HQ to water samples.

### B.I.5.2. Preconcentration strategy using the direct addition of iodide and cationic surfactant to the sample

Home-made silica phase columns were fabricated. For that purpose, a batch of silica gel (100-200 mesh) was activated by passing successively 20 mL/1 g silica methanol, 20 mL/1 g ultrapure water, 20 mL/1 g silica 2 mol/L nitric acid, 20 mL/1 g silica ultrapure water, 5 mL/1 g silica methanol, 10 mL/1 g ultrapure water. Then 1 g activated silica phase is packed in PTFE column (6 mL volume, 4.0 mm i.d., 60 mm length) and sealed with glass wool at both ends. Suitable 50 mL river water was spiked with a final concentration 0.04  $\mu\text{g/mL}$ , 0.01 mol/L KI, 0.0005 mol/L dodecyltrimethylammonium chloride (DTAB). The river water samples are left to stabilize for 1 hour and then passed through the column at a flow rate of 2 mL/min using a peristaltic pump. The retained analytes are desorbed from silica phase by using 8 mol/L nitric acid at a flow rate of 0.5 mL/min and analysed using ICP-MS (figure B.I.5).



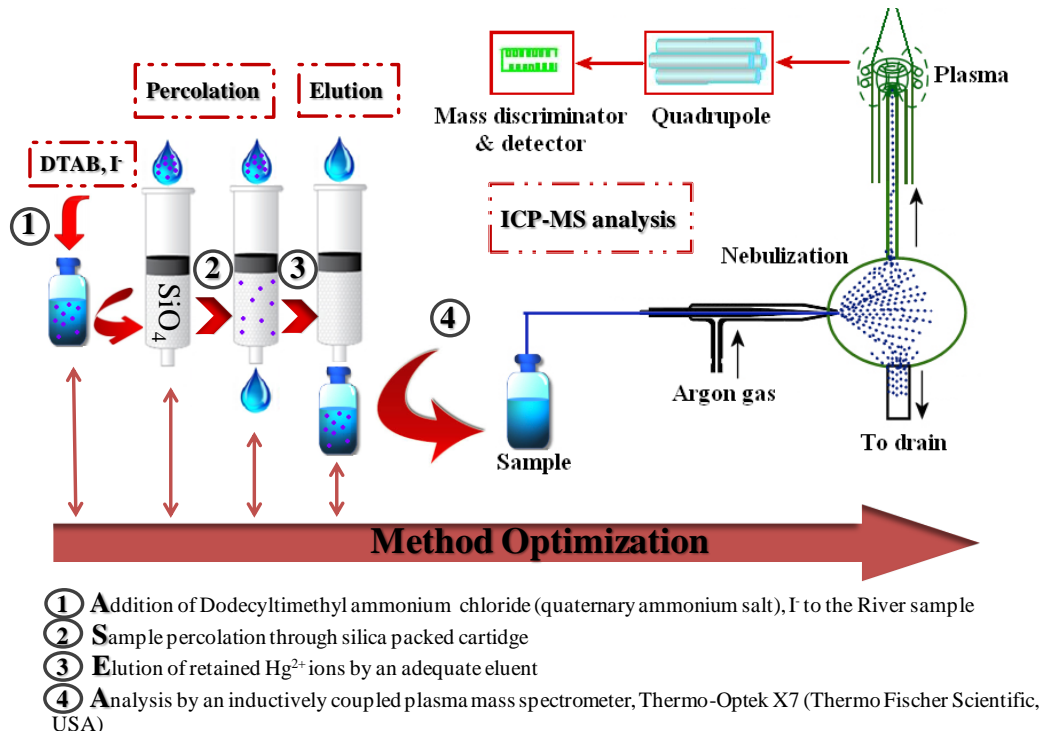


**Figure B.I.5.** Experimentale procedure for the extraction of mercury ions from river water based on I/DTAB/SiO<sub>2</sub> system.

### B.I.6. Batch sorption experiments

Among six different 8-HQ linked silica examined for the extraction of mercury ions, 5-phenylazo-8-hydroxyquinoline is chosen for mercury adsorption dynamics studies (figure B.I.6).

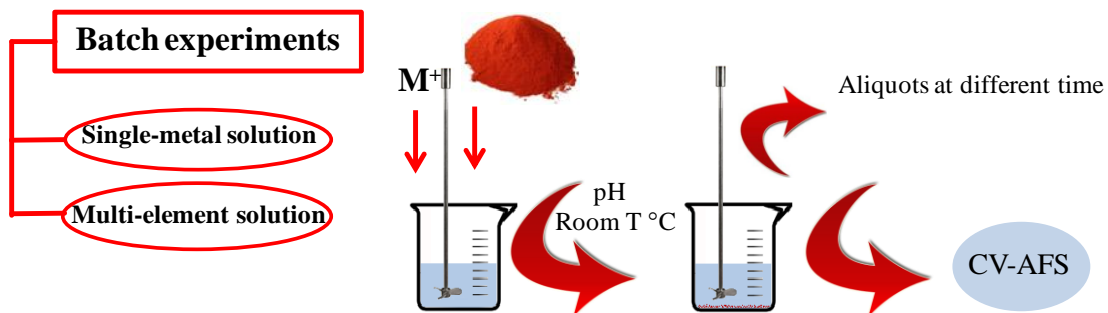


**Figure B.I.6.** Adsorption dynamics studies of mercury ions on 5-phenylazo-8-hydroxyquinoline using batch experiment mode.

### B.I.6.1. Adsorption experiments

A series of metal sorption experiments were conducted to study the effect of pH, sorption kinetics, selectivity, adsorption capacities, and interferences of mercury with other metals. Batch experiments were conducted using 1000 mL polyethylene (PE) bottles. The amount of adsorbent used was 1 g and the volume of ultra-pure water was maintained at 200 mL. A concentration of metal ion of 1 µg/mL was prepared by dilution of stock solution (1000 mg/L M<sup>+</sup>) and adjusted to the required pH using an adequate buffer system. The bottles were shaken at room temperature for a fixed period of time at constant speed 150 g. At the end of shaking time, the supernatant was separated from the solid phase by filtration using Millipore filters and analyzed by ICP-MS for metals and mercury analysis was performed using CV-AFS. The experiments were conducted in duplicates and the average results were reported. This methodology was followed to identify the pH effect, optimize shaking time and understand the competition between metals towards 5Ph8HQ sites and its effect on mercury adsorption efficiency.

Metal uptake or sorption capacity was calculated based on the difference of metal ion concentration before and after adsorption according to eq. (1). The percentage of mercury sorption, distribution coefficient, selectivity coefficients and half-life sorption (Rivas et al, 2012) were calculated using Eqs. (1)- (5) respectively.

$$\text{Sorption (\%)} = \frac{C_i - C_e}{C_i} \times 100 \quad (1)$$

$$Q = \frac{(C_i - C_e)V}{m} \quad (2)$$

$$K_d = \frac{Q}{C_e} \quad (3)$$

$$\alpha = \frac{K_d(\text{Hg(II)})}{K_d(X)} \quad (4)$$

$$t^{1/2} = \frac{1}{K_2 Q_e} \quad (5)$$

Here,  $C_i$  (mg/L) is the initial concentration;  $C_e$  (mg/L) the equilibrium concentration in the solution;  $V$ (L) the solution volume;  $m$  (g) the amount of sorbent;  $Q$ (mg/g) represents the sorption capacity;  $K_d$  distribution coefficient,  $\alpha$  is the selectivity coefficient for the binding of a specific metal in the presence of other competitive ions;  $X$  represents the metal ion species;  $K_2$  (g/mmol min) is the rate constant of pseudo second order reaction.

### B.I.6.2. Kinetics studies

A concentration of metal ion of 1 µg/mL was prepared and adjusted to the optimized pH using buffer system. An accurately measured sorbent of 1 g was added. Different aliquots were sampled and filtered at different time intervals for 24 hours. Sorption dynamics were studied in mercury single metal solution and binary solutions of Hg(II)-Cu(II), Hg(II)-Co(II), Hg(II)-Ni(II), Hg(II)-V(II), Hg(II)-Fe(III). Moreover, adsorption kinetics were performed in multi-element mixture composed of Hg(II), Cr(III), Fe(III), V(II), As(II), Co(II), Cu(II), Ni(II), Cd(II), Pb(II), Mn(II).

Sorption kinetics were analyzed using pseudo-first, pseudo-second order rate equation and intra particle diffusion model. Chemical reactions in homogenous systems are described as pseudo first-order rate equation. The linearized form of the first-order rate equation by Lagergren and Svenska. (1898) is given in eq. (6):

$$\text{Log}(Q_e - Q_t) = \text{log}Q_e - \frac{K_1 t}{2.303} \quad (6)$$

Where  $Q_e$  and  $Q_t$  are the amounts of metal ions adsorbed (mmol/g) and at contact  $t$  (min), respectively,  $K_1$  (1/min) is the rate constant.

The linearized equation of pseudo-second rate equation was given by Ho et al. 1999 as eq.(7):

$$\frac{1}{Q_t} = \frac{1}{K_2 Q_e^2} + \left(\frac{1}{Q_e}\right) t \quad (7)$$

Where  $K_2$  (g/mmol min) is the rate constant of pseudo-second order adsorption reaction.

Intra-particle diffusion can be described by the model given by Weber et al. 1963 by eq. (8):

$$Q_t = K_i t^{1/2} \quad (8)$$

Where  $K_i$  is the intraparticle diffusion rate constant (mmol/g min<sup>0.5</sup>).

### B.I.6.3. Adsorption isotherms

Adsorption isotherms were also determined for Hg(II). Accurately measured 1 g of the sorbent was mixed with 50 mL of solution adjusted to the Hg optimal pH. The concentration of metal ion was changed between 10-160 mg/L and shaken at a constant agitation speed of 150 r/min. The contact time was selected on the basis of the kinetics studies. At equilibrium time; an aliquot was sampled, filtered and analyzed. The results were adjusted to Langmuir,

Freundlich, Dubinin-Radushkevich D-R models (Freundlich et al 1907; Dikici et al 2010; Dubinin et al 1947). The Langmuir model linearized form is given by eq.(9):

$$\frac{1}{Q_e} = \frac{1}{Q_m} + \frac{1}{b Q_m C_e} \quad (9)$$

Where  $Q_e$  (mmol/g) is the amount of metal ion adsorbed,  $C_e$  is the equilibrium metal ion concentration (mmol/L),  $Q_m$  (mmol/g) is the maximum Langmuir uptake, when the surface of the adsorbent is completely covered with adsorbate,  $b$  (L/mmol) is the Langmuir adsorption constant.

The Freundlich linearized form is described by Eq. (10):

$$\log Q_e = \log K_F + n \log C_e \quad (10)$$

where  $Q_e$  is the equilibrium metal ion concentration on the adsorbent (mmol/g),  $C_e$  is the equilibrium concentration of metal ion (mmol/L),  $K_f$  is the Freundlich constant ( $\text{mmol}^{(1-1/n)} \text{L}^{(1/n)}/\text{Kg}$ ) which indicates the adsorption capacity and the strength of the adsorption and  $n$  is the heterogeneity factor representing bond distribution.

The D-R adsorption isotherm linearized form is given by the following eq. (11):

$$\ln Q = \ln Q_m - K \varepsilon^2 \quad (11)$$

where  $Q$  is the amount of metal ion adsorbed per unit weight of the sorbent (mol/g),  $K$  is a constant related to the adsorption energy ( $\text{mol}^2/\text{KJ}^2$ ),  $Q_m$  is the maximum adsorption capacity (mol/g),  $\varepsilon$  is the Polanyi potential (J/mol).

## Part II: Biogeochemistry behavior of mercury in aquatic environments

### B.II.1. Study sites

The major source of mercury pollution to the Deûle river is attributed to a former ore smelter called “Metaleurop” that was active for more than a century and finally closed in 2003. Its activities have led to huge discharges of ore minerals i.e. metal sulfides to the river and its surrounding environments. The Deûle and the Lys rivers are the principal confluences of the Scheldt river which is considered as a major source of pollution to the North Sea. Therefore, a biogeochemical study of mercury behavior was conducted and sediment cores were sampled downstream and upstream the Deûle and Lys rivers in order to determine the impact of the Deûle mercury pollution on Lys river (figure B.II.1).

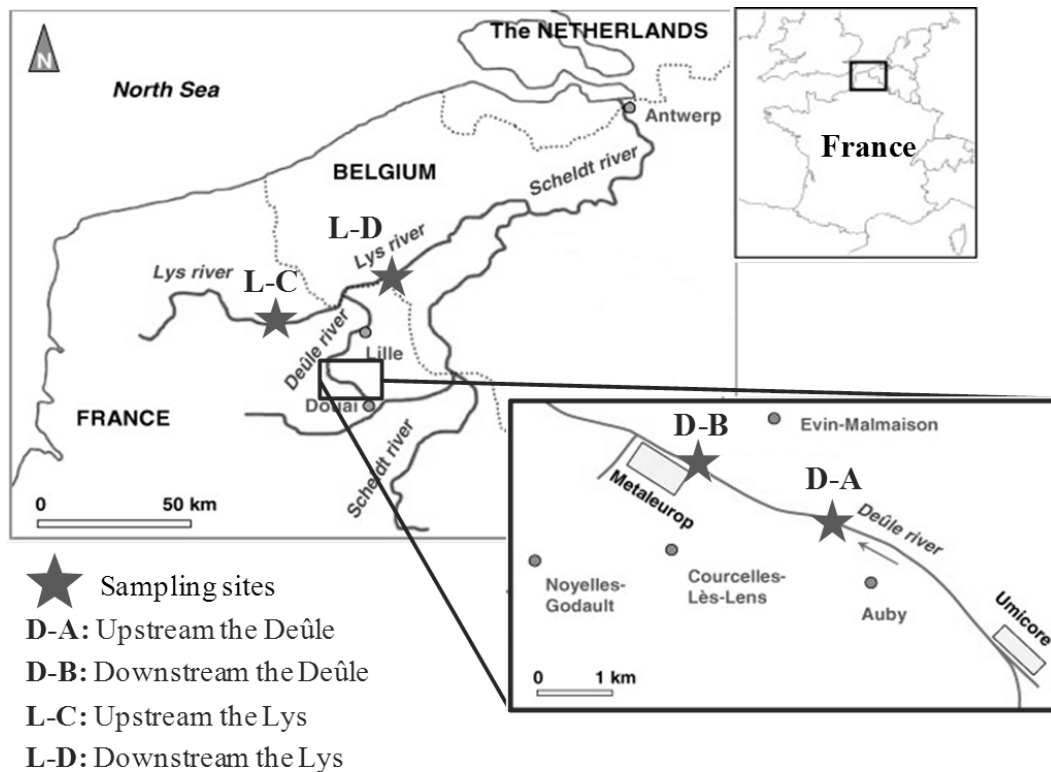


**Figure B.II.1.** Sampling sites in Deûle and Lys rivers.

**B.II.1.1. The Deûle river**

The Deûle river is located in the watershed of the Scheldt and is a major tributary of the Lys. This river is about 68 km long with an average flow rate of 8 m<sup>3</sup>/s. The river main source originates at Souchez (Pas-de-Calais), and then the river crosses successively Douai and Lille cities before merging with the Lys river (table B.II.1). This river runs along many areas of industrial and commercial activities, causing an eventual significant pollution to the watershed. The sites that were chosen in the Deûle river were selected in the surroundings of the former smelter “Metaleurop”. The area chosen for sampling is a highly polluted zone by the past metallurgic activities of Metaleurop which was operational for more than a century and closed for almost a decade. The latter smelter was located at Noyelles-Godault and it is a European group specialized in the production, transformation and the valorization of Zinc, Lead, Germanium and Indium. The chain of activities of the smelter starts up with production of metals from ore minerals, valorization of the industrial wastes and finally product marketing. Metaleurop was established in 1984 and was one of the largest lead smelters in Europe with an annual production of 170,000 tonnes in 1995. Its industrial activities were classified as Seveso 2, which had generated phenomenal pollution to the surrounding environments.

**B.II.1.2. The Lys river**

The Lys is a river in northern France and Belgium, a major tributary of the Scheldt in Ghent. The Lys river originates in Lisbourg (Pas-de-Calais) near Fruges at an altitude of 114.7 m with a total length of 195 km. It is a river that crosses the French territories in Wallon and Flamand with a total length of 85 km, and then it continues to Belgium with a total length of 24.6 km (table B.II.1).

**Table B.II.1.** Principal characteristics of Lys and Deûle rivers.

	<b>The Lys</b>	<b>The Deûle</b>
<b>Length (Km)</b>	195	68
<b>Flowrate (m<sup>3</sup>/s)</b>	29	8
<b>Countries</b>	France, Belgium	France
<b>Source</b>	Lisbourg	Souchez
<b>Outfall</b>	Scheldt	Lys
<b>Basin area (Km<sup>2</sup>)</b>	3910	1071

### **B.II.2. Field sampling and sediment processing**

Sediment cores were chosen based on their distance from Metaleurop smelter and the effect of major confluences of other rivers in this case Lys river (figure B.II.1). Therefore, sediment cores were collected at two sampling locations along the Deûle river, one near Metaleurop site (D-B) and the other (D-A) only 200 m upstream the river from Metaleurop location which represent locations directly influenced by past ore processing activities (Metaleurop smelter). Two other sediment cores were sampled in Lys river, one before the river confluence (Lys-C) and the other after Lys confluence with Deûle river (Lys-D). These sites represent distant location from the source of pollution. All cores were sampled in duplicates in March 2010, in which one core was dedicated to pH measurements on site and the other for Hg species and ancillary measurements. The core samples were collected using a hand-driven gouge sampler and polyethylene core (figure B.II.2 (a) and (b)). The length of the core was 80 cm and the inner diameter was 7 cm. The sediment cores were processed in a glove bag under nitrogen atmosphere (figure B.II.2(c)). Inside the glove, the sediments were sliced at 2-cm thickness. Each sediment slice was divided into several parts, one stored in hermetically closed plastic bags and frozen at -18°C for CRS and AVS analysis and other part for Hg species (HgT, MeHg) and organic carbon analysis in the solid phase. Aliquots from each sediment depth were transferred into teflon centrifuge bottles, spun at 3500 g for 15 minutes. Under nitrogen atmosphere, the supernatant was filtered (0.45 µm), acidified with HNO<sub>3</sub> for Fe and Mn analysis and porewater samples for the analysis of dissolved HgT were preserved with 1 % HCl. Additionally, surface water was collected from the two sampling sites, and filtered (0.45 µm). The filtrate was preserved with concentrated HCl for HgT in surface water and the filters containing particles were frozen unless analyzed for mercury in suspended solids.

Collection, storage and preservation followed US EPA Method 1631 (Revision E, 2002). All glass and Teflon vessels were cleaned by soaking in diluted nitric acid (HNO<sub>3</sub>:H<sub>2</sub>O = 1:10 v/v) for 24 hours, washing using Milli-Q (18.2 MΩ cm, Millipore) water and then drying under filtered air flow.

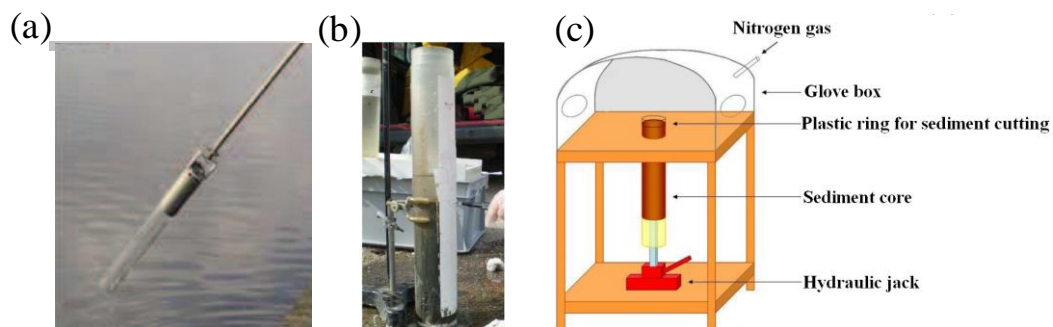


**Figure B.II.2.** Sampling and processing of sediment cores.

### B.II.3. Analysis of mercury species

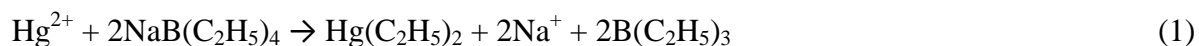
#### B.II.3.1. Mercury species determination in sediments

Total mercury in sediment phase can be extracted by various methods including digestion with a concentrated acid (Mikac et al, 1999) or acid mixture (Glimour et al, 1998). After extraction, all mercury species are transformed into inorganic mercury Hg(II) by the addition of a strong oxidant (BrCl, KBr/KBrO<sub>3</sub>). Oxidation is followed by a reduction step using SnCl<sub>2</sub> and NaBH<sub>4</sub> to elemental mercury Hg<sup>0</sup> which is purged out by an inert gas (e.g. Argon gas) to a preconcentration unit constituted of a gold trap. After thermal desorption of the gold trap, the desorbed mercury is transferred to the detection cell where it is measured at a wavelength of 253.7 nm.

The extraction and separation of methylmercury (MeHg) from sediments is more complicated than that of total mercury. There are three major methods for the separation of MeHg from sample matrix comprising of acid/solvent extraction, distillation, alkaline digestion (KOH/MeOH), acid leaching, supercritical extraction and microwave assisted extraction (Lorenzo et al 1999; Bowles and Apte 2000; Watsoo et al 1967; Hintelmann et al 2005; Emteborg et al 1998; Tseng et al 1999). Methylation artifacts are major problems of MeHg extraction from sediments that are caused by a very low concentrations of MeHg and high concentrations of Hg<sup>2+</sup>. MeHg artifacts can result in 30-80% overestimation of MeHg concentrations in the sediment. Acid leaching with H<sub>2</sub>SO<sub>4</sub>/KBr/CuSO<sub>4</sub> at room temperature followed CH<sub>2</sub>Cl<sub>2</sub> extraction and back extraction into water is an extraction method characterized by the lack of formation of MeHg artifacts (Bloom et al, 1997). After extraction of MeHg species, a derivatisation step is followed where different techniques exist for that purpose including hydride generation using sodium borohydride (NaBH<sub>4</sub>), ethylation using



sodium tetraethylborate (NaBEt<sub>4</sub>), propylation using tetrapropylborate (NaBPr<sub>4</sub>) and using Grignard reagent. By ethylation of Hg(II) and MeHg using NaBEt<sub>4</sub> at an optimal pH 4.9, volatile Hg species of diethylmercury and methylethylmercury can be formed respectively according to equations (1) and (2).



The volatile derivatised Hg species are purged out from the solution by an inert gas into a preconcentration unit formed of a sorbent e.g. Tenax or Carbotrap. After thermal desorption of the trapped mercury species, different mercury forms are separated by suitable separation technique. There exist different methods for mercury speciation where GC and LC are the most common chromatographic methods used for Hg separation. Mercury species in GC system can be separated by cryogenic, isothermal or temperature programmed GC. After separation and elution from the separation column, Hg species are thermally decomposed in pyrolytic unit before being quantified by a suitable detection technique. Different detectors can be used for Hg measurement including CV-AFS, CV-AAS, MIP-AES and ICP-MS.

### B.II.3.2. Total mercury in sediments

Total mercury analysis in dry sediments samples (HgT<sub>S</sub>) were analyzed without any pre-treatment by atomic absorption spectrometer Advanced Mercury Analyzer, model AMA 254 (Altec Ltd., Czech Republic). The analytical instrument is based on the dry decomposition of solid sample (100-500 mg) in an oxygen atmosphere. The combustion gases are then transferred to a catalytic column (Catalyst: cobalt oxalate and a mixture of manganese oxide, cobalt and calcium acetate) and then to a preconcentration unit composed of gold amalgamator. After thermal desorption of the gold amalgamator at a temperature of 900 °C, the released Hg<sup>0</sup> are transported into a system of measuring cells where mercury is quantified by atomic absorption spectrometry using a silicon diode detector at 253.6 nm (figure B.II.3).

The detection limit for AMA 254 based on 100 mg of sample was 0.1 µg/kg. The relative standard deviation of six replicate measurements was 1.2 %. For precision objectives, certified reference materials from the International Atomic Energy Agency were analyzed. The obtained values of HgT in IAEA 405, IAEA 433, and IAEA 158 were 0.81 ± 0.003

mg/kg,  $0.168 \pm 0.017$  mg/kg,  $0.132 \pm 0.014$  mg/kg respectively. The measured values were coherent with certified values of IAEA 405 ( $0.750 \pm 0.06$  mg/kg), IAEA-433 ( $0.155 \pm 0.01$ mg/kg) and IAEA-158 ( $0.121 \pm 0.013$ mg/kg). Particulate mercury ( $Hg_{Tp}$ ) in surface water was measured after filtration of surface water and the subsequent analysis of filters using AMA-254. Accuracy was determined by replicate analysis ( $n=3$ ) and was found to be < 25 %.

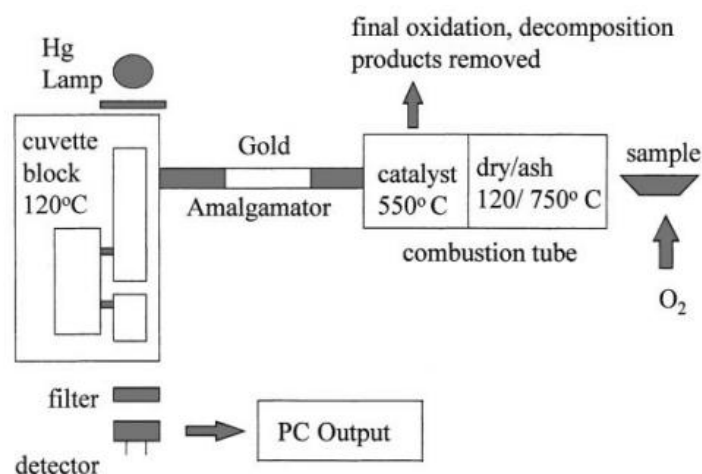


**Figure B.II.3.** Schematic diagram of AMA-254 (Costley et al 2000).

### B.II.3.3. Methylmercury in sediments

MeHg in sediments was determined as proposed by Leermakers et al. (2003), by aqueous ethylation followed by Headspace (HS) injection, Gas Chromatography separation (Clarus 500, PerkinElmer, USA), and detection by Atomic Fluorescence Spectroscopy (Tekran, Model 2600 CVAFS Mercury Analysis System, USA). Briefly, the extraction 100-200 mg sediment was performed in glass vial with 1 ml  $CuSO_4$  (Acros Organics, New Jersey, USA), 5 mL of 18% KBr (w/v) (Merck, Darmstadt, Germany) in 5%  $H_2SO_4$  (v/v) (Merck, Darmstadt, Germany). The mixture was shaken for 45 minutes at 400 g. Then, 10 mL  $CH_2Cl_2$  was added and shaken for 45 minutes, centrifuged for 15 min at 3000 g. After separation of the organic, aqueous phase, from solid layers, 5 ml of the organic phase was transferred to a conical glass bottle containing 20 mL Milli-Q water. Back-extraction of the organic layer in water phase was performed by solvent evaporation at  $46^\circ C$  using water bath (Compatible Control CC3, Offenburg, Germany) under constant  $N_2$  flow. The aqueous phase (5 mL) was transferred to Headspace vials and diluted with 5 mL of Milli-Q water and the pH was adjusted to optimum pH (between 4.8-5.2) using 0.1 M acetic acid-acetate buffer (82 g

CH<sub>3</sub>COONa, p.a., Merck, Darmstadt, Germany and 59 mL CH<sub>3</sub>COOH Scharlau Extrapur in 500 mL Milli-Q water). Finally, ethylation was performed using 50 µL of 1% tetraethyl borate (min 98 %, Stream Chemicals, Newburyport, USA). The vials were sealed with Teflon-coated butyl rubber septum and Al crimp caps and allowed to react for 1 hour in darkness before analysis. The detection limit of HS-GC-CVAFS was 1.12 ng/kg. The accuracy was examined by international reference materials (IAEA-405, IAEA-433). The obtained values of certified reference materials (IAEA-405: 5.85 ± 0.45 ng Hg/g, IAEA-433: 0.18 ± 0.09 ng Hg/g) were consistent with the certified values (IAEA-405: 5.49 ± 0.53 ng Hg/g, IAEA-433: 0.17 ± 0.07 ng Hg/g). Precision is given by the relative standard deviation of 5 replicate analyses, and was determined to be 4.86%.

#### **B.II.3.4. Dissolved mercury**

Total mercury in pore water (Hg<sub>TPW</sub>) as well as surface water (Hg<sub>TD</sub>) was determined according to US EPA Method 245.7 (Revision 2, 2005). It is based on the oxidation of Hg species by potassium bromated/potassium bromide reagent (J.T. Baker, USA). And sequentially pre-reduced with NH<sub>2</sub>OH.HCl (Sigma Aldrich) in order to destroy the excess bromine. The ionic mercury is then reduced with SnCl<sub>2</sub> (1% solution 5% HCl) (A & C American Chemicals Ltd) to volatile Hg<sup>0</sup>. The volatile species of Hg are separated from the solution by purging with high purity argon gas and transferred to gold cell for preconcentration cycles. After thermal desorption, the concentration of Hg is determined by atomic fluorescence spectrometry at 253.7 nm. The limit of detection as determined by CV-AFS was 1.8 ng/L, limit of quantification was 5 ng/L. Precision was determined by the relative standard deviation of 5 replicate analyses that was found to be 1.72 %

#### **B.II.4. Ancillary measurements**

##### **B.II.4.1. Sulfides in sediments**

The inorganic sulphides in the sediment are generally grouped into two main categories: unstable sulphides that are freshly precipitated (AVS: Acid Volatile Sulphides) and the more stable sulfides, mainly pyrite and elemental sulfur (CRS: Chromium Reducible Sulphur). The reduced sulfur species are determined by sequential extraction as described previously by Canfield et al. (1986). Manipulations are performed in a glove bag under inert atmosphere (N<sub>2</sub>). About 1 g of sediment is reacted 40 ml of 6 M hydrochloric acid, then the volatilized sulfide in the form of H<sub>2</sub>S, is purged by N<sub>2</sub>

flow and trapped in 20 mL of a basic solution ([NaOH] 1M [EDTA] 1M). CRS (Chromium Reducible Sulfides) sequentially follows AVS, and is extracted by adding about 40 mL of 1 mol/L chromium II solution, produced in the column of Jones and HCl solution. Again the volatile sulfur is trapped in 20 ml of a basic solution ([NaOH] 1M [EDTA] 1M). The concentration sulfide is then determined for each trap by potentiometry using an automatic titrator (Metrohm, model 736 GP Titrino). The titration is carried out with a cadmium solution of  $8.9 \times 10^{-3}$  mol/L, a calomel reference electrode ( $\text{Hg}/\text{Hg}_2\text{Cl}_2$ ,  $[\text{KCl}] = 3$  mol/L) and a measuring electrode specific to sulfide ions (Orion). The accuracy of the two methods is determined to be  $< 8\%$ . The lower limit of determination of 1 g of sediment was 20 mg/kg of S (Billon et al 2002).

#### **B.II.4.2. Organic carbon in sediments**

The organic carbon (Corg) was determined using LECO CS-125 Carbon-Sulfur Determinator. The accuracy was examined by testing standard of Carbon and Sulfur in White Iron (Leco Coporation) in which the mean obtained values of 6 determinations was  $3.34 \pm 0.03$  that were consistent with certified values ( $3.31 \pm 0.03$ ). The first measurement permits the determination of total carbon and a second one which is performed after calcination of the samples at  $450^\circ\text{C}$  for 24 hours, allows the measurement of mineral Carbon. By subtraction of the two determinations, organic carbon can be obtained.

## References

- Arıcı K, Yurdakul M, S Yurdakul. HF and DFT studies of the structure and vibrational spectra of 8-hydroxyquinoline and its mercury(II) halide complexes. *Spectrochim. Acta. A.* 61 (2005) 37.
- Asmy A, Sonbati A, Ba-Issa A. Synthesis and properties of 7-formyl-8-hydroxyquinoline and its transition metal complexes. *Transition Met. Chem.* 15 (1990) 222-225.
- Billon G, Ouddane B, Boughriet A. Chemical speciation of sulfur compounds in surface sediments from three bays (Fresnaye, Seine and Authie) in northern France, and identification of some factors controlling their generation. *Talanta.* 53 (2002) 2971-2981.
- Bowles K.C, Apte S.C. Determination of methylmercury in sediments by steam distillation/aqueous phase ethylation and atomic fluorescence spectrometry. *Anal. Chim. Acta.* 419 (2000) 145-151.
- Canfield D.E, Raiswell R, Westrich J.T, Reaves C.M, Berner R.A. *Chem. Geol.* 54 (1986) 149-155.
- Clemo G.R, and Howe R. 5-Formyl-8-hydroxyquinoline. *J. Chem. Soc.* (1955) 3552.
- Code De La Santé publique-Arrêté du 11/01/2007. Limites & références de qualité des eaux destinées à la consommation humaines; édictées à partir des directives de la CEE-1998-83.
- Costley C. T, Mossop K. F, Dean J.R, Garden L. M, Marshall J, Carroll J, 2000. Determination of mercury in environmental and biological samples using pyrolysis atomic absorption spectrometry with gold amalgamation. *Anal. Chim. Acta.* 405 (2000) 179-183.
- Dikici H and Salti K. Equilibrium and kinetics characteristics of copper(II) sorption into gyttja, *Bull. Environ. Contam. Toxicol.* 84 (2010) 147-151.
- Dubinin M.M, Raudushkevich, L.V. Equation of the characteristics curve of activated charcoal, *Proc. Acad. Sci. Phys. Chem. Sect. U.S.S.R.* 55 (1974) 331-333.
- Emteborg H, Bjorklund E, Odman F, Karlsson L, Mathiasson L, Frech W, D. C Baxter. Determination of methylmercury in sediments using supercritical fluid extraction and gas chromatography coupled with microwave-induced plasma atomic emission spectrometry. *Analyst* 121 (1996) 19.
- EPA-821-R-05-001 Method 245.7, 2005: Mercury in water by cold vapor atomic fluorescence spectrometry, U.S Environmental Protection Agency, Revision 2.0, Washington, DC, 1-30.
- Freundlich H. Ueber die adsorption in loesungen, *Z. Physik. Chem.* 57 (1907) 385-470.
- Goswami A, Singh A.K, Venkataramani B. 8-Hydroxyquinoline anchored to silica gel via new moderate size linker: synthesis and applications as a metal ion collector for their flame atomic absorption spectrometric determination. *Talanta.* 60 (2003) 1141.
- Glimour C, Riedel G.S, Ederington M.C, Bell J.T, Gill G.A, Stordal M.C, 1998. Methylmercury concentrations and production rates across a trophic gradient in the northern Everglades. *Biogeochemistry.* 40 (1998) 327-345.
- Hintelmann H, Nguyen H. T. Extraction of methylmercury from tissue and plant samples by acid leaching. *Anal. Bioanal. Chem.* 381 (2005) 360-365.

- Ho Y.S, McKay G. Pseudo-second order model for sorption processes, *Process Biochem.* 34 (1999) 451-465.
- Kamal M.M, Sayed A.Y, Ahmed S.M, Omran A.A, Shahata M.M. Pre-concentration of some heavy metal ions with AIO–HQ and AIO–PHQ and their studies by FTIR and spectroscopy. *Arab. J.Chem.* 2011, <http://dx.doi.org/10.1016/j.arabjc.2011.07.027>.
- Lagergren S. Zurtheorie der sorption geloster stoffe. *K. Sven. Vetenskapskad. Handl.* 24 (1989) 1-39.
- Leermakers M, Baeyens W, Quevauviller P, Horvat M. Mercury in environmental samples: speciation, artifacts and validation. *Trac-Trends in Analytical Chemistry* 24 (2005) 383-393.
- Lesven L, Lourino-Cabana B, Billon G, Proix N, Recourt P, Ouddane B, Fischer J. C, Boughriet A. Water-Quality Diagnosis and Metal Distribution in a Strongly Polluted Zone of Deûle River (Northern France). *Water Air Soil Pollut.* 198 (2009) 31–44.
- Lorenzo R.A, Vazquez M.J, Carro A.M, Cela R. Methylmercury extraction from aquatic sediments : A comparison between manual, supercritical fluid and microwave assisted techniques. *TrAC.* 18 (1999) 410-416.
- Mikac N, Niessen S, Ouddane B, Wartel M. Speciation of mercury in sediments of the Seine estuary (France). *Appl. Organometal. Chem.* 13 (1999) 715-725.
- Prygiel E. Impact des remises en suspension du sediment liées au trafic fluvial en rivières canalisé sur l'état des masses d'eau. Application au bassin Artois-Picardie. Thèse de doctorat (2013)-Université Lille 1.
- Pyell U and Stork G. Preparation and properties of an 8-hydroxyquinoline silica gel, synthesized via Mannich reaction. *Fresenius Z Anal Chem.* 342 (1992) 281.
- Rivas B.L, Urbano B, Pooley S.A, Bustos I, Escalona N. Mercury and lead sorption properties of poly(ethyleneimine) coated onto silica gel, *Polym. Bull.* 68 (2012) 1577-1588.
- Sugawara K.F, Weetall H.H, Schucker G.D. Preparation, properties, and applications of 8-hydroxyquinoline immobilized chelate. *Anal. Chem.* 46 (1974) 489.
- Tseng C. M, De Diego A, Wasserman J. C, Amouroux D, Donard O. F. X. Potential interferences generated during mercury species determination using acid leaching, aqueous ethylation, cryogenic gas chromatography and atomic spectrometry detection techniques. *Chemosphere* 39 (1999) 1119.
- Wang Z, Jing M, Lee F.S.C, Wang X. Synthesis of 8-hydroxyquinoline Bonded Silica (SHQ) and Its Application in Flow Injection-inductively Coupled Plasma Mass Spectrometry Analysis of Trace Metals in Seawater. *Chinese J anal Chem.* 34 (2006) 459.
- Weber W.J, Morris J.C. Kinetics of adsorption on carbon from solution, *J. Sanit. Eng. Div. Am. Soc. Civ. Eng.* (1963).

***Chapitre C: Evaluation des différentes résines chélatantes pour l'extraction du mercure***

***Chapter C: Evaluation of different chelating resins for mercury extraction***

## ***Résumé***

Les faibles concentrations de mercure dans les eaux de la rivière impliquent sa préconcentration par extraction en phase solide (SPE). 8-hydroxyquinoléine (8-HQ) est choisi comme ligand pour ses capacités extraordinaires et sa préférence de complexer une grande variété de métaux de transition par rapport aux métaux alcalins et alcalino-terreux. Le support de silice est adapté pour extraction de mercure pour sa stabilité mécanique et thermique et son faible coût. Pour la première fois, une méthode basée sur la formation des complexes Hg(II)-8-HQ dans des échantillons d'eau de rivière est examiné pour l'extraction du mercure. En outre, différents résines à base de 8-HQ ont été testés pour le recouvrement quantitatif du mercure de l'eau de rivière. Dans la première méthode (ajout direct de 8-HQ dans l'eau), différents paramètres tels que le pH, le débit de l'échantillon, la concentration de 8-HQ, éluant et le volume de l'échantillon ont été optimisés pour obtenir une extraction optimale de mercure. Dans la seconde méthode (extraction de mercure en utilisant les résines à base de 8-HQ), six méthodes d'immobilisations différentes ont été testés à la recherche de la meilleure silice fonctionnalisée de 8-HQ pour l'extraction de mercure.

Les résultats ont montré que, même après l'optimisation de tous les paramètres, l'ajout direct de 8-HQ dans l'eau MQ a atteint 80% de recouvrement de mercure tandis que dans l'eau de la rivière, la formation de complexe Hg(II)-8-hydroxyquinoline directement n'a pas donné de résultats exploitables, rendement faible pour le mercure (l'optimum d'extraction ne dépasse pas 10%). L'immobilisation de la 8-HQ sur le gel de silice, peut offrir une résine plus robuste avec une grande stabilité mécanique et une sélectivité améliorée. Parmi les six méthodes de greffage de 8-HQ, seuls trois résines (5-phenylazo-8-hydroxyquinoline et les deux imino-immobilisés 8-HQ), ont permis d'atteindre les objectifs de l'étude. Les positions d'ancrage sur le carbone 5 de la fraction 8-HQ et la nouvelle position sur le carbone 2 ont donné les meilleures performances, attribuées à une coordination améliorée du mercure avec les sites de liaison plus ouvertes (N-O).



### *Summary*

The low concentrations of mercury (Hg) in river water implicates its preconcentration by solid phase extraction (SPE). 8-Hydroxyquinoline (8-HQ) is chosen as a ligand for its extraordinary abilities for its preference of complexing a wide variety of transition metals over alkali and alkaline earth metals. Silica support is adapted for Hg SPE for its mechanical, thermal stability and its low cost. For the first time, Hg direct complexation in river water samples using 8-HQ was examined. In addition, different 8-HQ based chelating resins were tested for the quantitative recovery of Hg from river water. In the first method (direct addition of 8-HQ in water), different parameters including pH, flowrate, concentration of 8-HQ, eluent and sample volume were optimized to achieve optimal Hg extraction. In the second method (extraction of Hg using 8-HQ based chelating resins), six different immobilization methods were tried out in order to search for the best 8-HQ functionalized silica for Hg extraction.

Results have shown that even after the optimization of all parameters, direct addition of 8-HQ to MQ-water has reached 80% Hg recoveries while in river water, it failed in the quantitative recovery of Hg reaching an extraction of only 10%. Eventhough, 8-HQ was proven to be efficient for the extraction of many metals using direct complexation method, it is demonstrated to have poor results for Hg recovery in river water. The immobilization of 8-HQ on silica gel, can offer a more robust resin with high mechanical stability and an upgraded selectivity. Among the six different 8-HQ grafting methods, only three resins i.e. 5-phenylazo-8-hydroxyquinoline and two imino-immobilized 8-HQ silica attained the objectives of the study. Anchoring positions on Carbon 5 of the 8-HQ moiety and the novel position on carbon 2 gave the best performances attributed to an ameliorated coordination of Hg with the opened donor binding sites (NO).

## Development and evaluation of different chelating resins based on 8-hydroxyquinoline for the solid phase extraction of Hg(II) from water matrix†

Mirna Daye<sup>a,b</sup>, Baghdad Ouddane<sup>a\*</sup>, David Dumoulin<sup>a</sup> and Jalal Halwani<sup>b</sup>

<sup>a\*</sup> *University Lille 1, Géosystèmes, UMR - CNRS 8217, Villeneuve d'Ascq, France.*

<sup>b</sup> *Lebanese University, Water & Environmental Sciences Laboratory (L.S.E.E), Tripoli- Lebanon.*

\* **Tel.: +33 (0) 3 20 43 44 81, E-mail address: Baghdad.Ouddane@univ-lille1.fr.**

## C.1. Abstract

As a quest for the search of strong ligands for the retention of mercury, 8-hydroxyquinoline is proven to be a universal ligand for metal complexation. Thereby, 8-hydroxyquinoline was examined for the first time as a ligand for the retention of mercury ions from aqueous samples. In this study, two strategies were followed for solid phase extraction of mercury from river water matrix. In the first one, Hg(II)-8-HQ complexes were formed and retained on silica gel. The former method was optimized for maximal performances. In the second method, six different synthetic routes for 8-hydroxyquinoline immobilization on silica gel were tested for the retention of Hg(II) ions from river water. Results showed that, direct complexation of Hg(II) ions with 8-hydroxyquinoline gave poor results whereas, 8-hydroxyquinoline functionalized silica gel offered excellent retention. Not all types of 8-HQ immobilized silica have achieved quantitative extraction of mercury. Only anchoring positions at carbon 5 and the new grafting site on carbon 2 of 8-hydroxyquinoline moiety gave the ultimate results for the retention of Hg(II) ions from river water.

## C.2. Introduction

Mercury is ubiquitous element and is one of the most toxic environmental global pollutants.<sup>1</sup> In aquatic environments, mercury exists mainly as three forms, which are elemental mercury ( $\text{Hg}^0$ ), inorganic mercury Hg(II) and organic mercury (methylmercury and its complexes and dimethylmercury).<sup>2</sup> While all forms of mercury are poisonous, methyl mercury is the most toxic species due to its capacity of bioaccumulation through the aquatic food chain. In natural waters, mercury concentration is found to be at trace levels. While total mercury concentration ranges between 0.2-100 ng/L,<sup>3</sup> methylmercury levels are usually found to be much lower in the order of 0.05 ng/L.<sup>4</sup> The most employed analytical methods for trace metal determination are atomic absorption spectrometry<sup>5</sup> and inductively coupled plasma atomic emission spectrometry ICP-AES.<sup>6</sup> However, these modern analytical techniques often fail in the direct determination of Hg at trace levels due to matrix interferences and very low concentration. Subsequently, a separation/ preconcentration step is often indispensable.

In order to meet or enhance the detection limit of the selected analytical technique, various methods are used for the metal enrichment. Solid phase extraction (SPE) remains the most suited for trace metal analysis among the various preconcentration techniques. Depending on the nature of the sorbent, the mechanism of retention may include simple adsorption, chelation, ion-exchange or even ion-pairing. Silica gel has been extensively used as a solid

support for its mechanical, chemical and thermal stability under various conditions, fast kinetics and no swelling phenomena.<sup>7</sup> However, silica gel is also characterized by many drawbacks such as low ion exchange attributed to its surface silanol groups and its hydrolysis under basic conditions. Modification of silica gel by anchoring a specific chelating ligand further enhances the absorption capacity, sorption kinetics and selectivity. Selective extraction of target analytes is accomplished by anchoring the solid matrix with donor atoms such as oxygen, nitrogen and sulphur.<sup>8</sup>

8-Hydroxyquinoline (8-HQ) is a strong chelating agent according to its heterocyclic nitrogen and its phenolate oxygen atom. It has a universal chelating ability, capable of complexing over 60 metals.<sup>9</sup> Silica immobilized-8-quinolinol is a prominent material for metal extraction with high degree of recovery, matrix isolation with an exceptional preference for the retention of transition cations over alkali and alkaline earth metals.<sup>10, 11, 12, 13</sup> Several methods have already been described for silica gel functionalization with such oxine. The first immobilization technique was based on a diazo coupling of 8-HQ, and was widely adopted since the beginning of the 1970s.<sup>14, 15, 10, 16</sup> This time-consuming four steps procedure was further ameliorated by Marshall and Mottola, (1985) who considered direct functionalization of the silica surface using *p*-aminophenyltrimethoxysilane.

Goswami et al, (2003) proposed an alternative strategy involving the formation of a Schiff's base for 8-HQ covalent grafting on silica matrix. Amino-type linkages have been further examined to get around the possible hydrolysis of the imine bonds under acidic conditions. Mannich reaction, leading to the formation of aliphatic amine bond, was also employed for the immobilization of 8-hydroxyquinoline derivatives onto amino modified silica.<sup>19,20,21</sup> Many studies have proven that 8-HQ immobilized by diazo coupling, Mannich reaction and Schiff's base reaction are excellent sorbents for many metals (table C.1). Preconcentration studies of various metals are performed on these three different types 8-HQ immobilized silica and proven to be efficient.

**Table C.1.** Efficiency of three types of 8-HQ immobilized silica for the retention of metals.

Matrix	Trace elements	Sorbent	Immobilization method	Recovery (%)	Ref
Synthetic seawater	Ni/Cu/Mn/Ce Ag/V/Ti	CPG-HQ <sup>a</sup>	Diazo coupling	95-104	22
Seawater	La/Ce/Pr/Nd Sm/Eu/Gd/Tb Dy/Ho/Er/Tm/Yb/Lu	Si-8-HQ <sup>b</sup>	Diazo coupling	>80	23
Distilled-deionized water	Ni/Co/Fe/Cu/Zr/Ti/V/Al	CPG-HQ <sup>a</sup>	Diazo coupling	89-73	10
Synthetic seawater	Cd/Pb/Cu/Co/Ni	Si-8-HQ <sup>b</sup>	Diazo coupling	100-104	24
Seawater	Mn/Co/Ni/Cu/Zn/Ca/Pb	Si-8-HQ <sup>c</sup>	2-steps Mannich reaction	35-95	25
Seawater	Cd/Pb/Zn/Cu/Fe/ Mn/Ni/Co	Si-8-HQ <sup>b</sup>	Diazo coupling	74-115	13
Sea water	Mn/Co/Ni/Cu/Zn/Cd/Pb	Si-8-HQ <sup>b</sup>	Diazo coupling	59-126	26
Purewater	Cu/Pb/Ni/Co/Zn/ Fe/Cd	Si-8-HQ <sup>b</sup>	2-steps Schiff's base reaction	97-99	18
EPA quality control water	Cu	Si-8-HQ <sup>b</sup>	Diazo coupling	95-102	17

a: hydroxyquiniline immobilized on controlled pore glass; b: 8-hydroxyquinoline immobilized on silica gel; c: 8-hydroxyquinoline immobilized on silicone tubes

8-Hydroxyquinoline is a powerful organic soft base for its ability to form stable metal chelates. Its potency for the extraction of mercury was not demonstrated, highlighting the significance of revealing its capacity for mercury extraction. Direct complexation of metals with 8-hydroxyquinoline followed by SPE is a simple method for the preconcentration and determination of trace metals. Indeed, 8-HQ is able to form stable metal complexes with high stability constants (LogK) reaching for Fe(III), Cu(II), Cd(II), Ca(II), Mg(II) 13.7, 12.1, 7.3, 3.3, 4.2 respectively.<sup>27</sup> Numerous studies have been based on the latter principle and have accomplished quantitative recoveries for numerous metals including Cu, Cd, Pb, Zn, Fe, Mn, Ni, Sn, Co...etc. (table C.2). However, the direct addition of 8-HQ for the complexation of mercury ions in natural waters is not described previously accentuating the importance of the method development, considering 8-HQ as a universal ligand for metals. Moreover, immobilization of 8-HQ on a solid support can provide a more robust ligand with ameliorated

logK complex metal formation, mechanical & thermal stabilities and efficiencies. Higher stability constant was determined for Cd(II) with 8-HQ immobilized on controlled pore glass (CPG) ranging from  $10^9$ - $10^{11}$ .<sup>24</sup> Different types of 8-HQ immobilized silica were found to be effective for an upgraded extraction of metals. Therefore, it is indispensable to evaluate the capacity of these chelating resins and to develop a novel type of 8-HQ-grafted silica by discovering new grafting positions of 8-HQ moiety on amino-modified silica for the extraction of Hg.

**Table C.2.** Metal recovery results by the direct addition and the adsorption M<sup>+</sup>-ligand on silica phase.

Matrix	Ligand	Trace elements	Recovery (%)	Reference
Sea water	BPDB <sup>1</sup>	Hg	89 ± 3.22	28
Pond water	APDC <sup>2</sup>	Hg/MeHg	>95	29
NIST 1572, MESS-3, DOLT-2	DDTP <sup>3</sup>	Hg/MeHg	100	30
Sea water	APDC <sup>2</sup>	Se/Sb	94-97	31
Sea water	8-HQ <sup>4</sup>	Cd/Co/Fe/Mn/Ni/ Pb/Cr/Zn/Cu/V	85-95	32
Sea water	8-HQ <sup>4</sup>	Al/ Cd/Cu/Fe/Mn/ Ni/Pb/Sn/V/Zn	88-101	33
Sea water	8-HQ <sup>4</sup>	Cd/Zn/Cu/Mn/ Fe/Ni/Co	67-108	13
Sea water	8-HQ <sup>4</sup>	Cu/Mn	100	34
River water				
Tap water	8-HQ <sup>4</sup>	Hg	5-10	This study

<sup>1</sup>BPDB: 1,4-bis(4-pyridyl)-2,3-diaza-1,3-butadiene; <sup>2</sup>APDC: Ammonium pyrrolidine dithiocarbamate;

<sup>3</sup>DDTP dithiophosphoric acid diacyl ester; <sup>4</sup>8-HQ: 8-Hydroxyquinoline .

Herein, we wish to report two strategies employed for the study of Hg(II) solid phase extraction. First, we focused on the optimization of mercury ions complexation with 8-hydroxyquinoline and adsorption on C<sub>18</sub>-reverse phase silica gel columns. Four parameters that are pH of complexation, flow rate of the sample through the column, concentration of the complexing agent, volume of eluent and the preconcentration factor were also optimized. In the second approach, six strategies involving 8-HQ-immobilized silica gels (figure C.1) were examined for the recovery of Hg(II) ions under varied pH values. Mercury analysis was performed by using ICP-AES.

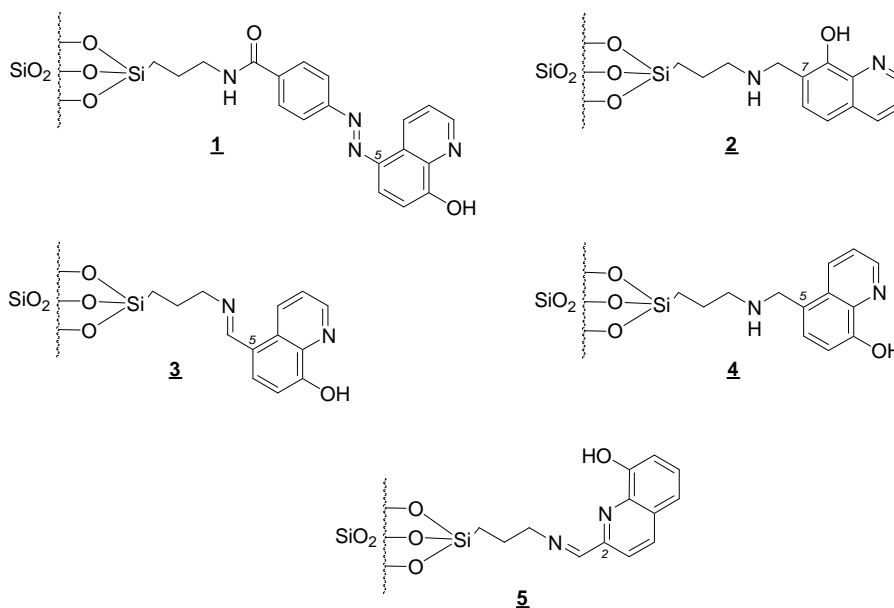


Fig.C.1. Studied 8-hydroxyquinoline modified silica gels

### C.3. Experimental procedure

#### C.3.1. Instrumentation

Concentration of Hg(II) ions were determined by using Inductively Coupled Plasma Atomic Emission Spectroscopy (ICP-AES; Varian Vista Pro, axial view, 253 nm). External calibration was performed using standard solution and blank correction was applied if necessary. pH measurements were conducted by pH meter calibrated using two standard buffer solutions of pH 4 and pH 7. Fourier Transform Infrared (FT-IR) spectra of functionalized silica were recorded using Nicolet 380 Smart *i*TR spectrometer (ThermoScientific, USA) and were silica-matrix corrected. Sample flow rates were adjusted using a Gilson Miniplus 3 peristaltic pump. PVC tubes (3.18 i.d) were used for the preconcentration process. PTFE (polytetrafluoroethylene) columns (65 mm × 13 mm i.d.) were used for packing the examined adsorbent. <sup>1</sup>H NMR spectra were recorded with a Bruker AM) using CDCl<sub>3</sub> as the solvent and TMS as the internal standard.

### C.3.2. Reagents

All chemicals and solvents used were analytical grade. Ultrapure water (with a resistivity of 18.2 M $\Omega$ .cm) was obtained using a Milli-Q system (Millipore, USA). Labware was soaked in 20% nitric acid and washed thoroughly with pure water prior to use. Inorganic mercury (Hg<sup>2+</sup>) stock solution (1000 mg/L) was prepared from mercuric chloride (Merck). Silica (100-200 mesh), chemicals and solvents were supplied from Sigma Aldrich (France). Buffer solutions were prepared from 1 M sodium acetate and the pH was adjusted to the desired pH value by addition of 1 M HNO<sub>3</sub>.

### C.3.3. Preconcentration procedure using column method

#### C.3.3.1. Preconcentration strategy using direct addition of reagent to the sample

We were first interested in studying mercury direct complexation with 8-hydroxyquinoline followed with adsorption of the complex onto octadecyl silica gel.

C<sub>18</sub> cartridges were prepared by activation of a batch of silica gel. Prior to use, C<sub>18</sub>-silica gel was washed with methanol, ultra pure water and 2 M aq. nitric acid HNO<sub>3</sub> in order to remove contaminants. Octadecyl silica gel was then prepared using ultrapure water (20 mL/g silica), methanol (5 mL/g silica) and ultrapure water (20 mL/g silica). PTFE columns (6 ml volume, 4.0 mm i.d., 60 mm length) were packed with one gram of activated silica gel. A suitable 50 mL model solution of 0.2  $\mu$ g/mL of Hg(II) and 72.58 mg/L ( $5 \times 10^{-4}$  M) of the ligand was prepared in ultrapure water. Under optimized conditions, water samples were adjusted to pH 4 and passed through a column containing the tested adsorbent at a constant flowrate of 2 mL/min. Retained Hg(II) ions were stripped off using 10 mL of 2 M HNO<sub>3</sub> at a flowrate of 0.5 mL/min. Quantitative analyses of eluents were performed by ICP-AES in order to determine the percentage of retention.

#### C.3.3.2. Preparation of the hydroxyquinoline functionalized silica gels

The second part of this work concerns the study of immobilized-8-quinolinol silica gels that differ from the nature and the position of the bond connecting the chelating agent to the surface of silica gel. Prior to use, silica gel was activated by hydrochloric acid, neutralized, and then dried at 110 °C till total dryness. For the preparation of aminopropyl silica gel (APSG), the dried silica gel (10 g) in toluene (150 mL) was refluxed with aminopropyltriethoxysilane (10 mL) for 18h. The resulting suspension was filtered and



washed successively with toluene, diethylether, ethanol (20 mL each), and finally dried at 60°C.

#### *Method 1*

The first strategy concerned loading of 8-hydroxyquinoline on activated silica gel as described by Kamal et al (2011). The non-covalent procedure for impregnation involved mixing of 8-HQ and silica gel in ethanol and ultra pure water with heating at 60°C for 24 hours. The synthesis yield of the produced chelating resin was high of 95 %. FT-IR spectrum of the prepared silica gel (resin **6**) showed bands in the region from 1700 to 1550  $\text{cm}^{-1}$  that could be assigned to the aromatic  $C=C$  bonds of 8-HQ (Annexe 1).

#### *Method 2*

Phenylazo-8-hydroxyquinoline silica gel **1** (figure C.1) was prepared according to the procedure proposed by Sugawara et al (1974). The procedure firstly consists in a coupling step between an arylamine moiety and aminopropyl silica gel (APSG) to permit further azo-linking of 8-hydroxyquinoline on position 5. APSG (10 g) was also acylated by treatment with *p*-nitrobenzoyl chloride (1 g) in chloroform (60 mL) in presence of triethylamine (2 mL). The nitro-adduct was then reduced by sodium dithionite (5% *w/v* solution) to yield aminobenzoyl-APSG. Oxidation of the amino-moiety with sodium nitrite afforded formation of the expected diazonium salt, which was rapidly filtered to be coupled with 8-HQ. Formation of the final adduct **1** was characterized by the rapid development of a deep red color, prominent feature of the formation of the expected diazo-linkage. The synthesis yield was about 85 %. Presence of the anchored 8-hydroxyquinoline was further ensured by FT-IR analysis, which revealed absorption bands from 1636 to 1524  $\text{cm}^{-1}$  relative to the presence of amide and heteroaromatic bonds (Annexe 2).

#### *Method 3*

Starting from aminopropyl silica gel (APSG), preparation of the 8-hydroxyquinoline silica gel **2** (figure C.1) was performed according to the procedure described by Pyell and Stork (1992). Involving a Mannich reaction, this strategy offers immobilization of 8-HQ on position 7 via a secondary amine bond linkage. Surface functionalization was performed by mixing APSG with formaldehyde (40 % aq.) in presence of acetic acid, followed by coupling of the intermediate iminium with 8-HQ at pH 9. The synthesis yield was also high using this protocole; of about 90%. Matrix-corrected IR spectrum of **2** was in accordance with the

observations described by Pyell and Stork (1992), in particular in the region from 1700 to 1450  $\text{cm}^{-1}$  where absorption bands could be assigned to aromatic ring vibrations (Annexe 3).

#### *Method 4*

The third strategy involved immobilization of 8-HQ on position 5 via formation of a Schiff base according to Goswami et al (2003) to give chelating resin **3** (figure C.1). Starting from 8-hydroxyquinoline, installation of the carbaldehyde function was accomplished by a Reimer-Tiemann reaction as described by Clemo et al. (1955).  $^1\text{H}$  nuclear magnetic resonance analysis of the isolated solid after Soxhlet purification (hexanes as eluant) revealed a mixture of 5-formyl-8-hydroxyquinolinol **9a** (80 %) and 7-formyl-8-hydroxyquinolinol **9b** (20 %) (Annexe 4). Formation of the corresponding imino-immobilized 8-HQ silica gels was performed by condensing the aldehyde mixture **9a** + **9b** with APSG in anhydrous diethylether. The synthesis yield using this synthetic route is very low of 12%. FT-IR spectrum of this silica gel exhibits a band at 1653  $\text{cm}^{-1}$  that appears to originate from  $\text{C}=\text{N}$  stretching. Additional bands at 1558, 1541, 1507 and 1457  $\text{cm}^{-1}$  further support the immobilization and matched the observations reported by Goswami et al (2003).

#### *Method 5*

The fourth studied strategy involved the one-step Mannich reaction described by Wang et al (2006), yielding to a mixture of amino-immobilized 8-HQ silica gels **4** and **2** (figure C.1). As stated by the optimized method, 8-HQ was allowed to react with silica gel in presence of formaldehyde and aminopropyltrimethoxysilane (0.8 eq. vs. 8-HQ) for 6 h in ethanol at 50°C. The synthesis yield using Wang et al protocole gave 90%. Immobilization of 8-HQ was confirmed after IR analysis according to Zheng's observations in the region from 1504 to 1374  $\text{cm}^{-1}$  (Annexe 5).

#### *Method 6*

We also embarked on the study of a new anchored silica gel concerned by a Schiff-base functionalization of APSG with 8-hydroxyquinoline on position 2. Such imino-derivative of 8-HQ was also described to exhibit a particular ability for complexation with metals.<sup>37,38</sup> Here, imino-immobilized 8-HQ silica gel **5** (figure C.1) was prepared by condensation of APSG with commercial 2-formyl-8-hydroxyquinoline. The synthesis yield using the novel method of immobilization is high of about 90%. IR bands observations from 1560 to 1474  $\text{cm}^{-1}$  support the immobilization of the 8-HQ moiety (Annexe 6).

### **C.3.3.2.a. Preconcentration procedure using the synthesized chelating resins**

Efficiency of the six above-mentioned immobilized-8-quinolinol silica gels was investigated for Hg(II) extraction from river water samples. Three hundred milligrams of Si-8-HQ were packed in the column and plugged with frit caps at both ends. Prior to sample percolation, solid phase was conditioned to the pH of the sample. The packed 8-HQ resins were tested by using river water samples spiked with 0.2 µg/mL of Hg(II). Samples were then adjusted to the desired pH value with buffer prior percolation.

## **C.4. Results and discussion**

### **C.4.1. Optimization direct addition method**

#### **C.4.1.1. Effect of pH**

pH is one of the most important factors controlling metal adsorption. Solution acidity can protonate the binding sites of the adsorbent whereas basicity can increase the hydroxide concentration leading to the formation of hydroxide-metal complexes. Therefore, any changes in the pH can influence formation of the complex between Hg(II) ions and 8-HQ. pH effect on the adsorption of Hg(II) chelates on C<sub>18</sub> was studied in a range from pH 3 to pH 8. Sample pH was adjusted using nitric acid and ammonia suprapur solutions (Figure C.2 (a)).

In the tested conditions, maximum recoveries of mercury ions occurred at pH 4 with an average retention reaching 65 %. As shown in figure C.2 (a), adsorption of Hg(II) rapidly decreases with increasing pH due to the probable formation of mercury hydroxides complexes as well as the possible hydrolysis of the octadecyl silica for pH above 8. Low retention was also observed at pH 2. Thereby, pH 4 was chosen for further determination studies of Hg(II) that was adjusted using a buffer solution of acetic acid-sodium acetate.

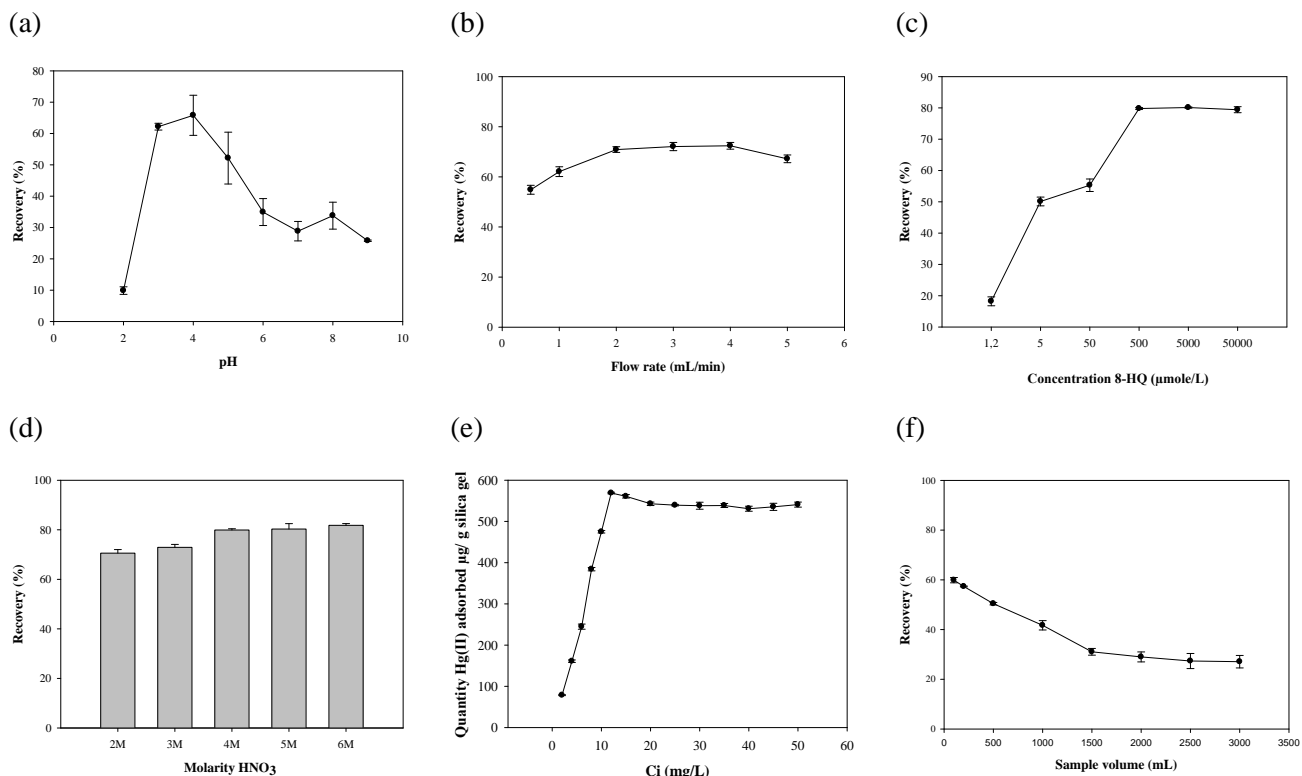


**Fig. C.2.** (a) Effect of solution's acidity on Hg(II) retention . Conditions: concentration of Hg(II): 0.2  $\mu\text{g/mL}$ , sample flowrate: 2 mL/min, elution: 10 mL/HNO<sub>3</sub> (2 M)/ 0.5 mL/min, Concentration 8-HQ:  $5 \times 10^{-4}$  mol/L. (b) Effect of sample flowrate on Hg(II) recovery. Conditions: concentration of Hg(II): 0.2  $\mu\text{g/mL}$ , pH 4, elution: 10 mL/HNO<sub>3</sub> (2 M)/0.5 mL/min, concentration 8-HQ:  $5 \times 10^{-4}$  mol/L (c) Effect of 8-HQ concentration on the retention of Hg(II). Conditions: concentration of Hg(II): 0.2  $\mu\text{g/mL}$ , pH 4, sample flowrate: 2 mL/min, elution: 10 mL/HNO<sub>3</sub> (2 M)/ 0.5 mol/min. (d) Effect of nitric acid concentration on the recovery of Hg(II) ions. Conditions: concentration of Hg(II): 0.2  $\mu\text{g/mL}$ , pH 4, sample flowrate: 2 mL/min, concentration 8-HQ:  $5 \times 10^{-4}$  mol/L, elution: 10 mL HNO<sub>3</sub>/0.5 mL/min. (e) Adsorption isotherm. Conditions: pH 4, sample flowrate: 2 mL/min, concentration 8-HQ:  $5 \times 10^{-4}$  mol/L, elution: 10 ml/HNO<sub>3</sub> (4 M)/0.5 mL/min. (f) Breakthrough volume. Conditions: 10  $\mu\text{g}$  Hg(II)/sample volume, pH 4, sample flowrate: 2 mL/min, concentration 8-HQ:  $5 \times 10^{-4}$  mol/L, elution: 10 mL/HNO<sub>3</sub> (4 M)/ 0.5 mL/min.

#### **B.4.1.2. Effect of flowrate of the sample and the eluent**

Sample flow rate is another important parameter affecting the time of adsorption, desorption and analysis. The sample flow-rate also needs to be optimized to ensure maximal retention along with minimization of the time required for sample processing. Hg(II) model solutions were percolated through the packed C<sub>18</sub> columns at defined conditions at different flow-rates ranging from 0.5 to 5 mL/min. Influence of the sample flow-rate on the retention is schematized on figure C.2 (b).

Maximum recoveries of mercury analytes were obtained for sample flow-rates between 2 and 4 mL/min. Performances slightly tend to decrease for flow-rates higher than 4 mL/min because of the lower contact time between the Hg(II)-HQ complexes and C<sub>18</sub> silica gel. Sample flow-rate of 2 mL/min was finally chosen to ensure the best compromise between retention performance and time-consumption.

#### **B.4.1.3. Effect of ligand and eluent concentration**

The amount of ligand added to the sample also plays a crucial role in the metal complex formation. Here, the optimal concentration of the ligand that allows complete complexation of Hg(II) ions was determined by varying the amount of 8-HQ. As shown on figure C.2 (c), it was found that a concentration of 0.5 mmol/L offers the best performance. This concentration was also chosen for the rest of this study. Higher concentrations of 8-HQ were avoided in order not to saturate the binding sites of octadecyl silica gel.

Concerning the nature of the eluent, the use of nitric acid was preferred to hydrochloric acid in order to prevent hydrolysis of silica gel. Nitric acid concentrations were varied in the range from 2 to 6 mol/L in order to investigate the impact on mercury desorption. (Figure C.2 (d)). For the same volume of eluent, 4 M HNO<sub>3</sub> was found to be sufficient for the recovery of Hg(II) analytes.

Different volumes of 4 M nitric acid (from 2 to 12 mL) were investigated for stripping off the retained Hg(II) ions on the column. It was noted that 10 mL of 4 M nitric acid was capable of a quantitative desorption of the analytes and therefore was selected as a proper volume for elution.

#### **B.4.1.4. Adsorption capacity**

This parameter allows the determination of the sorbent quantity that is able of quantitatively retaining all metal ions from solution. To investigate, the maximum amounts 8-HQ-Hg(II) chelates extraction by 1 g silica phase, a varying concentration of Hg(II) ions between 2  $\mu\text{g}/\text{mL}$  - 50  $\mu\text{g}/\text{mL}$  were percolated through the silica phase using the optimized working conditions. An adsorption isotherm curve (figure C.2 (e)) can be obtained by tracing the initial concentration of Hg(II) ( $\mu\text{g}/\text{mL}$ ) vs. the microgram of Hg(II) retained per gram of silica phase. The adsorption per unit mass of silica phase increases with the increase of the initial concentration of Hg(II) ions until reaching a plateau value which corresponds to silica phase saturation. The maximum capacity of the cartridge was found to be 568.95  $\mu\text{g Hg(II)}/\text{g silica gel}$  at pH 4.

#### **B.4.1.5. Breakthrough volume and real samples applications**

In order to find the maximum applicable volume for the adsorption of Hg(II) complexes on C<sub>18</sub>, different sample volumes (from 100 to 3000 mL) were percolated under optimum conditions while keeping constant the loaded quantity of Hg(II). As indicated in figure B.2 (f), increasing the sample volume leads to a decrease of Hg(II) recovery from 60% to 27% for sample volumes of 100 mL and 2500 mL respectively. The low breakthrough volume can be explained by the low stability constant of Hg(II)-HQ complex.

Consequently, the application of this direct 8-HQ addition method on tap and river water using 50 mL sample volume under optimum conditions further confirmed the former observations. The obtained results demonstrate low retention of Hg(II) ions in tap and river water, with values attaining 5 to 10% respectively, in contrast with the other results published for the retention of different metal ions other than mercury (Table C.2).

#### **B.4.1.6. Selectivity and Interferences studies**

The selectivity of a complexing agent towards a metal ion is conferred by the donor atoms (*O,N,S*) in the ligand function it adheres. For this purpose, the selectivity of 8-HQ towards Hg(II) ions was studied in binary metal ion mixtures. Binary equimolar mixtures consisting of Hg(II) and a single metal tested were percolated through silica column and eluted under the optimized conditions. As represented in figure C.3, 8-hydroxyquinoline presents high selectivity in case of presence of Zn(II) and Co(II), where mercury ions retention respectively reached 92% and 83%. However, binary mixtures Hg(II)-Pb(II) and Hg(II)-Cd(II) revealed a

competition trend between these soft metals towards 8-HQ ligand, revealed by a decrease of mercury recovery. Hg(II) extraction selectivity was further impacted by the presence of metal ions having high stability constant formation with 8-HQ. Indeed, Hg(II) extraction only reached 41% in the case of Hg(II)-Fe(III) mixture. Furthermore, the low selectivity of 8-HQ towards Hg(II) ions was also promoted in multi-element mixture where the recovery of Hg(II) drops off to 19%. In conclusion, the presence of metal ions can interfere with the Hg(II)-HQ complex formation, since the stability of metal-HQ complex is depending on the logK (table C.3).

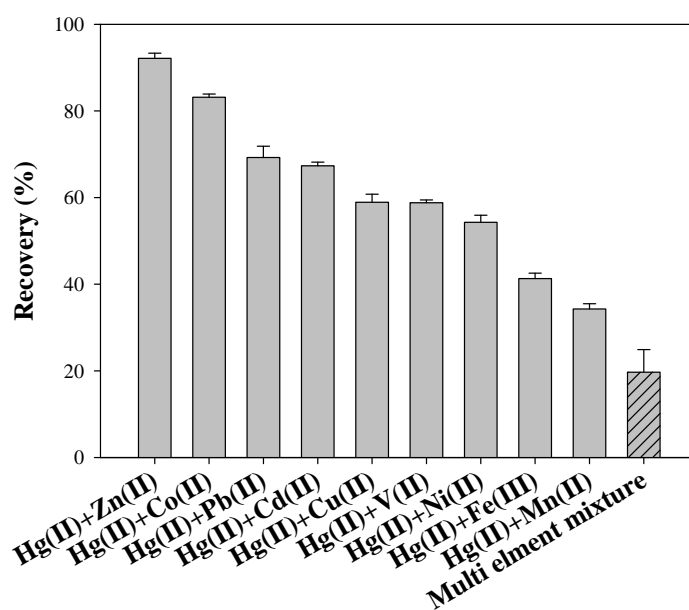


**Fig.C.3.** Study of 8-hydroxyquinoline selectivity towards Hg(II) ions. Conditions: concentration of Hg(II): 0.2  $\mu\text{g/mL}$ , pH 4, sample flow rate: 2 mL/min, concentration: 8-HQ:  $5 \times 10^{-4}$  mol/L, eluent: 10 mL nitric acid (4 M)/0.5mL/min.

Effects of other interfering substances normally encountered in natural water samples on the recovery of Hg(II)-HQ chelates by  $\text{C}_{18}$  columns were also studied. For this purpose, Hg(II) solutions (0.2  $\mu\text{g/mL}$ ) containing known amount of interfering substances were adsorbed on silica phase using the optimal-defined preconcentration parameters. The results presented in Table C.4, show that 300-1000 fold excess of humic acid, Ca(II),  $\text{C}_4\text{H}_4\text{O}_6^{2-}$ , Mg(II),  $\text{NO}_3^-$ ,  $\text{CN}^-$ ,  $\text{Na}^+$ , 200-50 fold excess of  $\text{CO}_3^{2-}$ ,  $\text{C}_2\text{O}_4^{2-}$ ,  $\text{K}^+$ ,  $\text{F}^-$ , 50-fold excess of Al(III) strongly interfered in Hg(II) extraction. The major cause behind the substantial effects of interfering substances is the formation of Hg(II)-HQ complex characterized by a low stability constant.

**Table C.3.** Stability constant metal-8HQ.<sup>39</sup>

Element	Zn	Co	Pb	Cd	Cu	V	Ni	Fe	Mn
Log K	8.56	8.65	9.02	7.78	12.56	10.97	9.27	14.5	6.8

In order to resolve the low recovery of Hg(II) from aqueous solution, 8-hydroxyquinoline functionalized silica gels were used for the subsequent experiments. Silica immobilized-8-quinolinol should indeed offer an enhanced thermal and mechanical stability, as well as a better selectivity and an upgraded efficiency. In addition, 8-HQ modified silica is known for their potential for matrix isolation with an extraordinary preference for the extraction of transition metals over alkali and alkaline earth metals.<sup>10,12,11,13</sup>

**Table C.4.** Effects of different electrolytes on the retention of Hg(II) ions.

Electrolytes (cations/anions)	Foreign ion	% Recovery
Humic acid <sup>a</sup>	30	24.2 ± 0.9
KCN <sup>a</sup>	224.01	8.8 ± 1.2
KNaC <sub>4</sub> H <sub>4</sub> O <sub>6</sub> <sup>a</sup>	117.69	57.1 ± 0.5
Na <sub>2</sub> C <sub>2</sub> O <sub>4</sub> <sup>a</sup>	77.71	29.8 ± 0.7
Na <sub>2</sub> CO <sub>3</sub> <sup>a</sup>	222.56	23.6 ± 1.1
Na <sub>3</sub> C <sub>6</sub> H <sub>5</sub> O <sub>7</sub> <sup>a</sup>	49.03	24.2 ± 1.3
Mg <sup>2+</sup> <sup>a</sup>	99.89	8.0 ± 0.8
Ca <sup>2+</sup> <sup>a</sup>	359.63	5.3 ± 0.4
Na <sup>+</sup> <sup>a</sup>	83.65	17.2 ± 1.7
K <sup>+</sup> <sup>a</sup>	10.17	13.1 ± 1.5
Al <sup>3+</sup> <sup>a</sup>	1.08	7.6 ± 0.8
Cl <sup>-</sup> <sup>a</sup>	49.98	8.1 ± 0.9
NO <sub>3</sub> <sup>-a</sup>	29.76	8.0 ± 1.3
F <sup>-</sup> <sup>a</sup>	1.89	10.3 ± 0.8
SO <sub>4</sub> <sup>2-</sup> <sup>a</sup>	600.38	38.3 ± 0.5

a: µg/mL

## B.4.2. Silica functionalized-8-hydroxyquinoline

### B.4.2.1. Immobilization of 8-HQ according to method 1

The quinolinol-impregnated silica gel studied by Kamal et al (2011) for Cu(II) and Fe(III) extraction was here tested at different pH values with the aim to examine its efficiency for mercury extraction. As shown on figure C.4 (f), this resin (resin **6**) exhibits poor affinity for Hg(II) extraction with recoveries ranging from 20 to 37% depending on the pH.



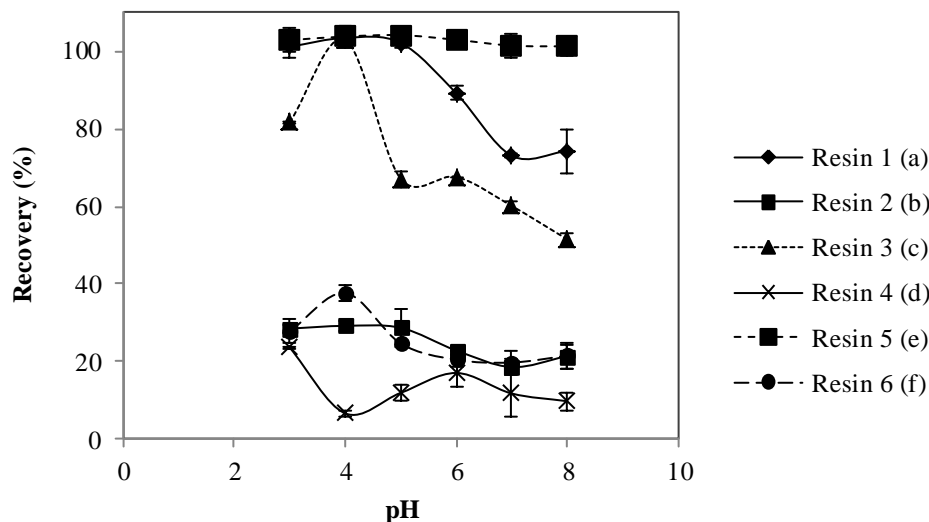


**Figure C.4** (a) Effect of pH variation on Hg(II) ions recovery. Conditions: River water, concentration of Hg(II): 0.2  $\mu\text{g/mL}$ , flow rate: 2 mL/min, 300 mg of 8-HQ immobilized on silica gel (**1**), elution: 10 mL/5 M HCl 5% CS(NH<sub>2</sub>)<sub>2</sub>/ 0.5 mL/min. (b) Effect of pH variation on Hg(II) extraction. Conditions: River water, concentration of Hg(II): 0.2  $\mu\text{g/mL}$ , flow rate: 2 mL/min, 300 mg of 8-HQ immobilized on silica gel (**2**), elution: 10 mL/2 M HCl 1 M HNO<sub>3</sub>/ 0.5 mL/min. (c) Effect of pH variations on Hg(II) retention. Conditions: River water, concentration of Hg(II): 0.2  $\mu\text{g/mL}$ , flow rate: 2 mL/min, 300 mg of 8-HQ immobilized on silica gel (**3**), elution: 10 mL/ 2 M HNO<sub>3</sub>/ 0.5 mL/min. (d) Effect of pH variations on Hg(II) ions extraction. Conditions: river water, concentration of Hg(II): 0.2  $\mu\text{g/mL}$ , flow rate: 2 mL/min, 300 mg of 8-HQ immobilized on silica gel (**4**), elution: 10 mL/2 M HCl 1 M HNO<sub>3</sub>/ 0.5 mL/min. (e) Effect of pH variation on the retention of Hg(II) ions. Conditions: river water, concentration of Hg(II): 0.2  $\mu\text{g/mL}$ , flow rate: 2 mL/min, 300 mg of 8-HQ immobilized on silica gel (**5**), elution: 10 mL/ 5 M HNO<sub>3</sub>/ 0.5 mL/min. (f) Effect of pH variation on the retention of Hg(II) ions. Conditions: River water, concentration of Hg(II): 0.2  $\mu\text{g/mL}$ , flow rate: 2 mL/min, 300 mg of 8-HQ immobilized on silica gel (physical bonding; resin (**6**)), elution: 10 mL/2 M HCl 1 M HNO<sub>3</sub>/ 0.5 mL/min.

#### B.4.2.2. Immobilization of 8-HQ according method 2

Mercury extraction using 5-phenylazo-8-hydroxyquinoline silica gel **1** was also studied. It was found that elution using HNO<sub>3</sub> alone did not allow total desorption of Hg(II) ions from the resin. Different types of eluents were also examined to address this desorption problem that could be probably due to the high chelating strength of the resin **1** (figure C.5).

Studies performed using 5-phenylazo-8-hydroxyquinoline showed that, the HCl-HNO<sub>3</sub> mixture was tested for the desorption of metals and was proven to be successful.<sup>26,23,25</sup> In this study, best performances for mercury elution were attained using the mixture 5 M HCl 5% thiourea. As depicted in figure C.4 (a), total recovery of Hg(II) ions was attained for pH

ranging from 3 to 5. Adsorption of the target ions then diminishes to 70% for pH above 5. As already mentioned<sup>13,17,23</sup> and moreover evidenced in this paper, phenylazo-8-hydroxyquinoline silica gel **1** turns out to be a good material for the adsorption of metals and in this study Hg(II) ions.

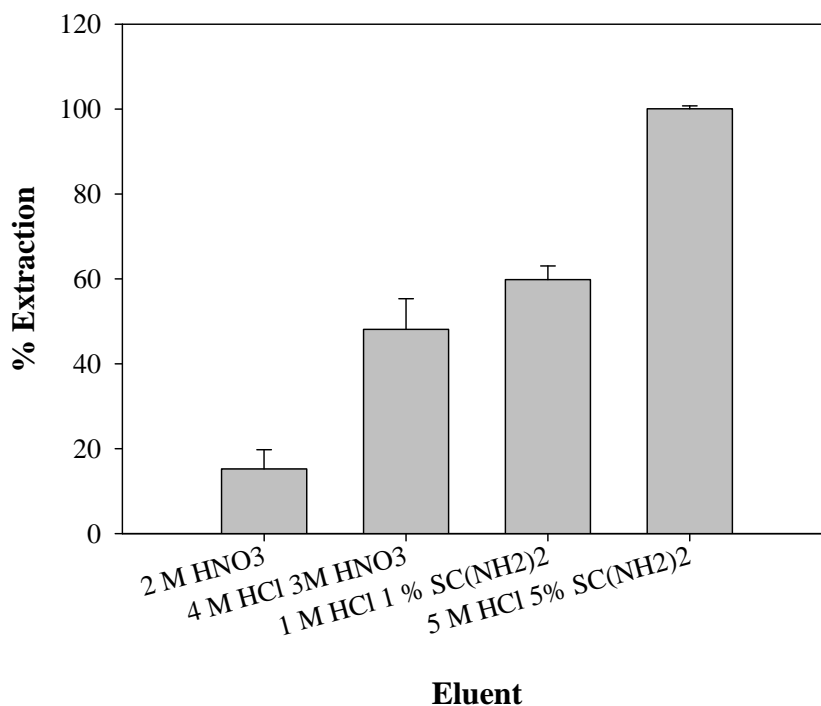


**Figure C.5.** Effect of eluent type on the desorption of Hg(II) ions. Conditions: River water, concentration of Hg(II): 0.2 µg/mL, flow rate: 2 mL/min, 300 mg of 8-HQ immobilized on silica gel, elution: 10 mL/ 0.5 mL/min.

#### B.4.2.3. Immobilization 8-HQ according to method 3

To examine the efficiency of 8-hydroxyquinoline silica gel (**2**) for Hg(II) ions recovery, river water adjusted to different pH values was percolated through 300 mg synthesized resin. 2 M HCl/1 M HNO<sub>3</sub> was found to be strong enough for complete removal of Hg(II) ions from the resin. Thereby, elution was performed using 10 mL of this mixture. Figure C.4 (b) represents the efficiency of this resin for pH values ranging from 3 to 8. Hg(II) ions extractions were found to be low (< 30%) whatever the sample pH. An increase in the quantity of the resin packed into the column to 500 mg permits a 20 % gain in the recovery of the studied ion as indicated in figure C.6, still not attaining quantitative retention. This evident change in retention is due to the fact that, the adsorbent dosage is one of many parameters which prominently affects the adsorption process. Modified silica gel **2** possessing an 8-HQ moiety

amino-linked through its position 7 also turns out to be unfit for efficient recovery of Hg(II). However, this resin remains suitable for the preconcentration of other metals (e.g. Mn(II), Co(II), Ni(II), Cu(II), Zn(II), Cd(II), Pb(II)) according to Willie et al (1998).

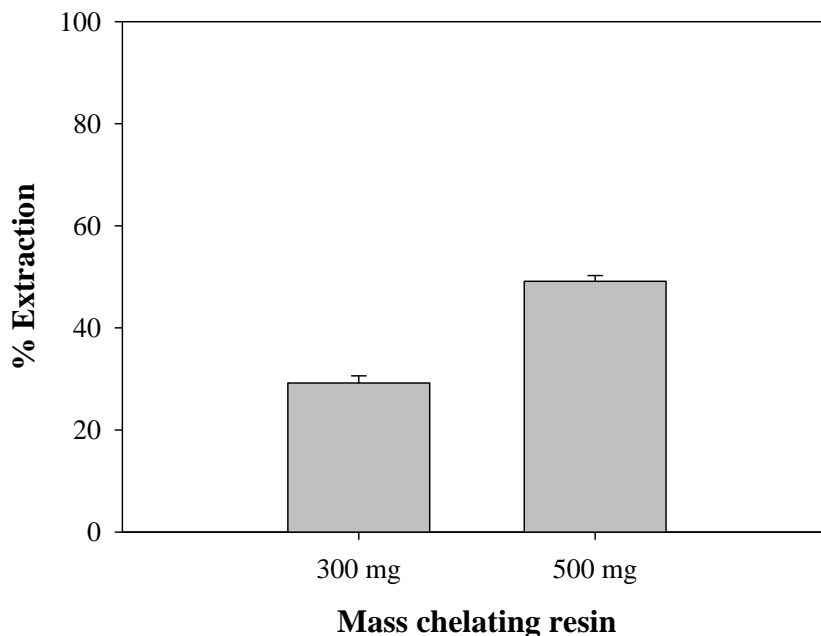


**Figure C.6** Effect of adsorbent amount on the recovery of Hg(II) ions. Conditions: River water, concentration of Hg(II): 0.2  $\mu\text{g/mL}$ , flow rate: 2 mL/min, elution: 10 mL/2 M HCl 1 M HNO<sub>3</sub>/0.5 mL/min.

#### B.4.2.4. Immobilization of 8-HQ according to method 4

Imino-immobilized 8-HQ silica gel (**3a** + **3b**) was also tested for Hg(II) extraction from river water. Retained Hg(II) were stripped off from the column using 10 mL of 2 M HNO<sub>3</sub>. The results shown in figure C.4 (c) demonstrate high performance with Hg(II) extraction reaching 100 % at pH 4. It should be noted that quantitative extraction of Cu(II), Pb(II), Ni(II), Fe(III), Cd(II), Zn(II) and Co(II) were also observed by Goswami et al (2003).

Such silica resin equipped with an 8-HQ moiety anchored through a flexible synthetic Schiff's base arm also provides a powerful resin for Hg(II) adsorption with performances that are comparable to 5-phenylazo-8-hydroxyquinoline silica gel **1**. The similarity between these two resins is also referable to the anchoring position at position 5 of 8-HQ. This linkage position indeed seems to offer a good affinity towards Hg(II) ions that can be explained by the formation of a dipotic ligand in both cases.

#### B.4.2.5. Immobilization of 8-HQ according to method 5

Method 5 involves the formation of a mixture of two 8-HQ amino-modified silica gels (4 + 2) in disproportionate ratios. As previously defined for method 3, best performances were obtained using a 2 M HCl/1 M HNO<sub>3</sub> mixture as eluent. However, low recoveries were attained whatever the sample pH (Figure C.4 (d)).

As depicted in figure C.7, increasing the quantity of resin to 1 g afforded Hg(II) recovery reaching 52%. This demonstrates that modified silica gel (4 + 2) possess a low adsorption capacity for mercury, as well as a possible low molar coverage of the ligand that can be inherent to the synthetic route. It can also be supposed that the amino-linkage provided by the Mannich reaction (method 3 and 5) is not suitable for mercury complexation. However, despite the poor performances exhibited in our case for mercury extraction, this resin has been used with success for Pb(II) preconcentration from seawater,<sup>24</sup> and exhibits a high adsorption capacity for Cu(II) reaching 347  $\mu\text{mol/g}$ .<sup>21</sup>

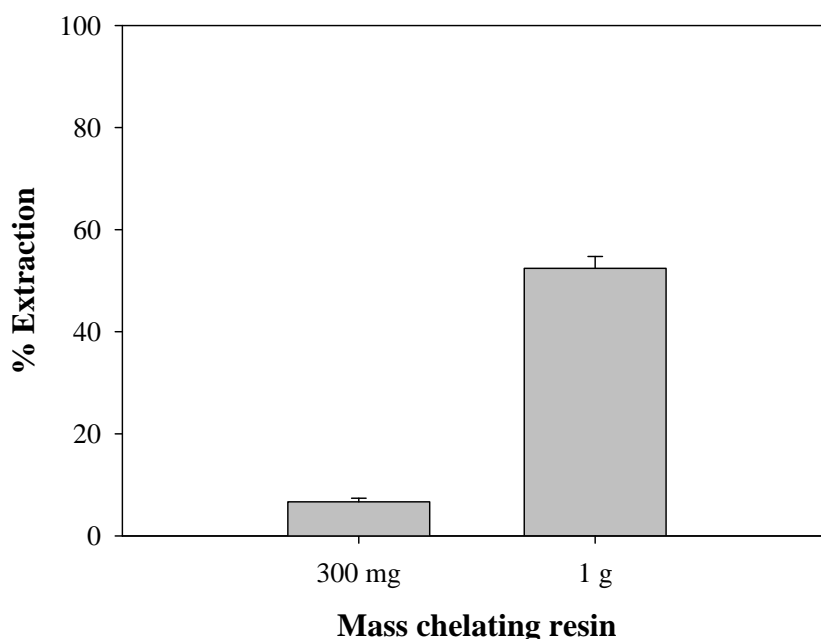


**Figure C.7.** Effect of adsorbent amount on the recovery of Hg(II) ions. Conditions: River water, concentration of Hg(II): 0.2  $\mu\text{g/mL}$ , flow rate: 2 mL/min, elution: 10 mL/2 M HCl 1 M HNO<sub>3</sub>/0.5 mL/min.

#### B.4.2.6. Immobilization of 8-HQ according to method 6

Efficiency of the novel imino-immobilized 8-HQ silica gel **5** was tested by passing river water samples at different pH values. Optimal elution was achieved using 5 M HNO<sub>3</sub>. As observed in figure C.4 (e), mercury ions were quantitatively extracted whatever the pH values. Such modified silica gel with an imino-embedded 8-HQ moiety on its position 2 offers an extraordinary capacity for Hg(II) retention. It seems that such a new immobilization-position offers the advantaged *N,O* binding site of the 8-hydroxyquinoline residue, to which the conjugated imine *N* atom can join to act as a planar tridentate *N,N,O* donor set. Moreover, the good performances are combined with an easy dilution step using nitric acid.

### B.5. Conclusion

For the first time, 8-Hydroxyquinoline was investigated for the adsorption of mercury ions by the formation of 8-HQ-Hg(II) complexes for its subsequent SPE and by the examination of different chelating resins based on 8-hydroxyquinoline. Mercury ion is proven to have an exceptional coordination with 8-hydroxyquinoline which is not demonstrated by any other metal. The Hg(II)-HQ chelate formation and its adsorption on silica column has been proven in this work to be poorly suited for mercury extraction due to its low formation constant for the constitution of Hg(II) chelates. However, the immobilization of 8-HQ on silica matrix can offer a better stability combined with an upgraded stability constant (table C.5) and an improved selectivity. Different synthetic routes for silica functionalization with 8-hydroxyquinoline were tried out for mercury extraction.

Among the six methods tested in this study, only three have been successfully able of quantitative extraction of Hg(II) ions from river water matrix. 5-Phenylazo-8-hydroxyquinoline silica gel **1** and the two imino-immobilized 8-HQ silica gel **3a/b** and the novel 8-HQ grafted silica ligand **5** gave the best performances for Hg(II) adsorption. These high potentials for mercury complexation were attributed to the anchoring position of 8-HQ (5 and 2). Such grafted 8-hydroxyquinolinols also offer opened donor set (ON) binding sites for mercury ions coordination.

**Table C.5.** Distribution ratios of metals on 8-HQ functionalized silica gel through position 5 on HQ moiety.<sup>19</sup>

Element	Cu	Ni	Co	Fe	Mn	Zn	Cd	Pb	Hg
Log K <sub>D</sub>	4.06	4.21	3.84	4.09	3.89	>4.85	>4.89	>4.72	>4.25

## B.6. References

- 1 Z. Li, Q. Wei, R. Yuan, X. Zhou, H. Liu, and H. Shan. *Talanta*, 2007, **71**, 68.
- 2 S.M. Ullrich, T.W. Tanton, and S.A. Abdrashitova. *Environ. Sci. Technol.* 2001, **31** 241.
- 3 D.Cossa, J. Sanjuan, J.Cloud, P.B. Stockwell, and W.T. Toms. *J. Anal. Spectrom.* 1995, **10**, 287.
- 4 M. Horvat, L. Liang, and N.S. Bloom. *Anal. Chim. Acta.* 1993, **282**, 153.
- 5 A. Detcheva, K.H. Grobecker. *Spectrochim,Acta.* 2006, **61**, 454.
- 6 J. Koh, Y. Kwon, and Y. Pak. *Microchem. J.* 2005, **80**, 195.
- 7 S. P. Boudreau and W. T .Cooper. *Anal. Chem.* 1989, **61**, 41.
- 8 R.J. Kvitek., J.F. Evans, and P.W. Carr. *Anal.Chim.Acta.* 1982, **144**, 93.
- 9 J.M. Gladis and T. P. Rao. *Anal Bioanal Chem.* 2002, **373**, 867.
- 10 K.F. Sugawara, H.H. Weetall, and G.D. Schucker. *Anal. Chem.* 1974, **46**, 489.
- 11 M.M. Guedes da Mota, F. G. Romer, and B. GriepInk. *Fresenius Z Anal Chem.* 1977, **287**, 19.
- 12 E. D. Moorhead and P. H. Davis. *Anal. Chem.* 1974, **46** ,1879.
- 13 R. E. Sturgeon, S. S. Berman, S. N Willie, and J.A.H. Desaulniers. *Anal. Chem.* 1981, **53**, 2337.
- 14 H.H. Weetall. *Biochim.Biophys.Acta.* 1970, **212**, 1.
- 15 J.M.Hill. *J. Chromatogr.* 1973, **76**, 455.
- 16 J.R. Jezorek and H.Freiser. *Anal. Chem.* 1979, **51**, 3.
- 17 M.A. Marshall and H.A. Mottola. *Anal. Chem.* 1985, **57**, 729.
- 18 A.Goswami, A.K. Singh, and B. Venkataramani. *Talanta*, 2003, **60**, 1141.
- 19 M. Luhrmann, N. Stelera, and A.Kettrup. *Fresenius Z Anal Chem.* 1985, **322**, 47.
- 20 U. Pyell and G. Stork. *Fresenius Z Anal Chem.* 1992, **342**, 281.
21. Z. Wang, M. Jing, F.S.C. Lee, and X. Wang. *Chinese J anal Chem.*, **2006**, 34, 459.
- 22 S.M. Nelms, G.M. Greenway, and R.C. Hutton. *J. Anal. At. Spectrom.* 1995, **10**, 929.
- 23 B.K. Esser, A.Volpe, J.M. Kenneally, and D.K. Smith. *Anal. Chem.* 1994, **66**, 1736.
- 24 M. Howard, H.A. Jurbergs, and J.A. Holcombe. *J. Anal. At. Spectrom.* 1999, **14**, 1209.
- 25 S.N. Willie, H. Tekgul, and R.E. Sturgeon. *Talanta*. 1998, **47**, 439.
- 26 J.W. McLaren, A.P. Mykytiuk, S.N. Willie, and S.S. Berman. *Anal. Chem.* 1985,**57**, 2907.
- 27 J. Malamas, M. Bengtsson, and G. Johansson. *Anal. Chim. Acta.* 1984, **160**, 1.
- 28 M. Soleimani, M.S.Mahmodi, A.Morsali, A.Khani, and M.G.Afshar, *J.Hazard.Mater.* 2011,**189**, 371.
- 29 S.R. Segade and J.F. Tyson. *Talanta*, 2007, **71**, 1696.
- 30 A.C.P. Monteiro, L.S.N. Andrade, and R.C. Campos. *Fresenius Z Anal Chem.* 2001 **371**, 353.
- 31 R.E. Sturgeon, S.N. Willie, and S.S. Berman. *Anal Chem.* 1985, **57**, 6.
- 32 G.Abbasse (2002). Mise au point de methodologies analytiques pour l'etude de la speciation de metaux traces en milieux aquatiques naturels: Application aux eaux de mer et interstitielles. PhD thesis, Université des Sciences et Technologie de Lille.
- 33 J. Otero-Roman, A. Moreda-Pineiro, A. Bermejo-Barrera, and P. Bermejo-Barrera. *Anal. Chim. Acta.* 2005, **536**, 213.

- 34 H.Watanabe, K. Goto, S. Taguchi, J.W. McLaren, S.S. Berman, and D. S. Russell. *Anal. Chem.* 1981, **53**, 738.
- 35 M.M. Kamal, A.Y. Sayed, S.M. Ahmed, A.A. Omran, and M.M. Shahata. *Arab. J. Chem.* 2011, <http://dx.doi.org/10.1016/j.arabjc.2011.07.027>
- 36 G.R. Clemo and R. Howe. *J. Chem. Soc.* 1955, 3552.
- 37 I. García-Santos, J. Sanmartín, A.M. García-Deibe, M. Fondo, and E. Gómez. *Inorg. Chim. Acta.* 2009, **363**, 193.
- 38 P. Hu, F. Wang, and G. Jin. *Organometallics.* 2011, **30**, 1008.
- 39 Martell A.E and Sillen L.G. *Stability constants of metal ion complexes*, second ed, Chemical Society, London, 1964.

***Chapitre D: Développement de méthode analytique pour la quantification de Hg(II) par extraction en phase solide***

***Chapter D: Analytical method development for the measurement of Hg(II) by solid phase extraction onto chelating resin***



## ***Résumé***

Nous avons montré dans le chapitre précédent que la méthode d'extraction par formation directe de complexe, en utilisant la 8-hydroxyquinoline (8-HQ) en solution n'est pas adaptée pour la détermination du mercure dans les eaux naturelles. L'immobilisation de 8-HQ sur un gel de silice peut offrir de meilleurs taux de recouvrement pour l'extraction du mercure dissous. Seuls trois résines parmi les six testés ont permis d'atteindre des recouvrements quantitatifs dans les eaux naturelles. Le 5-Phénylazo-8-hydroxyquinoline (5Ph8HQ) peut être considéré comme un bon choix pour l'extraction du mercure en phase solide du fait de son faible coût et du rendement élevé de la synthèse et la fixation sur le support. Dans cette partie, la dynamique d'adsorption du mercure avec le 5Ph8HQ a été étudiée pour arriver à la mise au point d'une méthode d'analyse simple du Hg(II) dans les eaux naturelles, en utilisant la Spectroscopie Fluorescence Atomique à Vapeur Froide (CV-AFS) et le 5Ph8HQ comme adsorbant.

Dans une solution mono-élémentaire, le temps nécessaire pour atteindre l'équilibre d'adsorption est de 30 minutes avec un temps demi-vie de sorption ( $t_{1/2}$ ) de 5 minutes. Le modèle de la cinétique de pseudo-deuxième ordre prévalait le mécanisme d'adsorption des ions de Hg (II), ce qui accentue la "chemisorption" qui est peut être considérée comme le mécanisme prédominant. La diffusion intra particulaire a régi, dans les premières heures, l'adsorption du Hg(II) sur l'absorbant, suivie par un contrôle du mécanisme de type "couche de diffusion". L'influence des métaux coexistant en solution sur l'adsorption de Hg(II) a également été testé dans des mélanges multi-élémentaire et binaire. Une valeur plus élevée de  $t_{1/2}$  a été obtenue pour le mercure (14,6) dans une solution multi-élémentaire. Le coefficient de partage ( $K_d$ ) pour est plus élevé (52,4) dans le cas d'une solution mono-élémentaire que dans une solution multi-élémentaires (49,8). Par conséquent, le 5Ph8HQ présente une sélectivité importante envers les ions Hg(II) dépassé seulement par le Cu(II) qui a une valeur de  $K_d$  plus élevé. L'étude de l'isotherme d'adsorption du mercure sur la phase solide montre qu'il suit un modèle de sorption monocouche de Langmuir.

L'excellente dynamique d'adsorption du mercure par le 5Ph8HQ a contribué au développement d'une méthode analytique pour la détermination de Hg(II) dans les eaux naturelles. La méthode mise au point est basée sur l'extraction en phase solide de Hg(II) en utilisant le 5Ph8HQ et la détection par CV-AFS. Divers paramètres ont été optimisés pour atteindre un recouvrement maximum. Les valeurs optimales des différentes conditions

expérimentales étaient les suivantes: pH = 4, éluant (4 mL de HCl 5 M + CS(NH<sub>2</sub>)<sub>2</sub> 5%), débit de percolation et d'élution 0,5-2 mL/min et un volume d'échantillon d'un litre. La limite de détection (LOD) de la méthode d'analyse développés est de = 0,21 pg/mL avec un écart type relatif < 6%.

### *Summary*

Based on previous studies of solid phase extraction of mercury (Hg) from river water using 8-HQ, direct ion complexations of Hg have shown to be poorly adapted for Hg determination in natural water samples. 8-hydroxyquinoline (8-HQ) immobilization on silica gel have offered better recoveries of Hg ions. However, only three 8-HQ resins have attained quantitative recoveries of Hg(II) from river water. As opposed to the two other imino-immobilized 8-HQ, 5-phenylazo-8-hydroxyquinoline (5Ph8HQ) has low cost of chemical reagents and high synthesis yields which makes it a good candidate as solid support for SPE studies. In this study, Hg adsorption dynamics with 5Ph8HQ were studied for the first time. Moreover, an analytical method for the determination of Hg(II) ions in river water was developed based on 5Ph8HQ as adsorbent and CV-AFS as an analytical instrument.

In a single metal solution, the time required for Hg to reach adsorption equilibrium was 30 minutes with half-life sorption ( $t_{1/2}$ ) of 5 minutes. Pseudo-second order kinetic model prevailed the adsorption mechanism of Hg(II) ions, accentuating chemisorption as the predominant adsorption mechanism. Intraparticle diffusion has governed in the first few hours of Hg adsorption on the sorbent followed by the over control of film diffusion. The influence of coexisting metals on the adsorption of Hg(II) ions was also tested in multi and binary element mixtures. In multi-element mixture, higher  $t_{1/2}$  of 14.6 minutes was obtained for Hg. The distribution coefficient ( $K_d$ ) of Hg showed a high value of 52.4 in single metal solution and 49.8 in multi-element mixture. Therefore, 5Ph8HQ have demonstrated significant selectivity towards Hg ions surpassed by only one element Cu(II) which have showed higher  $K_d$  value. The study of Hg adsorption isotherm showed that it follows Langmuir model of monolayer sorption at specific homogenous sites.

The excellent adsorption dynamics of Hg by 5Ph8HQ have contributed to analytical method development for Hg(II) determination in river water. The developed method is based on the solid phase extraction of Hg(II) using 5Ph8HQ and detection by CV-AFS. Various parameters were optimized for maximum recoveries of Hg. The optimal values of different experimental conditions were as follows: pH: 4, 4 mL of 5 M HCl + 5 % CS(NH<sub>2</sub>)<sub>2</sub> as eluent conditions, 0.5-2 mL/min as eluent and sample flow-rate and sample volume of 1000 mL. The figures of merit of the developed analytical method were: limit of detection (LOD)= 0.21 pg/ mL and relative standard deviation (RSD) < 6 %.

## **Solid phase extraction of inorganic mercury using 5-phenylazo-8-hydroxyquinoline and determination by cold vapor fluorescence spectroscopy in natural water samples†**

Mirna Daye<sup>a,b</sup>, Baghdad Ouddane<sup>a\*</sup>, Jalal Halwani<sup>b</sup>, Mariam Hamze<sup>a</sup>

<sup>a</sup>*University Lille 1, Géosystèmes, UMR - CNRS 8217, Villeneuve d'Ascq, France.*

<sup>b</sup>*Lebanese University, Water & Environmental Sciences Laboratory (L.S.E.E), Tripoli, Lebanon*

**\*Corresponding author. Tel.: +33 (0) 3 20 43 44 81, E-mail address: Baghdad.Ouddane@univ-lille1.fr**

## **D.1. Abstract**

8-hydroxyquinoline (8-HQ) was chosen as a powerful ligand for Hg solid phase extraction. Among several chelating resins based on 8-HQ, 5-phenylazo-8-hydroxyquinoline (5Ph8HQ) is used for mercury extraction in which the adsorption dynamics were fully studied. It has been shown, that Hg(II) is totally absorbed by 5Ph8HQ within the first 30 minutes contact time with  $t_{1/2}$  5 minutes, following Langmuir adsorption model. At pH 4, the affinity of mercury is unchallenged by other metals except for Cu(II) which has shown higher  $K_d$  value. With these latter characteristics, 5Ph8HQ was examined for the preconcentration of trace levels of Hg(II). The developed method, showed quantitative recoveries of Hg(II) with LOD= 0.21 pg/mL and RSD= 3-6% using CV-AFS with a preconcentration factor greater than 250.

Keywords: 5-phenylazo-8-hydroxyquinoline, Hg(II), adsorption, solid phase extraction, water samples.

## **D.2. Introduction**

8-hydroxyquinoline (8-HQ) has a complexing coordinating ability for over 60 metals with preference for transition metals over alkali and alkaline earth metals. It is even used for the extraction of rare earth metals using a binary mixture of sec-octylphenoxyacetic acid-8-HQ [1]. 8-HQ forms chelates with metals of varying stability.  $\log K_1$  values for Fe(III), Cu(II), Cd(II), Ca(II), Mg(II) with 8-HQ are 13.7, 12.1, 7.3, 3.3, 4.2 respectively [2]. Stability constant of Ca(II) with immobilized 8-HQ was also determined by [3] with slightly higher value with  $\log K_1$  of 3.7. Moreover, Weaver and Harris [4], calculated the stability constant of Aluminum with alkyl-immobilized 8-HQ and was found to be  $\log K_1$  0.8. High stability constants were found for Cd(II) with 8-HQ immobilized on controlled pore glass (CPG) ranging from  $10^9$ - $10^{11}$  [5]. 8-HQ has been used extensively for the preconcentration of trace metals from natural water samples and seawater. Silica has been used as a support in many applications for its numerous advantages as compared to polymers. 8-HQ has been immobilized on various solid matrices from XAD to activated carbon [6]. Adsorption capacities have been determined for some metals, i.e. Cu(II) using 8-HQ functionalized CPG of 58  $\mu\text{mole/g}$ , with Porasil C porous silica of 104  $\mu\text{mole/g}$  and silica gel of 216  $\mu\text{mole/g}$ . It is evident that silica gel confers the largest capacity with an average molar coverage of 0.39  $\mu\text{mole/m}^2$  attributed to increased surface area of 553.84  $\text{m}^2/\text{g}$  (decreased pore size) [7].

Numerous synthesis routes have been described since the first immobilization of 8-hydroxyquinoline (8-HQ) on silica gel. Diazo coupling of 8-HQ with p-aminobenzamide propyl silica was first reported [8, 9, 10]. The first technique was further ameliorated by diazo coupling of 8-HQ on p-amino phenyl silica [11] or glass [12]. Moreover, the formation of Schiff's base on position 5 of 8-HQ moiety enables its fixation on p-aminopropyl silica bestowing extraordinary coordination [13]. Finally, following Mannich reaction in the anchoring procedure, in two steps reactions [14, 15] and one-step reaction [16, 17]. Among these synthesis routes, immobilization involving the diazo coupling of 8-HQ on p-aminobenzamide propyl silica was shown by many studies to have an excellent retention of many trace metals. The most powerful chelating 8-HQ-grafted silica is that with an exceptional coordination potential given by its anchoring position on carbon 5 of 8-HQ moiety. Therefore, phenylazo-8-HQ was chosen in this study among other 8-HQ-5-grafted silica due its higher yield product.

Since then, much research has been conducted to fully understand the complexing ability of phenylazo-8-HQ (5Ph8HQ). Spectroscopic studies of metal complexes with 5Ph8HQ bound to silica, showed 1:1 metal ligand stoichiometry in  $\text{Cu}^{2+}$  solution complex [18]. Other studies have determined the protonation constants of 5Ph8HQ grafted silica to  $\text{pK}_{a1}=2.7$  and  $\text{pK}_{a2}=8.6$  [18]. However, the water soluble sulfo derivative of 8-HQ 5-(*p*-sulfophenylazo)-8-hydroxyquinoline, showed higher acid dissociation constants  $\text{pK}_{a1}$  of 3.78 and  $\text{pK}_{a2}$  of 7.94 [19]. These values would certainly change when the ligand is bound on silica. Equilibrium constants for 5Ph8HQ silica binding to metals have been determined. The stability constant of  $\text{Cu}^{2+}$  with the grafted material was  $K^{\circ}=4.8 \times 10^8$  [18], showing higher stability constant with sulfo-5Ph8HQ in water,  $K=1.4 \times 10^{10}$  [19]. Recent study has showed, higher equilibrium constant for  $\text{Cu}^{2+}$  than the previously reported ones for 5Ph8HQ in micelles, and colloidal fumed silica-5Ph8HQ,  $K^{\circ}=1.27 \times 10^{11}$ ,  $K^{\circ}=7 \times 10^{11}$  respectively [20]. Stability constant for  $\text{Ni}^{2+}$  was also determined and found to be  $K'_{\text{ext}}=5.9$  [11],  $K'_{\text{ext}}=0.8-1.2$  for 1:1 ligand/metal stoichiometry in presence of either acetate or chloride counter ion [20]. Stability constants for metals were also determined by Lührman et al [15] protocol which involved the functionalization of p-aminopropyl silica with 5-chloro-methyl-8-hydroxyquinoline. The use of the former protocol is not widely studied because of its extremely high cost. Distribution ratios  $\log K_D$  were determined for Cu, Ni, Co, Fe, Mn, Cr, Zn, Cd, Hg and Pb using batch equilibrium technique for 8HQ grafted silica. Many studies have used 5Ph8HQ for the

retention and preconcentration of metals with excellent recoveries [9, 21, 22, 23, 24, 5]. Nevertheless, the adsorption dynamics of 5Ph8HQ grafted silica is not completely studied particularly for mercury. Therefore in this study, we attempt to examine the adsorption kinetics of mercury in single and multi-element solution to discover the competition demonstrated between mercury and different metals for 5Ph8HQ affinity sites. Moreover, in this study, adsorption isotherms of mercury and other metals were determined for 5Ph8HQ. Finally, an analytical method for the determination of Hg(II) ions in river water was developed based on 5Ph8HQ-linked silica as adsorbent and Cold Vapor Atomic Fluorescence Spectroscopy (CV-AFS) as an analytical instrument.

### **D.3. Materials and methods**

#### **D.3.1. Chemicals and materials**

##### **D.3.1.1. Reagents and apparatus**

Analytical reagent-grade chemicals were used and obtained Sigma Aldrich (France). Ultrapure water (with a resistivity of 18.2 MΩ.cm) was obtained using a Milli-Q system (Millipore, USA). Silica (100-200 mesh), chemicals and solvents were supplied from Sigma Aldrich (France). Labware was soaked in 20% nitric acid and washed thoroughly with pure water prior to use. Working solutions of metals (Cr(III), Cu(II), Co(II), Zn(II), Ni(II), Pb(II), Cd(II), As(II), Fe(III), V(II), Hg(II)) were prepared from stock metal nitrate solution (1000 mg/L) (Merck). Buffer solutions were prepared from 1 M sodium acetate to which different volumes of 1 M nitric acid were added to obtain pH in the range 4-6. Ammonium acetate and phosphate buffer were used for obtaining pH 7 and pH 8 respectively.

Fourier Transform Infrared (FT-IR) spectra of functionalized silica were recorded using Nicolet 380 Smart *i*TR spectrometer (ThermoScientific, USA) and were silica-matrix corrected. An inductively coupled plasma mass spectrometer, Thermo-Optek X7 (Thermo Fischer Scientific, USA), equipped with a cross-flow pneumatic nebulizer, a Concentric glass-type nebulization chamber and a 1.5 mm i.d. quartz plasma torch, was used. All the operating parameters were those recommended by the manufacturer. The optimum operating conditions and measurement parameters for ICP-MS are listed in table D.1. Measurements were performed with high purity Argon gas. The pH measurements and adjustments were conducted by pH meter calibrated using two standard buffer solutions of pH 4 and pH 7. The flow rate of the samples was adjusted using a Gilson Miniplus 3 peristaltic pump. PVC tubes

(3.18 i.d) were used for the preconcentration process. Self-made PTFE (polytetrafluoroethylene) columns (65 mm × 4 mm i.d.) were used for packing the examined adsorbent. Mercury was measured by Cold vapor- Atomic Fluorescence Spectroscopy (Tekran, Model 2600 CVAFS Mercury Analysis System, USA). Ionic mercury is reduced with SnCl<sub>2</sub> (2% solution in 1 % HCl), subsequently converting Hg(II) to Hg<sup>0</sup>. The volatile species of mercury are separated from solution by purging with high purity argon gas through a semi permeable dryer tube. Volatile mercury is then carried by argon gas and preconcentrated into a gold cell of the Cold-Vapor Atomic Fluorescence spectrometer. After thermal desorption, the concentration of Hg is determined by atomic fluorescence spectrometry at 253.7 nm.

**Table D.1:** Operating conditions ICP-MS with CCT mode

Forward Power (W)	1050
Nebuliser Gas Flow (L/min)	0.7
Auxiliary Gas Flow (L/min)	0.95
Cool Gas Flow (L/min)	13.5
Quartz Plasma Torch I.D. (mm)	1.5
Cone type	Pt
Glass Impact Bead	3
Spray Chamber temperature (°C)	
Nebulizer type	Glass concentric
Sample Uptake Rate (mL/min)	1
Uptake delay (s)	35
Washout delay (s)	75
Analytes	<sup>51</sup> V, <sup>52</sup> Cr, <sup>55</sup> Mn, <sup>59</sup> Co, <sup>60</sup> Ni, <sup>65</sup> Cu, <sup>66</sup> Zn, <sup>111</sup> Cd, <sup>208</sup> Pb, <sup>56</sup> Fe, <sup>75</sup> As

### D.3.2. 5Ph8HQ synthesis

Phenylazo-8-hydroxyquinoline silica gel was prepared according to the procedure proposed by Sugawara et al (1974). The procedure firstly consists in a coupling step between an arylamine moiety and aminopropyl silica gel (APSG) to permit further azo-linking of 8-hydroxyquinoline on position 5. APSG (10 g) was also acylated by treatment with *p*-



nitrobenzoyl chloride (1 g) in chloroform (60 mL) in presence of triethylamine (2 mL). The nitro-adduct was then reduced by sodium dithionite (5% w/v solution) to yield aminobenzoyl-APSG. Oxidation of the amino-moiety with sodium nitrite afforded formation of the expected diazonium salt, which was rapidly filtered to be coupled with 8-HQ. Formation of the final adduct was characterized by the rapid development of a deep red color, prominent feature of the formation of the expected diazo-linkage. Presence of the anchored 8-hydroxyquinoline was further ensured by FT-IR analysis, which revealed absorption bands from 1636 to 1524  $\text{cm}^{-1}$  relative to the presence of amide and heteroaromatic bonds.

### D.3.3. Adsorption experiments

A series of metal sorption experiments were conducted to study the effect of pH, sorption kinetics, selectivity, adsorption capacities and interferences of mercury with some other metals. Batch experiments were conducted using 1000 mL polyethylene (PE) bottles. The amount of the adsorbent used was 1 g and the volume of ultra-pure water was maintained at 200 mL. A concentration of metal ion of 1  $\mu\text{g}/\text{mL}$  was prepared by dilution of stock solution (1000  $\text{mg}/\text{L}$   $\text{M}^+$ ) and adjusted to the required pH using an adequate buffer system. The bottles were shaken at room temperature for a fixed period of time at constant speed 150 g. At the end of shaking time, the supernatant was separated from the solid phase by filtration using Millipore filters and analyzed by ICP-MS for metals and mercury analysis was performed using CV-AFS. The experiments were conducted in duplicates and the average results were reported. This methodology was followed to identify the pH effect, optimize shaking time and understand the competition between metals towards 5Ph8HQ sites and its effect on mercury adsorption efficiency.

Metal uptake or sorption capacity was calculated based on the difference of metal ion concentration before and after adsorption according to eq. (1). The percentage of mercury sorption, distribution coefficient, selectivity coefficients and half-life sorption [25] were calculated using Eqs. (1)- (5) respectively.

$$\text{Sorption (\%)} = \frac{C_i - C_e}{C_i} \times 100 \quad (1)$$

$$Q = \frac{(C_i - C_e)V}{m} \quad (2)$$

$$K_d = \frac{Q}{C_e} \quad (3)$$

$$\alpha = \frac{K_d(\text{Hg(II)})}{K_d(\text{X})} \quad (4)$$

$$t^{1/2} = \frac{1}{K_2 Q_e} \quad (5)$$

Here,  $C_i$  (mg/L) is the initial concentration;  $C_e$  (mg/L) the equilibrium concentration in the solution;  $V$  (L) the solution volume;  $m$  (g) the amount of sorbent;  $Q$  (mg/g) represents the sorption capacity;  $K_d$  distribution coefficient,  $\alpha$  is the selectivity coefficient for the binding of a specific metal in the presence of other competitive ions;  $X$  represents the metal ion species;  $K_2$  (g/mmol min) is the rate constant of pseudo-second order adsorption reaction.

#### D.3.4. Kinetics studies

A concentration of metal ion of 1  $\mu\text{g/mL}$  was prepared and adjusted to the optimized pH using buffer system. An accurately measured sorbent of 1 g was added. Different aliquots were sampled and filtered at different time intervals for 24 hours. Sorption dynamics were studied in mercury single metal solution, binary solutions of Hg(II)-Cu(II), Hg(II)-Co(II), Hg(II)-Ni(II), Hg(II)-V(II), Hg(II)-Fe(III). Moreover, adsorption kinetics were performed in multi-element mixture composed of Hg(II), Cr(III), Fe(III), V(II), As(II), Co(II), Cu(II), Ni(II), Cd(II), Pb(II), Mn(II).

Sorption kinetics were analyzed using pseudo-first, pseudo-second order rate equation and intra-particle diffusion model. Chemical reactions in homogeneous systems are described as pseudo first-order rate equation. The linearized form of the first-order rate equation by Lagergren and Svenska [26] is given as eq. (6):

$$\text{Log}(Q_e - Q_t) = \text{log}Q_e - \frac{K_1 t}{2.303} \quad (6)$$

Where  $Q_e$  and  $Q_t$  are the amounts of metal ions adsorbed (mmol/g) and at contact  $t$  (min), respectively,  $K_1$  (1/min) is the rate constant.

The linearized equation of Pseudo-second rate equation was given by Ho et al [27] as eq.(7):

$$\frac{1}{Q_t} = \frac{1}{K_2 Q_e^2} + \left(\frac{1}{Q_e}\right) t \quad (7)$$

Where  $K_2$  (g/mmol min) is the rate constant of pseudo-second order adsorption reaction.

Intra-particle diffusion can be described to the model given by [28] by eq. (8):

$$Q_t = K_i t^{1/2} \quad (8)$$

Where  $K_i$  is the intraparticle diffusion rate constant ( $\text{mmol/g min}^{0.5}$ ).

### **D.3.5. Adsorption isotherms**

Adsorption isotherms were determined for Hg(II) ions. Accurately measured 1 g of the sorbent was mixed with 50 mL of solution adjusted to the Hg optimal pH. The concentration of metal ion was changed between 10-160 mg/L while shaken (agitation speed 150 r/min). The contact time was selected on the basis of the kinetic studies. At equilibrium time; an aliquot was sampled, filtered and analyzed. The results were adjusted to Langmuir, Freundlich, Dubinin-Radushkevich D-R models [29, 30, 31]. The Langmuir model linearized form is given by eq.(9):

$$\frac{1}{Q_e} = \frac{1}{Q_m} + \frac{1}{b Q_m C_e} \quad (9)$$

Where  $Q_e$  (mmol/g) is the amount of metal ion adsorbed,  $C_e$  is the equilibrium metal ion concentration (mmol/L),  $Q_m$  (mmol/g) is the maximum Langmuir uptake, when the surface of the adsorbent is completely covered with adsorbate,  $b$  (L/mmol) is the Langmuir adsorption constant.

The Freundlich linearized form is described by Eq. (10):

$$\log Q_e = \log K_F + n \log C_e \quad (10)$$

where  $Q_e$  is the equilibrium metal ion concentration on the adsorbent (mmol/g),  $C_e$  is the equilibrium concentration of metal ion (mmol/L),  $K_f$  is the Freundlich constant ( $\text{mmol}^{(1-1/n)} \text{L}^{(1/n)}/\text{Kg}$ ) which indicates the adsorption capacity and the strength of the adsorption and  $n$  is the heterogeneity factor representing bond distribution.

The D-R adsorption isotherm linearized form is given by the following eq. (11):

$$\ln Q = \ln Q_m - K \varepsilon^2 \quad (11)$$

where  $Q$  is the amount of metal ion adsorbed per unit weight of the sorbent (mol/g),  $K$  is a constant related to the adsorption energy ( $\text{mol}^2/\text{KJ}^2$ ),  $Q_m$  is the maximum adsorption capacity (mol/g),  $\varepsilon$  is the Polanyi potential (J/mol).

### **D.3.6. Preconcentration study**

For optimization procedure, the synthesized 5Ph8HQ was cleaned by 20 mL of 2 M  $\text{HNO}_3$  at flowrate 2 mL/min, washed by Milli-Q pure water until free from acid and finally

conditioned by acetate-acetic acid buffer system at a flow rate of 1 mL/min. Aliquots of 50 mL of river water containing of 2 ng/mL were adjusted to the optimal extraction pH using ammonia or HNO<sub>3</sub> suprapur solution. Samples were percolated through 300 mg pre-cleaned resin at optimized flowrate, eluted with a suitable eluent and finally analyzed by CV-AFS.

## **D.4. Results and discussion**

### **D.4.1. Effect of pH**

The effect of pH variation on metal uptake of Hg(II), Cr(III), V(II), As(II), Co(II), Cu(II), Ni(II), Cd(II), Pb(II), Mn(II), Zn(II) was investigated using batch procedure in single-metal solution. Solution acidity was varied between pH 3-8. At equilibrium time, aliquots were sampled, filtered and analyzed. Metal ion sorption can occur through several single or mixed mechanisms. Coordination with the functional groups adhered to the sorbent through chelation, electrostatic attraction and anion exchange with protonated amino group through proton or anion exchange.

Figure D.1, shows the effect of pH variation on metal retention on the grafted material. The optimal adsorption of mercury was found in the range 3-4 with pH 4 as the optimal acidity. Above pH 4, Hg(II) retention decreases to 80% and follows a steady trend between pH 4 and 8. At pH greater than 5 mercury form colloidal precipitate of Hg(OH)<sub>2</sub> or soluble Hg(OH)<sup>+</sup>. The chemistry of mercury in aqueous solutions is more complicated than any other metals. Mercuric ions can be easily hydrolyzed according to the equation [32]. The coordination of water influence mercury adsorption dynamics and can relatively allow for slow diffusion.



The presence of Cl<sup>-</sup> can result in the formation of HgCl<sup>+</sup>, HgCl<sub>2</sub> and Hg Cl<sub>4</sub><sup>2-</sup>, HgCl<sub>3</sub><sup>-</sup> [33] and the possible electrostatic adsorption on the resin depending on its charged form. The increase in retention might be attributed to these species and not due to free Hg(II). Lower pH values are expected to enhance protonated ligand sites available for adsorption. Beyond pH 6, mercury uptake can decrease due to precipitation for high concentration which is therefore not applicable in our case. The pH dependence of metal adsorption is the result of the effect of metal speciation and the ionization forms of different groups of the sorbent. The adsorption of mercury is possibly by complexation and not by chemical binding since the zeta potential of 5Ph8HQ is zero [20]. The affinity of mercury towards the donor set atoms of 5Ph8HQ is due

to hard and soft acid base theory. It correlates the degree of metal softness to the observed strength of interaction with the donor atoms (N, O). Mercury is considered as a soft metal, because of its relatively large ionic size, low electronegativity and high polarisability. The N=N, -NH and OH of 5Ph8HQ are considered as relatively soft bases leading to the observed high affinities between each others.

The stability constant of Cu(II) with 8-HQ is elevated ( $\log\beta = 12.56$ ) [34], which is demonstrated by high distribution coefficient value as discussed below. Quantitative adsorption of Cu(II) is found for pH values greater than 4 and then it slightly decreases due to the formation of strong complexes with carbonates  $\text{Cu}(\text{CO}_3)_2^{2-}$  ( $\log\beta = 10.69$ ) [35]. The retention of Cd(II) is shown to be low for  $\text{pH} < 6$ , in which Turner et al [35] reported that 96 % of Cd are found as ionic free species for  $\text{pH} = 6$ . In seawater, It has been reported that  $\text{pH} < 6$ , Cd forms chlorocomplexes  $\text{CdCl}_2$ ,  $\text{CdCl}_3^-$ ,  $\text{CdCl}_4^{2-}$  with high stability constant  $\log\beta = 2.59$ ,  $\log\beta = 2.4$ ,  $\log\beta = 1.47$  [35] respectively which impede its complexation with 8-HQ. Thereby, quantitative retention is achieved for pH values  $> 6$ , with the formation of weak hydroxide complexes  $\text{Cd}(\text{OH})^+$ ,  $\text{Cd}(\text{OH})_2$ ,  $\text{Cd}(\text{OH})_3^-$  of  $\log\beta = -10.08$ ,  $\log\beta = -20.35$ ,  $\log\beta = -33.3$  [35]. The stability constant of Cd with 8-HQ is high of  $\log\beta = 7.78$ , which can easily break down the weak complexes formed with hydroxides. As for Mn(II), quantitative retention is attained for pH values  $> 6$ . At basic medium, Mn forms weak complexes with hydroxides  $\text{Mn}(\text{OH})^+$  ( $\log\beta = -10.59$ ) and carbonates  $\text{Mn}(\text{CO}_3)$  ( $\log\beta = 4.1$ ) [35] which seems far from the competition with 8-HQ complexes ( $\log\beta = 6.8$ ).

At acidic pH value, the stability constant of Ni(II) ( $\log\beta = 9.27$ ) and  $\text{H}^+$  ( $\log\beta = 9.9$ ) with 8-HQ is comparable. Therefore, quantitative recoveries of Ni(II) are found for  $\text{pH} \geq 5$  values although at  $\text{pH} = 4$ , 92.4 % recovery of Ni(II) can be attained. As shown in figure D.1, the retention of Pb(II) at low pH values is almost negligible. This is due to the competition between Pb(II) and  $\text{H}^+$  to form stable complexes with 8-HQ with  $\log\beta = 9.1$ ,  $\log\beta = 9.9$  respectively. As has been described Ni(II) and Pb(II), Zn(II) follows the same behavior, with competition of  $\text{H}^+$  ions at low pH values ( $\log\beta = 9.9$ ) to form more stable complexes with 8-HQ than Zn-8-HQ complexes ( $\log\beta = 8.56$ ). Therefore quantitative retention of Zn(II) is observed for  $\text{pH} \geq 5$ .

Quantitative recovery of Vanadium is only seen for  $3 < \text{pH} < 4$ . At higher pH values, the retention decreases. This is explained by the formation of V(IV) species at pH values  $< 3.5$

which are mainly  $\text{VO}^{2+}$ ,  $\text{VO}(\text{OH})^+$ ,  $(\text{VO}(\text{OH}))_2^{2+}$ ,  $\text{VO}(\text{OH})_2$  [36]. At  $3.5 < \text{pH} < 7.5$ , anionic species form, mainly  $\text{H}_2\text{VO}_4^{2-}$  and for  $7.5 < \text{pH} < 13$ , the anionic form of  $\text{HVO}_4^{2-}$  dominates [37]. The retention of Cr(III) at the studied pH range (3-8) is lower than 36%. It is probably due to the formation of chromium, under the oxidation state (V) which forms  $\text{CrO}_4^{2-}$  which certainly hinders its complexation with 8-HQ [38].

Arsenic showed no adsorption by 5Ph8HQ at the studied pH range (pH= 3-8). In summary, the adsorption Pb(II) Cd (II), Mn(II), was almost negligible between pH 3 and 4, then it increased for  $\text{pH} > 5$ . It is shown that basic conditions are favorable for Pb(II) retention. At lower pH value, the retention of these metals drops off due probably to the partial protonation of active sites and stronger electrostatic repulsion between Pb(II) and the protonated amino and hydroxyl groups of 5Ph8HQ. At basic medium, the retention is higher which is appreciated in selective separation from Hg(II), V(II), Cu(II), Ni(II), Co(II). Moreover, at basic pH values, functional groups of the sorbent are free from protonation and therefore retention is controlled by chelation mechanism. The corresponding affinity of the resin is attributed to the protonation of the free lone pair of nitrogen suitable for coordination with metals. Values of pH higher than 8 were not examined to prevent hydrolysis of adsorbent and precipitation of metals. The optimal pH values for Hg(II) is 4, for V(II) is 4, for Cu(II) is 4, for Co(II) is 3-4, for Zn(II) and Ni(II) is 5-8, for Cd(II) and Pb(II) is 8, for Cr(III) and Mn(II) is 7-8. Therefore, at pH 4, simultaneous extraction Hg(II), V(II), Cu(II), Co(II), Ni(II) can be achieved by 5Ph8HQ with maximal extractions occurring for Hg(II), V(IV) and Cu(II) and Co(II) with prominent separation from Pb(II) Cd (II), Mn(II) and Zn (II).

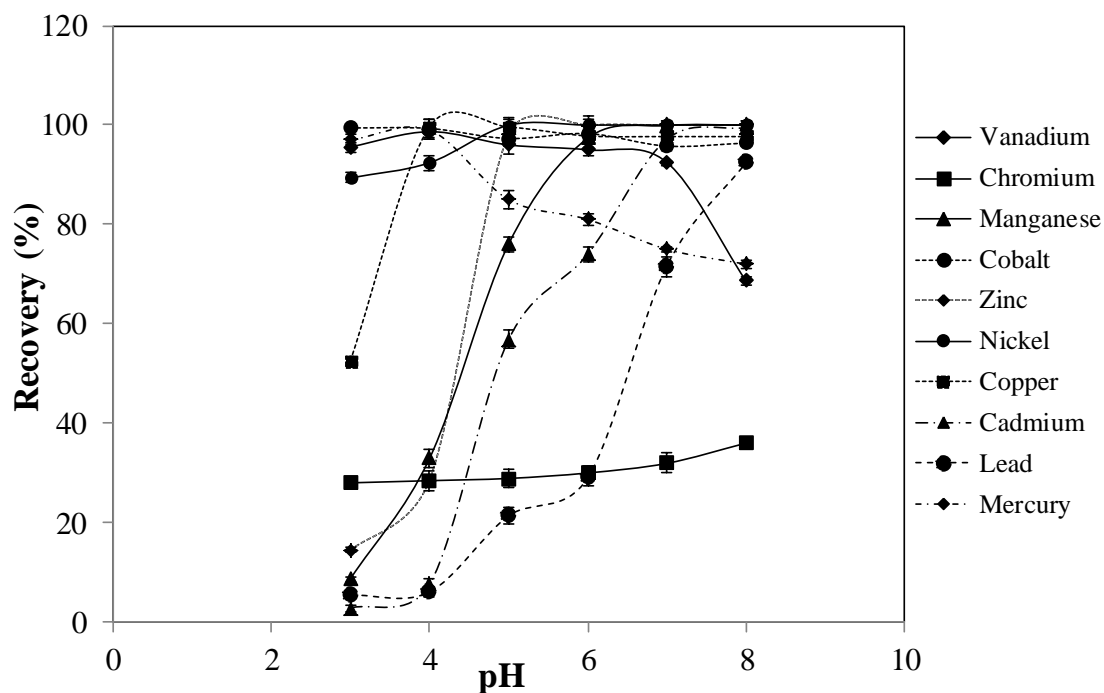


**Figure D.1:** Effect of pH variation on the adsorption of metals. Conditions: Volume 200 mL, m(5Ph8HQ): 1g,  $[M^+]$ : 1  $\mu\text{g/mL}$  in single metal solution. Bars represent standard deviation for two replicates.

#### D.4.2. Adsorption dynamics

In order to determine the optimum contact time between 5Ph8HQ, adsorption recoveries (%) were measured as a function of time in single metal solution and presented in figure D.2. Rapid uptake of metals by the resin was observed within the first 10 minutes. The time required to reach adsorption equilibrium was 30 minutes for V(IV), Cd(II), Cu(II), Zn(II), Hg(II), Ni(II), while slower equilibrium time was attained for Mn(II) of 1 hour, and 5 hours for Co(II) and Pb(II). Adsorption time equilibrium was comparable to other resins and in some cases the adsorption is faster than others reported in the literature [39, 40]. On the other hand, in multi-element mixture, equilibrium time of Hg and other metals have shifted to longer time, mainly because of interferences with other metals with stronger affinity to 5Ph8HQ. Mercury has reached equilibrium after 2 hours, while for Co(II), Ni(II), Zn(II), Fe(III), the adsorption time was longer and did not reach quantitative recoveries after 24 hours contact time. Still, the equilibrium time of Cu (II), V(IV) have not been influenced in multi-element mixture, revealing the significant affinity of these metals towards the studied resin.

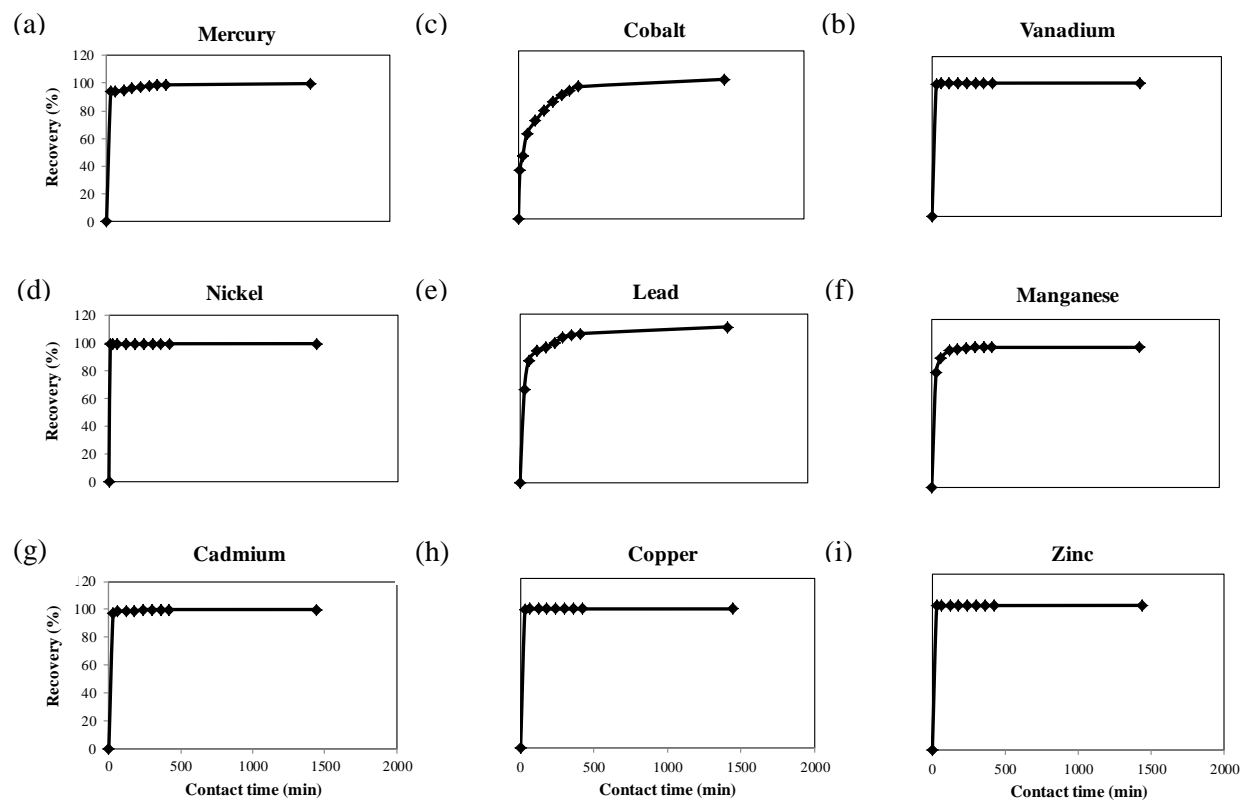


**Figure D.2:** Recovery percentage of metals as function of time in a single metal solution. Conditions: V (200 mL), m(5Ph8HQ)=1 g, element optimized pH,  $[M^+]=1\mu\text{g/mL}$ .



In a single metal solution, the lowest half-life sorptions were that of Cu(II) 0.06 min < V(IV) 0.28 min < Ni(II) 0.39 min < Zn(II) 0.41 min < Cd(II) 0.89 min respectively while slower sorption kinetics were found for Hg(II) 5.39 min < Pb 25.23 min < Co(II) 49.96 min (table D.2). Overall, the fast adsorption of metals on 5Ph8HQ can be attributed to the good hydrophilicity of silica and the chelating strength of 5Ph8HQ towards metals. In order to interpret the sorption kinetics, Lagergren first-order equation, pseudo-second order equation and Webber-Morris intraparticle diffusion models were used to evaluate the experimental data.

Table D.2 shows adsorption kinetic parameters of different metals in single metal solution. First order rate  $K_1$  was determined from the slope and intercept of the plot of  $\log(Q_e - Q_t)$  versus  $t$  (figure D.3 (a)). The correlation coefficient ( $R^2$ ) were between 0.99-0.79 for all studied metals and 0.9641 for Hg(II). As for pseudo second order model, correlation coefficients were superior to 0.999 for all systems. The inapplicability of the first kinetic model suggest the prevalence of pseudo-second order kinetic model on the adsorption of metals on the studied sorbent in which the calculated equilibrium adsorption capacities  $Q_e$  (theoretical) were in accordance with the experimental adsorption capacities  $Q_e$  (experimental). Thereby, chemisorption may control the adsorption mechanism involving valence forces through sharing or exchange of electrons between the resin and metals [41]. Moreover, the kinetic results were also fitted to intra-particle diffusion model by tracing  $qt$  versus  $t_{1/2}$ . If the plots were straight lines passing through the origin, then the adsorption mechanism is governed by intra-particle diffusion defining the sole rate limiting step. If plot  $qt$  versus  $t_{1/2}$  did not pass the origin, then the adsorption might be dominated by film diffusion or boundary layer diffusion [42]. As shown in figure D.3 (c), the corresponding plot was not linear over the studied time range. Hg adsorption had an initial linear portion followed by a plateau suggesting the governance of intra-particle diffusion in the few hours of adsorption then film diffusion over controlled. This two different stages of adsorption for Hg(II) is also seen for Co(II), V(IV), Cd(II), Cu(II), Zn(II), Ni(II), Pb(II) with good correlation coefficients attained for Zn of 0.8 and Co, Ni, Hg of 0.76. In contrast to other metals, Mn(II) demonstrated only film diffusion where a plateau is only seen.

In order to examine the influence of metals on the adsorption kinetics of mercury, adsorption kinetics was examined in multi-element mixture. For this purpose, a certain metal ion concentration containing V(IV), Cr(III), Co(II), Ni(II), Cu(II), Zn(II), Fe(III), Hg(II) was

added to 1 g of 5Ph8HQ at optimal pH for mercury sorption (pH 4). Metal mixture was shaken at 150 g and samples were taken at predetermined time as described above. As demonstrated in Table D.3, the experimental data fitted pseudo second order model with correlation coefficient between 0.9-1. The calculated equilibrium adsorption capacity for almost all metals tested were consistent with experimental data except for Co(II), Ni(II), Zn(II). It seems that the adsorption of Ni, Co and Zn is significantly affected in multi element mixture at pH 4. Similar to single metal solution, film diffusion predominated the trend of adsorption of metals in multi-element mixture except for Co which followed intra particular diffusion model with correlation coefficients of 0.97. Higher half time-sorption was found for all metals in multi element mixture, in which  $t_{1/2}$  of some metals was tremendously affected. The  $t_{1/2}$  of Ni(II) and Zn(II) were 230, 61 respectively higher in magnitude than in single metal solution. The sorption sequence of metals has been altered in multi-element solution with fast adsorption for Cu, V and Hg. The  $t_{1/2}$  sorption sequence became as follows: Cu(II) 0.7 min < V(IV) 1.86 min < Hg(II) 14.52 min < Zn(II) 25 min < Ni(II) 89.83 min < Fe(III) 124 min < Co(II) 119.61 min (table D.3). Therefore, in multi-element solution, Cu(II) and V(IV) appear to compete with Hg(II) for the adsorption sites of 5Ph8HQ since these metals have faster sorption time.

**Table D.2:** Adsorption kinetics of metals in single metal solution.

Metal	First-order rate constants				Second-order rate constant				Intra-particle diffusion	
	Q <sub>e</sub> (exp) (mmol/g)	Q <sub>e</sub> (theor) (mmol/g)	K <sub>1</sub> (1/min)	R <sup>2</sup>	Q <sub>e</sub> (mmol/g)	K <sub>2</sub> (g/mmol min)	R <sup>2</sup>	t <sub>1/2</sub>	K <sub>i</sub>	R <sup>2</sup>
Co	0.003394	0.0020068	0.00576	0.9988	0.00326	6.140	0.9997	49.9	0.00005	0.7041
V	0.003926	0.0000176	0.00461	0.7997	0.00392	913.816	1	0.3	0.0000006	0.5295
Pb	0.000965	0.0003075	0.00530	0.9559	0.00091	43.728	0.9999	25.2	0.000009	0.6236
Cd	0.001779	0.0000601	0.01313	0.9368	0.00178	627.455	1	0.90	0.000001	0.5016
Cu	0.003152	0.0000044	0.00668	0.9478	0.00311	5116.770	1	0.06	0.0000001	0.5123
Zn	0.003059	0.0000122	0.00299	0.9195	0.00303	819.968	1	0.40	0.0000004	0.8384
Mn	0.003640	0.0010354	0.01958	0.9961	0.00365	83.622	1	3.27	0.00005	0.3805
Ni	0.003408	0.0000186	0.00484	0.9743	0.00340	739.984	1	0.40	0.0000005	0.7674
Hg	0.000997	0.0000789	0.00507	0.9641	0.00100	186.063	1	5.39	0.000002	0.7665

**Table D.3:** Adsorption kinetics of metals in multi-element mixture at pH=4.

Metal	First-order rate constants			second-order rate constant				Intra-particle diffusion	
	Q <sub>e</sub> (theor) (mmol/g)	K <sub>1</sub> (1/min)	R <sup>2</sup>	Q <sub>e</sub> (mmol/g)	K <sub>2</sub> (g/mmol min)	R <sup>2</sup>	t <sub>1/2</sub>	K <sub>i</sub>	R <sup>2</sup>
Co	0.00146	0.00230	0.9533	0.00255	3.283	0.991	119.61	0.00004	0.9427
V	0.00007	0.00299	0.8843	0.00390	137.896	1	1.86	0.000003	0.4423
Cu	0.00004	0.00484	0.8318	0.00315	420.290	1	0.76	0.000001	0.6093
Zn	0.00033	0.00553	0.9541	0.00096	41.447	0.9998	25.04	0.000009	0.6659
Ni	0.00161	0.00345	0.9552	0.00267	4.169	0.9987	89.83	0.00004	0.7309
Fe	0.00193	0.00161	0.7571	0.00350	2.302	0.9993	124.09	0.000008	0.3698
Hg	0.00024	0.00668	0.7452	0.00100	68.596	0.9998	14.52	0.000009	0.4446

### D.4.3. Competitive adsorption

#### D.4.3.1. Multi-element mixture

The selectivity is determined by equilibrating a unit mass of the adsorbent in solution containing the same initial concentration for all metals. Solution acidity was adjusted to 4, which is the optimal pH for mercury adsorption. The overall adsorption efficiencies of Cu(II), V(IV), and Hg(II) remained unaffected in multi-component mixture. Maximum metal retention of 99.9%, 99.8%, 99.3 %, 94.2 %, 81%, 79%, 32.5 %, 14%, 10% were obtained for Cu(II), Hg(II), V(IV), Fe(III), Co(II), Ni(II), Zn(II), Pb(II), Cd(II) respectively. As a result, the affinity order can be as following Cu(II) > Hg(II) > V(IV) > Fe(III) > Ni(II) > Co(II) > Zn(II) > Pb(II) > Cd(II). The highest affinities ( $K_d$  (g/L)) were obtained for Cu(II) 154, Hg(II) 50, V(IV) 25 (table D.4). According to separation factor ( $\alpha$ ), mercury can be separated from metals of high affinity to 5Ph8HQ, that are V(IV), Fe(III), Co(II), Ni(II), however Cu(II) poses a potential concurrence with Hg(II) towards the resin binding sites. This is ascribed to the higher distribution coefficient  $K_d$  Cu(II) 145.48 >  $K_d$  Hg(II) 50 and  $\alpha < 1$ .

**Table D.4:** Metal distribution coefficient ( $K_d$ ) and separation factor ( $\alpha$ ) at pH 4 in Multi-element mixture.

Element	V	Co	Ni	Cu	Zn	Cd	Pb	Fe	Hg
$K_d$ (g/L)	25.12	0.48	0.58	153.65	0.05	0.02	0.03	3.26	49.76
$\alpha: K_d \text{Hg} / K_d \text{M}^+$	1.98	102.87	85.99	0.32	931.16	2638.32	1468.79	15.28	-

#### D.4.3.2. Binary and single metal-solution

Following the results of multi-element mixture, the highest affinities of metals towards 5Ph8HQ are obtained with an order Cu(II) > Hg(II) > V(IV) > Fe(III) > Ni(II) > Co(II). Therefore, it is interesting to identify the effects of these metal ions with mercury in binary metal mixture at pH 4. The outlined order of metal ion selectivity by 5Ph8HQ based on the values of distribution coefficient and separation factor  $\alpha$ : Cu(II) > Hg(II) > Co(II) > V(IV) > Ni(II) > Fe(III) (table D.5). It seems that the affinity order as seen in Table D.5 has changed in binary metal mixture as compared to multi-element mixture with increased values of  $K_d$  and a decrease in the separation factor  $\alpha_{\text{Hg}/\text{M}^+}$ . Change in the affinity of metals towards different sorbents with varying the competition potential was also observed in previous adsorption studies [44, 45]. According to Irving-Williams series, the stability of metal complexes with ligands is in the order: Mn(II) < Fe(II) < Co(II) < Ni(II) < Cu(II) > Zn(II) [46].

**Table D.5:** Selectivity of mercury at pH 4 in Binary mixtures.

	V	Cu	Ni	Co	Fe	Hg
$K_d$ (g/L)	27.011	159.800	12.829	35.836	5.260	52.376
$\alpha: K_d\text{Hg}/K_d\text{M}^+$	1.939	0.3278	4.0825	1.462	9.957	

The crystal field theory, suggests electrostatic interaction between the central atom and the ligand. Therefore, there is a direct relationship between stability of metal complexes and ionic potential that is charge to radius ratio ( $Z/r$ ). Following the  $Z/r$  ratio cited in table D.6 of the studied metals, the selectivity sequence is expected to be Mn(II) > Ni(II) > Co(II)=Zn(II) > V(II) > Cd(II) > Hg(II) and for trivalent metals As(III) > Cr(III) > Fe(III). The stability sequence of metals is not consistent with our results in either the two mixed metal studies. The adsorption selectivity can shift from the predicted affinities depending on the experimental conditions (pH...ect.) and sorbent properties. A direct correlation is made between  $Z/r$  ratio of metals and the metal complex stability in pure cation-exchange mechanism [47] that could be not ascribed to the studied resin. Therefore, it is also important to define the selectivity and the stability constants in single-metal solution without the presence of competitor elements.

**Table D.6:** Metal ion charge to radius ratio [43].

Ion	Oxidation state	Coordination number	Z/R
Pb	2	6	1.68
Zn	2	6	2.70
Cd	2	6	2.11
Cu	2	6	2.74
Ni	2	6	2.90
Cr	3	6	4.88
Co	2	6	2.70
V	2	6	2.53
Fe	3	6	4.65
Hg	2	6	1.96
As	3	6	5.12
Mn	2	6	2.98

Distribution coefficients are determined in single metal solution at element-optimized pH. As demonstrated by table D.7,  $K_d$  has tremendously been altered to high values as opposed to that observed in multi-element mixture, still  $K_d$  values (g/L) for Cu(IV), V(II), Hg(II) remained unchanged. Therefore, according to  $K_d$  values (g/L), metal affinity order towards 5Ph8HQ

can be as follow: Mn(II) 999.8> Co(II) 799.8>Cd(II) 199.8>Cu(II) 160>V(IV) 137.73>Ni(II) 59.5>Hg(II) 52.38>Zn(II) 18.84> Pb(II) 2.4.

**Table D.7:** Distribution coefficients of metals in single-metal solution at element optimized pH.

Element	V	Co	Ni	Cu	Zn	Cd	Pb	Mn	Hg
$K_d$ (g/L)	137.73	799.80	59.50	160.65	18.85	199.80	2.41	999.80	52.38

#### D.4.4. Adsorption isotherms

Adsorption isotherm studies are of great value for their importance in describing the interaction between the solute, adsorbant and the adsorbate. Thereby, the effect of initial concentration of metal ions on the sorption efficiency was investigated by varying the initial concentrations of metal ions at optimum pH. The obtained results were presented in Figure D.3. As indicated in figure D.4, as the concentration of metal ion increases, the larger is the equilibrium adsorption uptake by the adsorbent. There seems a direct relation between the loading capacity of the sorbent and metal ion concentration. It can be explained by the fact that, with higher concentration the transfer driving force is larger [48]. The adsorption data for metals were analyzed and fitted according to Langmuir, Freundlich and Dubinin-Radushkevich D-R models. The Langmuir isotherm model suggests monolayer sorption at specific homogenous site without interaction between the sorbed molecules, with sites having identical adsorption energies. The Freundlich isotherm sorption assumes monolayer sorption on heterogeneous sites with interaction between the adsorbent and adsorbate and all adsorption sites are energetically different. The D-R isotherm is considered more general than Langmuir model; it does not assume homogenous surface or constant adsorption potential. It is used to identify whether the adsorption is of chemical nature or physical one [30].

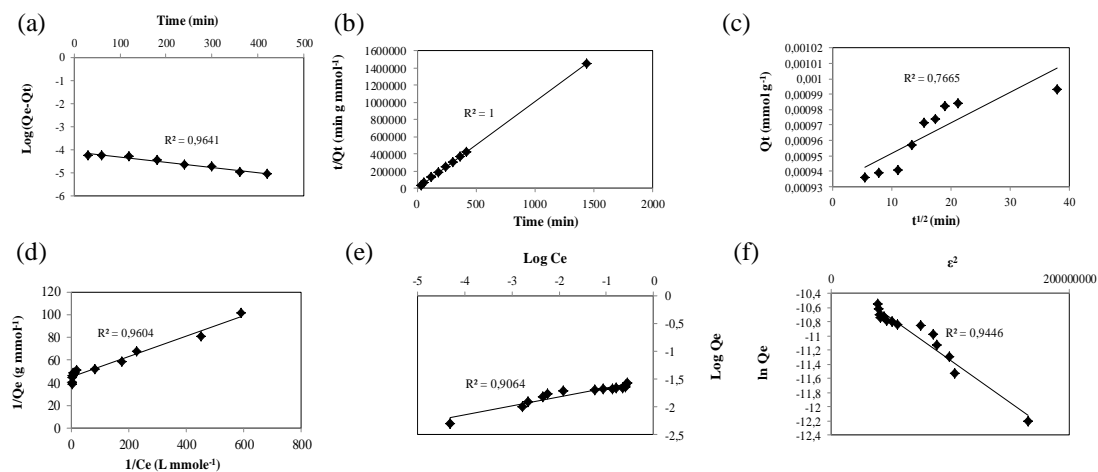


**Figure D.3:** Adsorption kinetics of Hg(II) according to (a) pseudo first order model, (b) pseudo second order model, (c) intra particle diffusion; [Hg(II)]: 0.005 mmol/L, V(200 mL), pH 4, m(5Ph8HQ): 1g. Adsorption isotherms of Hg(II) by 5Ph8HQ according to (d) Langmuir adsorption model, (e) Freundlich adsorption model, (f) Dubinin-Radushkevich adsorption model; [Hg(II)]: 10-160  $\mu\text{g/mL}$ , V(50 mL), pH 4, m(5Ph8HQ): 1g.

**Table D.8:** Langmuir, Freundlich and D-R isotherm constants of Hg.

Metal	Langmuir isotherms parameters			Freundlich isotherms parameters			D-R isotherms parameters		
	$Q_m$ (mmol/g)	$b$ (L/mmol)	$R^2$	$K_F$ (mmol/g)	$n$	$R^2$	$Q_m$ (mol/g)	$K$ (mol <sup>2</sup> / KJ <sup>2</sup> )	$R^2$
Hg	0.0224	492.815	0.9604	0.0311	6.1463	0.9064	0.000039	$1 \times 10^{-15}$	0.9446

The model constants of Langmuir, Freundlich and D-R isotherms along with correlation coefficients values are listed in table D.8. The  $R^2$  values indicate that Langmuir fit the experimental data better than Freundlich and D-R isotherm models, suggesting a monolayer coverage of Hg(II) on 5Ph8HQ resin. Langmuir isotherm adsorption-type was also found for Hg(II) with other studied resins, thiourea-modified chitosan [49] and poly-allyl thiourea [50]. The maximum adsorption capacity of Hg(II) on 5Ph8HQ was found to be 0.022 mmol Hg(II)/g corresponding to a maximum Hg(II) initial concentration of 90 mg/L (figure D.4). The determined adsorption capacity is considered as minimal as compared to other resins such as thiol-functionalized mesoporous silica magnetite nanoparticles with 0.8 mmol Hg(II)/g [51]; 0.39 mmol Hg(II)/g of silica supported dithiocarbamate [52] and 1.13 mmol Hg(II)/g of poly-allyl thiourea [50]. 8-Hydroxyquinoline silica synthesized according to Luhrmann et al [15] showed higher capacity for Hg(II) 0.448 mmol/g at optimized pH 6. The adsorption capacity for some metals has been also reported using HQ-silica synthesized according to different protocols. Marshall and Mottola [7], found an adsorption capacity for Cu(II) 0.227 mmol/g. While HQ-silica synthesized according to Pyell et al. [14] showed higher capacity of 0.414 mmol/g Cu(II), 0.248 mmol/g for Ni(II) and 0.333 mmol/g for Zn(II).

For Langmuir model, to determine if the resin is favorable for Hg(II) sorption, a dimensionless separation factor is defined as:

$$R_L = \frac{1}{1 + K_L C_i} \quad (13)$$

Where  $K_L$  (L/mmol) is the Langmuir equilibrium constant and  $C_o$  (mmol/L) is the initial concentration of metal ion. If  $R_L > 1$ , the isotherm is unfavorable;  $R_L = 1$ , the isotherm is linear;  $0 < R_L < 1$ , the isotherm is favorable;  $R_L = 0$  the isotherm is irreversible [53]. The value of  $R_L$  in this study was found to be 0.01, confirming the suitability of the resin for the recovery of Hg(II) ions. Moreover, the low  $R_L$  value  $< 0.1$  implies strong interaction between Hg(II) and 5Ph8HQ.



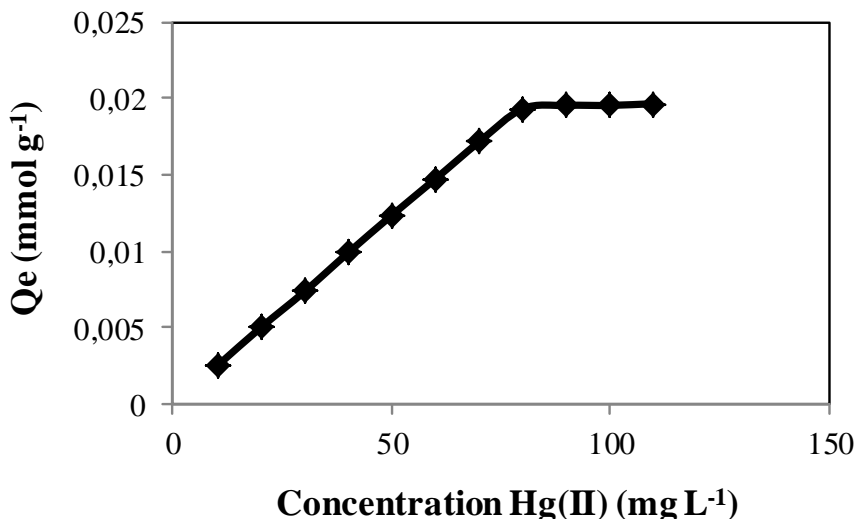


**Figure D.4:** Adsorption profile of Hg(II) as a function of increasing metal concentration. Conditions: [Hg(II)]: 10-160  $\mu\text{g/mL}$ , V(50 mL), pH 4, m(5Ph8HQ): 1g.

#### D.4.5. 5Ph8HQ column extraction of Hg(II)

##### D.4.5.1. Flow rate optimization

The flowrate of Hg(II) solution through the column is an important parameter, in order to ensure sufficient contact time between the sorbent and the adsorbate and to control time of analysis. The flow rate of samples was investigated in the range between 1-5 mL/min. As shown in figure D.5, quantitative recoveries were obtained for flowrates values between 2-3 mL/min. At flowrate >3 ml/min, recoveries drop off to 93 %. Therefore, a flowrate of 2 mL/min was used for the subsequent Hg(II) preconcentration.

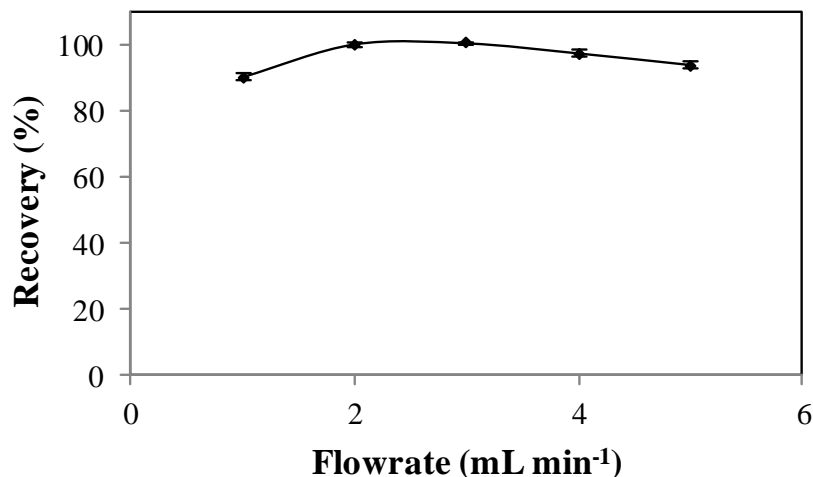


**Figure D.5:** Effect of flowrate mercury by 5Ph8HQ column extraction. Conditions: [Hg(II)]: 2 ng/mL, V(50 mL), pH: 4, eluent: 5 M HCl + 5% CS(NH<sub>2</sub>)<sub>2</sub>/10 mL. Bars represent standard deviation for two replicates.

#### D.3.5.2. Eluent type and volume optimization

Elution of Hg(II) from 5Ph8HQ column was investigated by using different types of eluents, following the general procedure. The results demonstrated in figure D.6, showed that even with a mixture of HCl+HNO<sub>3</sub>, Hg(II) ions have not been completely desorbed. Although the use HCl+HNO<sub>3</sub> as an eluent for metals from 5Ph8HQ was proven to be efficient [22, 23, 54]. This further accentuates the strong affinity of Hg(II) ions towards binding donor atoms (N, O) of 5Ph8HQ.

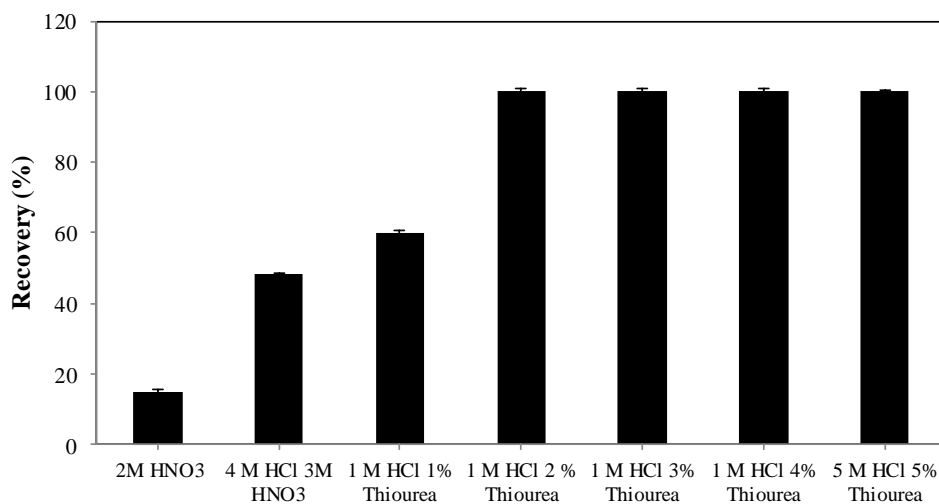


**Figure D.6:** Elution recovery of Hg(II) adsorbed on 5Ph8HQ by column method using different types of eluents. Conditions: [Hg(II)]: 2 ng/mL, V(50 mL), pH: 4, eluent volume: 10 mL. Bars represent standard deviation for two replicates.

In this case, as other studies have reported for the desorption of Hg(II) ions [50, 55], a strong complexing agent for mercury such as thiourea is added to varying concentrations of HCl. The obtained results, show that 1 M HCl mixed with [CS(NH<sub>2</sub>)<sub>2</sub>] ≥ 2 % was shown to be sufficient for quantitative desorption of Hg(II) ions (figure D.6). Eventhough 1 M HCl + 2% CS(NH<sub>2</sub>)<sub>2</sub> was enough for the elution of Hg(II) ions, a larger elution volume of 10 mL was required for stripping off all the target ions. Inorder to achieve higher enrichment factor, 4 mL of 5 M HCl + 5 % CS(NH<sub>2</sub>)<sub>2</sub> was used for complete desorption at an optimized eluent flowrate of 0.5 mL/min (figure D.7).

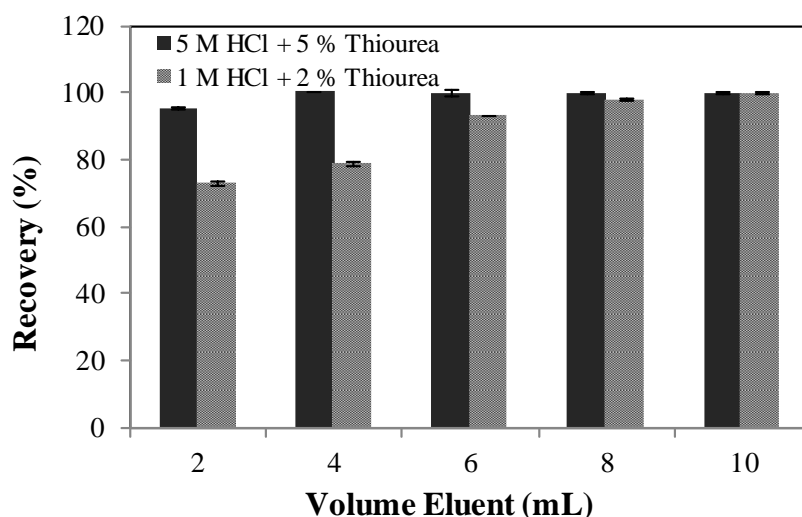


**Figure D.7:** Effect of eluent volume on the recovery of Hg(II) adsorbed on 5Ph8HQ by column method. Conditions: [Hg(II)]: 2 ng/mL, V(50 mL), pH: 4, eluent: 5 M HCl + 5% CS(NH<sub>2</sub>)<sub>2</sub>/ 1 M HCl + 2% CS(NH<sub>2</sub>)<sub>2</sub>. Bars represent standard deviation for two replicates.

#### D.4.5.3. Interferences

As shown in mercury adsorption dynamics section, the coexistence of equimolar metals with Hg(II), can prolong the equilibrium time due to the competition between mercury and other metals towards the relevant binding sites. Therefore, the effect of common interfering ions on the adsorption of Hg(II) ions was examined using batch experiment. For that purpose, 1 g of the studied resin was equilibrated at pH 4 with 1 mg/L of Hg(II) and a certain concentration of the interfering ion. The mixture was shaken at 150 g and aliquots were taken at Hg equilibrium time and analyzed using CV-AFS. Results of table D.9, showed that thousands fold excess of KNaC<sub>4</sub>H<sub>4</sub>O<sub>6</sub>, Na<sub>2</sub>CO<sub>3</sub>, Na<sub>3</sub>C<sub>6</sub>H<sub>5</sub>O<sub>7</sub> and humic acid had minor effect on the extraction of Hg(II) ions in which quantitative recoveries are still attained. Similarly, 10-100 fold excess of anions and major competing metals did not impose significant interferences. Yet, 4000 fold excess of Na<sub>2</sub>C<sub>2</sub>O<sub>4</sub> and KCN have decreased the Hg(II) retention to 94%, 87% respectively. The latter high concentrations of 2-4 g/L are rarely seen in aquatic environments which do not seem to impede the quantitative extraction of mercury from river water matrix.

**Table D.9:** Effects of different electrolytes on the retention of Hg(II) ions.

Electrolytes (cation/anion)	Foreign ion	Recovery (%)
Na <sub>2</sub> CO <sub>3</sub> <sup>a</sup>	0.93	95.49 ± 0.15
Na <sub>3</sub> C <sub>6</sub> H <sub>5</sub> O <sub>7</sub> <sup>a</sup>	2.23	95.99 ± 0.16
KNaC <sub>4</sub> H <sub>4</sub> O <sub>6</sub> <sup>a</sup>	4.36	96.71 ± 0.21
Na <sub>2</sub> C <sub>2</sub> O <sub>4</sub> <sup>a</sup>	4.03	94.22 ± 0.11
KCN <sup>a</sup>	2.62	86.76 ± 0.22
Humic acid <sup>a</sup>	0.42	96.33 ± 0.14
SO <sub>4</sub> <sup>2-</sup> <sup>a</sup>	0.09	97.00 ± 0.37
Cl <sup>-</sup> <sup>a</sup>	0.09	95.96 ± 0.26
NO <sub>3</sub> <sup>-</sup> <sup>a</sup>	0.09	96.98 ± 0.22
F <sup>-</sup> <sup>a</sup>	0.01	94.59 ± 0.14
Co <sup>2+</sup> <sup>a</sup>	0.08	99.1 ± 0.11
Fe <sup>3+</sup> <sup>a</sup>	0.08	97.02 ± 0.91
Ni <sup>2+</sup> <sup>a</sup>	0.08	99.16 ± 0.23
V <sup>4+</sup> <sup>a</sup>	0.08	99.25 ± 0.15
Cu <sup>2+</sup> <sup>a</sup>	0.08	98.35 ± 0.85

a: g L<sup>-1</sup>

#### D.4.5.4. Breakthrough volume

It is determined by using the recommended column procedure as described above, using increasing volumes of Hg(II) solution while keeping the total amount of Hg(II) adsorbed to the column constant at 2 µg. Results have shown that the maximum sample volume can be up to 2000 mL with the attainment of quantitative recovery and relative standard deviation < 12%. The quantitative recovery of Hg(II) ions at high sample volumes is attributed to its high affinity and stability constant with 5Ph8HQ, in which most resins fail in Hg(II) extraction from large volumes [50]. Though, a volume of 2000 mL was shown to extract effectively all target ions, 1000 mL was adopted for Hg(II) preconcentration in order to avoid long periods of extraction time (t>8 hours). Considering 1000 mL as the sample volume and an eluent volume of 4 mL, an enrichment factor of 250 can be achieved.

#### D.4.5.5. Analytical performance and applications

The optimized method was applied for the extraction of trace levels of Hg(II) ions in tap and river water samples. A volume of 1000 mL was spiked with varying quantities of 2 µg and 0.5 µg of Hg(II). Results shown in table D.10, show that Hg(II) spikes were quantitatively extracted from both tap and river water. As shown in pH section of the adsorption dynamics, V(II), Cu(II), Ni(II), Co(II) could be simultaneously extracted with Hg(II) ions at pH 4.

Previous studies, have reported a simultaneous extraction of metals at pH 6-8 [21, 23, 24, 22, 56]. For this purpose, 1000 mL of tap and river water were spiked with 2 µg/L of a multi-element mixture containing V(II), Cu (II), Ni(II), Co(II) and Hg(II) and percolated at pH 4 through 300 mg 5Ph8HQ, eluted using 4 mL of 5 M HCl + 5% CS(NH<sub>2</sub>)<sub>2</sub> and analyzed using ICP-MS for metals and CV-AFS for Hg(II) ions. Table D.10 and D.11, demonstrate simultaneous quantitative extraction of V(II),Cu(II), Ni(II),Co(II) and Hg(II) at pH 4.

The detection limit was calculated according to IUPAC [57], which is three times the standard deviation of eight runs of blank solution (3σ) was 0.21 ng/L for Hg(II) using CV-AFS. The detection limit of ICP-MS was also calculated for V(II), Co(II), Ni(II), Cu(II) 0.28 ng/L, 0.4 ng/L, 1.5 ng/L, 1.1 ng/L respectively. The relative standard deviation (RSD) of 6 runs of 2 ng/mL Hg(II) was lower than 6% indicating a good precision of the analytical method.

**Table D.10:** Analytical results for the determination of Hg(II) in natural water samples by CV-AFS.

Water samples	Concentration µg/L		Recovery (%)
	Added	Found <sup>a</sup>	
Tap water	0	0.774 ± 0.034	
	0.5	1.274 ± 0.082	100
	2	2.769 ± 0.066	99.814
River water	0	0.382 ± 0.069	
	0.5	0.882 ± 0.085	100
	2	2.380 ± 0.055	99.924

<sup>a</sup> The value following "±" is the standard deviation (n=2)

**Table D.11:** Simultaneous determination of metals in natural water samples by ICP-MS at pH 4.

Water samples	Element	Concentration $\mu\text{g/L}$		Recovery (%)
		Added	Found	
Tap water	V	0	0.320 $\pm$ 0.106	
		2	2.315 $\pm$ 0.21	99.79
	Co	0	0.059 $\pm$ 0.004	
		2	2.041 $\pm$ 0.02	99.11
	Ni	0	4.392 $\pm$ 0.037	
		2	6.172 $\pm$ 0.05	96.55
	Cu	0	0.762 $\pm$ 0.137	
		2	2.759 $\pm$ 0.32	99.89
River water	V	0	0.606 $\pm$ 0.428	
		2	2.602 $\pm$ 0.52	99.84
	Co	0	0.041 $\pm$ 0.014	
		2	2.030 $\pm$ 0.05	99.47
	Ni	0	2.964 $\pm$ 0.377	
		2	4.790 $\pm$ 0.52	96.45
	Cu	0	0.066 $\pm$ 0.42	
		2	2.065 $\pm$ 0.32	99.97

<sup>a</sup> The value following " $\pm$ " is the standard deviation (n=2)

## D.5. Conclusion

The optimized method was compared to previously developed analytical techniques for the measurements of trace levels of Hg(II). As can be seen from Table D.12, the preconcentration factor is high in comparison to other methods. Moreover, LOD achieved by CV-AFS is also low as compared to other reported techniques. Even though, the adsorption capacity of the studied resin is considered low, it does not seem to restrict the objectives of the analytical technique developed, i.e. recovery of trace levels of mercury. High adsorption capacities of resins are rather preferable for the removal studies of mercury.

In summary, 5Ph8HQ has been widely used for the preconcentration of trace levels of metals. It has been proven to be robust and exhibiting excellent affinity towards transition elements. However, it has not been examined for the extraction of mercury. Therefore, in this study we have reported the adsorption dynamics of mercury. Results have shown, that it is totally absorbed by 5Ph8HQ within the first 30 minutes contact time with  $t_{1/2}$  5 minutes, following Langmuir adsorption model. At pH 4, the affinity of mercury is unchallenged by other metals

except for Cu(II) which has shown higher K<sub>d</sub> value. With these latter characteristics, 5Ph8HQ was examined for the preconcentration of trace levels of Hg(II). The developed method, showed quantitative recoveries of Hg(II) with LOD= 0.21 pg/mL and RSD= 3-6% using CV-AFS.

**Table D.12:** Comparison of figures of merits for different preconcentration methods for Hg(II) ion.

Chelating resin	DT <sup>a</sup>	pH	Capacity (mmol/g)	LOD <sup>b</sup> (pg/mL)	PF <sup>c</sup>	Ref <sup>d</sup>
<b>1</b> poly(acrylamide) grafted onto cross-linked poly(4-vinyl pyridine) (P4-VP-g-PAm)	AFS	1-8	4.1	2	20	58
<b>2</b> Silica gel/2-Thiophenecarboxaldehyde	AAS	2	2	4.75	1000	59
<b>3</b> Sodium dodecyl sulphate-coated magnetite nanoparticles/Michler's Thioketone complexes	ICP-AES	3	-	40	1230	60
<b>4</b> Magnetic nanoparticles doped with 1,5-diphenylcarbazine	CV-AAS	6	0.22	160	100	61
<b>5</b> Poly-allylthiourea	CV-AAS	2	1.1	80	160	50
<b>6</b> Silica gel/ 2-(2-oxoethyl)hydrazine	ICP-AES	4	0.18	100	50	62
<b>7</b> Polyaniline (PANI)	gold trap-CVAAS	1-12	0.49	0.05	120	63
<b>8</b> Hg(II)-Ionic imprinted polymers-Thymine	AFS	8	0.014	30	200	64
<b>9</b> Silica gel/cysteine	CV-AAS	1-7	0.69	1.5	40	65
<b>10</b> Alumina/ dimethylsulfoxide	AAS	1-2	381	-	1000	66
<b>11</b> C18/ Isoprosyl 2-[(isopropoxycarbothioly)disulfany]ethane thioate	CV-AAS	3-7	0.015	5	>150	67
<b>12</b> Hg(II)-imprinted ion polymer	CV-AAS	8	0.205	50	200	55
<b>13</b> Agar powder modified with 2-mercaptobenzimidazole	CV-AAS	2-3	1.89	20	100	68
<b>14</b> Hg(II)-imprinted thiol-functionalized mesoporous sorbent	ICP-AES	4-8	0.022	390	150	69
<b>15</b> Silica gel immobilized 5-phenylazo-8-hydroxyquinoline	CV-AFS	4	0.027	0.21	>250	This work

<sup>a</sup> Detection technique; <sup>b</sup> Preconcentration factor; <sup>c</sup> Limit of detection; <sup>d</sup> Reference



## D.6. References

- [1] M. Tian, N. Song, D. Wang, X. Quan, Q. Jia, W. Liao, L. Lin, Applications of the binary mixture of sec-octylphenoxyacetic acid and 8-hydroxyquinoline to the extraction of rare earth elements, *Hydrometallurgy* 111–112 (2012) 109–113.
- [2] J. Malamas, M. Bengtsson and G. Johansson, Online trace enrichment and matrix isolation in atomic absorption spectrometry by a column containing immobilized 8-quinolinol in a flow injection system, *Anal. Chim. Acta* 160 (1984) 1-10.
- [3] P. Y. T. Chow, F. F. Cantwell, Calcium Sorption by Immobilized Oxine and Its Use in Determining Free Calcium Ion Concentration in Aqueous Solution, *Anal. Chem.* 60 (1988) 1569-1573.
- [4] M. R. Weaver and J.M. Harris, In-situ fluorescence studies of aluminum ion complexation by 8-hydroxyquinoline covalently bound to silica, *Anal. Chem.* 61 (1989) 1001.
- [5] M. Howard, H.A. Jurbergs, J.A. Holcombe, Comparison of silica-immobilized poly(L-cysteine) and 8-hydroxyquinoline for trace metal extraction and recovery, *J. Anal. At. Spectrom.* 14 (1999) 1209–1214.
- [6] S. Cerutti, M.F. Silva, J. A. Gasquez, R.A. Olsina, L. D. Martinez, Online preconcentration/determination of cadmium in drinking water on activated carbon using 8-hydroxyquinoline in a flow injection system coupled to an inductively coupled plasma optical emission spectrometer, *Spectrochim Acta B* 58 (2003) 43-50.
- [7] M.A. Marshall, H.A. Mottola, Synthesis of Silica- Immobilized 8-Quinotinol with (Amino phenyl)trimethoxysilane, *Anal. Chem.* 55 (1983) 2089-2093.
- [8] J.M.Hill, Silica gel as an insoluble carrier for the preparation of selective chromatographic adsorbents : The preparation of 8-hydroxyquinoline substituted silica gel for the chelation chromatography of some trace metals, *J. Chromatogr.* 76 (1973) 455.
- [9] K.F. Sugawara, H.H. Weetall, G.D. Schucker, Preparation, properties, and applications of 8-hydroxyquinoline immobilized chelate, *Anal. Chem.* 46 (1974) 489-492.
- [11] M.A. Marshall, H.A. Mottola, Performance Studies under Flow Conditions of Silica-Immobilized 8-Quinolinol and Its Application as a Preconcentration Tool in Flow Injection/Atomic Absorption Determinations, *Anal. Chem.* 57 (1985) 729-733.
- [12] J.R. Jezorek, K.H. Faltynski, L.G. Blackburn, P.J. Henderson, H.D Medina, Silica-bound complexing agents: some aspects of synthesis, stability and pore size, *Talanta* 32 (1985) 763-770.
- [13] A. Goswami, A.K. Singh and B. Venkataramani, 8-Hydroxyquinoline anchored to silica gel via new moderate size linker: synthesis and applications as a metal ion collector for their flame atomic absorption spectrometric determination, *Talanta.* 60 (2003) 1141-1154.
- [14] U. Pyell, G. Stork, Preparation and properties of an 8-hydroxyquinoline silica gel, synthesized via mannich reaction, *Fresenius Z Anal Chem.* 342 (1992) 281-286.
- [15] M. Luhrmann, N. Steltera and A.Kettrup, Synthesis and properties of metal collecting phases with silica immobilized 8-Hydroxyquinoline, *Fresenius Z Anal Chem.* 322 (1985) 47-52.
- [16] V.A. Tertykh, V.V. Yanishpolskii and O.Panova, Covalent attachment of some phenol derivatives to silica surface by use of single-stage aminomethylation, *J. Therm. Anal. Calorim* 62 (2000) 545-549.
- [17] W. Zheng, J. Miao, F. S.C. Lee and W.Xiaoru, Synthesis of 8-hydroxyquinoline bonded silica (SHQ) and its application in flow injection inductively coupled plasma mass spectrometry analysis of trace metals in seawater, *Chinese J anal Chem.* 34 (2006) 459-463.

- [18] R.H. Uibel, J.M. Harris, Fiber-optic Raman spectroscopy studies of metal ion complexation by 8-hydroxyquinoline covalently bound to silica surfaces, *Anal.Chem.* 74 (2002) 5112-5120.
- [19] R.H. Uibel, J.M. Harris, Spectroscopic studies of proton-transfer and metal-ion binding of a solution phase model for silica immobilized 8-hydroxyquinoline, *Anal. Chim. Acta* 494 (2003) 105-123.
- [20] M. Hebrant, M. Rose-Helene, A. Walcarius, Metal ion removal by ultrafiltration of colloidal suspensions of organically modified silica. *Colloids and surfaces A: Physicochem. Eng. Aspects* 417 (2013) 65-72.
- [21] R. E. Sturgeon, S.S. Berman, S.N. Willie, J.A.H. Desaulniers, Preconcentration of trace elements from seawater with silica-immobilized 8-hydroxyquinoline, *Anal. Chem.* 53 (1981) 2337-2340.
- [22] J.W. McLaren, A.P. Mykytiuk, S.N. Willie, S.S. Bermann, Determination of Trace Metals in Seawater by Inductively Coupled Plasma Mass Spectrometry with Preconcentration on Silica-immobilized 8-Hydroxyquinoline, *Anal. Chem.* 57 (1985) 2907-2911.
- [23] B.K. Esser, A. Volpe, J.M. Kenneally, D.K. Smith, Preconcentration and Purification of Rare Earth Elements in Natural Waters Using Silica- Immobilized 8-Hydroxyquinoline and a Supported Organophosphorus Extractant, *Anal. Chem.* 66 (1994) 1736-1742.
- [24] S.M. Nelms, G.M. Greenway, R.C. Hutton, Application of Multi-element Time resolved Analysis to a Rapid On-line Matrix Separation System for Inductively Coupled Plasma Mass Spectrometry, *J. Anal. Atom. Spectrom.* 10 (1995) 929-933.
- [25] B.L. Rivas, B. Urbano, S.A. Pooley, I. Bustos, N. Escalona, Mercury and lead sorption properties of poly(ethyleneimine) coated onto silica gel, *Polym. Bull* 68 (2012) 1577-1588.
- [26] S. Lagergren, Zurtheorie der sorgnannten adsorption geloster stoffe, *K. Sven. Vetenskapsakad. Handl.* 24 (1898) 1-39.
- [27] Y.S. Ho, G. Mckay, Pseudo-second order model for sorption processes, *Process Biochem.* 34 (1999) 451-465.
- [28] W.J. Weber, J.C. Morris, Kinetics of adsorption on carbon from solution, *J. Sanit. Eng. Div. Am. Soc. Civ. Eng.* 1963.
- [29] H. Freundlich, Ueber die adsorption in loesungen, *Z.Physik. Chem.* 57 (1907) 385-470.
- [30] H. Dikici, K Salti, Equilibrium and kinetics characteristics of copper(II) sorption into gytija, *Bull. Environ. Contam. Toxicol.* 84 (2010) 147-151.
- [31] M.M. Dubinin, L.V. Raudushkevich, Equation of the characteristics curve of activated charcoal, *Proc. Acad. Sci. Phy. Chem. Sect. U.S.S.R.* 55 (1947) 331-333.
- [32] M.L.Ferreira, M.E. Gschaidler, Theoretical and Experimental Study of Pb<sup>2+</sup> and Hg<sup>2+</sup> Adsorption on Biopolymers, *Macromol. Biosci.* 1 (2001) 233- 248.
- [33] A.W. Adamson, *Physical Chemistry of Surfaces*, fifth ed., Wiley, New York, 1990.
- [34] A.E. Martell, L.G. Sillen, *Stability constants of metal ion complexes*, second ed, Chemical Society, London, 1964.
- [35] D.R. Turner, M. Whitfield, A.G. Dickson, The equilibrium speciation of dissolved components in fresh water and sea water at 25 °C and 1 atm pressure, *Geochim. Cosmochim. Ac* 45 (1981) 855-881.
- [36] W.T.Rees, Fluorimetric Determination of Very Small Amounts of Aluminium, *Analyst* 87 (1962) 202.
- [37] K.L. Yang, S.J. Jiang, T.J. Hwang, Determination of titanium and vanadium in water samples by inductively coupled plasma mass spectrometry with on-line preconcentration. *J. Anal. At. Spectrom.* 11 (1996) 139.
- [38] J.R. Dojlido, G.A. Best, *Chemistry of water and water pollution. Ellis Horwood Series in Water and Wastewater Technology*, (1993) 65-66.

- [39] A. Denizili, K. Kesenci, Y. Arica, E. Peskin, Dithiocarbamate-incorporated monosize polystyrene microspheres for selective removal of mercury ions, *Reat. Funct. Polym.* 44 (2000) 235-243.
- [40] P. Stathi, K. Dimos, M.A. Karakassides, Y. Deligiannakis, Mechanism of heavy metal uptake by a hybrid MCM-41 material: Surface complexation and EPR spectroscopic study, *J. Colloid Interface Sci.* 343 (2010) 374-380.
- [41] V.C. Taty-Costodes, H. Fauduet, C. Porte, A. Delacroix, Removal of Cd(II) and Pb(II) ions from aqueous solutions, by adsorption onto sawdust of *Pinus sylvestris*, *J. Hazard. Mater.* 105 (2003) 121-142.
- [42] M.V. Dinu, E.S. Dragan, Evaluation of Cu<sup>2+</sup>, Co<sup>2+</sup> and Ni<sup>2+</sup> ions removal from aqueous solution using a novel chitosan/clinoptilolite composite: kinetics and isotherms, *Chem. Eng. J.* 160 (2010) 157-163.
- [43] R. D. Shannon, Revised Effective Ionic Radii and Systematic Studies of Interatomic Distances in Halides and Chalcogenides, *Acta Cryst A* 32 (1976) 751-767.
- [44] M. Muresanu, A. Reiss, I. Stefanescu, E. David, V. Parvulescu, G. Renard, V. Hulea, Modified SBA-15 mesoporous silica for heavy metal ions remediation, *Chemosphere* 73 (2008) 1499-1504.
- [45] A. Sayari, S. Hamoudi, Y. Yang, Applications of pore-expanded mesoporous silica.1- Removal of heavy metal cations and organic pollutants from wastewater, *Chem. Mater.* 17 (2008) 212-216.
- [46] H. Irving, R.J.P. Williams, Order of stability of metal complexes, *Nature* 162 (1948) 746-747.
- [47] A. Benhamou, M. Baudu, Z. Derriche, J.P. Basly, Aqueous heavy metals removal on amine-functionalized Si-MCM-41 and Si-MCM-48, *J.Hazard.Mater.* 171 (2009) 1001-1008.
- [48] N. Unlu, M. Ersoz, Adsorption characteristics of heavy metal ions onto low cost biopolymeric sorbent from aqueous solution, *J. Hazard. Mater. B* 136 (2006) 272-280.
- [49] L. Wang, R. Xing, S. Liu, S. Cai, H. Yu, J. Feng, R. Li, P. Li, Synthesis and evaluation of a thiourea-modified chitosan derivative applied for adsorption of Hg(II) from synthetic wastewater, *Int. J. Biol. Macromol* 46 (2010) 524-528.
- [50] W. Qu, Y. Zhai, S. Meng, Y. Fan, Q. Zhao, Y. Fan, Q. Zhao, Selective solid phase extraction and preconcentration of trace mercury(II) with poly-allylthiourea packed columns, *Microchim. Acta* 163 (2008) 277-282.
- [51] O. Hakami, Y. Zhang, C.J. Banks, Thiol-functionalized mesoporous silica-coated magnetite nanoparticles for high efficiency removal and recovery of Hg from water, *Water. Res* 46 (2012) 3913-3922.
- [52] L. Bai, H. Hu, W. Fu, J. Wan, X. Cheng, L. Zhug, L. Xiong, Q. Chen, Synthesis of a novel silica-supported dithiocarbamate adsorbent and its properties for the removal of heavy metal ions, *J. Hazard. Mater.* 195 (2011) 261-275.
- [53] L. Qi, Z. Xu, Lead sorption from aqueous solutions on chitosan nanoparticles, *Colloids Surf. A* 251 (2004) 114-190.
- [54] S.N. Willie, H. Tekgul and R.E. Sturgeon. Immobilization of 8-hydroxyquinoline onto silicone tubing for the determination of trace elements in seawater using flow injection ICP-MS. *Talanta* 47. (1998) 439-445.
- [55] Y. Liu, X. Chang, D. Yang, Y. Guo, S. Meng, Highly selective determination of inorganic mercury(II) after preconcentration with Hg(II)-imprinted diazoaminobenzene-vinylpyridine copolymers, *Anal. Chim. Acta* 538 (2005) 85-91.

- [56] H.Watanabe, K. Goto, S. Taguchi, J.W. McLaren, S.S. Berman and D. S. Russell, Preconcentration of trace elements in sea water by complexation with 8-hydroxyquinoline and adsorption on C18 bonded silica gel, *Anal. Chem.* 53 (1981) 738-739.
- [57] Long, G.L., Winefordner, J.D., 1983. Limit of Detection A Closer Look at the IUPAC Definition. *Anal. Chem.* 55, 712A.
- [58] O. Yayayuruk, E. Henden, N. Bicak. Determination of Mercury(II) in the Presence of Methylmercury after Preconcentration Using Poly(acrylamide) Grafted onto Cross-linked Poly(4-vinyl pyridine): Application to Mercury Speciation, *27 Anal. Sci.* 833.
- [59] E. Soliman, M. Saleh, S. Ahmed, New solid phase extractors for selective separation and preconcentration of mercury (II) based on silica gel immobilized aliphatic amines-2-thiophenecarboxaldehyde Schiff's bases, *Anal. Chim. Acta.* 523 (2004) 133–140.
- [60] M. Faraji, Y. Yamini, M. Rezaee, Extraction of trace amounts of mercury with sodium dodecyl sulphate-coated magnetite nanoparticles and its determination by flow injection inductively coupled plasma-optical emission spectrometry, *Talanta* 81 (2010) 831–836.
- [61] Y. Zhai, S. Duan, Q. He, X. Yang, Q. Han, Solid phase extraction and preconcentration of trace mercury(II) from aqueous solution using magnetic nanoparticles doped with 1,5-diphenylcarbazine, *Microchim. Acta.* 169 (2010) 353–360.
- [62] X. Chai, X. Chang, Z. Hu, Q. He, Z. Tu, Z. Li, Solid phase extraction of trace Hg(II) on silica gel modified with 2-(2-oxoethyl)hydrazine carbothioamide and determination by ICP-AES, *Talanta* 82 (2010) 1791–1796.
- [63] M.V.B. Krishna, D. Karunasagar, S.V. Rao, J. Arunachalam, Preconcentration and speciation of inorganic and methyl mercury in waters using polyaniline and gold trap-CVAAS, *Talanta* 68 (2005) 329–335.
- [64] S. Xu, L. Chena, J. Li, Y. Guan, H. Lu, Novel Hg<sup>2+</sup>-imprinted polymers based on thymine–Hg<sup>2+</sup>–thymine interaction for highly selective preconcentration of Hg<sup>2+</sup> in water samples. *J. Hazard. Mater.* 237–238 (2012) 347–354.
- [65] E.K. Mladenova, I.G. Dakova, D.L. Tsalev, I.B. Karadjova, Mercury determination and speciation analysis in surface waters, *Cent. Eur. J. Chem.* 10 (2012) 1175-1182.
- [66] E.M. Soliman, M.B. Saleh, S.A. Ahmed, Alumina modified by dimethyl sulfoxide as a new selective solid phase extractor for separation and preconcentration of inorganic mercury(II), *Talanta* 69 (2006) 55–60.
- [67] M. Shamsipur, A. Shokrollahi, H. Sharghi, M.M. Eskandari, Solid phase extraction and determination of sub-ppb levels of hazardous Hg<sup>2+</sup> ions, *J. Hazard. Mater. B* 117 (2005) 129–133.
- [68] N.Pourreza, K.Ghanemi, Determination of mercury in water and fish samples by cold vapor atomic absorption spectrometry after solid phase extraction on agar modified with 2-mercaptobenzimidazole, *J.Hazard. Mater. B* 161 (2009) 982–987
- [69] Z. Fan, Hg(II)-imprinted thiol-functionalized mesoporous sorbent micro-column preconcentration of trace mercury and determination by inductively coupled plasma optical emission spectrometry, *Talanta* 70 (2006) 1164–1169.

***Chapitre E: Développement de méthodes analytiques pour la mesure de Hg(II) par complexation directe et extraction en phase solide***

***Chapter E: Analytical method development for the measurement of Hg(II) by direct complexation and subsequent solid phase extraction***

## ***Résumé***

Dans les eaux naturelles, le mercure (Hg) est présent à de très faibles concentrations ce qui rend sa détermination difficile par les techniques analytiques. En conséquence, la préconcentration est requise. L'extraction en phase solide est considérée comme la technique la plus adaptée pour les métaux traces. A la recherche d'une méthode d'analyse simple, rapide et peu coûteuse pour la détermination du Hg(II) dans des les eaux naturelles, une nouvelle méthode d'analyse a été développée basée sur le mécanisme d'échange d'anions en utilisant l'ICP-MS. Cette méthode est fondée sur l'ajout d'une base faible, compte tenu que le mercure dissous est considéré comme un acide faible. Parmi les nombreux ligands étudiés, l'iodure a été choisi pour son efficacité d'extraction du mercure. Il forme des complexes iode-mercure avec une constante de stabilité élevée. En présence de Hg(II), I forme  $\text{HgI}_4^{2-}$  l'espèce la plus stable des complexes iode-mercure. Après l'addition d'un contre-ion, un agent tensio-actif cationique est ajouté ce qui assure la formation de la paire d'ions hydrophobes pour une extraction ultérieure à travers une phase de silice.

Différents paramètres ont été optimisés pour obtenir une extraction optimale du mercure. Les résultats ont démontré que la concentration optimale de I<sup>-</sup> est de 0,01 mol/L. En ce qui concerne le tensioactif cationique, le chlorure de dodécyltriméthylammonium (DTAB) a été choisi en raison de son caractère hydrophobe et ses capacités d'échanges des complexes de métaux, la concentration optimale utilisée est de 0,5 mmol/L. L'extraction de Hg a été jugée stable entre les valeurs de pH entre 3 et 8. Ceci est attribué à la charge positive permanente de DTAB, permettant la formation de sels sous une gamme de pH plus large. Néanmoins, un pH 4 a été choisi pour l'extraction et pour s'assurer de la présence des espèces de mercure ionique libre. Le débit de l'échantillon et l'élution a été ajusté à 2 mL/min et 0,5 mL/min respectivement. Les conditions d'élution permettant le recouvrement maximum, était de 10 mL d'acide nitrique (concentration entre 4-8 mol/L). Un volume de 500 mL d'échantillon est suffisant pour l'analyse et un facteur de préconcentration de 50 peut être obtenu. L'effet des substances interférentes a également été étudié et les résultats ont démontré que la plupart des composés ont montré peu d'interférences avec l'extraction du mercure. Cependant, ces concentrations élevées d'électrolytes ajoutés dans les expériences, sont rarement rencontrées dans des eaux naturelles.

L'optimisation de tous les paramètres a permis d'avoir un recouvrement de 100% pour le mercure dans des les eaux de rivière. La limite de détection (LOD) de la méthode analytique développée est de 8 pg/mL avec un écart type relatif < 5%. La méthode développée présente des avantages par rapport aux autres études utilisant le même principe de formation directe des complexes avec les ions de mercure dans l'eau. Un nombre limité de ligands permet d'atteindre des recouvrements quantitatifs de mercure, i.e. dithiophosphoriques diacyl ester (Monteiro et al, 2001)\* et le 1,4-bis (4-pyridyl) -2,3-diaza-1,3-butadiène (Soleiman et al, 2011)\*\*. Ces ligands exigent une longue et fastidieuse synthèse puisqu'ils ne sont pas commercialisées. Par conséquent, la méthode développée ici est simple, peu couteuse et peut convenable pour des préconcentrations *in situ*. Tous les instruments de mesure peuvent être utilisés, comme ICP-MS qui nous a permis d'atteindre une faible limite de détection et une application effective sur des échantillons dilués.

\*A.C.P. Monteiro, L.S.N. Andrade and R.C. Campos. Fresenius Z Anal Chem. 2001 **371**, 353.

\*\*M. Soleimani, M.S.Mahmodi, A.Morsali, A.Khani and M.G.Afshar, J.Hazard.Mater, 2011,**189**, 371.

### ***Summary***

In natural water samples, mercury (Hg) is present at very low concentrations which render its determination a defying task to most analytical techniques. Therefore, preconcentration is required in which solid phase extraction is chosen as the most adapted technique for metal extraction. In the search of a simple, rapid and cheap analytical method for the measurement of Hg(II) ions in natural water samples, an analytical method was developed based on anion exchange mechanism using ICP-MS. It is based on the addition of a soft base, considering Hg as a soft acid. Among many ligands studied for that purpose, iodide was chosen to be the most efficient for mercury extraction. It forms iodo-mercury complexes with high stability constant overcoming all other tested ligands. In the presence of Hg(II),  $I^-$  forms  $HgI_4^{2-}$  the most stable species of iodo-mercury complexes. After the addition of a counter ion, a cationic surfactant is added which ensures the formation of hydrophobic ion pair for its subsequent extraction on silica phase.

Different parameters were optimized to obtain optimum Hg extraction. Results have demonstrated that the optimal concentration of  $I^-$  was 0.01 mol/L. As for the cationic surfactant, dodecyltrimethylammonium chloride (DTAB) was chosen because of its hydrophobic character and its metal ion complexes exchange capacities. The optimal concentration of DTAB used for the extraction was found to be 0.0005 mol/L. Moreover, Hg extraction was found to be little changed between pH values of 3-8. This attributed to the permanent positive charge of DTAB, permitting the formation of salts under wider pH range. Nevertheless, pH: 4 was chosen for subsequent extraction to assure the presence of free Hg species. Sample flowrate and elution were adjusted at 2 mL/min and 0.5 mL/min respectively. The elution conditions allowing maximum recoveries were 10 mL of nitric acid of a concentration between 4-8 mol/L. Sample breakthrough volume was found to be 500 mL; thereby an enrichment factor of 50 can be obtained. The effect of interfering substances was also studied and results have demonstrated that most substances showed little interferences with the extraction of Hg. However, such high concentrations of the coexisting electrolytes as added in the experiment, are rarely encountered in natural water samples.

The optimization of all possible parameters has allowed a 100 % recovery of mercury ions from river water samples. The limit of detection (LOD) of the developed analytical method is 8 pg/mL and relative standard deviation (RSD) < 5%. The developed method shows advantages over other studies using the same principle of direct complexation of Hg ions in



water samples. In fact, not all ligands succeed in the formation of stable Hg complexes such as 8-hydroxyquinoline. Only few ligands can achieve quantitative recoveries of Hg e.g dithiophosphoric diacyl ester (Monteiro et al, 2001)\* and 1,4-bis(4-pyridyl)-2,3-diaza-1,3-butadiene (Soleiman et al, 2011)\*\*. Such ligands require long and tiresome synthesis that are not necessarily commercialized. Therefore, our developed method is simple, cheap and suitable for *in situ* sampling. All-element analysis instrument i.e. ICP-MS is used in this study, which allowed low LOD and an effective application to diluted samples.

\*A.C.P. Monteiro, L.S.N. Andrade and R.C. Campos. Fresenius Z Anal Chem. 2001 **371**, 353.

\*\*M. Soleimani, M.S.Mahmodi, A.Morsali, A.Khani and M.G.Afshar, J.Hazard.Mater, 2011, **189**, 371.

## **Preconcentration of total mercury in river water by anion exchange mechanism†**

Mirna Daye<sup>1,2</sup>, Baghdad Ouddane<sup>1\*</sup>, Jalal Halwani<sup>3</sup>, Mariam Hamze<sup>1</sup>

<sup>1</sup>*University Lille 1, Géosystèmes, UMR - CNRS 8217, Villeneuve d'Ascq, France.*

<sup>2</sup>*Lebanese University, Water & Environmental Sciences Laboratory, Tripoli, Lebanon*

**\*Corresponding author. Tel.: +33 (0) 3 20 43 44 81**

**E-mail address: Baghdad.Ouddane@univ-lille1.fr**

# Preconcentration of Total Mercury from River Water by Anion Exchange Mechanism

Mirna DAYE,\* Baghdad OUDDANE,\*† Jalal HALWANI,\*\* and Mariam HAMZE\*

\**Université Lille 1, Equipe Chimie Analytique et Marine, UMR-CNRS 8217 Géosystèmes, 59655 Villeneuve d'Ascq Cedex, France*

\*\**Lebanese University, Water & Environmental Sciences Laboratory (L.S.E.E), Lebanon*

A simple and cheap analytical technique was developed for the measurement of total mercury in river water samples using inductively coupled plasma-mass spectrometry (ICP-MS). It is based on the direct complexation of mercury ions using iodide and a cationic surfactant in water for its subsequent solid-phase extraction. Mercury ions are retained on the silica phase as ion pairs in the presence of iodide ions and dodecyltrimethylammonium bromide. Parameters having influential influence on the retention of Hg(II) were investigated: sample flowrate, eluent type, sample volume, iodide and surfactant concentrations. The retained mercury ions are stripped off from silica phase using 10 mL of 8 mol L<sup>-1</sup> HNO<sub>3</sub> and quantified by ICP-MS. An enrichment factor of 50 was achieved with a maximum adsorption capacity of 718 µg Hg(II) g<sup>-1</sup>. The limit of detection of Hg(II) was 8 pg mL<sup>-1</sup>. The developed method was applied for the determination of total mercury in river and tap-water samples.

**Keywords** Solid phase extraction, anion exchange, silica, mercury, ICP-MS

(Received July 8, 2013; Accepted August 30, 2013; Published October 10, 2013)

## Introduction

Mercury is one of the most toxic environmental pollutants due to its bioaccumulative character in the food chain *via* its organic form (methylmercury). The major anthropogenic sources of mercury pollution are coal-fired power plants, cement kilns, chlor-alkali plants, gold mining and batteries. Most modern analytical techniques do not succeed in the detection of mercury in natural water due to its low concentration. Preconcentration becomes a necessity to meet the detection limit of the analytical technique used. Among numerous preconcentration techniques, solid phase extraction (SPE) is the well adapted for the preconcentration of mercury from aqueous samples.<sup>1</sup> There are two methods for the SPE of metals from water matrix. The first is the direct addition of a ligand into the sample and its percolation through the solid phase.<sup>2</sup> The second method requires the immobilization of a ligand on the solid matrix used through a well-defined synthetic procedure.<sup>3</sup> Then, the aqueous sample can be preconcentrated through the synthesized resin. The second method offers a stronger resin capable of the formation of stable metal complexes with resin that is evidenced by a high preconcentration factor.<sup>4</sup> However, the immobilization method is exhaustive, and demands precautions while synthesizing the resin to eliminate cross-contamination. As compared to the second method, the first one is simple, rapid and easy. Nevertheless, not all ligands succeed in the formation of stable metal chelates with high-stability constants, such as 8-hydroxyquinoline.

The retention of metal ions on the solid matrix can be either by simple adsorption, chelation or ionic exchange. There are studies that developed methods for the retention Cd-chelates on the silica phase. It is based on the formation of anionic metal species in the aqueous phase. Also, by the anion-exchange mechanism with quaternary ammonium salts, metal chelates are readily adsorbed on the silica matrix.<sup>5,6</sup> Mercury is considered as soft acid, which makes its complexation with anionic soft bases possible. Its adsorption on silica phase is ensured by the formation of hydrophobic ion pairs with a suitable counter cation. By anion exchange mechanism, the anionic metal complexes are transformed to ion pairs in the presence of a cationic surfactant.

The aim of this study is to develop a simple, cheap and efficient method for the *in situ* extraction of total mercury from river-water samples and analysis using inductively coupled plasma-mass spectrometry (ICP-MS). Mercury ions in the sample form iodo-mercury complexes (HgI<sub>4</sub><sup>2-</sup>) with iodide. In the presence of an anion exchanger dodecyltrimethyl ammonium chloride (DTAB), the iodo-mercury complexes form ion pairs, [HgI<sub>4</sub><sup>2-</sup>][DTA<sup>+</sup>]<sub>2</sub>. The hydrophobic ion pair is adsorbed on the silica-phase column. Mercury ions are desorbed from the solid phase using nitric acid, and determined by ICP-MS. In this method, total mercury in river samples could be preconcentrated *in situ* on silica columns. Thus, mercury ions are directly preserved at the sampling field without the need of large-volume water sampling and preservation techniques, which could risk a deterioration of Hg contents in the sample. Besides, the solid-phase extraction of minute concentrations of Hg(II) had made the analysis possible with such techniques as ICP-MS other than the known sensitive CV-AFS and CV-AAS.

† To whom correspondence should be addressed.  
E-mail: baghdad.ouddane@univ-lille1.fr

Table 1 Operating conditions ICP-MS

Forward Power/W	
Nebuliser Gas Flow/L min <sup>-1</sup>	1050
Auxiliary Gas Flow/L min <sup>-1</sup>	0.7
Cool Gas Flow/L min <sup>-1</sup>	0.95
Quartz Plasma Torch/mm	13.5
Cone type	1.5
Glass Impact Bead	Pt
Spray Chamber temperature/°C	3
Nebulizer type	Concentric glass
Sample Uptake Rate/mL min <sup>-1</sup>	1
Uptake delay/s	35
Washout delay/s	150
Analyte	<sup>202</sup> Hg

## Experimental

### Reagents and apparatus

Analytical reagent-grade chemicals were used and obtained from Sigma Aldrich (France). Ultra-pure water was used for preparing the reagent solutions. An inorganic mercury (Hg<sup>2+</sup>) stock solution (1000 mg L<sup>-1</sup>) was prepared from mercuric chloride (Merck). Buffer solutions were prepared from 1 M sodium acetate, and the pH was adjusted to the desired pH value by adding different volumes of 1 M HNO<sub>3</sub>.

An inductively coupled plasma mass spectrometer, Thermo-Optek X7 (Thermo Fischer Scientific, USA), equipped with a cross-flow pneumatic nebulizer, a concentric glass-type nebulization chamber and a 1.5 mm i.d. quartz plasma torch, was used. All of the operating parameters were those recommended by the manufacturer. The optimum operating conditions and measurement parameters for ICP-MS are listed in Table 1. Measurements were performed with high-purity Argon gas. The pH measurements and adjustments were conducted by a pH meter, calibrated using two standard buffer solutions of pH 4 and 7. The flow rate of the samples was adjusted using a Gilson Miniplus 3 peristaltic pump. PVC tubes (3.18 i.d.) were used for the preconcentration process. Self-made PTFE (polytetrafluoroethylene) columns (65 × 4 mm i.d.) were used for packing the examined adsorbent.

### General extraction procedure

River water was used throughout the optimization procedure. For that, river-water samples were filtered through a 0.45 µm pore size Millipore filter and acidified by nitric acid (0.5% v/v), and frozen till used.

Home-made silica phase columns were fabricated. For that purpose, a batch of silica gel (100 - 200 mesh) was activated by passing successively 20 mL/1 g silica methanol, 20 mL/1 g silica ultrapure water, 20 mL/1 g silica 2 mol L<sup>-1</sup> nitric acid, 20 mL/1 g silica ultrapure water, 5 mL/1 g silica methanol, 10 mL/1 g silica ultrapure water. Then 1 g of activated silica phase was packed in PTFE column (6 mL volume, 4.0 mm i.d., 60 mm length) and sealed with glass wool at both ends. Suitable 50 mL river water was spiked with a final concentration 0.04 µg mL<sup>-1</sup>, 0.01 mol L<sup>-1</sup> KI, 0.0005 mol L<sup>-1</sup> DTAB. The river-water samples were left to stabilize for 1 h, and then passed through the column at a flow rate of 2 mL min<sup>-1</sup> using a peristaltic pump. The retained analytes were desorbed from silica phase by using 8 mol L<sup>-1</sup> nitric acid at a flow rate of 0.5 mL min<sup>-1</sup>.

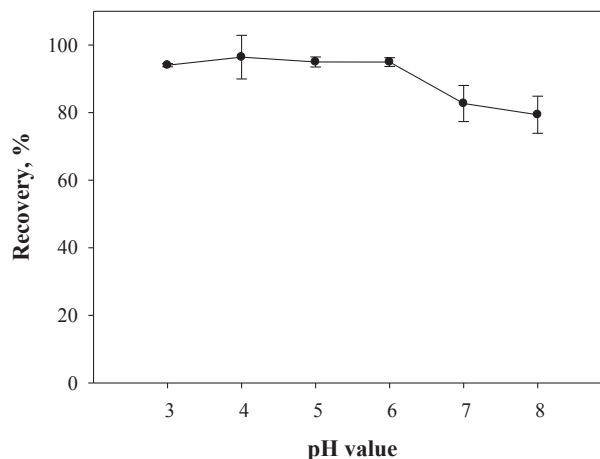
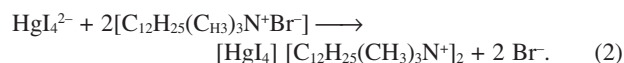
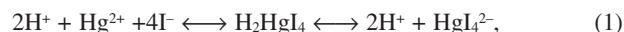


Fig. 1 Effect of pH on the retention of [HgI<sub>4</sub><sup>2-</sup>][DTA<sup>+</sup>] on silica gel. Conditions: 2 µg Hg(II) 50 mL<sup>-1</sup>; flow rate, 2 mL min<sup>-1</sup>; [I<sup>-</sup>], 0.01 mol L<sup>-1</sup>; [DTAB], 0.0005 mol L<sup>-1</sup>; [HNO<sub>3</sub>], 10 mL/4 mol L<sup>-1</sup>/0.5 mL min<sup>-1</sup>.

## Results and Discussion

### Effect of the pH

Mercury ions form iodo-mercury complexes in the presence of iodide ions (Eq. 1). The addition of quaternary ammonium salts forms a hydrophobic ion pair with anionic metal complexes (Eq. 2) that assure its adsorption on the silica matrix:



One of the most influential factors affecting the adsorption of metals is the pH value of the water sample. For that reason, different pH values in the range of 3 - 8 were tested in order to obtain the optimum extraction of mercury ions. As observed in Fig. 1, the pH values examined are shown not to significantly influence the extraction efficiency with the optimum recovery reaching 95% at pH 4. Moreover, the extraction of mercury ions decreases slightly to 82% for pH > 4. For the following optimization experiments, pH 4 of the sample solution was adopted. The extraction of mercury ions was found to be unchanged in the tested pH range. This is attributed to the nature of quaternary ammonium salts with permanent positive charge, which enables it to form salts with different anions over a wider pH range than primary, secondary and tertiary amines.<sup>7</sup> Unlike quaternary amines, triisooctylamine (TIOA) is pH-dependent. At low pH values, TIOA can form an amine mineral salt acid, which has been shown to be the most efficient for the extraction of metals.<sup>8</sup>

### Effect of the flow rate

The flow rate of the sample is another factor affecting the adsorption of the metal chelate on the silica phase, thus controlling the time of analysis. As a result, different water samples are passed through the column at different flowrates (1 - 5 mL min<sup>-1</sup>) controlled by a peristaltic pump. As can be seen in Fig. 2, the sample flowrate does not seem to considerably influence the extraction of mercury ions. A flowrate of 2 mL min<sup>-1</sup> was selected for further experiments. The eluent flowrate is another parameter that affects the desorption of the

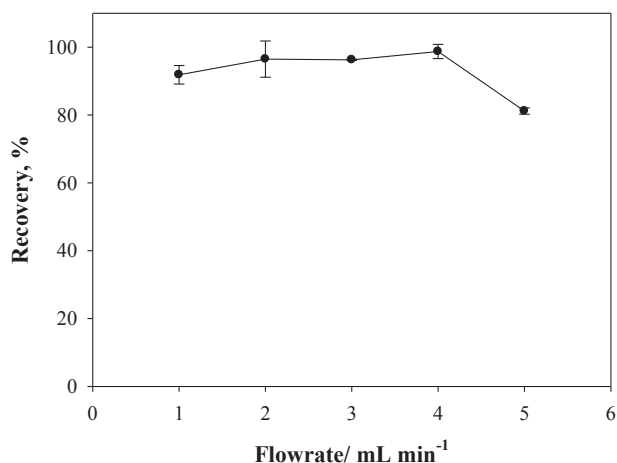


Fig. 2 Effect of the flowrate on the retention of  $[\text{HgI}_4]^{2-}[\text{CTA}^+]$  on silica gel. Conditions:  $2 \mu\text{g Hg(II)}$   $50 \text{ mL}^{-1}$ ; pH, 4;  $[\text{I}^-]$ ,  $0.01 \text{ mol L}^{-1}$ ;  $[\text{DTAB}]$ ,  $0.0005 \text{ mol L}^{-1}$ ;  $[\text{HNO}_3]$ ,  $10 \text{ mL}/4 \text{ mol L}^{-1}/0.5 \text{ mL min}^{-1}$ .

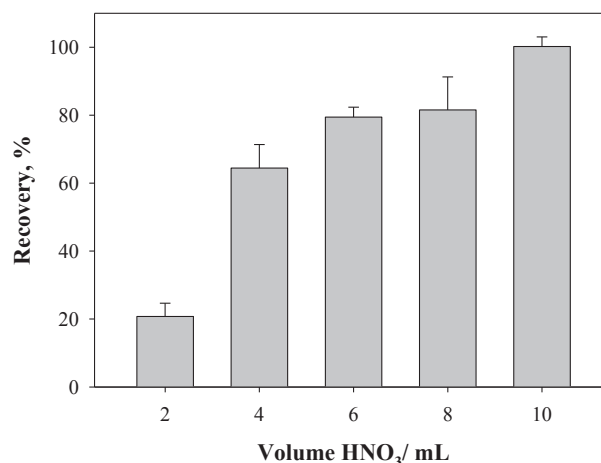


Fig. 3 Effect of the  $\text{HNO}_3$  volume on the desorption of  $\text{Hg(II)}$  ions from the silica phase. Conditions:  $2 \mu\text{g Hg(II)}$   $50 \text{ mL}^{-1}$ ; pH, 4; flow rate,  $2 \text{ mL min}^{-1}$ ;  $[\text{I}^-]$ ,  $0.01 \text{ mol L}^{-1}$ ;  $[\text{DTAB}]$ ,  $0.0005 \text{ mol L}^{-1}$ ;  $[\text{HNO}_3]$ ,  $8 \text{ mol L}^{-1}/0.5 \text{ mL min}^{-1}$ .

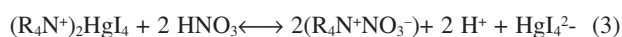
Table 2 Effect of different concentrations of the eluent on the extraction of mercury

	Eluent	Extraction, %	
Concentration $\text{HNO}_3/$ mole $\text{L}^{-1}$	0.5	$4.3 \pm 1.1$	
	1	$8.3 \pm 1.5$	
	2	$32.1 \pm 0.3$	
	3	$63.8 \pm 4.8$	
	4	$96.7 \pm 5.3$	
	5	$97.7 \pm 2.8$	
	6	$98.2 \pm 2.1$	
	8	$104.6 \pm 1.5$	
	9	$88.7 \pm 2.2$	
	10	$89.1 \pm 1.1$	
	14	$90.2 \pm 1.2$	
	Concentration $\text{HCl}/\text{mole}$ $\text{L}^{-1} + \text{CS}(\text{NH}_2)_2, \%$	0.5 + 0.5	$84.4 \pm 2.4$

retained analytes. Therefore, the influence of the eluent flowrate on the extraction of mercury ions was also studied. It was found that  $0.5 \text{ mL min}^{-1}$  was sufficiently low to ensure the maximum desorption of mercury ions from the silica phase.

#### Effect of the eluent type & volume

Since numerous sorbents form strong bonds with  $\text{Hg(II)}$ , it becomes a challenging task to elute mercury ions. High concentrations of  $\text{HNO}_3$ ,  $\text{HCl}$  were insufficient for a quantitative elution of  $\text{Hg(II)}$ . Only acidified thiourea by  $\text{HCl}$  was able to complete elution.<sup>9</sup> As a result,  $10 \text{ mL}$  of  $0.5 \text{ mol L}^{-1}$   $\text{HCl}$  and  $0.5\%$  thiourea was examined, and showed an  $84\%$  recovery of mercury ions, which is comparable to elution with  $4 \text{ mol L}^{-1}$   $\text{HNO}_3$ . Consequently, the elution conditions were studied by varying the concentration of nitric acid. In the desorption reaction,  $\text{NO}_3^-$  is interchanged with  $\text{HgI}_4^{2-}$  in an acidic medium (Eq. 3). The obtained results given in (Table 2) showed that  $10 \text{ mL}$  of  $4 - 8 \text{ mol L}^{-1}$   $\text{HNO}_3$  allowed a quantitative elution of mercury ions.



The volume of the eluent should also be examined to guarantee complete elution of the analytes. Thereby,  $10 \text{ mL}$  of  $8 \text{ mol L}^{-1}$

Table 3 Ligands tested for  $\text{Hg(II)}$  extraction

Ligand	Recovery Hg, %
$\text{I}^-$	$102.5 \pm 4.2$
$\text{CS}_2^-$	$42.9 \pm 0.06$
$\text{SCN}^-$	$44.6 \pm 2.9$
$\text{O}_6\text{S}_4^{2-}$	$40.9 \pm 1.8$
$\text{Cl}^-$	$20.1 \pm 1.3$
$\text{Br}^-$	$10.2 \pm 1.5$

Table 4 Stability constant for different ligands at  $25^\circ\text{C}$  and  $1(\text{NaClO}_4)$  as ionic medium<sup>10</sup>

Ligand	Log K
$\text{I}^-$	29.3
$\text{SCN}^-$	27.9
$\text{Cl}^-$	6.7
$\text{Br}^-$	1.6

$\text{HNO}_3$  was passed through the column in five aliquots. The results given in Fig. 3, show that a volume of  $10 \text{ mL}$  allowed the recovery of  $100\%$  of the mercury ions.

#### Ion pair formation

Based on HSAB theory, soft metals like mercury form adducts with soft bases. To investigate the efficiency of complex formation with anionic bases, different ligands were examined for that purpose. The results given Table 3 show that the iodide- $\text{Hg}$  complex has the capacity of hydrophobic complex formation with a counter ion, allowing its adsorption on the silica phase. This is attributed to the high stability constant of the iodide- $\text{Hg}$  complex, which overcomes all other tested ligands (Table 4).

The effect of the iodide concentration on mercury extraction was also examined by varying the concentration of iodide ions from  $0.005 - 0.1 \text{ mol L}^{-1}$ . It was noteworthy that the iodide concentration had an influential role on  $\text{HgI}_4^{2-}$  formation. Thus, it is evident from Fig. 4 that as the concentration of  $\text{I}^-$  increased from  $0.005$  to  $0.1 \text{ mol L}^{-1}$ , the extraction efficiency with  $\text{DTAB}$  increased from  $63$  to  $100\%$ . However, beyond  $0.1 \text{ mol L}^{-1}$  the

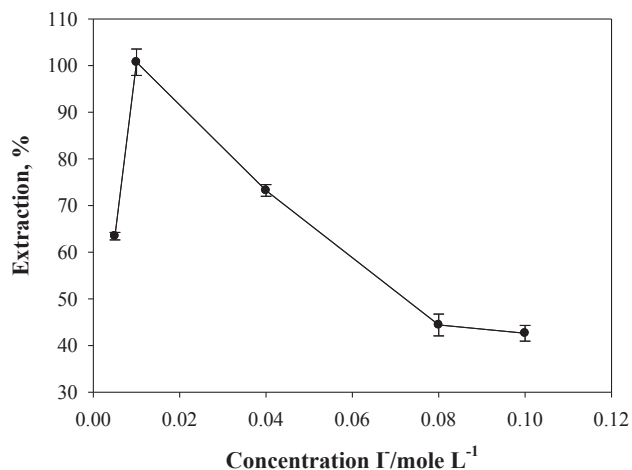


Fig. 4 Effect of the iodide concentration on the adsorption of  $[\text{HgI}_4^{2-}][\text{DTA}^+]$  Hg(II) on the silica phase. Conditions:  $2 \mu\text{g Hg(II)}$   $50 \text{ mL}^{-1}$ ; pH, 4; flow rate,  $2 \text{ mL min}^{-1}$ ; [DTAB],  $0.0005 \text{ mol L}^{-1}$ ;  $[\text{HNO}_3]$ ,  $10 \text{ mL}/8 \text{ mol L}^{-1}/0.5 \text{ mL min}^{-1}$ .

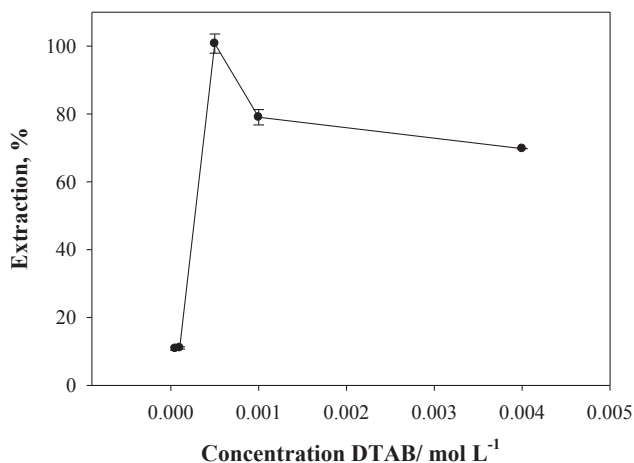


Fig. 5 Effect of the DTAB concentration on the adsorption of  $[\text{HgI}_4^{2-}][\text{DTA}^+]$  on the silica phase. Conditions:  $2 \mu\text{g Hg(II)}$   $50 \text{ mL}^{-1}$ ; pH, 4; flow rate,  $2 \text{ mL min}^{-1}$ ;  $[\text{I}^-]$ ,  $0.01 \text{ mol L}^{-1}$ ;  $[\text{HNO}_3]$ ,  $10 \text{ mL}/8 \text{ mol L}^{-1}/0.5 \text{ mL min}^{-1}$ .

recovery of mercury ions dropped off to 42% when the concentration of  $\text{I}^-$  increased to  $0.08 \text{ mol L}^{-1}$ . This can be explained by competition between  $\text{I}^-$  and  $\text{HgI}_4^{2-}$  for DTAB, and the saturation of the silica phase with the  $[\text{I}^-][\text{DTA}^+]$  ion pair.

There are many reasons to consider amines as being powerful extractants for mercury. Being a soft metal, mercury tends to form strong complexes with ligands particularly containing nitrogen, sulphur electron donor atoms. Moreover, metal cations in strong electrolytic solutions form anionic complexes with halides.<sup>11</sup> High-molecular-weight quaternary amines are an efficient anion exchanger for anionic metal complexes.<sup>8</sup> There is a large repertory of quaternary ammonium salts, from methyltriethylammonium chloride, aliquat 336 (tri-octyl methylammonium chloride), alamine 336 (tri-octyl amine), cetyltrimethylammonium bromide and Primene JMT (1,1,3,3,5,5,7,7,9,9-decamethyl decyl amine), all used as counter ions for the extraction of anionic metal complexes.<sup>5,6,12</sup> Quaternary ammonium salts are readily adsorbed on hydrophobic

Table 5 Effect of electrolytes on the adsorption of  $2 \text{ ng mL}^{-1}$  of Hg(II)

Interferents	Foreign ion/ $\mu\text{g mL}^{-1}$	Recovery, %
$\text{F}^-$	0.2	$100 \pm 1.2$
$\text{K}^+$	1	$100 \pm 0.5$
$\text{Al}^{3+}$	0.1	$96.15 \pm 1.1$
$\text{Na}_2\text{C}_2\text{O}_4$	51.7	$96.00 \pm 1.4$
KCN	77	$94.84 \pm 0.6$
$\text{NO}_3^-$	3	$93.17 \pm 0.4$
$\text{KNaC}_4\text{H}_4\text{O}_6$	12.7	$92.78 \pm 0.8$
$\text{Na}^+$	8	$91.20 \pm 2.1$
$\text{Na}_3\text{C}_6\text{H}_5\text{O}_7$	70.2	$89.55 \pm 1.3$
$\text{Mg}^{2+}$	10	$89.56 \pm 0.6$
$\text{Ca}^{2+}$	30	$87.50 \pm 0.9$
$\text{SO}_4^{2-}$	60	$86.97 \pm 0.7$
$\text{Na}_2\text{CO}_3$	31.6	$83.99 \pm 1.4$
Humic acid	13.1	$70.91 \pm 0.8$

sorbents, like the silica phase.<sup>13</sup> This hydrophobic character of the surfactant is attributed to its high molecular weight. Therefore, the effect of the DTAB concentration was studied by varying its concentration in the range of  $5.10^{-5}$  –  $4.10^{-3} \text{ mol L}^{-1}$  (Fig. 5). The extraction of  $\text{HgI}_4^{2-}$  becomes quantitative with a DTAB concentration of  $5.10^{-4} \text{ mol L}^{-1}$ . Beyond that concentration, the recovery of mercury ions decreases slightly to reach 79%. High concentrations of the surfactant tend to saturate the silica phase column, contributing to a low extraction of  $\text{HgI}_4^{2-}$ . Thereby, for subsequent extraction, concentrations of  $5.10^{-4} \text{ mol L}^{-1}$  and  $0.01 \text{ mol L}^{-1}$  of  $\text{I}^-$  were used.

#### Effect of coexisting interferences

The effect of different interferences on the adsorption of  $\text{HgI}_4^{2-}$  on a silica column was studied (Table 5). Various interfering species are examined based on their potential presence in natural river water. Anions like  $\text{SO}_4^{2-}$ ,  $\text{NO}_3^-$  were tested for their potential interferences in complexing mercury ions acting as ligands. Major cations *i.e.*  $\text{Mg}^{2+}$ ,  $\text{Ca}^{2+}$  were also examined for their potential competition with mercury ions to form stable complexes with iodide using the developed analytical method. The likely presence of organic ligands such as humic acid, oxalic acid, etc. in river water emphasizes the importance of examining their effects on the extraction of mercury ions acting as powerful complexing agents for mercury. Ligands such as thiocyanate and citrate could be anthropogenically present in river water due to urban and agricultural effluents as it seems the case of most rivers around the world. Concentrations of interfering substances are chosen on the basis of their natural occurrence in natural river water or/and river water affected by urban effluents and agricultural runoffs.

A solution of  $2 \mu\text{g L}^{-1}$  containing the optimized concentration of  $\text{I}^-$  and DTAB and the added interfering substance was passed through a silica column. The results given in Table 5 showed that most substances interfered in the recovery of mercury ions. A 50-fold  $\text{Al}^{3+}$ , 160-fold  $\text{Na}_2\text{C}_2\text{O}_4$  have decreased the extraction of mercury ions to 96%. A 150 – 4000-fold KCN,  $\text{NO}_3^-$ ,  $\text{KNaC}_4\text{H}_4\text{O}_6$ ,  $\text{Na}^+$ ,  $\text{Na}_3\text{C}_6\text{H}_5\text{O}_7$  have reduced the extraction of mercury ions to 91 – 95%. A 3000 – 500-fold  $\text{Ca}^{2+}$ ,  $\text{Na}_2\text{CO}_3$ ,  $\text{SO}_4^{2-}$ ,  $\text{Mg}^{2+}$  decreased the extraction to 84 – 89%. A 650-fold humic acid has the most substantial influence on mercury ions extraction, which diminishes to 70.9%.

The effect of heavy metals on the adsorption of mercury ions was also investigated (Table 6). A binary metal mixture was passed through the column under the optimized conditions.

Table 6 Single metals competition in binary element mixture

Metal	Foreign ion/ $\mu\text{g mL}^{-1}$	Recovery, %
Mn <sup>2+</sup>	3	100 $\pm$ 0.2
Pb <sup>2+</sup>	3	98.36 $\pm$ 0.5
Zn <sup>2+</sup>	3	94.98 $\pm$ 1.2
Ni <sup>+</sup>	3	94.40 $\pm$ 1.3
Co <sup>2+</sup>	3	93.67 $\pm$ 0.9
Fe <sup>3+</sup>	3	85.67 $\pm$ 1.1
Cu <sup>2+</sup>	3	85.95 $\pm$ 0.6
V <sup>2+</sup>	3	83.16 $\pm$ 1.5
Cd <sup>2+</sup>	3	72.25 $\pm$ 1.1

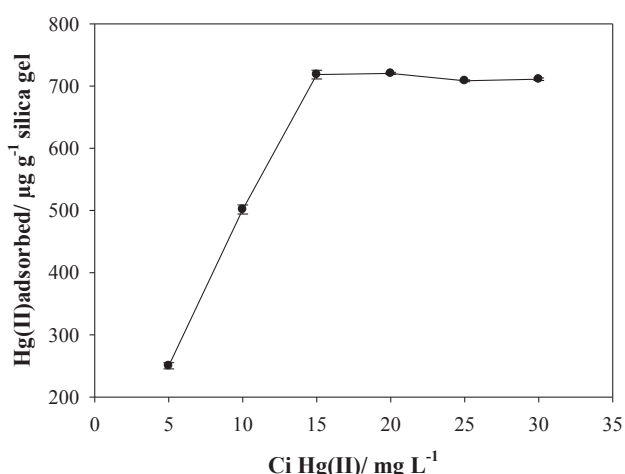


Fig. 6 Maximum adsorption capacity of 1 g of the silica phase. Conditions: pH, 4; flow rate, 2 mL min<sup>-1</sup>; [I<sup>-</sup>], 0.01 mol L<sup>-1</sup>; [DTAB], 0.0005 mol L<sup>-1</sup>; [HNO<sub>3</sub>], 10 mL/8 mol L<sup>-1</sup>/0.5 mL min<sup>-1</sup>.

Mainly, the adsorption of metals depends on many factors, such as the pH, temperature, sorbent dose and metal concentration. Moreover, other factors can considerably vary the adsorption of metals, such the presence of a competitive metal ion, which can either promote or decrease the sorption.<sup>14</sup> The competition of the coexisting metal depends on its stability constant with the functional groups of the adsorbent and metal ion to the charge radius ( $Z/r$ ). In the ion-exchange mechanism, the adsorption depends on the metal charge-to-radius ratio ( $Z/r$ ).<sup>15</sup> The results show that, 15-fold Cd(II) had the most potent effect on the Hg(II) adsorption among all of the examined metals, which decreased the extraction to 72%. Therefore, the results may vary from the predicted behaviour of the metals based on the ( $Z/r$ ) ratio. This difference sets off other factors, like the experimental conditions (anion exchange) and the sorbent properties. The competitive adsorption between cadmium and mercury was also found by Dalali *et al.*<sup>6</sup> but with a higher tolerance concentration for mercury.

This significant decrease in the retention of mercury ions is due to either competition between the soft metals to form a complex with iodide ions, or the competition of other ligands to form complexes with the Hg(II) ion. Normally, high concentrations of interfering substances are not encountered in natural water, which is manifested by a high recovery of HgI<sub>4</sub><sup>2-</sup> with DTAB on the silica phase using a river water matrix.

#### Adsorption capacity

The adsorption capacity of the silica phase is the amount of

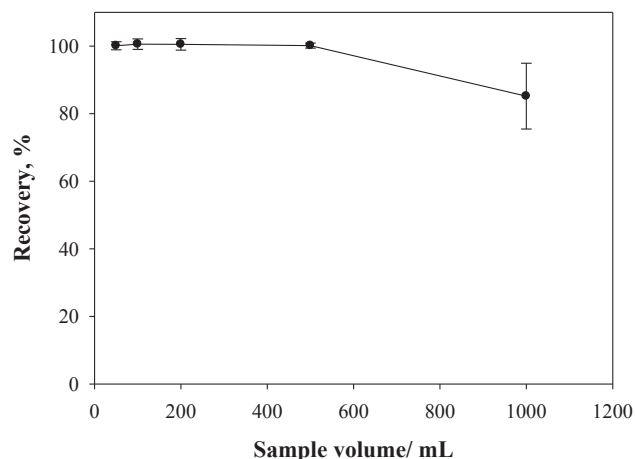


Fig. 7 Effect of the sample volume on the retention of [HgI<sub>4</sub><sup>2-</sup>][DTA<sup>+</sup>] on the silica gel. Conditions: 2  $\mu\text{g Hg(II) V mL}^{-1}$ ; pH, 4; flow rate, 2 mL min<sup>-1</sup>; [I<sup>-</sup>], 0.01 mol L<sup>-1</sup>; [DTAB], 0.0005 mol L<sup>-1</sup>; [HNO<sub>3</sub>], 10 mL/8 mol L<sup>-1</sup>/0.5 mL min<sup>-1</sup>.

Table 7 Analytical results for the determination of Hg(II) in natural water samples

Water samples	Concentration Hg(II)/ $\mu\text{g L}^{-1}$		Recovery, %
	Added	Found <sup>a</sup>	
River water	0	0.4897 $\pm$ 0.07	100
	2	1.49 $\pm$ 0.21	
Tap water	0	0.102 $\pm$ 0.12	100
	2	1.1 $\pm$ 0.11	

a. The value following “ $\pm$ ” is the standard deviation ( $n = 3$ ).

sorbent needed to quantitatively adsorb a specific amount of the [HgI<sub>4</sub><sup>2-</sup>][DTA<sup>+</sup>]<sub>2</sub> ion pair. Different volumes of Hg(II) solutions with different concentrations in the range of 5 – 30 mg L<sup>-1</sup> were percolated through 1 g of the silica phase. Variations in the adsorption of mercury ions were measured as shown in Fig. 6. The adsorption capacity of the [HgI<sub>4</sub><sup>2-</sup>][DTA<sup>+</sup>]<sub>2</sub> ion pair on silica phase was found to be 718  $\mu\text{g/1 g}$  of silica.

#### Breakthrough volume

It is important to determine the maximum sample volume while allowing the enrichment of low concentrations of mercury ions from large volumes. For this purpose, different volumes (50, 100, 200, 500 and 1000 mL) containing the same amount of 2  $\mu\text{g}$  of Hg(II) ions were percolated through 1 g of the silica phase at the optimum flow rate (Fig. 7). The maximum applicable volume that allowed a quantitative retention of mercury ions was 500 mL, and at greater volume the recovery drops off significantly. The breakthrough volume was up to 1000 mL for the retention of Cd<sup>2+</sup>;<sup>5,6</sup> however, lower breakthrough volumes were determined for Hg(II) ions. This can be attributed to the more stable complex formation of CdI<sub>4</sub><sup>2-</sup> than HgI<sub>4</sub><sup>2-</sup> with quaternary ammonium salts. Considering the final elution volume of 10 mL, the preconcentration factor (PF) becomes 50.

#### Analytical performance and applications

The detection limit (LOD) was calculated according to IUPAC,<sup>16</sup> which is three-times the standard deviation of eight runs of the blank solution ( $3\sigma$ ), which was 0.008  $\mu\text{g L}^{-1}$ . The

Table 8 Comparison of figures of merits for different preconcentration methods for Hg(II) ion

Chelating resin	pH	Adsorption capacity/mg g <sup>-1</sup>	LOD <sup>a</sup> /pg mL <sup>-1</sup>	PF <sup>b</sup>	Ref. <sup>c</sup>
<b>Poly(acrylamide)</b> grafted onto cross-linked poly(4-vinyl pyridine) (P4-VP-g-PAm)	1 – 8	817	2	20	[18]
<b>Silica gel</b> functionalized diphenylthiocarbazon	5 – 6	49	—	200	[19]
<b>Poly-allylthiourea</b>	2	227	80	160	[20]
<b>Silica gel</b> functionalized 2-(2-oxoethyl)hydrazine carbiothioamide	4	37.5	100	50	[ 9]
<b>Polyaniline</b> (PANI)	1 – 12	100	0.05	120	[21]
<b>C18</b> modified sodium diethyldithiocarbamate	3 – 8	—	5.2	50	[22]
<b>Silica gel</b> /cysteine	1 – 7	140	1.5	40	[23]
<b>Alumina</b> modified dimethylsulfoxide	1 – 2	381	—	100	[24]
<b>C18</b> modified hexiathia-18-crown-6-tetraone	1 – 7	24.1	6	75	[25]
<b>Silica gel</b> functionalized dithizone	7	60.2	—	200	[26]
<b>Silica gel</b> functionalized aminopropylbenzoylazo-2-mercaptobenzothiazole	0 – 6	8.3	—	111	[27]
<b>XAD-2</b> functionalized 2-(methylthio)aniline	3 – 7	37.9	28	300	[28]
<b>Sulfur</b> loaded <i>N</i> -(2-chloro benzoyl)- <i>N</i> -phenylthiourea	2 – 3	—	3	333	[29]
<b>Agar</b> powder modified with 2-mercaptobenzimidazole	2 – 3	0.049	20	100	[30]
<b>Mesoporous silica</b> functionalized Hg(II)-imprinted thiol- sorbent	4 – 8	4.46	390	150	[ 4]
<b>C18</b> modified dithizone	4	—	150	200	[31]
<b>C18, I<sup>-</sup>, DTAB</b>	3 – 8	25	8	50	TW <sup>d</sup>

a. Limit of detection, b. Preconcentration factor, c. References, d. This work.

relative standard deviation (RSD) of 6 runs of 2 ng mL<sup>-1</sup> Hg(II) was lower than 5% indicating a good precision of the analytical method.

The proposed procedure was applied to river and tap-water samples *via* spike recovery experiments. About 500 mL of river and tap-water samples were spiked 2 µg L<sup>-1</sup> and passed through a silica column according to the general procedure. As shown in Table 7, the proposed methodology efficiently preconcentrates mercury ions from both river and tap-water matrices with recoveries in the range 95 – 105%.

#### Comparison with other SPE Hg(II) methods

Table 8 represents a comparison of the developed method with some SPE methods for the preconcentration of Hg(II). The suggested method is superior to the others in terms of its applicability in a wider pH range, but comparable in LOD. However, the other methods possess the advantages of adsorption capacity and enrichment factor. The developed method surpasses the others in its simplicity. The fact that there is no modification needed for the adsorbent, is because it is based on the direct addition of a ligand (I<sup>-</sup>). In addition, there are few direct addition methods that succeeded in the recovery mercury ions by solid-phase extraction.<sup>2,17</sup>

## Conclusions

In this work, a simple, cheap and reliable method was developed for the *in situ* determination of trace levels of mercury ions from river water samples. It is based on the adsorption of [HgI<sub>4</sub><sup>2-</sup>][DTA<sup>+</sup>]<sub>2</sub> ion pairs on a silica phase column. The developed procedure can be performed in wide pH range (1 – 8), interference-free extraction of mercury ions, simplicity (direct addition of reagent in the sample), rapidity (no modification of the sorbent is required) and possible analysis by ICP-MS. It allows *in situ* sampling and is particularly suited for distant sites and long-term monitoring programs, while avoiding the sampling of large volumes of water. With the developed analytical method, an all-element analytical technique is used, *i.e.* ICP-MS, overcoming Hg memory effects conferred to the

preconcentration principle. Besides, the great value of the I<sup>-</sup>/DTAB/SiO<sub>2</sub> extraction system is for its application to diluted water samples.

## Acknowledgements

The authors thank David Dumoulin, Romain Descamps (Université Lille 1) and Abdel Boughriet (Université d'Artois) for technical assistance.

## References

1. X. Jia, D. Gong, Y. Han, C. Wei, T. Duan, and H. Chen, *Talanta*, **2012**, *88*, 724.
2. S. R. Segade and J. F. Tyson, *Talanta*, **2007**, *71*, 1696.
3. Z. Fan, *Talanta*, **2006**, *70*, 1164.
4. J. Fan, C. Wu, Y. Wei, C. Peng, and P. Peng, *J. Hazard. Mater.*, **2007**, *145*, 323.
5. A. M. H. Shabani, S. Dadfarnia, F. Motavaselian, and S. Ahmadi, *J. Hazard. Mater.*, **2009**, *162*, 373.
6. N. Dalali and S. Nakisa, *Int. J. Chem. Environ. Eng.*, **2012**, *3*, 1.
7. F. M. Fabrega and M. B. Mansur, *Hydrometallurgy*, **2007**, *87*, 83.
8. R. Caban and T. Chapman, *AIChE J.*, **1972b**, *18*, 904.
9. X. Chai, X. Chang, Z. Hu, Q. He, Z. Tu, and Z. Li, *Talanta*, **2010**, *82*, 1791.
10. A. E. Martell and L. G. Sillen, “*Stability Constants of Metal Ion Complexes*”, 2nd ed., **1964**, Chemical Society, London.
11. L. Tavlarides, J. Bae, and C. Lee, *Sep. Sci. Technol.*, **1987**, *22*, 581.
12. R. Kumbasar, *J. Membr. Sci.*, **2008**, *325*, 460.
13. M. Shamsipur, A. R. Ghiasvand, and Y. Yamini, *Anal. Chem.*, **1999**, *71*, 4892.
14. A. Benhamou, M. Baudu, Z. Derriche, and J. P. Basly, *J. Hazard. Mater.*, **2009**, *171*, 1001.
15. P. Wu and Y. S. Zhou, *J. Hazard. Mater.*, **2009**, *168*, 674.
16. G. L. Long and J. D. Winefordner, *Anal. Chem.*, **1983**, *55*,



- 712A.
17. M. Soleimani, M. S. Mahmodi, A. Morsali, A. Khani, and M. G. Afshar, *J. Hazard. Mater.*, **2011**, *189*, 371.
  18. O. Yayayuruk, E. Henden, and N. Bicak, *Anal. Sci.*, **2011**, *127*, 833.
  19. A. Moghimi and M. J. Poursharifi, *World Appl. Sci. J.*, **2011**, *12*, 624.
  20. W. Qu, Y. Zhai, S. Meng, Y. Fan, and Q. Zhao, *Mircrochim. Acta*, **2008**, *163*, 277.
  21. M.V. B. Krishna, D. Karunasagar, S.V. Rao, and J. Arunachalam, *Talanta*, **2005**, *68*, 329.
  22. R. M. Blanco, M.T.Villanueva, J. E. S. Uria, and A. Sanz-Medel, *Anal. Chim. Acta*, **2000**, *419*, 137.
  23. E. K. Mladenova, I. G. Dakova, D. L. Tsalev, and I. B. Karadjova, *Cent. Eur. J. Chem.*, **2012**, *10*, 1175.
  24. E. M. Soliman, M. B. Saleh, and S. A. Ahmed, *Talanta*, **2006**, *69*, 55.
  25. Y. Yaminia, N. Alizadeha, and M. Shamsipur, *Anal. Chim. Acta*, **1997**, *355*, 69.
  26. M. E. Mahmoud, M. M. Osman, and M. E. Amer, *Anal. Chim. Acta*, **2000**, *415*, 33.
  27. W. X. Ma, F. Liu, K. A. Li, W. Chen, and S.Y. Tong, *Anal. Chim. Acta*, **2000**, *416*, 191.
  28. Y. Guo, B. Din, Y. Liu, X. Chang, S. Meng, and M. Tian, *Anal. Chim. Acta*, **2004**, *504*, 319.
  29. N. Pourreza, H. Parham, A. R. Kiasat, K. Ghanemi, and N. Abdollahi, *Talanta*, **2009**, *78*, 1293.
  30. N. Pourreza and K. Ghanemi, *J. Hazard. Mater.*, **2009**, *161*, 982.
  31. D. M. Sanchez, R. Martin, R. Morante, J. Marin, and M. L. Munuera, *Talanta*, **2000**, *52*, 671.
-

***Chapitre F: Distribution, spéciation et transport du mercure dans le milieu aquatique***

***Chapter F: Mercury distribution, speciation and transport in the aquatic environment***

## *Résumé*

La pollution des sédiments de la Deûle par les métaux est très importante et historique en particulier pour le mercure. L'étude de la distribution de ce métal dans cette rivière est très importante pour comprendre son comportement. Pour connaître les différents facteurs biogéochimiques régissant la distribution du mercure et le transport potentiel à des sites distants comme la rivière Lys en aval, quatre sites ont été étudiés: D-A en amont du site "Metaleurop", D-B près de fonderie "Metaleurop", L-C (rivière la Lys, en amont de la confluence avec la rivière Deûle) et L-D (rivière la Lys en aval de la confluence).

Des concentrations élevées en mercure total HgT ont été détectées dans les sites de la Deûle (11,37 mg/kg à D-A, 9,28 mg/kg à D-B), sur la Lys les concentrations sont plus faibles (L-D <1 mg/kg). Sur le site amont de la Lys (L-C), les concentrations moyennes de HgT sont inférieures aux fonds géologiques de la région (0,042 mg/kg). Cela montre que L-C n'est pas affecté par la pollution en mercure. Les concentrations en méthylmercure suivent la même tendance avec une concentration de 2,06 µg/kg à D-A, 7,03 µg/kg à D-B, 1,63 µg/kg à L-D et 1,86 µg/kg à L-C. Cependant, les pourcentages de méthylmercure (%MeHg) ont montré une tendance opposée. Des valeurs plus élevées ont été relevés dans la Lys (4,21% à L-C et 0,42% en L-D) alors que dans la Deûle les pourcentages de méthylmercure sont beaucoup plus faibles 0,02% à DA et 0,09% à D-B. Dans les sites de la Lys, les conditions semblent être plus favorables à la méthylation que les sites de la Deûle. Des niveaux de HgT, des sulfures et des matières organiques plus bas dans la Lys ont contribué à une production plus prononcée de méthylmercure. Les déchargements de minerais (HgS, CdS, ZnS ...ect.), pour alimenter l'ancienne fonderie "Metaleurop", avaient contribué à une accumulation des sulfures de métaux (dont le mercure) dans les sédiments. Des niveaux élevés de sulfures sont capables de réduire la biodisponibilité du mercure et ralentir sa méthylation. En plus, la déméthylation biotique renforcée dans des environnements très pollués en mercure comme le cas de la Deûle, est capable de diminuer la concentration en méthylmercure. Toutes ces conditions sont suffisantes pour contribuer à des faibles potentiels de méthylation dans la Deûle par rapport aux zones non-contaminées ou moins contaminées comme les sites de la Lys. Les associations importantes établis entre %MeHg et AVS, CRS dans le site D-B, montrent que la production de MeHg a été initiée dans le passé et continue même avec la persistance des conditions favorables de méthylation. D'autre part, l'absence de relation entre %MeHg et les CRS et une bonne corrélation avec les AVS dans les sites de Lys, démontre une activité de

méthylation plus récente par les communautés microbiennes. Il semble y avoir de différentes conditions biogéochimiques contrôlant la production de MeHg dans les deux rivières. Dans la Deûle, lorsque les niveaux de sulfures (AVS) et Corg augmentent, la méthylation est favorisée. Dans des environnements riches en sulfures comme dans la Deûle, la formation de polysulfures peut améliorer la solubilisation du mercure combinée à l'effet synergique du carbone organique. En bref, les relations importantes observées entre %MeHg et %Corg, AVS et %Corg et AVS suggèrent l'importance de l'activité microbienne dans la méthylation et la production *in situ* du MeHg dans les deux rivières.

Le mercure dissous ( $Hg_D$ ) dans les eaux de surface ne montre aucune variation spatiale entre les différents sites de la Deûle et la Lys avec une concentration variant entre 19,4 à 20,8 ng/L. Cependant, le mercure particulaire ( $Hg_{Tp}$ ) a montré une tendance de diminution de D-B (4,3  $\mu\text{g/g}$ ) à L-D (2,5  $\mu\text{g/g}$ ). Les conditions hydrologiques et climatiques sont capables d'éroder les sédiments de surface de la Deûle et de lessiver des polluants par les eaux de ruissellement de l'entourage contaminé de la rivière. Les particules en suspension sont la principale phase porteuse du mercure et considérée comme le véhicule de la pollution de la Deûle à la Lys.

Les concentrations dans l'eau interstitielle varient dans les deux sites, des valeurs élevées ont été mesurées dans les sédiments de la Deûle (D-A : 17,4 ng/L) et plus faible dans la Lys (L-C : 3,9 ng/L). Les conditions réductrices dans les sites de la Deûle, confirmées par de fortes concentrations de sulfures peuvent provoquer une dissolution de Hg par réduction des phases porteuses comme le oxydes de fer et manganèse. Par conséquent, il est évident de trouver des flux de diffusion du mercure beaucoup plus élevés dans la Deûle (223,9  $\text{ng/cm}^2/\text{an}$ ) que dans la Lys (LC: 51  $\text{ng/cm}^2/\text{an}$ , LD: 2,1  $\text{ng/cm}^2/\text{an}$ ).

## Summary

The Deûle is a highly polluted river by heavy metals caused by the ancient discharges of ore minerals from the former ore smelter “Metaleurop”. The potential mercury (Hg) pollution in the Deûle river, implicates the importance of Hg distribution study in the river and the Lys river. As well as, to configure the different biogeochemical factors governing Hg distribution and the potential transport to distant sites. Four different sites were studied, D-A upstream the river, D-B near Metaleurop smelter, L-C (Lys river, a site located upstream the confluence of the Deûle with Lys river) and L-D (downstream the rivers confluence).

Results showed high concentrations of total mercury in sediments ( $HgT_s$ ) in the Deûle sites with 11.37 mg/Kg in D-A and 9.28 mg/Kg in D-B becoming attenuated at L-D to < 1 mg/Kg downstream the rivers merging. Upstream of Lys river at L-C, the average  $HgT$  concentrations was found to be 0.042 mg/Kg which is less than the background concentration. This shows that L-C is unaffected by Hg Deûle river pollution. MeHg concentrations followed the same trend with a concentration of 2.06  $\mu\text{g/Kg}$  at D-A, 7.03  $\mu\text{g/Kg}$  at D-B. In Lys river, MeHg contents showed lower values of 1.63  $\mu\text{g/Kg}$  at L-D and 1.86  $\mu\text{g/Kg}$  at L-C. However, the % MeHg has demonstrated opposite trend. Higher value of %MeHg was obtained in Lys river with 4.21 % at L-C and 0.42 % at L-D. Whereas, in the Deûle river, much lower %MeHg were acquired with 0.02 % at D-A and 0.086 % at D-B. In Lys sites, conditions seems to be more favorable to methylation than Deûle sites. Lower  $HgT$ , sulfides, organic matter in Lys river have contributed to more pronounced *in situ* MeHg production. The old discharges of minerals ( $HgS$ ,  $CdS$ ...ect.) by the former smelter had triggered old/recent methylation events contributing to sulfide build-up in sediments. High sulfide levels are able in reducing the bioavailability of mercury by forming strong complexes with Hg. In addition to, the enhanced biotic demethylation in highly polluted environments i.e. Deûle river, capable of decreasing bulk phase MeHg contents. All of these conditions are sufficient in rendering lower methylation potentials in Deûle river as compared to pristine or less contaminated areas such as Lys sites. The important associations established between % MeHg and AVS, CRS in D-B, shows that MeHg production has been initiated in the past and continued with presence of favoring conditions. On the other hand, the lack of relation between % MeHg and CRS with important relation with AVS in Lys sites, demonstrate more recent activities of methylating microbial communities. Thereby, there are different biogeochemical conditions governing MeHg production in the two rivers. In the Deûle,

increasing levels of sulfides (AVS) and Corg promote methylation whereas in the Lys, these conditions decrease methylation. In high sulfidic rich environments such as in the Deûle, the formation of polysulfides can enhance the solubilization of mercury solid phases combined with the synergetic effect of Corg. In short, the important relations found between % MeHg and %Corg, AVS and %Corg and AVS suggest the importance of microbial activity in methylating and producing mercury in the two rivers.

Dissolved Hg ( $Hg_D$ ) in surface water showed no spatial variations between different sites of the Deûle and Lys river with concentrations varying between 19.4-20.8 ng/L. However, particulate mercury ( $Hg_{T_P}$ ) have showed a decreasing trend from D-B (4.3  $\mu\text{g/g}$ ) to L-D (2.5  $\mu\text{g/g}$ ). Hydrological and climatic conditions are capable of eroding the Deûle river surface sediment and Hg leaching from the surrounding river environments. Suspended particles are the major Hg carrier phase and transporters of Hg pollution from the Deûle to the Lys river. Eventhough L-C is a pristine/uncontaminated Hg environment, high levels of  $Hg_{T_D}$  (18.5 ng/L),  $Hg_{T_P}$  (1.5  $\mu\text{g/g}$ ) are measured in the surface water of Lys river at site C. This could be ascribed to agricultural runoffs and the participation of the Deûle river in the propagation of Hg pollution to Lys river (L-D, L-C) by river flows and resuspension events. Boat traffic in both rivers can cause sediment remobilization and effective dispersion of pollution. As well as, the contribution of Hg solubilization by DOC and possible microbial degradation of particulate organic matter, an important carrier of Hg, disseminating Hg in the surrounding surface water.

Pore-water distribution has varied from high values at D-A (17.39 ng/L) to lower levels at L-D (11.42 ng/L) and L-C (3.98 ng/L). The governance of reducing conditions in Deûle sites conferred by high concentrations of sulfides; induce dissolution of Hg by polysulfides and the reduction of Fe/Mn oxyhydroxides. Therefore, it is evident to find much higher HgT diffusional fluxes in the Deûle river (223.91  $\text{ng/cm}^2/\text{y}$ ) than the Lys river (L-C: 51  $\text{ng/cm}^2/\text{y}$ , L-D: 2.1  $\text{ng/cm}^2/\text{y}$ ).

## **Biogeochemical factors affecting the distribution, speciation and transport of Hg species in the Deûle and Lys rivers †**

Mirna Daye<sup>a</sup>, Baghdad Ouddane<sup>a\*</sup> and Milada Kadlecova<sup>a</sup>

<sup>a</sup>*University Lille 1, Géosystèmes, UMR - CNRS 8217, Villeneuve d'Ascq, France.*

**\*Corresponding author. Tel.: +33 (0) 3 20 43 44 81,**

**E-mail address: Baghdad.Ouddane@univ-lille1.fr**

† Submitted to *Applied Geochemistry*

## F.1. Abstract

Mercury distribution was studied in the Deûle river and Lys river at two different sites, after and before the rivers merging. Total mercury concentration in sediments ( $HgT_S$ ) decreases downstream from the Deûle river sites with a mean value of  $11.37 \pm 0.34$  mg/kg to L-D with a mean value of  $0.53 \pm 0.018$  mg/kg at the confluence. The unaffected side of Lys river, localized before the confluence (L-C) is characterized by low  $HgT_S$  concentrations below Hg background levels of the region and high %MeHg reaching 4.2. Whereas, the highly contaminated Deûle sites are designated with low %MeHg of an average value of 0.053. Low pristine environments like that found in L-C with more favorable biogeochemical conditions of lower levels of HgT, sulfides, Corg, host more active biotic methylation than that of the highly polluted Hg Deûle sites with high contents of HgT and sulfides levels. Methylation in D-B, the closet site to Metaleurop smelter, is an old and recent methylation activity that has contributed to MeHg accumulation in the sediments as opposed to the recent events of methylation in Lys sites. MeHg in all sites is produced *in situ* rather than exported from other potential sources confirmed by significant relations of %MeHg with %Corg and AVS. Mercury pollution is transported to Lys river (L-C, L-D) through suspended particles leached or remobilized from the river catchment. The dominance of reducing conditions in the Deûle attributed to higher sulfide content, have contributed to higher  $HgT_{PW}$  than the Lys. Diffusive fluxes of HgT from sediment to water column for the Deûle and Lys river sites (L-C, L-D) were estimated to be  $223.91$  ng/cm<sup>2</sup>/y,  $51.70$  ng/cm<sup>2</sup>/y and  $2.11$  ng/cm<sup>2</sup>/y respectively.

## F.2. Introduction

In natural ecosystems, understanding the biogeochemistry of mercury is substantial, because of increasing concerns regarding Hg toxicity and the biomagnification of methylmercury (MeHg) through the food web. Mercury is a global pollutant, because of its long-range transport in the atmosphere. Combustion of fuels, especially coal and gold mines are the major sources of Hg to the atmosphere contributing to a global pollution. Plants are the primary receivers of elemental mercury in which it is adsorbed, and consequently oxidized to a highly water soluble Hg(II). Inorganic mercury produced is further transported into the aquatic systems: major pathway for global scale pollution (Grigal, 2002). The local contributors of Hg to riverine environments are non-point sources of atmospheric deposition, river input through erosion (Coquery et al, 1997). The most potential point sources of Hg to the river systems include, sewage effluents (Hammerschmidt et al, 2004), industries such as



chloroalkali (Bloom et al, 1999) and ore refining industries (Kadlecova et al, 2011), and mines such as mercury (Hines et al, 2006) and gold mines (Yan et al, 2013). Mercury mobility and diffusion to the overlying water depends on numerous factors, including the redox cycle of Fe and Mn (Gagnon et al, 1996), vertical position of redox transition zone, redox gradients affecting the potential binding phases of mercury (organic matter and sulfides), microbial activity and bioturbation (Hammerschmidt et al, 2004).

The primary vector of transport of mercury away from sources are riverine flows, which can transport mercury through the dissolved and solid phases mainly by suspended solids to several hundreds of kilometers to coastal zones. Therefore mercury can be deposited downstream and can be subject to resuspension events from riverine high flows and floods to active bioturbation phenomena or anthropogenic remobilization (boat traffic, dredging..) exposing mercury to methylation. As a result, MeHg can be produced at distant areas from the source of pollution. The fate of transported mercury through the river is governed by biogeochemical parameters affecting its mobility, speciation and availability to the microbial communities for subsequent transformations.

The region of Northern France (Nord Pas-de-Calais) is highly populated and industrialized by metallurgical activities. Two of the most important smelters in the region are Metaleurop and Umicore which are localized at the banks of the Deûle river, which have perturbed the natural balance of the ecosystem significantly. Furthermore, the agricultural and urban inputs in the river have provided additional favorable biogeochemical conditions for the production and the transport of Hg pollution throughout the river system. The Lead and Zinc smelter "Metaleurop" was active for more than a century and was the major contributor of metal pollution to the river. Fortunately, Metaleurop was closed in January 2003; however untreated or not well refined ore wastes are disposed in the former smelter location, certainly contributing to continuous metal pollution to soil and to the surrounding river system. Besides Metaleurop, Umicore is another relevant source of metal pollution localized at the upstream river from Metaleurop which is still active since 1869. Previous studies, have shown important metal pollution in the Deûle sediments near Metaleurop site, particularly in Cd, Zn, Pb, Cu and Ni (Lourino-Cabana et al, 2011) and Hg species including MeHg (Kadlecova et al, 2011).

The present study investigates the spatial distribution of Hg species in the Deûle and Lys rivers and the potential transport of Hg and its consequent methylation at distant regions. Additionally, evaluating the biogeochemical factors controlling the distribution and transport of Hg species emphasizing on the significance of these controls in regulating mercury levels in the system.

### **F.3. Methods and Materials**

#### **F.3.1. Field sampling and sediment processing**

Sediment cores were chosen based on their distance from Metaleurop smelter and the effect of major confluences with other rivers in this case Lys river (figure F.1). Therefore, sediment cores were collected at two sampling locations along the Deûle river, one near Metaleurop site (D-B) and the other (D-A) only 200 m upstream the river from Metaleurop location which represent locations directly influenced by past ore processing activities (Metaleurop smelter). Two other sediment cores were sampled in Lys river, one before the river confluence (Lys-C) and the other after Deûle confluence with Lys river (Lys-D). These sites represent distant location from the source of pollution. All cores were sampled in duplicates in March 2010, in which one core was dedicated to pH measurements on site and the other for Hg species and ancillary measurements. The core samples were collected using a hand-driven gouge sampler and polyethylene core. The length of the core was 80 cm and the inner diameter was 7 cm. The sediment cores were processed in a glove bag under nitrogen atmosphere. Inside the glove, the sediments were sliced at 2-cm thickness. Each sediment slice was divided into several parts, one stored in hermetically closed plastic bags and frozen at -18°C for CRS and AVS analysis and other part for Hg species (HgT, MeHg) and organic carbon analysis in the solid phase. Aliquots from each sediment depth were transferred into teflon centrifuge bottles, spun at 3500 g for 15 minutes. Under nitrogen atmosphere, the supernatant was filtered (0.45µm), acidified with HNO<sub>3</sub> for Fe and Mn analysis and porewater samples for the analysis of dissolved HgT were preserved with 1 % HCl. Additionally, surface water was collected from the two sampling sites, and filtered (0.45 µm). The filtrate was preserved with concentrated HCl for HgT in surface water and the filters containing particles were frozen for the subsequent analysis of mercury in suspended solids.

Collection, storage and preservation followed US EPA Method 1631 (Revision E, 2002). All glass and Teflon vessels were cleaned by soaking in diluted nitric acid (HNO<sub>3</sub>:H<sub>2</sub>O = 1:10

v/v) for 24 hours, washing using Milli-Q (18.2 MΩ cm, Millipore) water and then drying under filtered air flow.

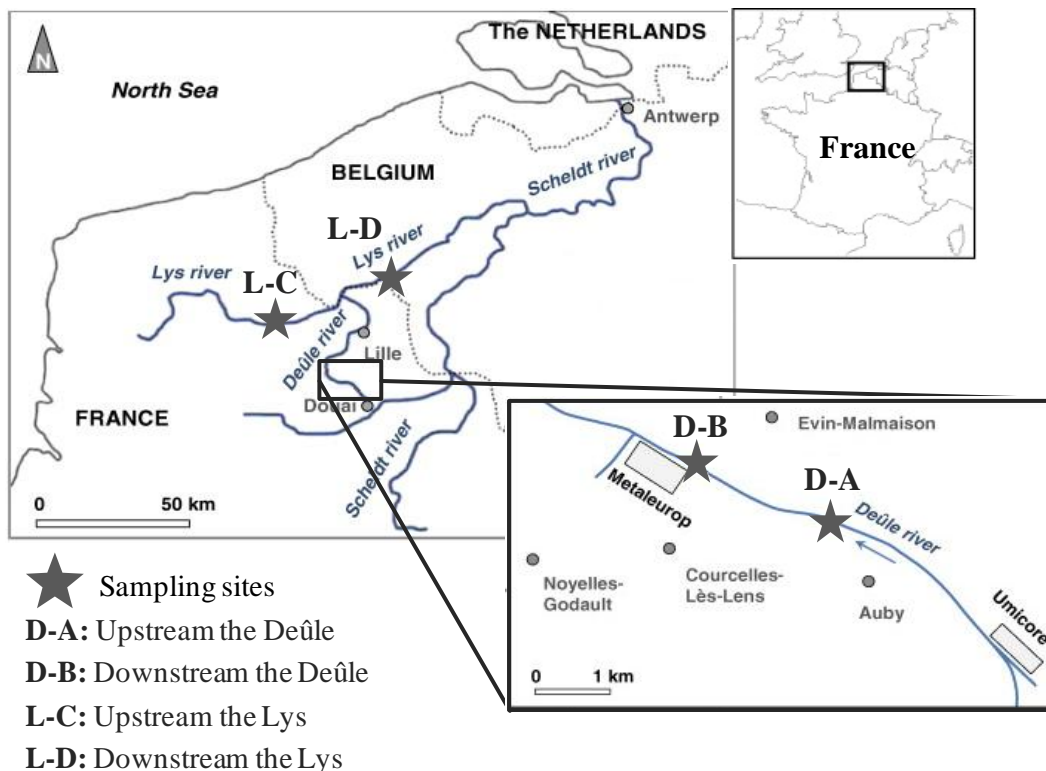


**Fig.F.1.** Sampling sites in the Deûle and Lys rivers.

### F.3.2. Analysis of mercury species

Total mercury analysis in dry sediments samples ( $HgT_S$ ) were analyzed without any pre-treatment by atomic absorption spectrometer Advanced Mercury Analyzer, model AMA 254 (Altec Ltd., Czech Republic). The detection limit for AMA 254 based on 100 mg of sample was 0.1  $\mu\text{g}/\text{kg}$ . The relative standard deviation of six replicate measurements was 1.2 %. For precision objectives, certified reference materials from the International Atomic Energy Agency were analyzed. The obtained values of  $HgT$  in IAEA 405, IAEA 433, and IAEA 158 were  $0.81 \pm 0.003$  mg/kg,  $0.168 \pm 0.017$  mg/kg,  $0.132 \pm 0.014$  mg/kg respectively. The measured values were coherent with certified values of IAEA 405 ( $0.750 \pm 0.06$  mg/kg), IAEA-433 ( $0.155 \pm 0.01$  mg/kg) and IAEA-158 ( $0.121 \pm 0.013$  mg/kg). Particulate mercury ( $HgT_P$ ) in surface water was measured after filtration of surface water and the subsequent analysis of filters using AMA-254. The accuracy was determined by replicate analysis ( $n=3$ ) and was found to be  $< 25$  %.

MeHg in sediments was determined as proposed by Leermakers et al. (2003), by aqueous ethylation followed by Headspace (HS) injection, Gas Chromatography separation (Clarus 500, PerkinElmer, USA), and detection by Atomic Fluorescence Spectroscopy (Tekran, Model 2600 CVAFS Mercury Analysis System, USA). Briefly, the extraction 100-200 mg sediment was performed in glass vial with 1 ml  $\text{CuSO}_4$  (Acros Organics, New Jersey, USA), 5 mL of 18% KBr (w/v) (Merck, Darmstadt, Germany) in 5%  $\text{H}_2\text{SO}_4$  (v/v) (Merck, Darmstadt, Germany). The mixture was shaken for 45 minutes at 400 g. Then, 10 mL  $\text{CH}_2\text{Cl}_2$  was added and shaken for 45 minutes, centrifuged for 15 min at 3000 g. After separation of the organic, aqueous phase, from solid layers, 5 ml of the organic phase was transferred to a conical glass bottle containing 20 mL Milli-Q water. Back-extraction of the organic layer in water phase was performed by solvent evaporation at 46°C using water bath (Compatible Control CC3, Offenburg, Germany) under constant  $\text{N}_2$  flow. The aqueous phase (5 mL) was transferred to Headspace vials and diluted with 5 mL of Milli-Q water and the pH was adjusted to optimum pH (between 4.8-5.2) using 0.1 M acetic acid-acetate buffer (82 g  $\text{CH}_3\text{COONa}$ , p.a., Merck, Darmstadt, Germany and 59 mL  $\text{CH}_3\text{COOH}$  Scharlau Extrapur in 500 mL Milli-Q water). Finally, ethylation was performed using 50  $\mu\text{L}$  of 1% tetraethyl borate (min 98 %, Stream Chemicals, Newburyport, USA). The vials were sealed with Teflon-coated butyl rubber septum and Al crimp caps and allowed to react for 1 hour in darkness before analysis. The detection limit of HS-GC-CVAFS was 1.12 ng/kg. The accuracy was examined by international reference materials (IAEA-405, IAEA-433). The obtained values of certified reference materials (IAEA-405:  $5.85 \pm 0.45$  ng Hg/g, IAEA-433:  $0.18 \pm 0.09$  ng Hg/g) were consistent with the certified values (IAEA-405:  $5.49 \pm 0.53$  ng Hg/g, IAEA-433:  $0.17 \pm 0.07$  ng Hg/g). Precision is given by the relative standard deviation of 5 replicate analyses, and was determined to be 4.86%.

Total mercury in pore water ( $\text{Hg}_{\text{TPW}}$ ) as well as surface water ( $\text{Hg}_{\text{TD}}$ ) was determined according to US EPA Method 245.7 (Revision 2, 2005). It is based on the oxidation of Hg species by potassium bromated/potassium bromide reagent (J.T. Baker, USA). And sequentially pre-reduced with  $\text{NH}_2\text{OH}\cdot\text{HCl}$  (Sigma Aldrich) in order to destroy the excess bromine. The ionic mercury is then reduced with  $\text{SnCl}_2$  (1% solution 5% HCl) (A & C American Chemicals Ltd) to volatile  $\text{Hg}^0$ . The volatile species of Hg are separated from the solution by purging with high purity argon gas and transferred to gold cell for preconcentration cycles. After thermal desorption, the concentration of Hg is determined by

atomic fluorescence spectrometry at 253.7 nm. The limit of detection as determined by CV-AFS was 1.8 ng/L, limit of quantification was 5 ng/L. Precision was determined by the relative standard deviation of 5 replicate analyses that was found to be 1.72 %

### F.3.3. Ancillary measurements

The inorganic sulphides in the sediment are generally grouped into two main categories: unstable sulphides that are freshly precipitated (AVS: Acid Volatile Sulphides) and the more stable sulfides, mainly pyrite and elemental sulfur (CRS: Chromium Reducible Sulphur). The reduced sulfur species are determined by sequential extraction as described previously by Canfield et al. (1986). Manipulations are performed in a glove bag under inert atmosphere ( $N_2$ ). About 1 g of sediment is reacted 40 ml of 6 M hydrochloric acid, then the volatilized sulfide in the form of  $H_2S$ , is purged by  $N_2$  flow and trapped in 20 mL of a basic solution ([NaOH] 1M [EDTA] 1M). CRS (Chromium Reducible Sulfides) sequentially follows AVS, and is extracted by adding about 40 mL of 1 mol  $L^{-1}$  chromium II solution, produced in the column of Jones and HCl solution. Again the volatile sulfur is trapped in 20 ml of a basic solution ([NaOH] 1M [EDTA] 1M). The concentration sulfide is then determined for each trap by potentiometry using an automatic titrator (Metrohm, model 736 GP Titrino). The titration is carried out with a cadmium solution of  $8.9 \times 10^{-3}$  mol/L, a calomel reference electrode ( $Hg/Hg_2Cl_2$ , [KCl] = 3 mol/L) and a measuring electrode specific to sulfide ions (Orion). The accuracy of the two methods is determined to be < 8 %. The lower limit of determination of 1 g of sediment was 20 mg/kg of S.

The organic carbon (Corg) was determined using LECO CS-125 Carbon-Sulfur Determinator. The accuracy was examined by testing standard of Carbon and Sulfur in White Iron (Leco Coporation) in which the mean obtained values of 6 determinations was  $3.34 \pm 0.03\%$  that were consistent with certified values ( $3.31 \pm 0.03\%$ ). The first measurement permits the determination of total carbon and a second one which is performed after calcination of the samples at  $450^\circ C$  for 24 hours, allows the measurement of mineral Carbon. By subtraction of the two determinations, organic carbon can be obtained. Porewater Fe and Mn were measured using ICP-MS (Thermo-Optek X7, Thermo Fischer Scientific, USA).

## F.4. Results and discussion

### F.4.1. Spatial distribution of HgT and MeHg

The general vertical depth profiles of HgT in the Deûle cores, was a decreasing trend of HgT levels from depth to surface, which corroborate the halt of Metaleurop smelter. Therefore, one can estimate sedimentation rates relative to the gradual decrease in HgT<sub>s</sub> which is approximated to be 0.43 cm/year. Dating of the Deûle sediments using <sup>137</sup>Cs and <sup>210</sup>Pb radionuclides should provide accurate measurement of accumulation rate for the possible determination of Hg background levels in the river. In D-A, the HgT concentration varied between 6.89-16.03 mg/kg with an average value of 11.37 mg/kg ± 0.34, while in the downstream river (D-B) HgT concentration are less pronounced with varying concentrations between 6.36-11.76 mg/Kg and an average value of 9.28 mg/Kg ± 0.22 (Figure F.2(a), (e)). The overall concentrations of HgT are greatest near the historic smelter, becoming attenuated downstream the river to < 1 mg/Kg at Lys D. In the uncontaminated side of Lys river (Lys C), HgT concentrations were low with levels varying between 0.04-0.06 mg/kg with an average value of 0.042 mg/kg ± 0.0032, which is less than the background concentration of Hg in Northern France 0.1 mg/kg (Agence de l'eau, 1997). Thereby, Lys C is not affected by any Hg contamination. Whereas, in the contaminated side of the river affected by Deûle effluents, concentrations were 10 times higher in magnitude with concentration between 0.18-0.944 mg/Kg and an average value of 0.53 mg/Kg ± 0.018. The vertical depth profiles of HgT in Lys cores did not show significant variations within depth. The primary transport vector for Hg species in aquatic environments is organic matter which binds strongly to mercury and can be transported far away from their point sources (Bishop and Lee 1997). In the Deûle sites and Lys D, HgT concentrations profiles tend to decrease from depth to surface, suggesting a decline in Hg inputs to the river and burial of mercury, effectively preserved under anoxic conditions.

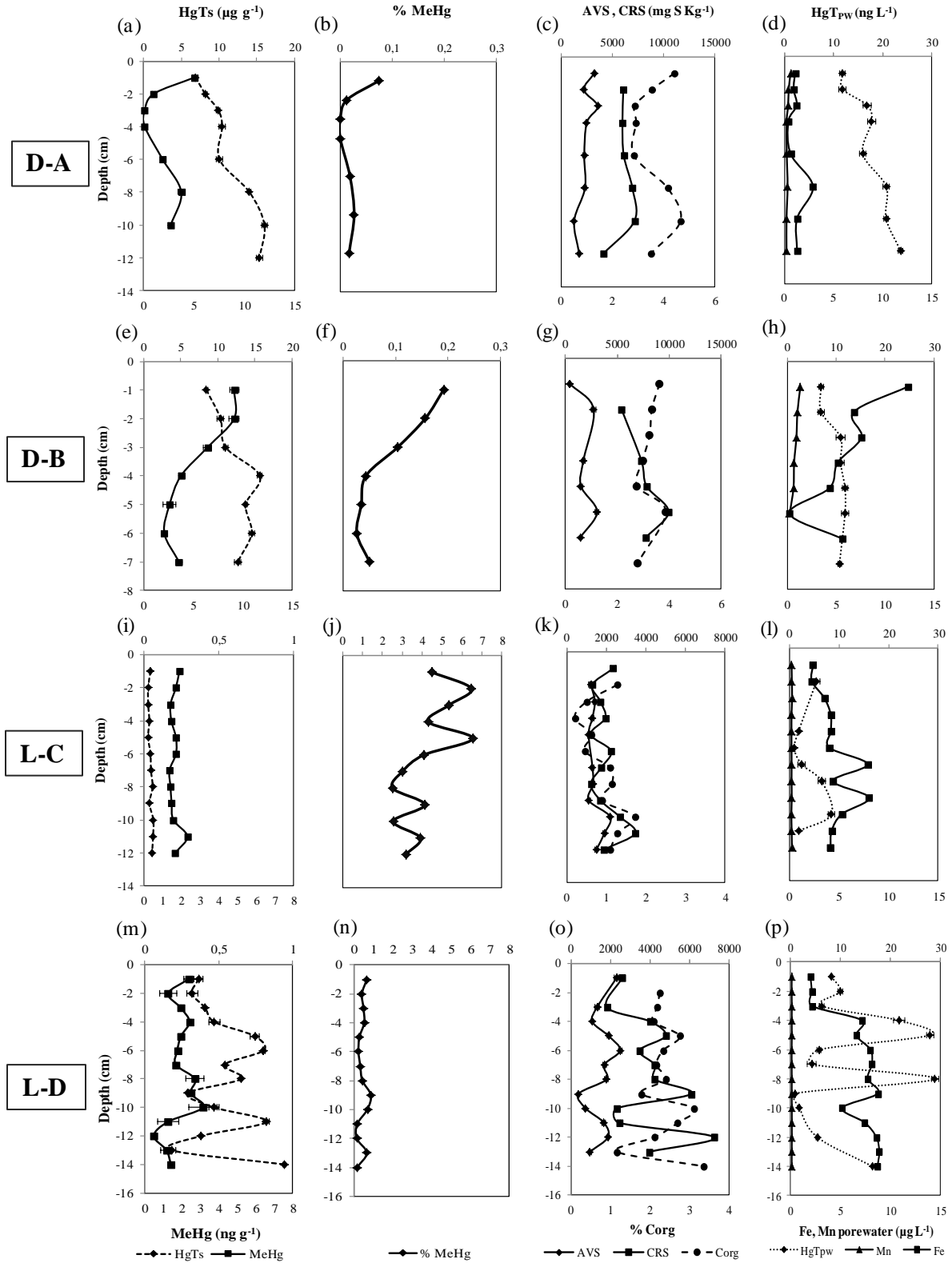


**Fig.F.2.** Sediment depth profiles of Hg species and geochemical determinants in D-A, D-B, L-C and L-D.

The concentration of MeHg in Deûle A and B showed pronounced maximum near sediment surface of 5.0 ng/g, 12.22 ng/g respectively, with a rapid decrease over the first few centimeters core depth. The average concentration of MeHg in D-A and D-B  $2.06 \mu\text{g/Kg} \pm 0.13$  and  $7.03 \mu\text{g/Kg} \pm 0.50$  respectively (figure F.2 (a), (e)). Concentrations of MeHg in both Deûle sites were highest near sediment-water interface corresponding to methylation zone. Moreover, a minimum of MeHg in Deûle A and B occurred at depth between 6-7 and between 3-4 cm respectively. The low concentrations in MeHg correspond to the high levels of sulfides. At these depths, sulfide accumulates and induces the precipitation of  $\text{HgS}_{(s)}$  and its further pyritization (Morse and Luther, 1999). In Lys river, levels of MeHg had consistent gradients with depth with an average concentration of MeHg  $1.63 \mu\text{g/Kg} \pm 0.094$  for L-C and  $1.86 \mu\text{g/Kg} \pm 0.23$  for L-D (figure F.2 (i), (m)). Concentrations of both HgT and MeHg in the Deûle are considered to be high as compared to other contaminated estuarine and riverine ecosystems as Seine and Adour estuaries (Ouddane et al, 2008; Stoichev et al, 2004), Long Island sound (Hammerschmidt et al, 2004), San Francisco Bay-Delta, (Choe et al, 2004). However, much higher concentrations of Hg are found in locations near point source pollution as Lavaca bay (Bloom et al, 1999), Tagus estuary (Canario et al, 2005). The average % MeHg at D-A is 0.02 %, increasing at downstream river to 0.086% at D-B and to higher extent at L-D and L-C reaching 0.42 %, 4.21% respectively (figures F.2 (b), (f), (j), (n)). It is expected that % MeHg drops off away from the pollution source; this was the case for  $\text{HgT}_s$  and not % MeHg. High % of MeHg did not coincide with  $\text{HgT}_s$  levels, especially in L-C and L-D. This is explained by the site intrinsic characteristics with more favorable hydrological, climatic and environmental conditions for methylation. Similar spatial trend of MeHg and HgT was observed in Idrijca mine, where the highest % MeHg was found in the upstream river (20%) to less than 1.5% downstream the river from the mine (Kocman et al, 2011). Moreover, in the gulf of Trieste affected by Idrijca mine, % of MeHg increases gradually downstream from 0.0078 % at the mouth of the estuary to 0.022 % away from the gulf (Hines et al, 2000). The high values of % MeHg of L- C and L- D are also found in other uncontaminated sites in Ore river estuary (4-13 %) (Lambertsson et al, 2006), Krka estuary (0.65%) (Kwokal et al, 2002) and in pristine lakes in Wisconsin (% MeHg in surface water > 58 %) (Eckely et al, 2005). Higher methylation potentials of 21.7 % were also observed in the uncontaminated sediments of Carson river (Oremland et al, 1995). This suggests that active mercury methylation is more promoted in pristine environments rather than highly Hg contaminated sites. Another explanation could be attributed to the possible outfall of waste water from sewage treatment



plants and agricultural runoffs in the Lys river. Hg methylation can be enhanced by the supply of nutrients full of sulfates and organic matter which are considered as the most important promoters of methylation (Benoit et al, 2002). Furthermore, waste water could be source of MeHg to receiving body of water (Mason and Lawrence, 1999) leading to high % MeHg. On the other hand, high concentrations of MeHg can be also detected in enclosed bodies of water such as lakes, parts of rivers subject to impoundments and wetlands. As wetlands are considered as a sink of Hg and a source for MeHg (Galloway and Branfireun, 2004) and water stagnation can promote methylation by favorable high reductive conditions and nutrient concentrations (sulfate, organic matter) (Guedron et al, 2011). Therefore, further investigations are needed to clarify the reasons behind high levels of % MeHg in Lys sediments, such as organic carbon determination which is discussed below. The lower % MeHg in the Deûle sites can be elucidated by significantly higher HgT content. High mercury concentrations can enhance MeHg degradation and volatilization through reductive demethylation process via Hg-resistant-type microbes. Thereby, demonstrating high demethylation potentials as shown in a previous study where D-A site showed a value of 27.3 %/day and D-B 28.8 %/day (In preparation). In addition to the toxicity induced by highly burdened sediments in Hg and heavy metals towards sulfate reducing bacteria (SRB) the principal microbial species for mercury methylation decreasing their efficiency in methylating mercury in polluted sites.

The percentage of MeHg at the Deûle sites are relatively low, but are comparable to other highly polluted estuaries affected by chloroalkali discharges as Tagus estuary (% MeHg 0.02-0.4%) (Canario et al, 2005), Lavaca Bay (0.02-0.1%) (Bloom et al, 1999) and Paglia river affected Abbadia San Salvatore mercury mine (0.06-0.1 %) (Rimondi et al, 2012), Baihu reservoir influenced by an ancient gold mine (0.05-0.81 %) (Yan et al, 2013), Kuskokwim river (Southwest Alasca) affected by an abandoned Hg mines (< 1%) (Gray et al, 2000), and gulf of Trieste affected by Idrijca Hg mine 0.035 % (Hines et al, 2006). Higher values of % MeHg are observed in other ecosystems affected by nonpoint source inputs as Seine river 0.5 % (Mikac et al, 1999) and less contaminated sites as Patuxent River (0.1-0.5%) (Benoit et al, 1998), Thau lagoon ranging between 0.02-0.8% (Muresan et al, 2007), Baltimore Harbor at 0.6% (Mason and Lawrence 1999) Chesapeake Bay of 1 % (Mason et al, 1999), 0.2 % in Hudson River and Grinode estuary (Heyes et al, 2004; Schafer et al, 2010). In contrast, mercury in highly contaminated sites are more Hg burdened than observed in the Deûle river

as found in Idrija river affected by Idrija mine % MeHg (1-5%) (Hines et al, 2000), and Saguenay Fjord affected by chloralkali plant 0.4 % (Gagnon et al, 1997). Eventhough, L-C and L-D are 10 times less in magnitude of HgT contents than the Deûle sites; they exhibit higher percentage of MeHg of 4.21 % and 0.42 % respectively. Estuarine and marine sediments tend to have % MeHg < 0.5%. However, lakes and wetlands are more prone to methylation and therefore the % MeHg > than 10% (Glimour et al, 1992) and eutrophic ecosystems can have also relatively high methylation potentials 0.3-5% (Gray and Hines, 2009). Sources of MeHg in a natural ecosystem can be either from anthropogenic inputs (sewage effluents, industries) or from natural methylation processes. However, it seems that the agricultural nature of Lys river and less Hg contamination have attributed favorable conditions for Hg methylation with supply of organic matter and less toxicity of Hg exerted on Sulfate Reducing Bacteria. *In situ* MeHg concentrations can provide estimates about methylation potentials. Mercury in aquatic environments is rapidly recycled and can vary from one season to another within the same location in response to changes in the microbial activity and supply of organic matter (Benoit et al, 2001). Evidently, there are different factors controlling MeHg production and methylation between Lys and Deûle rivers. Although the factory is closed, sediments are still burdened with HgT particularly in D-A and D-B and therefore are still considered as permanent and important source of Hg in the area.

#### **F.4.2. Sulfide and organic carbon distribution**

Two of the most determinative controls of Hg dynamics are sulfides and organic carbon content. Sulfides are important solid phase carriers of mercury. The determination of their levels is crucial for the reason that sulfides govern the availability, speciation and methylation of Hg. Therefore, sulfides can be used as a proxy for the degree of methylation in a given site (AVS: recent event, CRS: old event). The vertical sediment profiles of sulfides followed variable patterns. The highest average values of sulfides were determined in D-B of AVS 1799 mg/Kg  $\pm$  114, CRS 7644 mg/Kg  $\pm$  92, followed by D-A of AVS 2398 mg/Kg  $\pm$  89, CRS 6062 mg/Kg  $\pm$  99 (figure 2(c), (g)). On the other hand, significantly lower average values of sulfides were obtained in Lys sites, with AVS 1438 mg/Kg  $\pm$  66, CRS 1952 mg/Kg  $\pm$  83 for L-C, AVS 1520 mg/Kg  $\pm$  72, CRS 3806 mg/Kg  $\pm$  82 for L-D (figure F.2 (k), (o)). The higher sulfidic concentrations in sediments of the Deûle sites, signify that methylation is provoked long time ago by the high Hg discharges particularly those that are the most proximal to the former smelter site. Considering that, Lys sites as less contaminated

particularly L-C. The higher methylation and lower sulfide concentrations in these sites indicate that methylation is the result of a current process. Further interpretations are needed to point out relations between Hg species and relevant geochemical proxies. In D-A, the percentage of Corg varied between 2.9-4.6 % with an average value of 3.61 % (figure F.2 (c)). D-B site showed comparable values with Corg varying between 2.8-3.6 % with an average value of 3.23 % (figure F.2 (g)). Similar high values of organic matter are found in Bay of Biscay of sediments sampled near urban discharges (Stoichev et al, 2004) and in Seine estuary also affected by industrial and urban effluents (Ouddane et al, 2008) with % MeHg ranging from 0.01-0.6% and 0.2-0.4 % respectively. Therefore, we can assume that the high bulk organic contents in the river could be attributed to two possible sources, urban effluents and agricultural runoffs. In Lys sites, the values of Corg are 1-2 orders of magnitude lower than the Deûle sites (figure F.2 (k), (o)). In L-D site, % Corg varied between 1.17-3.36% with an average value of 2.34% while in L-C showed lower values ranging between 0.20-1.72% and an average value of 0.93%. Similar values of Corg (1.5-0.74 %) were obtained in the Gulf of Trieste affected by mercury inputs from Idrijca mine with an observed % MeHg in surficial sediments of 1.8% (Covelli et al, 1999). The higher Corg content in the Deûle sites can be attributed to the more intense agricultural activities and/or the possible presence of organic substances in the discharges of an active ore smelter (Umicore) located upstream D-A site. Accordingly, a gradual decrease is observed in % Corg from site D-A to L-D while L-C (before confluence) showed the lowest % Corg.

#### **F.4.3. Effects of geochemical factors on sedimentary Hg species**

In D-B site, significant correlation existed between HgT and MeHg ( $r^2 = 0.795$ ;  $p < 0.01$ ). Linear relationships were detected for HgT and MeHg with Fe, Mn, CRS (Table F.1) with  $p < 0.05$ . Therefore, the major binding phases in site D-B for HgT and MeHg species were Fe/Mn oxyhydroxides and sulfides. Methylation potential (%MeHg) were also significantly associated with Fe, Mn, AVS, CRS & Corg with  $0.01 < p < 0.05$ . This indicates the importance of the reductive dissolution of Fe/Mn hydroxides for the bioavailability of dissolved Hg species for methylation. Important relationship was established between Corg and % MeHg ( $r^2 = 0.922$ ;  $p < 0.01$ ) (figure F.3) revealing the relevance of organic carbon content to fuel up the heterotrophic bacteria deriving methylation. Previous studies have showed that MeHg production is enhanced in organic-rich sediments (Ullrich et al, 2001; Rimondi et al, 2012)

with significant relation established between % MeHg and Corg in Cheesequake estuary ( $r^2=0.835$ ) (Choi and Bartha, 1994).

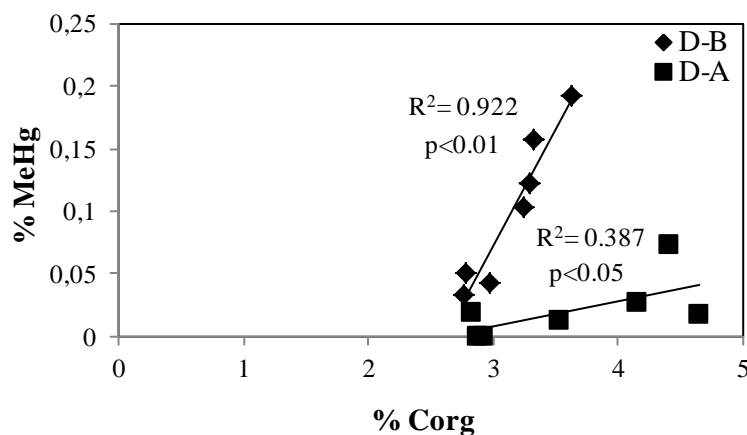


**Fig.F.3.** Correlation between percentage organic carbon (% Corg) and percentage methylmercury formation (%MeHg) in Deule site (D-A and D-B).

Additionally, methylation is contributed to an old and recent events of MeHg production since significant associations were found between %MeHg and AVS ( $r^2=0.914$ ,  $p<0.01$ ) (figure F.4) and CRS ( $r^2=0.722$ ;  $p<0.05$ ) (figure F.5). This site is characterized by high sulfide concentrations with an average value of AVS ( $n=6$ )  $1799 \pm 114$  mg/Kg and an average value of CRS ( $n=5$ )  $7644 \pm 92$ . This is due to the accumulation of sulfides and their subsequent pyritization during the past decades of intensive methylation with the persistence of favoring conditions for methylation. Metal sulfide minerals (ZnS, CdS...ect.) discharged by the old smelter could also participate with active old and recent methylation activities and in the build-up sulfide in the sediments. Therefore, high levels of sulfides are relevant in scavenging and trapping processes of mercury in deep sediments.  $HgS^{\circ}$  is shown to be the bioavailable pool for methylation, that is tightly coupled with the concentrations of S(-II) (Benoit et al, 1999).  $HgS^{\circ}$  becomes dominant at low concentrations of S(-II), however at high levels,  $HgHS^{2-}$  becomes the dominant complex (Hammerschmidt et al, 2004). The overall partitioning of Hg depends on the interaction of Hg with different factors, including organic matter, sulfides, Fe/Mn oxyhydroxides under oxic and anoxic conditions respectively (Merrit and Amirbahman, 2009). A poor association has been found between  $\log K_D$  and  $HgT_{PW}$  was discerned with a significant correlation between %MeHg and  $HgT_{PW}$  ( $r^2= 0.8836$ ;  $p<0.01$ ), revealing that dissolved Hg is the bioavailable pool for methylation. Since, site B is characterized by high % methylation as compared to site D-A.

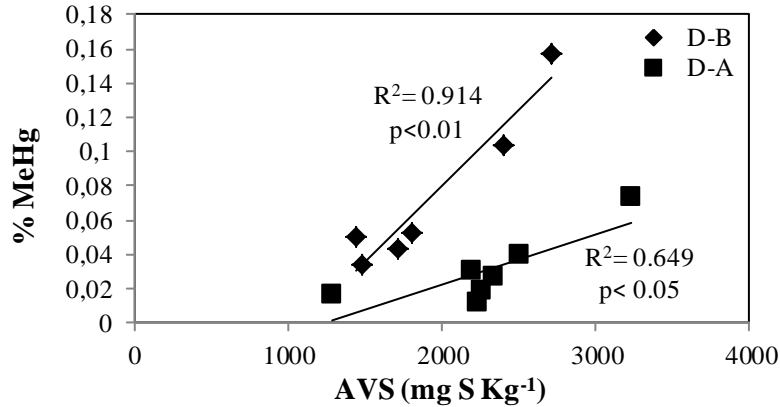


**Fig.F.4.** Associations between acid volatile sulfides (AVS) and percentage of methylmercury formation (% MeHg) in Deûle sites (D-A and D-B).

In D-A site, insignificant association between HgT and MeHg was found. Mn oxyhydroxides and AVS are relevant binding phases controlling the dissolution of HgT solid phases ( $r^2=0.553$ ;  $p<0.05$  (Mn),  $r^2=0.538$ ;  $p<0.05$  (AVS),  $r^2= 0.888$ ;  $p<0.001$  (HgT<sub>PW</sub>)). Sulfides, particularly CRS and Corg are the major controllers of MeHg in solid phase ( $r^2= 0.715$ ;  $p<0.05$  (CRS),  $r^2=0.636$ ;  $p<0.05$ (Corg)). This reflects the affinity of MeHg to organic and sulphide bulk phases. From correlation coefficients, methylation (%MeHg) seems not to be controlled by dissolution of Fe solid phases, eventhough a relation was discerned with Mn ( $r^2=0.542$ ,  $p<0.05$ ) but not with Fe. Therefore, there are other binding phases implicated in the bioavailability of Hg species, such as dissolution of organic matter and sulfide phases. Significant correlation between %MeHg and AVS ( $r^2=0.645$ ,  $p<0.05$ ) (figure F.4), with weaker association with CRS ( $r^2=0.408$ ,  $p<0.1$ ) (figure F.5) as shown in previous studies (Mikac et al, 1999; Kadlecova et al, 2011) with an important association discerned with Corg ( $r^2=0.387$ ,  $p<0.05$ ) (figure F.3). The strong relationship of MeHg with the active freshly precipitated sulfides, indicate that MeHg production in this site, is a more recent event. In the light of the weaker occurrence of % MeHg in site A than site B, less significant associations were found between LogK<sub>D</sub> and HgT<sub>PW</sub> and %MeHg and HgT<sub>PW</sub> with relevant association between logK<sub>D</sub> and Corg ( $r^2= 0.838$ ,  $p<0.001$ ). This reveals that mercury is preferentially retained to the organic solid phase in which exerts a prevailing effect on Hg binding, transformation and transport processes (Wallschlager et al, 1998).

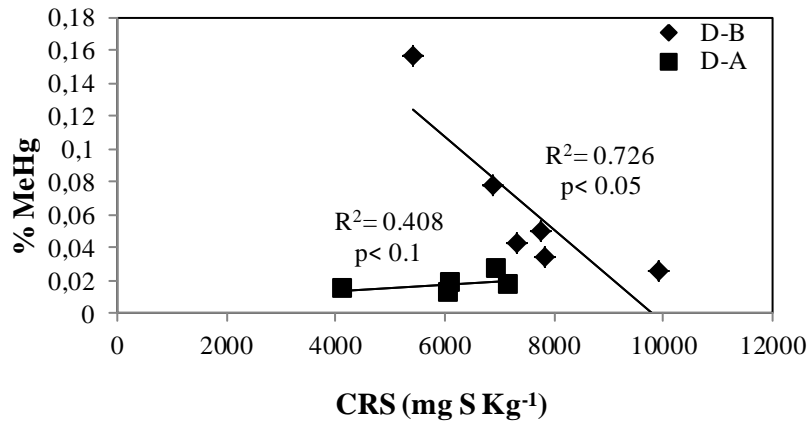


**Fig.F.5.** Correlations between chromium reactive sulfides (CRS) and percentage of methylmercury formation (% MeHg) in Deûle sites (D-A and D-B).

In L-C site, weak association was also found between MeHg and HgT with significant relation between HgT and %MeHg ( $r^2=0.744$ ,  $p<0.001$ ). For HgT, sulfides and Corg out-competed Fe/Mn hydroxides as binding phases for Hg species ( $r^2=0.554$ ;  $p<0.01$  (AVS),  $r^2=0.363$ ;  $p<0.05$  (CRS),  $r^2=0.414$ ;  $p<0.05$  (Corg)). The predominant binding phase for MeHg is shown to be sulfides, since good relation was established between the two parameters ( $r^2=0.466$ ,  $p<0.01$  (CRS)). Weak but still significant correlations were detected between % MeHg and AVS ( $r^2=0.402$ ;  $p<0.05$ ) (figure F.6). It appears that other factors may control methylation more probably organic matter. Therefore, correlation was made between % MeHg and Corg, and was found to be important ( $r^2=0.557$ ;  $p<0.01$ ) (figure F.7) emphasizing the overriding control of organic matter on methylation. Significant correlations were found between  $HgT_{PW}$  and  $\log K_D$  ( $r^2=0.676$ ;  $p<0.01$ ) and Corg ( $r^2=0.625$ ;  $p<0.05$ ), emphasizing the active dissolution of organic phase by intense microbial degradation and the role of dissolved Hg for methylation. This is elucidated by the high % MeHg found in L-C site. This site is distinguished by high % MeHg, assuming its possible export from other sources. Yet, the important relation discerned between Corg and AVS ( $r^2=0.719$ ;  $p<0.01$ ) along with %MeHg and Corg and AVS make evident the relevance of *in situ* methylation of mercury.

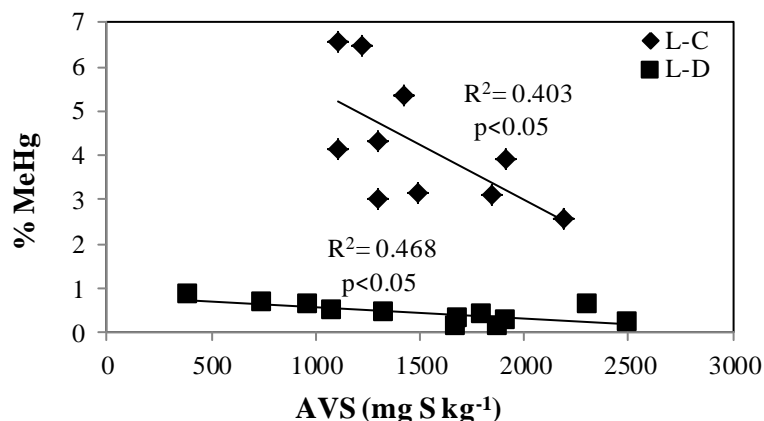


**Fig.F.6.** Correlations between acid volatile sulfides (AVS) and percentage of methylmercury formation (% MeHg) in Lys sites (L-C and L-D).

In L-D site, weak relations were established between HgT and MeHg, still significant correlations were determined for HgT and %MeHg ( $r^2=0.496$ ;  $p<0.01$ ). While, sulfides and Corg govern the distribution of Hg species for the whole sediment depth ( $r^2= 0.317$ ;  $p<0.05$  (AVS),  $r^2=0.529$ ;  $p<0.01$  (CRS),  $r^2=0.575$ ;  $p<0.01$  (Corg)). Methylation appears not to be controlled by the dissolution of Fe/Mn oxides but rather with sulfides (AVS) and Corg since significant relations were found of  $r^2= 0.468$ ;  $p<0.05$ ,  $r^2=0.640$ ;  $p<0.01$  respectively (figure F.6 & F.7). Dissolved HgT is suggested to prevail since strong correlations were determined between  $\log K_D$  and  $HgT_{PW}$  ( $r^2=0.690$ ;  $p<0.01$ ).

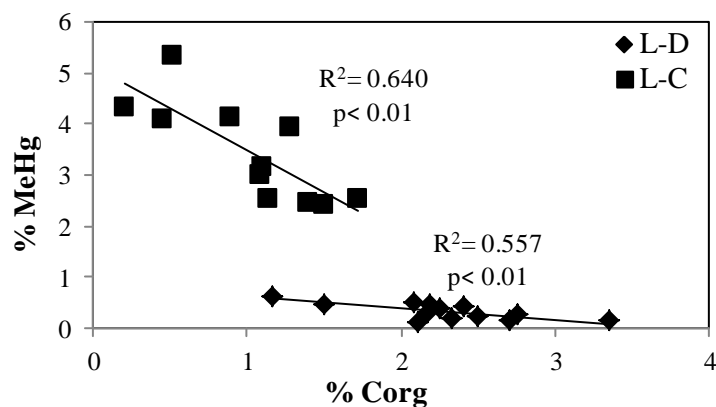


**Fig.F.7.** Correlations between percentage of organic carbon (%Corg and percentage of methylmercury (% MeHg) formation in Lys sites (L-C and L-D).

Overall, the relations between  $\log K_D$  and  $Hg_{TPW}$  were more determinative for Lys sites than Deûle sites, accounting for the more intensive methylation events in Lys sediments. Moreover, no associations were established between %MeHg and  $Hg_{TPW}$  in all study sites, except for D-B ( $r^2=0.883$ ,  $p<0.01$ ). Therefore,  $Hg_{TPW}$  cannot be the available pool for methylation in the active sites of L-C, L-D as opposed to D-B site. In sulfidic-rich environments such as that of D-B,  $Hg_T$  in pore water control methylation process since good associations were discerned, while in Lys-sites no relationship was discovered between the two latter controls. It is unclear till now, which form of Hg is bioavailable. Many studies have demonstrated that methylation is driven by dissolved inorganic mercury (IHg) (Hammerschmidt and Fitzgerald 2006) others have evidenced that methylation is correlated to particulate IHg species and not  $Hg_T$  (Benoit et al, 1999). Microbial availability of IHg is controlled by  $Hg-S(-II)$  ( $HgS^0$ ) (Benoit et al, 1999). In contrary, Jay et al. (2002) have shown no relation between the increased solubility of IHg and MeHg methylation.

Significant correlations between  $Hg_T$  and MeHg were found in previous studies (Benoit et al, 1998; Kadlecova et al, 2011; Hammerschmidt and Fitzgerald, 2006; Ouddane et al, 2008; Rimondi et al, 2012; Sunderland et al, 2006) and others demonstrated lack of dependence between  $Hg_T$  and MeHg in the upper surface sediments (Kadlecova et al, 2011). Lack of relations were established between  $Hg_T$  and MeHg in L-C, L-D and D-A sites as shown in previous studies (Tseng et al, 2001; Conaway et al, 2003; Han et al, 2007; Miles et al, 2010; Yanez et al, 2013). This points out to the less significant role of  $Hg_T$  and the prevalence of other factors in these sites. It seems that in Lys sites, the available fraction of  $Hg_T$  is not a limiting factor for methylation. Still, D-B has showed important associations between  $Hg_{TS}$  and MeHg in the bulk phase, primarily ascribed to the significant high  $Hg_{TS}$ . This is coherent



with a recent study, that showed that MeHg production is enhanced with increasing concentrations of mercury (Glimour et al, 2011).

Numerous studies have demonstrated significant relations between Hg and organic matter (Conaway et al, 2003; Benoit et al, 1998; Gagnon et al, 1997; Gray and Hines, 2009; Mikac et al, 1999; Shi et al, 2005; Lambertsson et al, 2006; Rimondi et al, 2012). It is shown that sediments with high organic content host the highest methylation with important MeHg concentrations (Macalady et al, 2000; Ullrich et al, 2001; Stoichev et al, 2004; Rimondi et al, 2012). However, this is not found in our study case, highest % MeHg was observed in Lys river sites of minimal Corg as compared to the Deûle river. MeHg concentrations is needed to be considered with other important geochemical characteristics such as sulphides, fine fraction, heterotrophic bacterial load and activity, dissolved inorganic mercury, and dissolved organic carbon. Therefore, the relationship between Corg and Hg could not be found in many aquatic sediments, surpassed by other determinative parameters (Thomas et al, 2002; Yan et al, 2012).

Significant correlations between % Corg and % MeHg were demonstrated in all sites of Deûle and Lys rivers. However, two different trends are noted between the two sites as shown in figures F.3 & F.7. In Deûle sites, there appears to be an increasing tendency of % MeHg with Corg. On the other hand, Lys sites showed a decreasing tendency of % MeHg with Corg. Sunderland et al. (2006) have found high MeHg methylation rates in the presence of both high levels of dissolved organic matter (DOM) and S(-II). This is explained by the formation of a mixed DOM-Hg-SH complex in organically sulfide rich sediments. In fact, the presence of DOM can enhance the bioavailability of Hg(II) by stabilizing HgS nanoparticles against growth and aggregation (Gerbig et al, 2011). Whereas, in Lys sites, increasing levels of Corg may have negative effect on %MeHg, efficiently trapping Hg species by forming stable complexes resistant to transformation. The high affinity of Hg to organic matter is attributed to high stability constant formed between Hg and thiol functional groups of organic compounds. High organic content in bulk phases of sediments, can lead to high dissolved organic carbon (DOC) by equilibrium process although it is not measured in this study. DOC is among the main geochemical parameters affecting Hg methylation (Balogh et al 2008; Yan et al, 2012). High DOC tends to have inhibitory effects on the bioavailability of Hg(II) (Simonin et al, 1995; Grieb et al, 1990). Barkay et al. (1997) showed that increasing concentrations of DOC reduce the availability of Hg(II) which is more pronounced under

neutral conditions. This can ultimately affect the speciation of Hg by forming strong complexes with Hg species influencing the amount of inorganic mercury available for methylating bacteria, since DOC molecules are too large to cross cell membrane of bacteria (Ullrich et al, 2001).

Again, a general decreasing trend is observed when all sites % MeHg is correlated with Corg (figure F.8). This shows the important role and control of organic carbon on the fate and bioavailability of mercury with important associations with % MeHg ( $r^2$ : 0.664;  $p < < 0.001$ ). Another important feature observed is the increasing tendency of %MeHg with sulfides (AVS) in D-A & D-B, as opposed to Lys sites following a decreasing tendency with AVS. Sulfides control the speciation of mercury by the formation of neutral  $HgS^0$  species, known to be as the bioavailable form for methylation. Sulfide concentrations above certain limits as defined by many studies can decrease methylation by the formation of strong complexes, less bioavailable to methylating microorganisms. However, in D-A & D-B increasing levels of AVS promoted methylation, by the solubilization of solid phase mercury rendering more bioavailable pool of mercury. In sulfidic rich environments, the formation of polysulfides and dissolved organic carbon can solubilize Hg (Paquette et al, 1995). This is confirmed by high HgT in porewater observed in these sites, more discussion will be provided in following sections.

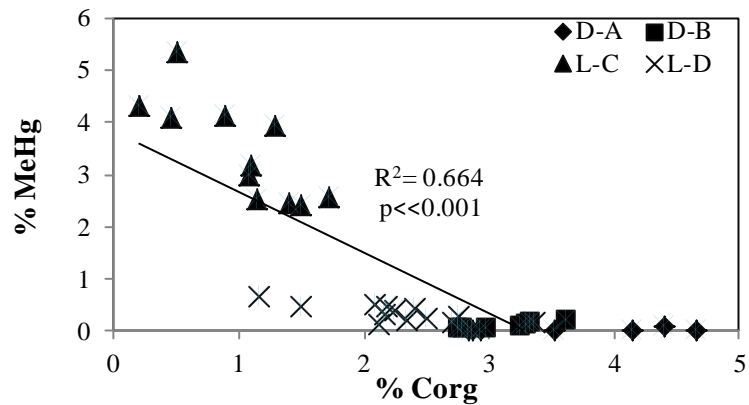


**Fig.F.8.** Correlation between percentage of organic carbon (% Corg) and percentage of methylmercury formation (% MeHg) in all sites (D-A, D-B, L-C & L-D).

Despite the fact that the major portion of sulfides is supplied by the ore minerals discharges of the past smelter in the Deûle sites particularly D-B. Significant association between % Corg and AVS with an increasing trend is established for all sites with  $r^2 = 0.539$ ;  $p < < 0.001$  (figure F.9). This demonstrates the active microbial degradation of organic matter with the use of

electron acceptors such as sulfate ( $\text{SO}_4^{2-}$ ) implying its reduction to sulfides  $\text{S}^{2-}$ . The good associations found between % MeHg and % Corg, AVS in all sites shows the significance of sulfate reducing bacteria (SRB) activity in methylating mercury. Thereby, mercury is produced *in situ* in the Lys & Deûle rivers rather than exported from other sources.

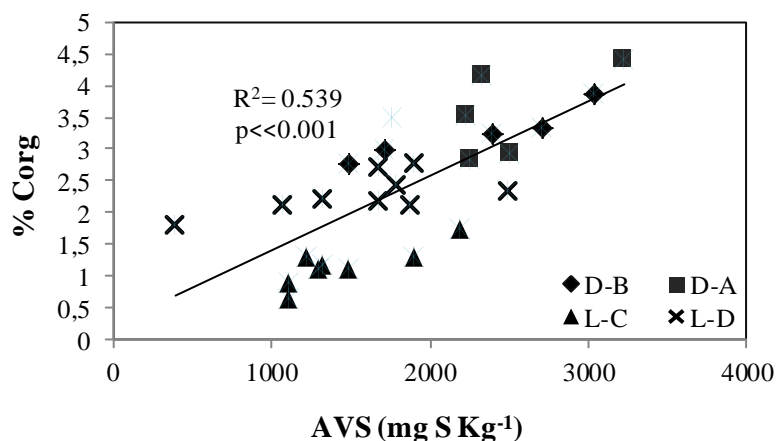


**Fig.F.9.** Correlation between percentage of organic carbon (% Corg) and acid volatile sulfides (AVS) in all sites (D-A, D-B, L-C & L-D).

Despite the higher levels of HgT in sediments of the the Deûle sites, lower % MeHg is found as compared to Lys sediments. This finding is similar to other areas affected by mining operations of intense Hg contamination and chloroalkali industries, where concentrations of MeHg found are not far from the background concentration of MeHg resulting in low %MeHg (Canario et al, 2005; Bloom et al, 1999; Higuera et al, 2006; Hines et al, 2000; Martin-Doimeadios et al; 2000). Estuaries and brackish waters are characterized by high methylation potentials, for the favoring conditions of low but unlimited supply of sulfate (Lambertsson and Nilsson, 2006). Because, Lys river terrestrial surroundings are of agricultural nature, it is probable that the use of sulfate fertilizers have contributed to increased nutrient load in the river further strengthening methylation. It seems in highly polluted environments, methylation can be reduced as compared to pristine or less contaminated areas. The high metal pollution, high sulphidic and organic contents are all factors affecting the bioavailability of Hg and activity of methylating bacteria in the Deûle river. In comparison to the Deûle river, Lys sites conditions seem to be optimal for Hg methylation, attributed to the coupling factors of lower sulphidic contents, lower HgT contents and organic carbon and high nutrients (Sulfate). In sulphate-limited environments, DOC is used by heterotrophic bacteria as source of energy and therefore its presence is indispensable for stimulating methylation in sediments (Ravichandran et al, 2004).

**Table F.1.** Correlation matrix between mercury species and biogeochemical determinants from Deûle river (D-A (n=8); D-B (n=7)) and Lys river (L-C and L-D (n=12)).

	Fe	Mn	AVS	CRS	LogK <sub>D</sub>	Corg	HgT <sub>S</sub>	HgT <sub>PW</sub>	MeHg	%MeHg
D-B										
HgT <sub>S</sub>	<b>0.691*</b>	<b>0.752*</b>	0.182	0.441	0.028	0.098	1	<b>0.669*</b>	<b>0.795**</b>	<b>0.872**</b>
HgT <sub>PW</sub>	<b>0.557*</b>	<b>0.704*</b>	0.091	<b>0.725</b>	0.181	0.102	<b>0.669*</b>	1	<b>0.873**</b>	<b>0.884**</b>
MeHg	<b>0.684*</b>	<b>0.864**</b>	0.077	<b>0.780*</b>	0.029	0.092	<b>0.795**</b>	0.873**	1	<b>0.965***</b>
%MeHg	<b>0.738**</b>	<b>0.864**</b>	<b>0.914**</b>	<b>0.722*</b>	0.011	<b>0.922**</b>	<b>0.872**</b>	<b>0.884**</b>	<b>0.965***</b>	1
D-A										
HgT <sub>S</sub>	0.205	<b>0.553*</b>	<b>0.538*</b>	0.0003	<b>0.411*</b>	0.107	1	<b>0.888***</b>	0.006	0.106
HgT <sub>PW</sub>	0.165	<b>0.596*</b>	0.303	0.065	0.127	0.007	<b>0.888***</b>	1	0.003	0.173
MeHg	0.234	0.231	0.008	<b>0.715*</b>	0.029	<b>0.636*</b>	0.005	0.003	1	<b>0.823**</b>
%MeHg	0.035	<b>0.542*</b>	<b>0.645*</b>	<b>0.408</b>	0.024	<b>0.387*</b>	0.107	0.173	0.823**	1
L-C										
HgT <sub>S</sub>	0.040	0.138	<b>0.554**</b>	<b>0.363*</b>	0.028	<b>0.414*</b>	1	0.138	0.077	<b>0.744***</b>
HgT <sub>PW</sub>	0.009	0.031	0.182	0.011	<b>0.676*</b>	<b>0.625*</b>	0.137	1	0.149	0.126
MeHg	0.171	0.006	0.182	<b>0.466**</b>	0.169	0.062	0.077	0.149	1	0.031
%MeHg	0.216	0.095	<b>0.402*</b>	0.129	0.023	<b>0.557**</b>	<b>0.744***</b>	0.126	0.032	1
L-D										
HgT <sub>S</sub>	0.091	0.004	<b>0.317*</b>	<b>0.529**</b>	0.027	<b>0.575**</b>	1	0.232	0.0005	<b>0.496**</b>
HgT <sub>PW</sub>	0.019	0.019	0.059	<b>0.306*</b>	<b>0.690**</b>	0.059	<b>0.232</b>	1	0.017	0.089
MeHg	0.049	0.00001	0.101	0.004	0.024	0.054	0.001	0.017	1	<b>0.392**</b>
%MeHg	0.059	0.007	<b>0.468*</b>	<b>0.352*</b>	0.117	<b>0.640**</b>	<b>0.496**</b>	0.089	<b>0.392**</b>	1

Bold: p<0.1; bold+\* p<0.05; bold+\*\* p<0.01; bold+\*\*\* p<0.001

#### **F.4.4. Spatial distribution dissolved and particulate HgT in water column**

There was a slight decline in concentrations of Hg in surface river water ( $HgT_D$ ) from D-A ( $20.8 \text{ ng/L} \pm 0.8$ ) decreasing slightly, downstream at the confluence with Lys river at Lys-D to  $19.4 \text{ ng/L} \pm 1.71$  and  $18.5 \text{ ng/L} \pm 1.50$  at Lys-C (Table F.2). Various parameters can influence the distribution of  $HgT_D$ , in which dissolved organic matter (DOC) is the most substantial environmental control ruling the spatial variation of  $HgT_D$  between sites (Coquery et al, 2003). DOC can promote the solubilization of Hg by complexation promoting its mobility from solid phase to water (Wallschlager et al, 1996). The enhanced mobility results in increased water column concentration. Additionally, the degradation of organic matter of suspended particles can lead to the release of trapped Hg, thereby enhancing Hg levels in surface waters. Similarly, for particulate Hg ( $Hg_P$ ), there was a decreasing trend from Deûle sites, the ancient source of pollution ( $4.3 \text{ } \mu\text{g/g} \pm 0.31$ ) to Lys C ( $1.5 \text{ } \mu\text{g/g} \pm 0.42$ ) and Lys D ( $2.6 \text{ } \mu\text{g/g} \pm 0.91$ ) (Table F.2). Suspended particles seem to be enriched with mercury relative to erosion of sediment bed surface of highly polluted Deûle sites, contributing to suspended particles consisting of the finest granulometric fraction.

**Table F.2.** Concentrations of mercury species and partition coefficient of HgT in surface water and in sediment phase.

Sites	Surface water			Porewater		Sediment		
	HgT <sub>D</sub> (ng/L)	HgT <sub>P</sub> (μg/g)	Log K <sub>D</sub> (L/Kg)	HgT <sub>PW</sub> (ng/L)	HgT <sub>S</sub> (μg/g)	MeHg (ng/g)	% MeHg	Log K <sub>D</sub> (L/Kg)
D-A	20.81 ± 0.80	4.3 ± 0.31	2.3	16 ± 3.20	9.92 ± 2.22	3.56 ± 1.31	0.02	5.81
D-B	8 ± 0.71	3.8 ± 0.25	2.7	9.83 ± 2.03	9.11 ± 1.85	7.61 ± 3.67	0.09	5.97
L-C	18.51 ± 1.50	1.5 ± 0.42	1.9	5.88 ± 0.35	0.042 ± 0.0023	1.63 ± 0.09	4.21	4.13
L-D	19.41 ± 1.70	2.6 ± 0.91	2.1	11.4 ± 3.50	0.527 ± 0.01	1.86 ± 0.23	0.42	4.82

At the river confluence,  $HgT_P$  dropped off by a factor 2 as compared to the Deûle sites. The polluted water of Deûle River is diluted by Lys additional water. The spatial distribution of Hg in the basin is associated to the distance from the riverine pollution source. Strong riverine flows and winds can cause both erosion and suspension, transporting more Hg- rich sediment away from their origins (Foucher et al, 2009). In addition to the participation of boat traffic in the sediment remobilization events of the river.

However  $HgT_D$  did not follow the same trend as  $HgT_P$ , in which it decreased slightly after the rivers merging. This is in contrast to the spatial distribution of  $HgT_D$  at Idrijca river where concentrations of  $HgT_D$  have decreased from 283 ng/L at the closest site to the source point pollution to < 0.5 ng/L measured at remote sites after river confluence with river Soca (Kocman et al, 2011). Mercury tends to decrease further downstream the river relative to its high volatile nature and its scavenging by iron and manganese hydroxides and organic matter entraining their deposition (Jenne, 1970). The distribution of  $HgT_P$  seems to be controlled by similar factors governing the distribution of suspended matter (fine grained sediments). The dissolved HgT in surface water were similar to those measured downstream Idrijca river (10-15 ng/L) affected by former Hg mine (Kocman et al, 2011) with extremely higher  $HgT_D$  proximal to the mine (283 ng/L). Likewise,  $HgT_D$  was significantly elevated near El Entredicho mine (11 000- 13000 ng/L), decreasing downstream to reach 9.1 ng/L at distant places (Gray et al, 2004). Downstream the gold mining activities of Sacramento River basin at Cache Creek (Sierra Nevada),  $HgT_D$  reached 12 ng/L (Domagalski et al, 1998). Lower values of  $HgT_D$  were observed in Thur River affected by an active chloroalkali plant (0.7-1.3 ng/L) (Hissler et al, 2006).

#### **F.4.5. Porewater distribution**

The vertical profiles of Fe in porewater were variable within sediment depth in all studied sites (figure F.2 (d), (h), (l), (p)). The highest average values were that of L-D 6.52  $\mu\text{g/L}$  >D-B of 6.01  $\mu\text{g/L}$  < L-C 4.55  $\mu\text{g/L}$  < D-A 1.22  $\mu\text{g/L}$ . On the other hand, sediment depth pore water profiles of Mn followed homogenous trend with comparable average values in Lys sites (0.24 ng/L), D-A (0.33 ng/L), D-B (0.83 ng/L). The notable high concentrations of Fe and Mn occurring in D-B (the site of highest methylation in the Deûle river) is attributed to the accumulation of sulfides through long years of MeHg production and discharges by the former smelter. Subsequently, developing anoxic conditions significantly more important than other sites.

The porewater distribution of HgT followed variable pattern across sites from high concentrations at D-A with an average value of  $17.39 \pm 0.64$  ng/L to lower levels obtained in L-D with an average value  $11.42 \pm 0.45$  ng/L and L-C of  $3.98 \pm 0.41$  ng/L. All sites demonstrated low HgT<sub>PW</sub> near sediment-water interface and a progressive increase in concentrations with depth. In solid phase, Hg can associate with many sedimentary phases, including clay, Fe and Mn oxyhydroxides, sulfides and organic matter (Huerta-Diaz and Morse, 1990). At surface suboxic conditions, dissolved mercury species are scavenged by Fe/Mn oxyhydroxides, whereas in deeper parts of the sediments, reducing conditions promote the dissolution of Fe/Mn oxides and sulfides. HgT<sub>PW</sub> in L-C and L-D sediments were in the range to those reported in other less contaminated sites as in St. Lawrence estuary (0.87-4.35 ng/L) (Goulet et al, 2007), San Francisco Bay-Delta (2.2 ng/L-10 ng/L) (Choe et al, 2004), Patuxent River (2.2-8.7 ng/L) (Benoit et al, 1998), Thau lagoon (2.3-18.49 ng/L) (Muresan et al, 2007). The average value of HgT<sub>PW</sub> in D-A is 17.39 ng/L which is 7 times higher in magnitude than D-B ( $10 \text{ ng/L} \pm 0.32$ ) and L-D ( $11.42 \text{ ng/L} \pm 0.45$ ). D-B site which is the nearest to the pollution source, did not exhibit higher porewater Hg concentrations than D-A despite the fact that this site contained over 3.5 times more sedimentary MeHg. Porewater values of Deûle sediments are comparable to others found in sediments affected by point source pollution as Lavaca Bay (10-21.8 ng/L) (Bloom et al, 1998), Everglades (2.17-16.32 ng/L) (Glimour et al, 1998), Gulf of Trieste (3.4-14.39 ng/L) (Covelli et al, 1999). The high values of Hg porewater can be explained by sulfide dissolution of Hg(II) (Dyrssen and Wedborg, 1991) or the release of Hg from the reduction of Fe oxyhydroxides (Gobeil et Cossa 1993). Significant associations were found between HgT<sub>PW</sub> and HgT<sub>S</sub> in bulk sediment in both Deûle sites ( $r^2=0.881$ ;  $p<0.001$  A,  $r^2=0.669$ ;  $p<0.05$  B) while weaker and insignificant correlations were detected for Lys sites. The distribution of HgT<sub>PW</sub> and HgT<sub>S</sub> were mirror images in the Deûle sites. This suggests that concentrations of dissolved mercury are controlled by dissolution processes out of equilibrium of solid phases. Contrary to the Deûle sites, mercury levels in porewater of the Lys river are not significantly correlated to HgT<sub>S</sub>, reflecting exchange equilibrium between the dissolved and solid phase where HgT<sub>PW</sub> and HgT<sub>S</sub> distributions were parallel. Many proxies can affect the availability and the release of Hg including organic matter mineralization in the oxic zone, Fe and Mn oxyhydroxides reduction in the suboxic zone and finally solubilization of HgS<sup>0</sup> complexes enhanced by the presence of polysulfides (Benoit et al, 1998).



#### F.4.6. Controls of mercury porewater

As demonstrated in figure F.2, vertical profiles of HgT in pore water were coincident occasionally with those of Fe and sulfides. The dissolved mercury species in D-B is controlled by Fe/Mn hydroxides and sulfide phases. This is confirmed by significant correlations found between HgT<sub>PW</sub> and Fe, Mn ( $r^2 = 0.557$ ;  $p < 0.05$ ,  $r^2 = 0.704$ ;  $p < 0.05$ ) and HgT<sub>PW</sub> with CRS ( $r^2 = 0.725$ ;  $p < 0.1$ ). In D-A, dissolved mercury is more associated to the dissolution Mn oxyhydroxides phases ( $r^2 = 0.596$ ;  $p < 0.05$ ) than sulfide solid phases. In suboxic conditions, solid phases (Organic matter, oxides/hydroxides, and sulfides) contribute to HgT content in porewater. HgT<sub>PW</sub> in D-A is two times higher in magnitude than D-B, attributed to higher levels of AVS (2397 mg/Kg) and lower CRS (6062 mg/Kg) than site B. This is also explained, by the increased dissolution of mercury phases in the form of soluble HgS complex induced by S<sup>0</sup> generated by polysulfides. The lower concentrations of dissolved mercury observed in D-B can be attributed to the precipitation of insoluble HgS and the coprecipitation with iron sulfides (Gobeil and Cossa, 1993) since D-B site is characterized by high values of CRS (7644 mg/Kg). At oxidized conditions, Fe/Mn oxides are known to scavenge mercury and reduce its concentrations in the dissolved phase. MeHg concentrations in the sediment phase are more pronounced in D-B, this suggest a more active sulfate reduction by SRB. MeHg production is associated with the production of hydrogen sulfides that could potentially transform Hg(II) into metacinnabar (HgS) and also convert MeHg into dimethylmercury sulfides with further decomposition into volatile dimethylmercury and metacinnabar (Baldi et al, 1995). These transformations can ultimately influence Hg contents in porewaters.

In L-C site, the concentration of Hg in pore water is governed by the dissolution and degradation of organic matter phases. It is verified by significant associations found between HgT<sub>PW</sub> and Corg ( $r^2 = 0.625$ ;  $p < 0.05$ ). Whereas, in L-D site, it seems that sulfides controlled the dissolution/precipitation processes with good associations discerned between HgT<sub>PW</sub> and CRS ( $r^2 = 0.306$ ;  $p < 0.05$ ). D-B and L-C are characterized by lower HgT<sub>PW</sub> than other sites. This is explained by higher methylation activities, contributing to higher reducing conditions. Therefore, affecting negatively the mobility of Hg (Hines et al, 1997).

Deûle A and B are considered to be the most affected by the discharges of the former smelter. However, HgT<sub>PW</sub> are low as compared to Seine (35-350 ng/L) with significantly lower average HgT<sub>S</sub> (0.3-1 µg/L) (Mikac et al, 1999), Saguenay fjord (17-500 ng/L) with average

HgT<sub>s</sub> 10 µg/g (Gagnon et al, 1997), Tagus estuary (15 ng/L-1.26 µg/L) with an average HgT<sub>s</sub> (0.6-12 µg/g) (Canario et al, 2003). Similar concentrations of porewater were observed in Gulf of Trieste affected by Hg pollution from Hg mining (10-13.58 ng/L), but with lower HgT<sub>s</sub> (2.82-3.84 µg/g) (Covelli et al, 1999). Higher porewater concentrations (0.014 µg/L-1.16 µg/L) were observed in Tagus estuary affected by discharges of chloroalkali plant with similar HgT<sub>s</sub> (4.6 - 12 µg/g) (Canario et al, 2003). Mercury behavior and bioavailability in aquatic environments may differ from one site to another, depending on the intrinsic characteristics of the site controlling Hg mobility and dynamics.

Dissolved Mn and Fe can be used as indicators for redox conditions in sediment phase. The low concentrations of dissolved Fe and Mn near surface water interface followed by the increase in their contents within the first 2 cm depth indicate the weak oxygen penetration and the development of suboxic conditions. Under these conditions, Fe/Mn oxyhydroxides are reduced releasing Hg into porewater. In sub-oxic zones, Fe/Mn hydroxides are used as electron acceptors for the microbial degradation of organic matter, consequently releasing the sequestered mercury from both phases. The occurrence of high levels of Hg in porewaters near sediment water interface could be attributed to organic matter degradation (Gobeil and Cossa, 1993) as noted in D-B with Fe<sub>PW</sub> maxima (12.33 µg/L) occurring at sub-surface level. Organic matter is the major binding site of Hg in oxic sediments while in anoxic conditions, sulfides are important controllers of Hg partitioning and availability (Winfrey and Rudd, 1990). The relatively low Hg concentrations in porewater in L-C of 1 ng/L and 0.95 ng/L for L-D occurring at 6 cm and 9 cm sediment depth respectively can be explained by the possible precipitation of HgS and coprecipitation with iron sulfides (Gobeil and Cossa, 1993). The formation of dissolved complexes with polysulfides and organic matter further enhances the solubilization and mobility of mercury (Emerson et al, 1983). Sulfides (pyrite FeS, Fe<sub>2</sub>S) are known to be important scavengers and sinks of mercury in anoxic sediments. Upon remobilization, Hg associated to AVS may be released to porewater since AVS are reactive to oxygen (Huerta-Diaz and Morse, 1992). Important peaks of mercury in anoxic zones can be explained by the oxidative releases of mercury from sulfidic phases mainly from AVS due to remobilization (bioirrigation, bioturbation, resuspension) as observed in all studied sites (Gagnon et al, 1996). Moreover, Bioturbation can promote Hg methylation and mercury diffusive fluxes from sediments (Hammerschmidt et al, 2004).

Organic matter may also control mercury partitioning between solid and dissolved phases. Important correlations between  $\log K_D$  of Hg species and sedimentary organic carbon were found in Lavaca Bay, TX (Bloom et al, 1999) and Long Island Sound (Hammerschmidt et al, 2004). Additionally, organic matter was found to be the major controller of Hg phase distribution in surface sediments of Baltimore Harbor (Mason and Lawrence, 1999). However in our study sites, only D-A and L-D presented associations between  $\log K_D$  of HgT and Corg with  $r^2 = 0.838$   $p < 0.001$  and  $r^2 = 0.432$ ;  $p < 0.01$  respectively. However, in D-B and L-C sites, insignificant associations were determined between  $\log K_D$  and Corg. With respect to %MeHg in study sites in both rivers, the percentage of MeHg increases in sites with less associations with organic matter such as in L-C as compared to L-D and D-B as compared to D-A. It is supposed that the association of Hg with Corg is less favorable to methylation as opposed in L-C where less association with Corg can indeed enhance methylation through solubilization.

The presence of typical levels of organic matter in sediments can enter into competition with sulfides for the overcontrol of Hg speciation in sediments and porewater phases. Both rivers are dominated by agricultural activities, in addition to urban discharges in the Deûle river which accentuate, the presence of organic ligands with high stability constant of  $10^{30}$ . The presence of such organic substances can break down the complexes formed between sulfides and mercury (Hsu et Sedlak 2003).

The concentration of mercury in porewater is comparable to the concentration of Hg in surface water. This means, that recent sediment could not be the source of dissolved mercury in water column. There must exist other sources of Hg concentrations found in surface water and particulate phase. The high values of mercury in surface water in the Deûle river and L-D sites may be attributed the proximity of the latter sites to the source of pollution (former smelter) and to the possible active methylation in low-oxygen zones in the water column. Also, atmospheric deposition of Hg and the subsequent oxidation of  $Hg^0$  in the presence of Cl<sup>-</sup> can also participate in observed Hg pool (Yamamoto et al, 1996) and the active dissolution of Hg bulk phases by DOC complexation. In addition to the colloidal fraction of Hg complexed with humic-hydrous oxides and Fe hydroxides could also contribute to high mercury contents in water, since the large filters  $< 0.45 \mu m$  were used in this study for the defined dissolved mercury (Roth et al, 2001). Elevated levels of HgT<sub>P</sub> in water can originate from the weathering processes and contaminated soil erosion. Hg binds to humic substances

and Al/Fe hydroxides of the weathering products and is subsequently leached to river water. Substantial hydrological events of heavy-rain, snow melting, flood events, wind, fluvial discharges and the associated river turbulence are a characteristic of the region's climate trend during spring season, coinciding with our sampling period (March). Heavy rainfall can cause overland flow and consequent surficial runoff that results in high Hg concentration in surface water. Therefore, high quantities mercury deposited in the surrounding river boundaries near D-B site can be easily leached, eroded and end up in surface water during such events.  $HgT_P$  can be redistributed throughout the river by wind and seasonal high river discharges. In addition to the contribution of rainfall to Hg in water bodies. MeHg content in continental rain can be up to 5% of total Hg (Bloom and Watras, 1989) and up to 2 % in coastal areas. Lower  $HgT_D$  are observed in D-B (8 ng/L) can be explained by possible complexation and trapping of Hg by sulfides and organic matter and their subsequent enrichment in river sediments. D-B is the closest site to the former pollution source; therefore, it is possible that active reductive demethylation in addition to mercury sequestration by sulfides by active methylation are behind the observed  $HgT_D$  concentration. L-C is considered to be slightly affected by the Deûle Hg-polluted river as regard to its high  $HgT_D$  observed. During low river flows, the Deûle can desorb and cause wider dispersion of Hg pollution reaching even the remote site of Lys river (L-C). Still, this site (L-C) is characterized by high  $HgT_P$  (1.5  $\mu\text{g/g}$ ) relative to its low  $HgT_S$  in the sediment phase (0.042  $\mu\text{g/g}$ ). Probable sources of  $HgT_D$  and  $HgT_P$  can be agricultural runoffs and from boat traffic. The active boat traffic in both rivers cause much resuspension of polluted sediments and dissipation of  $HgT_P$  from the Deûle sites reaching even L-C. Furthermore, the high levels of  $HgT_P$  could participate in the observed  $HgT_D$  concentrations through solubilization of Hg by DOC and organic matter mineralization consequently releasing enriched mercury from suspended particles. Moreover, another explanation for the high Hg surface concentrations can be attributed to the leaching and weathering of mercury bearing rocks which is unlikely to be present. As discussed previously, Lys river particularly L-C is considered as hotspot for methylation as demonstrated in sediment phase and most probably in water column. Therefore, it is not surprising to find  $HgT_D$  concentrations in pristine environments i.e. (L-C) obviously comparable with polluted ones (D-A, D-B).

#### F.4.7. Mercury partitioning $K_D$

To examine the spatial distribution trend of  $HgT_D$ ,  $\log K_D$  values were determined (table F.2). Mercury transport in the riverine ecosystem is controlled by its distribution between solid and dissolved phases. Hence, distribution ratio coefficients  $K_D$  were used to evaluate the extent of Hg diffusion within the aquatic system. Mercury partitioning between the different compartments of the aquatic system is mainly controlled by various processes including: environmental mechanisms of erosion, weathering and atmospheric deposition, anthropogenic inputs, physico-chemical conditions of the environment (pH, DOC, presence of ligands). Total suspended solids (TSS) is considered to be the most influential factor controlling mercury in the particulate phase (Quesmerais et al, 1998).

In river surface water,  $\log K_D$  value of  $HgT$  in the Deûle sites are comparable and are relatively higher in magnitude than Lys sites. Higher  $\log K_D$  values observed in D-B (2.7) than D-A (2.3) can be the consequence of remobilization events, eroding particulate mercury from river bed sediment. In addition to the contribution of Hg contaminated soil erosion in the river catchment, atmospheric deposition as a consequence of long years of ore processing, can also furnish high particulate mercury to the river. In addition, terrestrial organic matter leached from surrounding soils can lead to Hg complexation.

Slightly lower  $\log K_D$  values of  $HgT$  are observed in Lys sites are mainly attributed to mercury solubilization. This means that mercury is more controlled by dissolved phases rather than TSS.  $\log K_D$  values in L-C (1.9) with similar values occurring in L-D (2.1).  $K_D$  values can tend to decrease as a result of desorption processes under specific environmental conditions and to colloidal effect of Hg in the dissolved phase. Water acidity plays an important role in controlling the values of  $K_D$ , where high pH values were recorded for L-C of pH 7.5 and pH 7.2 for L-D due the leaching of carbonate rich rocks in the catchment. For pH values  $> 7.5$ ,  $K_D$  tend to decrease, due to the increased dissolved phase complexation with  $Cl^-$  and  $OH^-$ , forming  $Hg(OH)_2$  and  $HgCl_2$ , the dominant species in the absence of organic ligands (Dyrssen and Wedborg, 1991). In the presence of DOC, Hg-DOC are the dominant species with a high stability constant  $10^{21}$ - $10^{22.9}$  (Lamborg et al, 2003). In sulfide rich environments, mercury form  $HgS^\circ(aq)$ ,  $Hg(SH)^\circ_2$  with  $K=10^{26.5}$ ,  $10^{37.5}$  respectively (Benoit et al, 1999).

Overall, the particle-water coefficient in surface water ranged from 1.9 to 2.7 for  $HgT$  as fairly seen in other estuaries (Benoit et al, 1998; Schafer et al, 2010; Stordal et al, 1996;

Sunderland et al, 2006). Mercury tends to bind to particles and mercury reactivity is controlled by the partitioning between solid and dissolved phases. In aquatic systems, Hg has a high tendency to bind to suspended particles (Coquery et al, 1997; Tseng et al, 2001). Positive correlations were obtained between  $HgT_S$  and  $HgT_P$  in the four sampling sites ( $r^2=0.900$ ,  $p<0.05$ ). Therefore, particles seem to be the transporters of mercury pollution from the source point to the downstream of the river where  $HgT_P$  are shown to decrease with contribution of aqueous phase as an additional transport vector in the river. The binding of Hg on suspended particles can be achieved through organic matter by sulfur donor atom that is major carrier of mercury in sediments (Loring et al, 1983). Hereby, even more than a decade of the smelter closure, Hg pollution persists, and the catchment area still supplies prominent Hg to the river potentially transported to distant places i.e. the Lys river.

In sediment phase, Hg distribution between solid and dissolved phases has considerable effect on the availability of mercury for methylation and mobility.  $\log K_D$  of HgT profiles were homogenous in all sites with an average values of  $4.13 \text{ L-C} < 4.82 \text{ L-D} < 5.81 \text{ D-A} < 5.97 \text{ D-B}$  (table F.2). From the high % MeHg found in Lys sites, it is evident to have lower  $K_D$  values than the Deûle sites which strengthen the possibility of dissolved HgT availability for Hg methylation. Relatively similar high values of  $\log K_D$  were found in Marano and Grado Lagoon, Italy (3.34-5.61 L/Kg) (Hines et al, 2012), Hudson River ( 4.88-5.70 L/Kg) (Heyes et al, 2004), Gironde estuary ( $\log K_D \text{ Hg(II)}=4.2$ ) (Schafer et al, 2010). Lower values of  $\log K_D$  (3.12-3.76) were found for Passamaquoddy Bay (Sunderland et al, 2006). Three times higher partition coefficients are observed in sites affected by ore mines particularly mercury and gold, signifying higher association of Hg with solid phase (Guedron et al, 2011; Thomas et al, 2002). It is surprising to find that in all sites,  $\log K_D \text{ HgT}$  in surface water is less than  $\log K_D \text{ (HgT)}$  in sediment phase which is in contrast to other findings (Schafer et al, 2010; Rothenberg et al, 2008). This signifies the predominant distribution of mercury between different organic, Fe/Mn hydroxides, sulfide phases in sediment with varying binding strengths in our study sites.

#### **F.4.8. Estimated sediment-water flux of HgT**

Sediments can be a potential source of HgT and MeHg to the water column through diffusive fluxes of dissolved Hg species. Diffusional fluxes were calculated in the Deûle and Lys sites according to Fick's first law as previously described (Covelli et al, 2008):

$$F = - \left( \frac{\phi D_w}{\theta} \right) \frac{\delta C}{\delta x}$$

Where F is the flux of solute with concentration C at depth x,  $\phi$  is the sediment porosity that is determined from weight loss of sediments after drying,  $\theta$  is the tortuosity, estimated from porosity (Bourdeau, 1996) as  $\theta = 1 - \ln(\phi^2)$ . The  $D_w$  is the diffusion coefficient which is assumed to be  $D_w$  of  $\text{HgCl}_4^{2-} = 8.65 \cdot 10^{-6} \text{ cm}^2/\text{s}$  (Muresan et al, 2007). Diffusional fluxes at all sites were estimated from average porewater of HgT collected from the first sediment depth interval (0-1 cm).

Calculated diffusional fluxes of the Deûle site was  $223.91 \text{ ng/cm}^2/\text{y}^1$  and for Lys-C was  $51.70 \text{ ng/cm}^2/\text{y}$  and Lys-D of  $2.11 \text{ ng/cm}^2/\text{y}$ . Hg fluxes in Deûle site is considered to be extremely high and even comparable Valdeazogues river affected by Almaden Hg Mine ( $0.11\text{-}949 \text{ ng/cm}^2/\text{y}$ ) (Gray et al, 2004).

Hg fluxes in Lys-C are considered to be high for a pristine river and were found to be much more higher than that of Patuxent River ( $0.0059\text{-}0.0089 \text{ ng/cm}^2/\text{y}$ ) (Benoit et al, 1998), Thau Lagoon ( $0.00137 \text{ ng/cm}^2/\text{y}$ ) (Muresan et al, 2007), but comparable with Seine estuary ( $38\text{-}58 \text{ ng/cm}^2/\text{y}$ ) (Mikac et al, 1999), and Saguenay Fjord ( $26\text{-}36 \text{ ng/cm}^2/\text{y}$ ) (Gagnon et al, 1996). Diffusive Fluxes of L-D are similar to MeHg diffusive fluxes of the eutrophic Salmon Falls Creek Reservoir ( $0.18\text{-}3.29 \text{ ng/cm}^2/\text{y}$ ) (Gray and Hines, 2009), diffusive fluxes of HgT in Laurentian Trough ( $1\text{-}20 \text{ ng/cm}^2/\text{y}$ ) (Gobeil and Cossa, 1993) and Lavaca Bay ( $0.062\text{-}2.38 \text{ ng cm}^2/\text{y}$ ) (Gill et al, 1999).

It seems that strong reductive conditions prevail in Deûle sites, conferred by the high sulphidic contents contributing to dissolution of reactive Fe/Mn oxyhydroxides near surface-water interface and the release of metals to the overlying water. In Lys particularly, L-D, we assume that more oxidative conditions predominate and control the distribution and the mobility by trapping metals and reducing their fluxes to water.

## F.5. Conclusion

Deûle river sediments are characterized by high  $\text{HgT}_s$  contents of an average value of  $10.33 \mu\text{g/g}$  near the former Metaleurop smelter.  $\text{HgT}_s$  contents are shown to decrease downstream at the Deûle confluence with Lys river. Upstream the Lys river at L-C,  $\text{HgT}_s$  are lower than the established background values of Hg in the region. However, after merging with Deûle river,

10 times higher  $HgT_S$  was observed at L-D (downstream Lys river). The high  $HgT_P$  found in L-D confirms the transport of Hg from the source of pollution of the Deûle river and that suspended particles are the major carriers of mercury pollution. Eventhough, Metaleurop smelter is closed since 2003, Deûle sediments are still considered as potential sources of Hg through erosion, remobilization and solubilization. In Deûle sites, MeHg production is assumed to be contributed to both old and recent events of methylation as compared to more recent events of methylation in Lys sites. This is attributed to more important relations established in Deûle sites between % MeHg and AVS, CRS as opposed to Lys sites where associations were only determined between % MeHg and AVS with lack of correlation between %MeHg and CRS. The high  $HgT_S$ , Corg, sulfides are all factors responsible for much lower % MeHg in the Deûle sites as compared to the less contaminated Lys river sites. This is assigned to the complexing capacity of sulfides and organic matter to Hg, limiting its bioavailabilty as well as the toxicity towards methylating microorganisms induced by heavy metals heavily burdened in the Deûle sediments. Results have delineated, that % MeHg increases by a factor 10 from L-D affected by the Deûle river pollution to L-C (uncontaminated side of Lys river). This confirms that in pristine environments characterized by optimal geochemical conditions (sulfides, Corg....) methylation is stimulated and enhanced and further strengthened by the export of nutrients from the agricultural terrains as seen in L-C.

In all sampling sites, strong correlations were established between % MeHg and Corg, AVS and % Corg and AVS which corroborate that MeHg is produced *in situ* rather than exported from other sources such as sewage effluents, industries...ect. Higher  $HgT_P$  and  $LogK_D$  were observed in Deûle sites than Lys sites. The high Hg in the particulate phases of the Deûle is assigned to the sulfides and organic carbon enrichment, in addition to hydrological conditions contributing to sediment resuspension, soil erosion and leaching of the polluted surroundings of the former smelter. High levels of  $HgT_P$  in the Deûle are sufficient in transporting mercury pollution to more distant places such as that of L-D. Lower  $logK_D$  in L-C (the uncontaminated side of the river) is consistent with more significant %MeHg in this site. Despite the low concentrations of  $HgT_S$  in L-C,  $HgT_D$  and  $HgT_P$  are considered high to a pristine environment. Sources of pollutions can be attributed to agricultural runoffs and the dispersion/propagation of Deûle river pollution assisted by boat traffic, significantly enriching



the site with Hg. The dominance of reducing conditions in the Deûle has contributed to higher diffusive flux of HgT than the Lys river.

## F.6. References

- Baldi, F., Parati, F. & Filippelli, M., 1995. Dimethylmercury and dimethylmercury-sulfide of microbial origin in the biogeochemical cycle of Hg. *Water, Air. Soil. Poll.* 80, 805–815.
- Balogh, S.J., Swain, E.B., Nollet, Y.H., 2008. Characteristics of mercury speciation in Minnesota rivers and streams. *Environ. Pollut.* 154, 1, 3-11.
- Barkay, T., Gillman, M., Turner, R.R., 1997. Effects of dissolved organic carbon and salinity on bioavailability of mercury. *Appl. Environ. Microbiol.* 4267-4271.
- Bishop, K.H., Lee, Y.H., 1997. Catchments as a source of mercury/methylmercury in boreal surface waters. In: Sigel, A., Sigel, H. (Eds.), *Mercury and its effects on environment and biology. Metal ions in biological systems*, vol 34. Marcel Dekker, New York, pp. 113-130.
- Benoit, J.M., Gilmour, C.C., Heyes, A., Mason, R.P., Miller, C.L., 2002. Geochemical and biological controls over methylmercury production and degradation in aquatic ecosystems, vol 835. *ACS Symposium Series.*, American Chemical Society, pp 262-297.
- Benoit, J.M., Gilmour, C.C., Mason, R.P., 2001a. The influence of sulfide on solid phase mercury bioavailability for methylation by pure cultures of *Desulfobulbus propionicus*(1pr3). *Environ. Sci. Technol.* 35, 127 – 132.
- Benoit, J.M., Gilmour, C.C., Mason, R.P., Heyes, A., 1999. Sulfide controls on mercury speciation and bioavailability to methylating bacteria in sediment pore-waters. *Environ. Sci. Technol.* 33, 6, 951–957.
- Benoit, J.M., Gilmour, C.C., Manson, R.P., Riedel, G.S., Riedel, G.F., 1998. Behaviour of mercury in the Patuxent River estuary. *Biogeochemistry.* 40, 249-265.
- Benoit, J.M., Mason, R.P., Gilmour, C.C., Aiken, G.R., 2001. Constants for mercury binding by dissolved organic matter isolates from the Florida Everglades. *Geochim.Cosmochim. Ac.* 65, 24, 4445 – 4451.
- Bloom, N.S., Gill, G.A., Cappellino, S., Dobbs, C., Mcshea, L., Driscoll, C., Mason, R., Rudd, J., 1999. Speciation and Cycling of Mercury in Lavaca Bay, Texas, Sediments. *Environ. Sci. Technol.* 33, 7-13.
- Bloom, N.S., Watras, C.J., 1989. Observations of methylmercury in precipitation. *Sci. Total. Environ.* 87-88, 199-207.
- Bloom, N.S., Watras, C.J., Hurley, J.P., 1991. Impact of acidification on the methylmercury cycle of remote seepage lakes. *Water. Air. Soil. Pollut.* 56, 477-491.
- Canario, J., Vale, C., Caetano, M., 2005. Distribution of monomethylmercury and mercury in surface sediments of the Tagus estuary (Portugal). *Mar. Pollut. Bull.* 50, 1142- 1145.
- Choi, S.C., Bartha, R., 1994. Environmental factors affecting mercury methylation in estuarine sediments. *Bull. Environ. Contam. Toxicol.* 53, 805-812.
- Choe, K-Y., Gill, G.A., Lehman, R.D., Han, S., Heim, WA., Coale, KH., 2004. Sediment-water exchange of total mercury and monomethyl mercury in the San Francisco Bay-Delta. *Limnol. Oceanogr.* 49, 5, 1512–1527.
- Conaway, C.H., Squire, S., Mason, R.P., Flegal, A.R., 2003. Mercury deposition in a tidal

- marsh of South San Francisco Bay estuary. *Mar. Chem.* 80, 199-225.
- Conaway, CH., Squire, S., Mason, RP., Flegal, A. R., 2003. Mercury speciation in the San Francisco Bay estuary. *Mar. Chem.* 80, 199 – 225
- Coquery, M., Cossa, D., Sanjuan, J., 1997. Speciation and sorption of mercury in two macro-tidal estuaries. *Mar. Chem.* 58, 213–227
- Covelli, S., Faganeli, J., Horvat, M., Brambati, A., 1999. Porewater distribution and benthic flux measurements of mercury and methylmercury in gulf of Trieste (Northern Adriatic sea). *Estuar. Coast. Shelf. Sci.* 48, 415-428.
- Dyrssen, D., Wedborg, P., 1991. The sulphur-mercury(II) system in natural waters. *Water. Air. Soil Poll.* 56, 507-519.
- Domagalski, J., 1998. Occurrence and transport of total mercury and methylmercury in the Sacramento River Basin, California. *J. Geochem. Explor.* 64, 277-291.
- Eckley, C.S., Watras, C.J., Hintelmann, H., Morrison, K., Kent, A.D., Regnell, O., 2005. Mercury methylation in the hypolimnetic waters of lakes with and without connection to wetlands in northern Wisconsin. *Can. J. Fish. Aquat. Sci.* 62, 400-411.
- Emerson, S., Jacobs, L.J., Tebo, B., 1983. The behaviour of trace metals in marine anoxic waters: Solubility at the oxygen-hydrogen sulfide interface. In: Wong, C.S. et al. (Eds.), *Trace Metals in seaWater*. Plenum, New York, pp. 579-608.
- Foucher, D., Ogrinc, N., Hintelmann, H., 2009. Tracing mercury contamination from the Idrija mining region (Slovenia) to the gulf of Trieste using Hg isotope ratio measurements. *Environ. Sci. Technol.* 43, 33-39.
- Gagnon, C., Mucci, A., Pelletier, E., 1996. Behaviour of anthropogenic mercury in coastal marine sediments. *Mar. Chem.* 52, 195.
- Galloway, M.E., Branfireun, B.A., 2004. Mercury dynamics of a temperate forest wetland. *Sci. Total. Environ.* 325, 239-254.
- Gill, G.A., Bloom, N.S., Cappellino, S., Driscoll, C.T., Dobbs, C., Mcshea, L., Manson, R., Rudd, J., 1999. Sediment-Water Fluxes of Mercury in Lavaca Bay, Texas. *Environ. Sci. Technol.* 33, 663- 669.
- Glimour, C., Elias, D., KuchenA., Brown, S., Palumbo, A., Schadt, C., Wall, J., 2011. Sulfate reducing bacterium *Desulfovibrio desulfuricans* ND 132 as a model for understanding bacterial mercury methylation. *App. Environ. Microbiol.* 77, 3938-3951.
- Glimour, C., Henry, E.A., Mitchell, R., 1992. Sulfate stimulation of mercury methylation in freshwater sediments. *Environ. Sci. Technol.* 26, 2281.
- Glimour, C., Riedel, G.S., Ederington, M.C., Bell, J.T., Benoit, J.M., Gill, G.A., Stordal, M.C., 1998. Methylmercury concentrations and production rates across a trophic gradient in the northern Everglades. *Biogeochem.* 40, 327–345, 1998.
- Gray, J.E., Hines, M.E., 2009. Biogeochemical mercury methylation influenced by reservoir eutrophication, salmon Falls Creek Reservoir, Idaho, USA. *Chem. Geol.* 258, 157- 167.
- Gray, J., Hines, M., Higuera, P.L., Adatto, I., Lasorsa, B.K., 2004. Mercury speciation and microbial transformations in mine wastes, stream sediments, and surface waters at Almaden mining district, Spain. *Environ. Sci. Technol.* 38, 4285-4292.

- Gerbig, C., Kim, C., Stegemeier, J., Ryan, J.N., Aiken, G.R., 2011. Formation of nanocolloidal metacinnabar in mercury-DOM-sulfide systems. *Environ. Sci. Technol.* 74 4693-4708.
- Gray, J.E., Theodorakos, P.M., Bailey, E.A., Turner, R.R., 2000. Distribution, speciation and transport of mercury in stream-sediment, stream-water and fish collected near abandoned mercury mines in southwestern Alaska, USA. *Sci. Total. Environ.* 260, 21-33.
- Grieb, T.M., Driscoll, C.T., Glass, S.P., Schofield, C.L., Bowie, G.L., Porcella, D.B., 1990. Factors affecting mercury accumulation in fish in the upper Michigan peninsula. *Environ.Toxicol. Chem.* 9, 919-930.
- Gobiel, C., Cossa, D., 1993. Mercury in sediments and sediment porewater in the Laurentian Trough. *Can.J.Fish.Aquat.Sci.* 50, 1794.
- Goulet, R.R., Holmes, J, Page, B., Poissant, L., Siciliano, S.D., Lean, D., Wang, F., Amyot, M., Tessier, A., 2007. Mercury transformations and fluxes in sediments of a riverine wetland. *Geochim. Cosmochim. Ac.* 71, 3393–3406.
- Guedron, S., Grimaldi, M., Grimaldi, C., Cossa, D., Tisserand, D., Charlet, L., 2011. The Amazonian gold mined soils as source of methylmercury: Evidence from a small scale watershed in French Guinea. *Water research.* DOI: 101016/J. waters. 2011.02.022.
- Grigal, D.F., 2002. Inputs and outputs of mercury from terrestrial watersheds: a review. *Environ. Rev.* 10, 1-39.
- Hammerschmidt, C.R., Fitzgerald, W.F., 2006. Methylmercury cycling in sediments on the continental shelf of southern New England. *Geochim. Cosmochim. Ac.* 70, 918-930.
- Hammerschmidt, C.R., Fitzgerald, W.F., Lamborg, C.H., Balcom, P.H., Visscher, P.T., 2004. Biogeochemistry of methylmercury in sediments of Long Island Sound. *Mar. Chem.* 90, 31-52.
- Han, S., Obratsova, A., Pretto, P., Coe, K., Gieskes, J., Deheyn, D., Tebo, B., 2007. Biogeochemical factors affecting mercury methylation in sediments of the Venice Lagoon, Italy. *Environ. Toxicol. Chem.* 26, 4, 655-663.
- Heyes, A., Miller, C., Mason, R.P., 2004. Mercury and methylmercury in Hudson River sediment: impact of tidal resuspension on partitioning and methylation. *Mar. Chem.* 90, 75-89.
- Hines, M.E., Faganeli, J., Adatto, I., Horvat, M., 2006. Microbial mercury transformations in marine, estuarine and freshwater sediment downstream of Idrija mine Slovenia. *Appl. Geochem.* 21, 1924-1939.
- Hines, M.E., Faganeli, J., Planinc, R., 1997. Sedimentary anaerobic microbial biogeochemistry in the Gulf of Trieste, northern Adriatic: influence of bottom water oxygen depletion. *Biogeochemistry.* 39, 65-86.
- Hines, M.E., Horvat, M., Faganeli, J., Bonzongo, J-C., Barkay, T., Major, E.B., Scott, K.J., Bailey, E.A., Warwick, J.J., Lyons, W.B., 2000. Mercury Biogeochemistry in the Idrija River, Slovenia, from above the Mine into the Gulf of Trieste. *Environ.Res.* 83, 2, 129-139.

- Hines, M.E., Poitras, E.N., Covelli, S., Faganeli, J., Emili, A., Zizek, S., Horvat, M., 2012. Mercury methylation and demethylation in Hg-contaminated lagoon sediments (Marano and Grado Lagoon, Italy). *Estuar. Coast. Shelf. Sci.* 113, 85-95.
- Higuera, P., Oyarzun, R., Lillo, J., Sanchez Hernandez, J.C., Molina, J.A., Esbri, J. M., Lorenzo, S., 2006. The Almaden district (Spain): Anatomy of one of the world's largest Hg contaminated sites. *Sci.Total. Environ.* 356, 112-124.
- Hissler, C., Probst, J-L., 2006. Chlor-alkali industrial contamination and riverine transport of mercury: Distribution and partitioning of mercury between water, suspended matter, and bottom sediment of the Thur River, France. *Appl. Geochem.* 21, 1837-1854.
- Huerta-Diaz, M.A., Morse, J.W., 1992. Pyritization of trace metals in anoxic marine sediments. *Geochim. Cosmochim. Acta.* 56, 2681-2702.
- Hsu, H., Sedlak, D.L., 2003. Strong Hg(II) complexation in municipal wastewater effluent and surface waters. *Environ. Sci. Technol.* 37, 2743-2749.
- Jay, J., Murray, K., Glimour, C., Mason, R., Morel, F., Roberts, A., Hemond, H., 2002. Mercury methylation by *Desulfovibrio desulfuricans* ND132 in the presence of polysulfides. *Appl. Environ. Microbiol.* 68, 5741-5745.
- Jenne, E.A., 1970. Atmospheric and fluvial transport of mercury. In: *Mercury in the environment*. U.S. Geological Survey Professional Paper 713, 40-45.
- Kadlecova, M., Ouddane, B., Docekalova, H., 2012. Speciation of mercury in the strongly polluted sediments of the Deûle River (France). *J. Environ. Monitor.* 14, 961-967.
- Kocman, D., Kanduc, T., Ogrinc, N., Horvat, M., 2011. Distribution and partitioning of mercury in a river catchment impacted by former mercury mining activity. *Biogeochemistry.* 104, 183-201.
- Kwokal, Z., Franciskovic-Bilinski, S., Bilinski, H., Branica, M., 2002. A comparison of anthropogenic mercury pollution in Kastela Bay (Croatia) with pristine estuaries in Ore (Sweden) and Krka (Croatia). *Mar. Pollut. Bull.* 44, 1152-1169.
- Lambertsson, L., Nilsson, M., 2006. Organic material: The primary control on mercury methylation and ambient mercury concentrations in estuarine sediments. *Environ. Sci. Technol.* 40, 1822-1829.
- Lamborg, C.H., Tseng, C.M., Fitzgerald, W., Balcom, P.H., Hammerschmidt, C.R., 2003. Determination of the mercury complexation characteristics of dissolved organic matter in natural waters with "reducible mercury" titrations. *Environ. Sci. Technol.* 37, 3316-3322.
- Lourino-Cabana, B., Lesven, L., Charriau, A., Billon, G., Ouddane, B., Boughriet, A., 2011. Potential risks of metal toxicity in contaminated sediments of Deûle river in northern France. *J. Hazard. Mater.* 186, 2-3, 2129-2137.
- Loring, D.H., Rantala, R.T.T., Smith, J.N., 1983. Response time of Saguenay fjord sediments to metal contamination. *Environ. Biogeochem. Ecol. Bull.* 35, 59-72.
- Macalady, J.L., Mack, E.E., Nelson, K.M., Scow, K.M., 2002. Sediment microbial community structure and mercury methylation in mercury-polluted clear lake, California. *Appl. Environ. Microbiol.* 2000, 1479-1488.

- Mason, R., Lawrence, A., 1999. Concentration, distribution, and bioavailability of mercury and methylmercury in sediments of Baltimore harbor and Chesapeake bay, Maryland, USA. *Environ. Toxicol. Chem.* 11, 2438-2447.
- Martin-Doimeadios, R.C.R., Wasserman, J.C., Garcia Bermejo, L.F., Amouroux, D., Berzas Nevado, J.J., Donard, O.F.X., 2000. Chemical availability of mercury in stream sediments from Almaden area, Spain. *J. Environ. Monit.* 2, 360-366.
- Mason, R., Lawson, N., Lawrence, A., Leaner, J., Lee, J., Sheu G-R., 1999. Mercury in the Chesapeake Bay. *Mar. Chem.* 65, 77-96.
- Mikac, M., Niessen, S., Ouddane, B., Wartel, M., 1999. Speciation of Mercury in sediments of the Seine estuary (France). *Appl. Organomet. Chem.* 13, 715-725.
- Miles, A.K, Rica, M.A., 2010. Temporal and spatial distributions of sediment mercury at salt pond wetland restoration sites, San Francisco Bay, CA, USA. *Sci. Total. Environ.* 408, 1154-1165.
- Muresan, B., Cossa, D., Jezequel, D., Prevot, F., Kerbellec, S., 2007. The biogeochemistry of mercury at the sediment-water interface in the Thau lagoon.1. Partition and speciation. *Estuar. Coast. Shelf. Sci.* 3, 472-484.
- Ouddane, B., Mikac, N., Cundy, A.B., Quillet, L., Fischer, J.C., 2008. A comparative study of mercury distribution and methylation in mudflats from two macrotidal estuaries: The Seine (France) and the Medway (United Kingdom). *Appl. Geochem.* 23, 618-631.
- Oremland, R.S., Miller, L.G., Dowdle, P., Connell, T., Barkay, T., 1995. Methylmercury Oxidative Degradation Potentials in Contaminated and Pristine Sediments of the Carson River, Nevada. *Appl. Environ. Microbiol.* 61, 7, 2745-2753.
- Paquette, K.E., Helz, G., 1995. Solubility of cinnabar (red HgS) and implications for mercury speciation in sulfidic waters. *Water. Air. Soil. Poll.* 80, 1053-1056.
- Quesmerais, B., Cossa, D., Rondeau, B., Pham, T.T., Fortin, B., 1998. Mercury distribution in relation to iron and manganese in the St. Lawrence River. *Sci. Total Environ.* 213, 193-201.
- Ravichandran, M., 2004. Interactions between mercury and dissolved organic matter- a review. *Chemosphere*, 55, 319-331.
- Rimondi, V., Gray, J.E., Costagliola, P., Vaselli, O., Lattanzi, P., 2012. Concentration, distribution, and translocation of mercury and methylmercury in mine-waste, sediment, soil, water, and fish collected near Abbadia San Salvatore mercury mine, Monte Amiata district, Italy. *Sci. Total. Environ.* 414, 318-327.
- Rothenberg, S., Ambrose, R., Jay, J., 2008. Mercury cycling in surface water, pore water and sediments of Mugu Lagoon, Ca, USA. *Environ. Pollut.* 154, 32-45.
- Roth, D.A., Taylor, H.E., Domagalski, J., Dileanis, P., Peart, D.B., Antweiler, R.C., Alpers, C.N., 2001. Distribution of inorganic mercury in Sacramento River water and suspended colloidal sediment material. *Arch. Environ. Contam. Toxicol.* 40, 2, 161-172.
- Schafer, J., Castelle, S., Blanc, Gerard., Dabrin A., Masson M., Lancelleur, L., Bossy, C., 2010. Mercury methylation in the sediments of a macrotidal estuary (Gironde Estuary, south-west France). *Estuar. Coast. Shelf. Sci.* 90, 80-92.
- Shi J, Liang L, Jiang G, Jin X. The speciation and bioavailability of mercury in sediments of Haihe River, China. *Environ. Int.* 31 (2005) 357-365.

- Simonin, H.A., Loukmas, J.J., skinner, L.C., Roy, K.M., 2008. Lake variability: Key factors controlling mercury concentrations in Newyork state Fish. Environ. Pollut. 154, 107-115.
- Sunderland, E.M., Gobas, F., Branfireun, B.A., Heyes, A., 2006. Environmental controls on the speciation and the distribution of mercury in coastal sediments. Mar. Chem. 102, 111-123.
- Stordal, MC., Gill, GA., Wen, L-S, Santschi, PH., 1996. Mercury phase speciation in the surface waters of three Texas estuaries: Importance of colloidal forms. Limnol.Oceanogr. 41, 52-61.
- Stoichev, T., Amouroux, D., Wasserman, J.C., Point, D., De Diego, A., Bareille, G., Donard, O.F.X., 2004. Dynamic of mercury species in surface sediments of a macrotidal Estuarine–Coastal system (Adour River, Bay of Biscay). Estuar. Coast. Shelf. Sci. 59, 5111.
- Thomas, M.A., Conaway, C.H., Steding, D.J., Marvin-Dipasquale, M., Abu-Saba, K.E, Flegal, A.R., 2002. Mercury contamination from historic mining in water and sediment Guadalupe River and San Fransico Bay, California. Geochem. Explor. Env.A. 2, 211-217.
- Tseng, CM., Amouroux, D., Abril, G., Tessier, E., Etcheber, H., Donard, OFX., 2001. Speciation of mercury in a fluid mud profile of a highly turbid macrotidal estuary (Gironde, France). Environ. Sci. Technol. 35, 13, 2627–2633.
- Ullrich, S.M., Tanton, T.W., Svetlana, A., Abdrashitova, S.A., 2012. Mercury in the aquatic environment: A review of factors affecting methylation. Crit. Rev. Env. Sci. Tec. 31, 3, 241-293.
- Wallschager, D., Desai, M., Wilken, R.D., 1996. The role of humic substances in the aqueous mobilization of mercury from contaminated floodplain soils. Water. Air. Soil. Pollut. 90, 507-520.
- Wallschlager, D., Desai, M., Spengler, M., Windmoller, C.C., Wilken, R.D., 1998. How humic substances dominate mercury geochemistry in contaminated floodplain soils and sediments. J. Environ. Qual. 27/5, 1044-1054.
- Winfrey, M.R., Rudd, J.W.M., 1990. Environmental factors affecting the formation of methylmercury in low pH lakes. Environ.Toxicol. Chem. 9, 853-869.
- Yamamoto, M., 1996. Stimulation of elemental mercury oxidation in the presence of chloride ion in aquatic environments. Chemosphere, 32, 6, 1217-1224.
- Yan, H., Li, Q., Meng, C., Wang, C., Feng, X., He, T., Dominik, J., 2013. Spatial distribution and methylation of mercury in a eutrophic reservoir heavily contaminated by mercury in Southwest China. Appl.Geochem. 33, 182-190.
- Yanez, J., Guajardo, M., Miranda, C., Soto., C, Mansilla, H., Flegal, A.R., 2013. New assessment of organic mercury formation in highly polluted sediments in the Lenga estuary , Chile. Mar. Pollut.Bull. DOI:10.1016/j.marpolbul.2013.06.015.

***Chapitre G: Conclusion et perspectives***

***Chapter G: Conclusion and perspectives***



## Conclusion générale

Dans ce travail nous avons abordé deux aspects de recherche sur la contamination des eaux par le mercure. Le premier aspect est orienté sur le développement de méthodes analytiques pour la mesure des traces de mercure dans les eaux naturelles. Le deuxième aspect est consacré à l'étude et la compréhension de la distribution et le comportement du mercure dans la Deûle.

Le premier aspect de l'étude comprend un développement analytique pour mesurer des traces de mercure dissous dans les eaux naturelles en se basant sur les méthodes d'extraction en phase solide. Nous avons orienté notre recherche pour trouver des méthodes simples, peu coûteuses, sensibles et précises, applicables sur le terrain pour préconcentrer les échantillons. La formation de complexe Hg(II)-8-hydroxyquinoline directement n'a pas donné de résultats exploitables, rendement faible pour le mercure (l'optimum d'extraction ne dépasse pas 10%). Pour pallier à ce problème, une autre méthode basée sur le même principe de formation de complexes métalliques ioniques directe dans l'échantillon a été développée. Nous avons réussi à atteindre un rendement de 100% pour le Hg(II) dans l'eau de rivière avec une limite de détection de 8 pg/mL en utilisant comme technique d'analyse l'ICP-MS. Cette méthode est basée sur l'addition d'iodure (I<sup>-</sup>) pour former des complexes avec Hg(II), suivie par l'addition d'un agent tensio-actif cationique qui a permis la formation de paire d'ions hydrophobes extractible en phase solide, le mercure est analysé, après élution avec une solution acide, par ICP-MS.

D'autres méthodes ont été développées avec le même principe extraction-préconcentration en utilisant la 8-hydroxyquinoline, cette fois immobilisé sur une phase de silice pour améliorer la stabilité et la sélectivité. Six différentes silices fonctionnalisées à la 8-hydroxyquinoline ont été examinés pour l'extraction du Hg(II) des eaux naturelles. Seulement, le 5-phenylazo-8-hydroxyquinoline et deux imino-immobilisé 8-hydroxyquinoline ont permis d'atteindre des recouvrements quantitatifs et acceptables. Cela est attribué aux groupes fonctionnels imino/azo nouvellement formés et ancrés au carbone 5 et la nouvelle position du carbone 2 de la fraction 8-HQ. Le 5-phenylazo-8-hydroxyquinoline (5Ph8HQ) a été choisi pour une étude approfondie de l'adsorption et la préconcentration du mercure. Les résultats ont montré que la cinétique d'adsorption du mercure avec 5Ph8HQ est rapide avec un temps de demi-vie de sorption de 5 minutes et un coefficient de distribution élevé de 52,4. A la lumière des résultats de l'étude d'adsorption du mercure avec 5Ph8HQ, une méthode d'analyse a été développée

basée sur l'extraction en phase solide des ions Hg(II) de l'eau de rivière en utilisant 5Ph8HQ comme une résine de chélation et la technique CV-AFS pour la quantification. Dans des conditions optimales, les recouvrements quantitatifs ont été atteints avec un facteur d'enrichissement élevé de 250 et une limite de détection de 0,21 pg/ml.

La spéciation et la distribution du mercure ont été étudiées dans la Deûle et la Lys. Les sédiments de la Deûle sont considérés comme très pollués en mercure avec une concentration moyenne de HgT de 10,3 mg/Kg. La partie amont de la Lys avant le confluent est considérée comme non-contaminée, la concentration moyenne de HgT est de 0,042 mg/Kg. Cependant, après la jonction avec la Deûle, le niveau de concentration en mercure est 24 fois plus élevée que le côté non-contaminée de la rivière. La principale source de pollution par mercure est apportée par la matière en suspension enrichie en mercure par de la Deûle. Ceci est confirmé par les concentrations élevées du mercure particulaire (HgT<sub>P</sub>) trouvé dans l'eau de surface et par la relation entre HgT dans les phases dissoute et particulaire. Par conséquent, les conditions hydrologiques, climatiques et anthropiques peuvent éroder/remobiliser les sédiments et sols contaminés de la rivière et contribuer à la propagation spatiale de la pollution à des endroits éloignés tels que la Lys. Bien que les sédiments de la Deûle soient très chargés en mercure par rapport aux sédiments de la Lys, des pourcentages de méthylmercure (%MeHg) sont beaucoup plus élevés dans la Lys (4,21% dans le site L-C). Cela est dû à des conditions de méthylation plus favorables et disponibles dans la rivière Lys avec des niveaux de concentration plus faibles en mercure, en carbone organique et en sulfures que dans la Deûle. Des niveaux plus élevés de sulfures dans la Deûle qui peuvent rendre le mercure moins biodisponible pour la méthylation associés aux taux de déméthylation plus élevés occasionnés dans des sites contaminés. En plus, la Deûle est une rivière fortement polluée par des effluents chargés en métaux, ce qui peut manifester une toxicité accrue vers la communauté microbienne. Tous ces facteurs peuvent contribuer à baisser le pourcentage de MeHg dans la Deûle par rapport à la Lys. Des relations significatives ont été observées dans tous les sites entre %MeHg et %Corg, AVS et %Corg et AVS révélant l'importance de la méthylation microbienne et la production *in situ* de MeHg dans les deux rivières étudiées. Les sédiments de la Deûle sont considérés comme un puits de contamination par le mercure engendré par l'ancienne fonderie "Metaleurop". Par conséquent, les sédiments sont considérés comme une source potentielle de pollution sous l'effet de remobilisation avec un éventuel transport des polluants vers des zones non polluées. Malgré la

fermeture de la fonderie "Metaleurop" depuis près d'une décennie, les niveaux de mercure sont encore élevés et la rivière continue à engendrer des sources de pollution en mercure, potentiellement transportable à des endroits éloignés.

## Perspectives

La distribution et la spéciation du mercure dans des régions plus éloignées autre que la Lys peut être également étudié afin de déterminer l'étendue de transport du mercure et de sa transformation de la source de pollution vers d'autres sites. Les campagnes d'échantillonnages peut être élargie en choisissant des sites plus en amont la fonderie "Umicore" pour identifier sa contribution à la pollution. Une étude supplémentaire pour étudier l'origine de mercure dans la Lys par les traceurs isotopiques du mercure et la mise en évidence de son provenance de la Deûle. La détermination du flux diffusifs de MeHg de la Deûle est également nécessaire, pour contrôler ses niveaux, sa bioaccumulation et la possibilité de son transfert vers d'autres sites non contaminés. La détermination de paramètres supplémentaires tels que le carbone organique dissous est essentiel pour confirmer les suggestions formulées ci-dessus, de l'augmentation de la solubilisation des phases solide du mercure dans les environnements riches en sulfures. En outre, la détermination de la réduction des sulfates dans les sédiments dans des différents sites peut donner une vision plus claire de la différence de l'activité des bactéries sulfato-réducteur entre les sites fortement contaminés en mercure i.e. rivière de la Deûle et les environnements moins contaminés comme les sites de la Lys. L'examen des potentiels de méthylation et de déméthylation des communautés microbiennes impliquées et la variation saisonnière de la dynamique du mercure est nécessaire pour être exploré dans la Deûle et la Lys particulièrement sur le site en amont (L-C). Quant à la partie analytique, de nouvelles résines peuvent être développées avec des thiols comme groupe fonctionnel pour la spéciation des espèces de mercure en utilisant des techniques chromatographiques ou non-chromatographiques. En plus de l'évaluation de l'efficacité des différentes résines pour la préconcentration de la forme mercure  $Hg^{\circ}$ .

## General conclusion

This study has involved two different aspects of Hg study. The first aspect encompasses method development for the measurement of Hg(II) ions in river water. The second aspect of the work is dedicated to the study and understanding of mercury distribution and the biogeochemical behavior in the highly polluted Deûle river.

The first aspect of the study include the development of analytical methods for the determination of Hg(II) based on solid phase extraction. In the search of simple, cheap, sensible and accurate methods for the measurement of Hg(II) ions, direct complexation of Hg(II) in water samples is the most suitable for rapid and *in situ* sampling. The direct complexation of Hg(II) with 8-HQ failed in the quantitative recoveries of mercury from river water with an optimal mercury extraction reaching only 10 %. As a complement for the study, another method based on the same principle of direct complexation was able of 100 % recovery of Hg(II) ions from river water with limits of detection reaching 8 pg/ml. This technique is based on the addition of soft base i.e. I to form complexes with Hg(II) ions. It is followed by the addition of a cationic surfactant that allowed the formation of hydrophobic ion pair for its subsequent solid phase extraction on silica support. Finally, mercury ions were eluted and detected by ICP-MS showing good figures of merit.

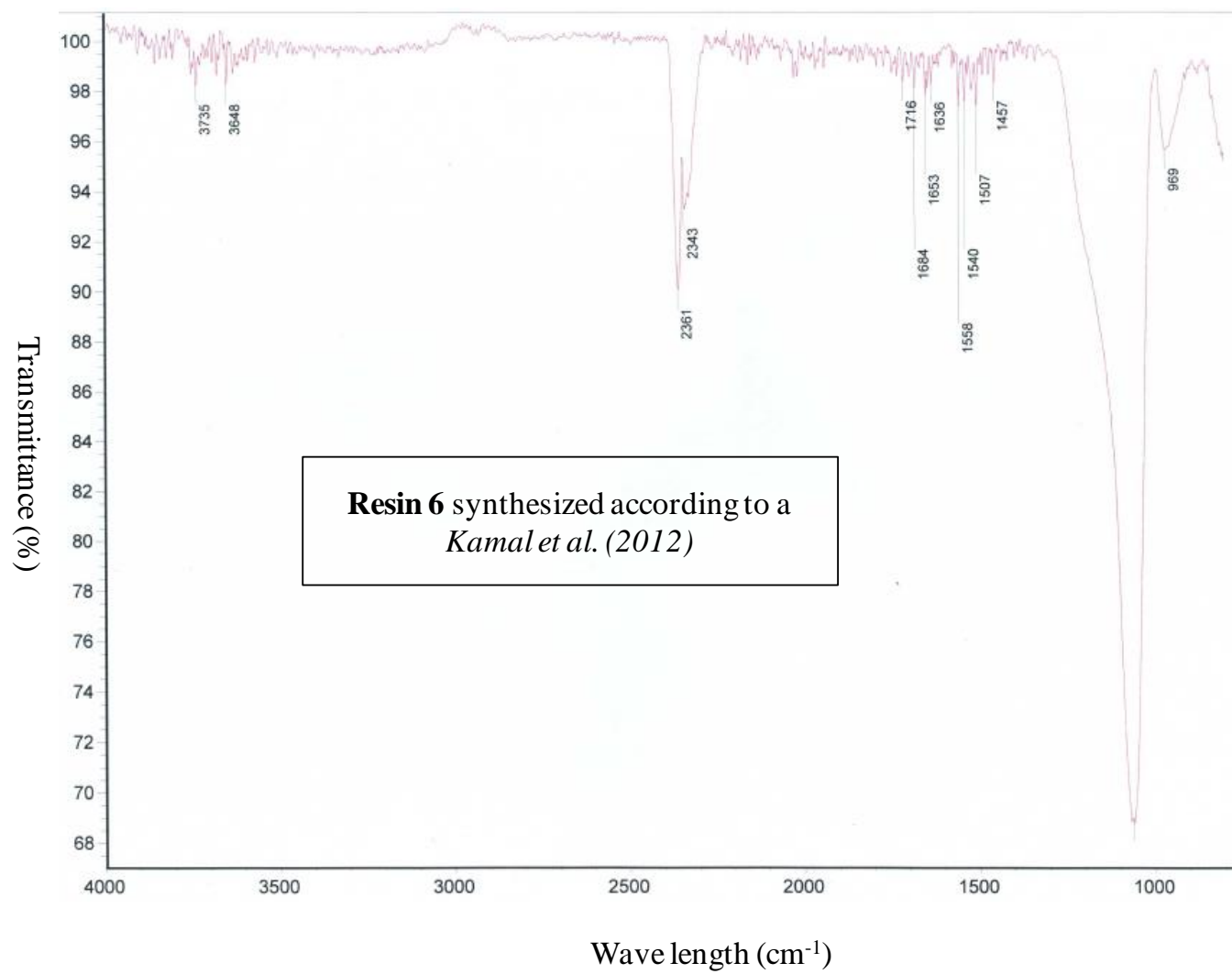
In order to defy the analytical failure of the direct complexation of Hg(II) ions by 8-HQ, the latter ligand was immobilized on silica phase to offer upgraded stability, selectivity and stability constant formation. Six different 8-HQ functionalized silica were examined for the extraction of Hg(II) from river water. Only 5-phenylazo-8-hydroxyquinoline and two imino-immobilized 8-HQ have achieved quantitative recoveries. This is attributed to the newly formed imino/azo functional groups anchored at carbon 5 and the new position of carbon 2 of 8-HQ moiety opening new coordination and binding sites for Hg ions. As a complementary study, 5-phenylazo-8-hydroxyquinoline (5Ph8HQ) was chosen for further adsorption and application studies with Hg ions. Mercury is shown to have fast adsorption kinetics with 5Ph8HQ with half time sorption of 5 minutes and high distribution coefficient of 52. In the light of the adsorption study of Hg with 5Ph8HQ, an analytical method was developed based on the solid phase extraction of Hg(II) ions from river water using 5Ph8HQ as chelating resin and CV-AFS for quantification. Under optimized conditions, quantitative recoveries were attained with high enrichment factor reaching 250 and low detection limit of 0.21 pg/mL.

Mercury speciation and distribution was studied in Deûle and Lys rivers. Sediments of the Deûle river are shown to be highly polluted in Hg with an average concentration of HgT reaching 10.3 mg/Kg. The upstream side of Lys river before the confluence is considered as uncontaminated since its average HgT concentrations are less than the background concentration of Hg. However, the side of the Lys river after the confluence with Deûle river has demonstrated levels of mercury 24 times higher than the uncontaminated side of the river. The major transporters of mercury pollution are suggested to be the suspended particulate matter enriched with mercury. This is confirmed by high particulate mercury (HgT<sub>p</sub>) concentrations found in the surface water of the rivers and the relation found between HgT in bulk and particulate phases. Therefore, hydrological, climatic and anthropogenic conditions can erode/resuspend the contaminated sediments and soils of the river catchment, contributing to spatial spread of pollution to distant places such as Lys river. Although Deûle sediments are highly burdened with HgT as compared to the Lys sediments, much higher % MeHg is found in Lys river reaching an average value of 4.21 %. This is attributed to the most suitable methylation conditions available in Lys river of lower levels of HgT, organic carbon and sulfides as compared to the Deûle river. Higher levels of sulfides as shown in the Deûle, the highly polluted Hg river, can render Hg less bioavailable for methylation associated with higher demethylation potentials occurring in Hg polluted sites. In addition, the Deûle is heavily polluted by past discharges loaded with metals of the former smelter "Metaleurop", which can manifest an important toxicity towards the present microbial community. All these factors may contribute to lower % MeHg in the Deûle as compared to the Lys. Increasing levels of Corg and sulfides in the Deûle are shown to promote methylation as opposed to the Lys enhanced by lower levels of Corg and sulfides. Significant relations were observed in all sites between % MeHg and % Corg, AVS and % Corg and AVS revealing the importance of microbial methylation and the *in situ* production of MeHg in the two rivers. Sediments of the Deûle river are considered as a sink and reservoir of Hg generated by the former Metaleurop smelter. Therefore, the river's sediments are considered as a potential source of pollution upon remobilization under different conditions potentially transporting mercury to remote unpolluted areas. Despite, the fact that the former Metaleurop smelter is closed for almost a decade, HgT/MeHg levels are still high, creating an Hg hotspot for mercury pollution to surrounding environments carrying Hg hundred kilometers downstream the river possibly reaching the sea.

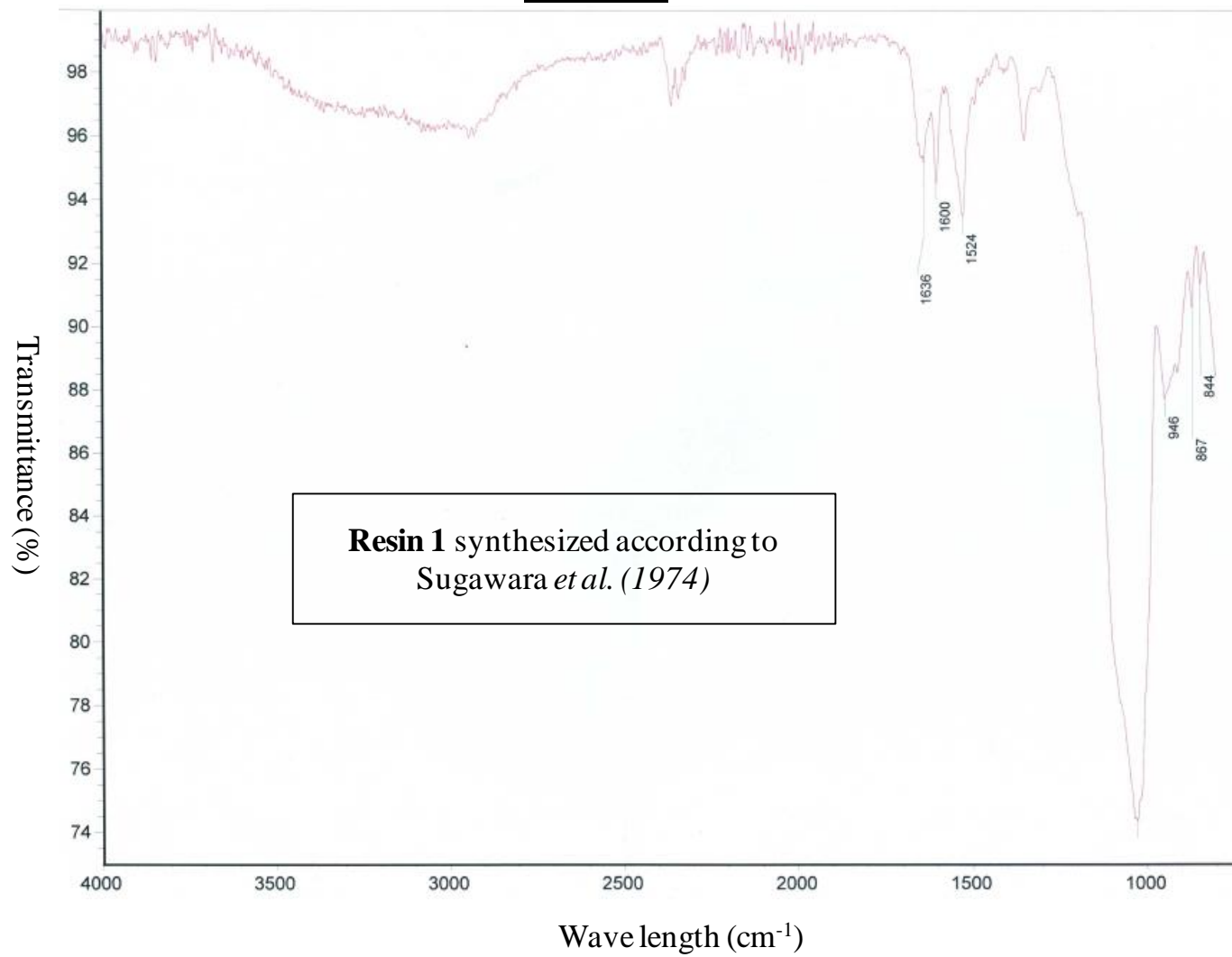
## Perspectives

Mercury distribution and speciation in more distant areas other than Lys river can be also studied to determine the range of mercury transport and transformation at distant places. The campaign of sampling sites can be broadened by choosing sampling locations upstream and downstream "Umicore" smelter to identify its contribution to pollution along the Deûle river. In addition to MeHg diffusive fluxes are needed to be calculated for Deûle river, to control its levels, its bioaccumulation and its possible transfer to uncontaminated sites. Besides, the determination of supplementary ancillary measurements such as dissolved organic carbon is essential to confirm the suggestions made above, of the increase of solubilization of Hg bulk phases in sulfidic rich environments. Moreover, the determination of sulfate reduction in sediments in different sites can give a more clear view of the difference of sulfate reducing activities between highly Hg contaminated site i.e. the Deûle sites and the less contaminated/pristine environments i.e. the Lys sites. Investigations of methylation and demethylation potentials of the microbial community involved and seasonal variations of mercury dynamics are needed to be explored in the Deûle and the Lys particularly L-C. As for the analytical part, new resins can be developed incorporating thiol functional groups for the speciation of mercury species using chromatographic or non-chromatographic techniques. In addition to, the evaluation of different resins for the online preconcentration of Hg<sup>0</sup>.

## ANNEXE 1

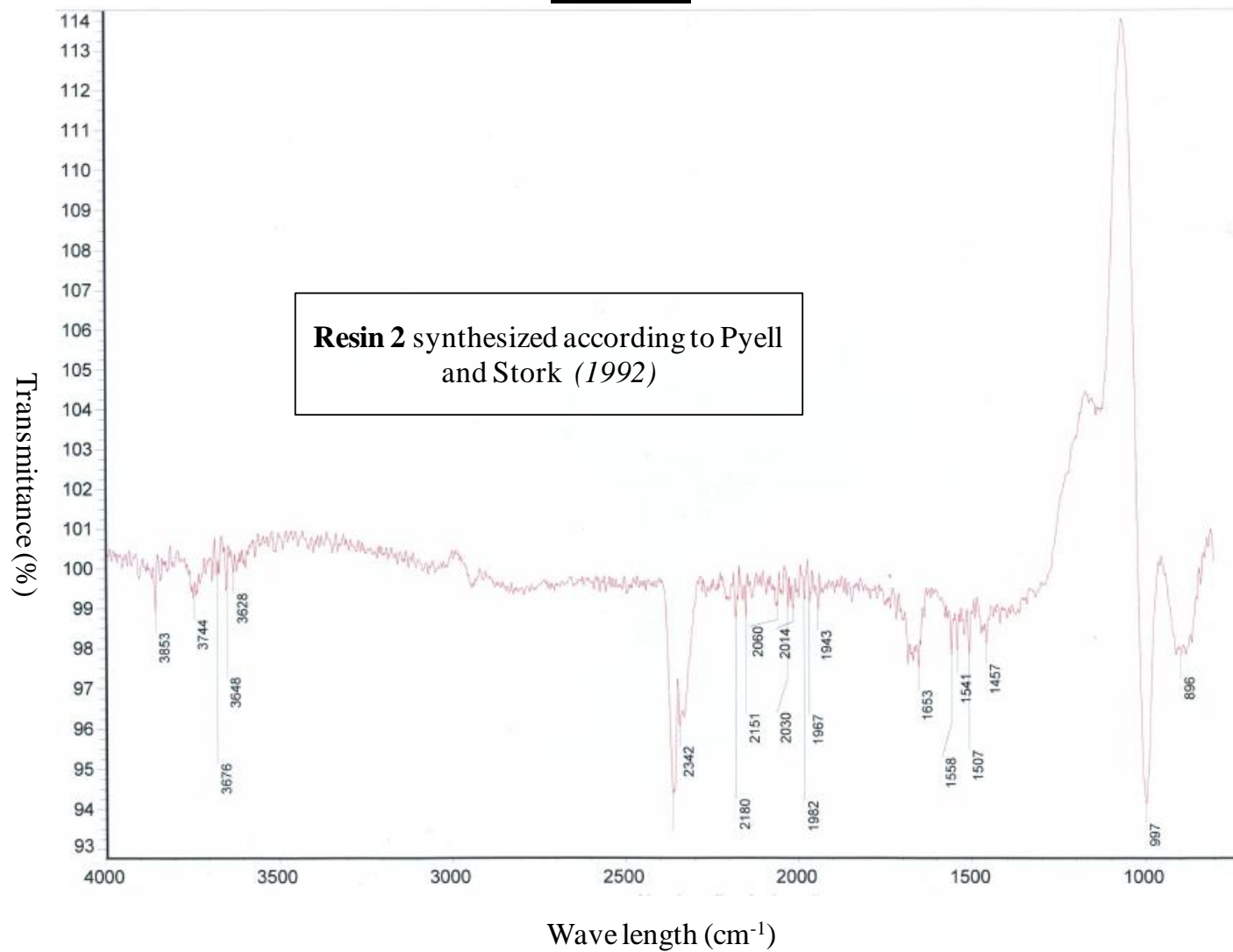


**ANNEXE 2**

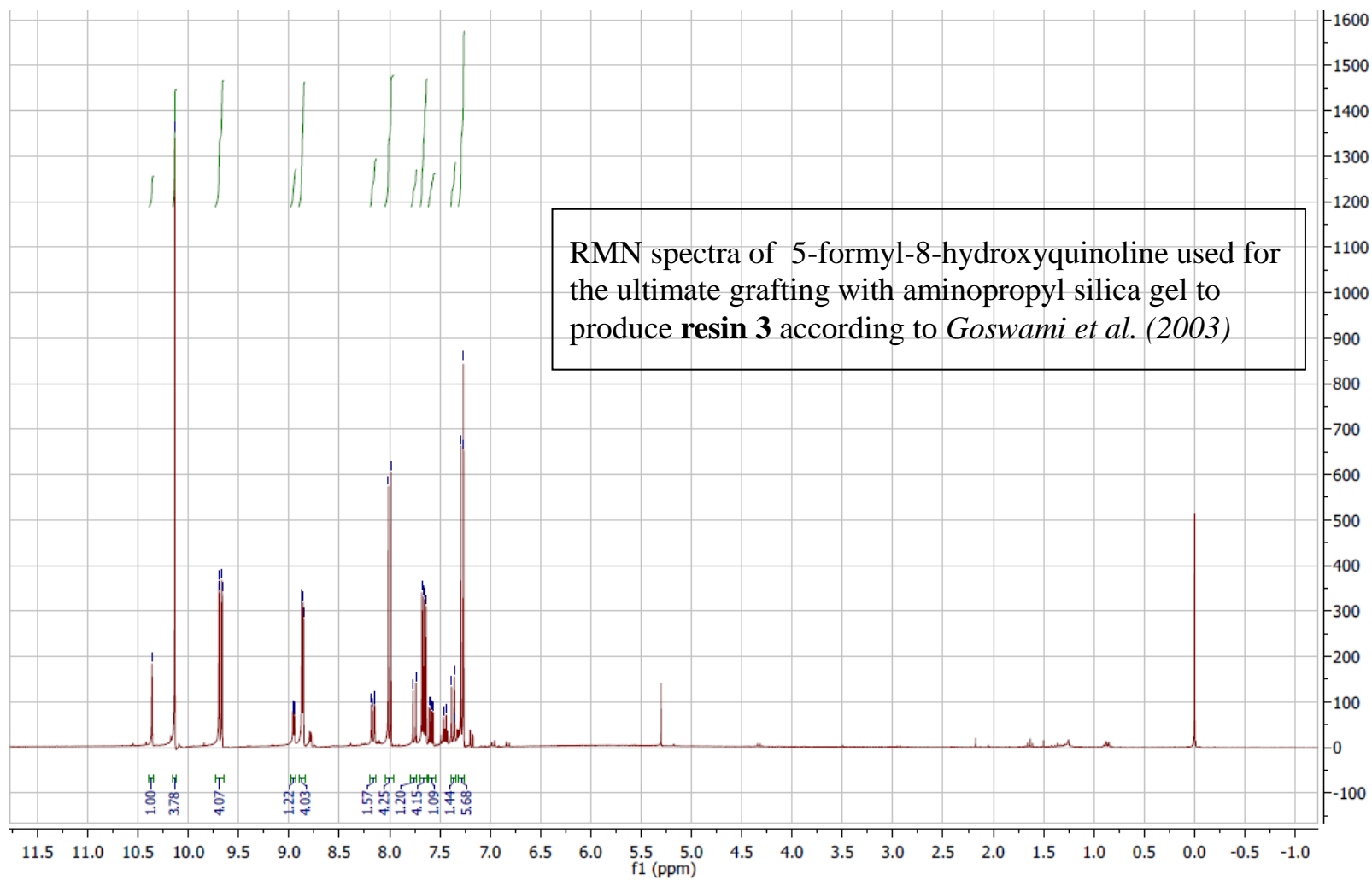




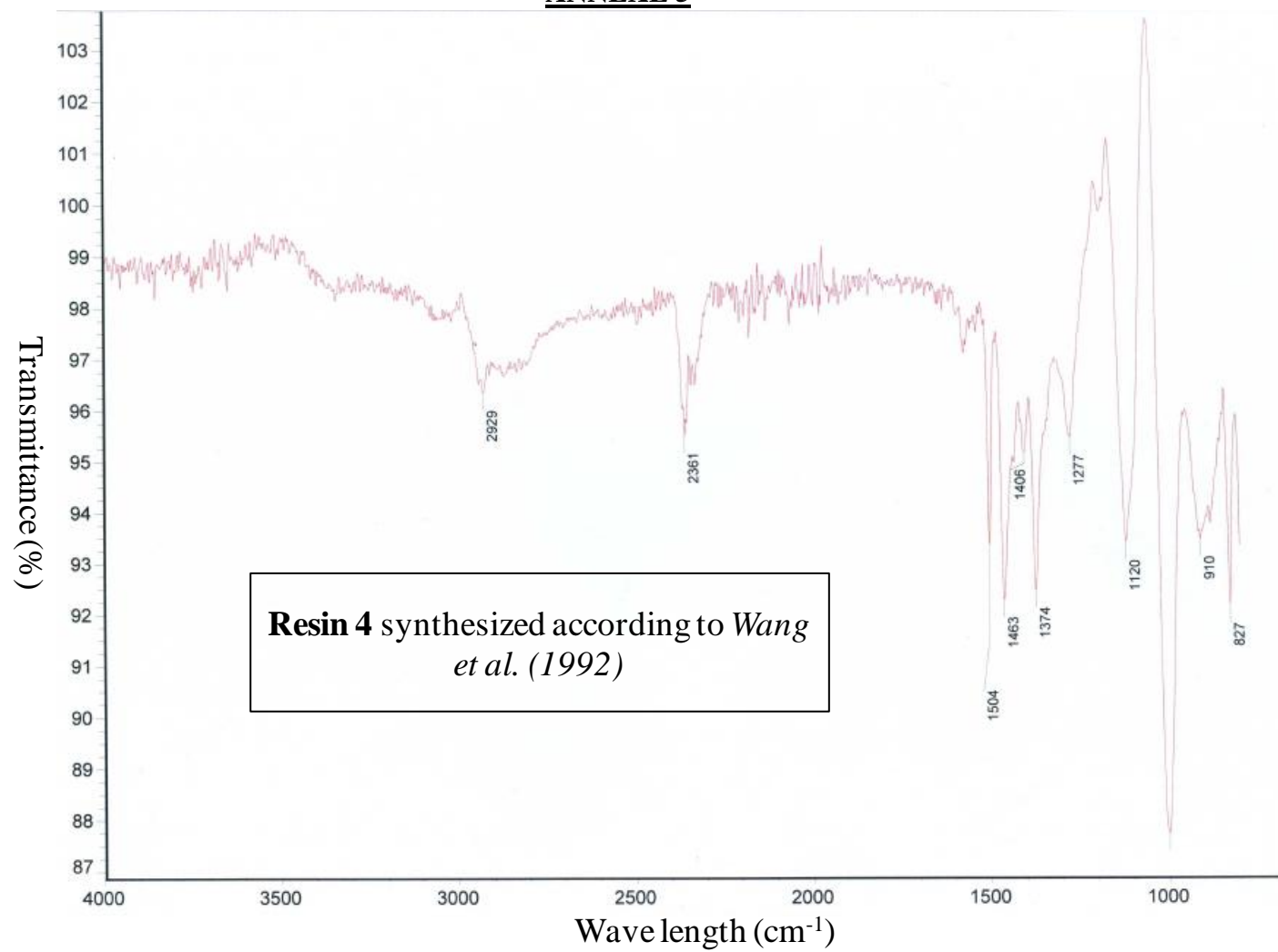
### ANNEXE 3



#### ANNEXE 4



## ANNEXE 5



**ANNEXE 6**

